TRANSPORTATION RESEARCH RECORD 602

Pavement Design, Evaluation, and Performance

TRANSPORTATION RESEARCH BOARD

COMMISSION ON SOCIOTECHNICAL SYSTEMS
NATIONAL RESEARCH COUNCIL

NATIONAL ACADEMY OF SCIENCES
WASHINGTON, D.C. 1976

Transportation Research Record 602
Price $5.40
Edited for TRB by Marianne Cox Wilburn

subject areas
25 pavement design
26 pavement performance
40 general maintenance
51 highway safety
62 foundations (soils)
63 mechanics (earth mass)

Transportation Research Board publications are available by ordering directly from the board. They may also be obtained on a regular basis through organizational or individual supporting membership in the board; members or library subscribers are eligible for substantial discounts. For further information, write to the Transportation Research Board, National Academy of Sciences, 2101 Constitution Avenue, N.W., Washington, D.C. 20418.

Notice
The project that is the subject of this report was approved by the Governing Board of the National Research Council, whose members are drawn from the councils of the National Academy of Sciences, the National Academy of Engineering, and the Institute of Medicine. The members of the committee responsible for the report were chosen for their special competence and with regard for appropriate balance.

This report has been reviewed by a group other than the authors according to procedures approved by a Report Review Committee consisting of members of the National Academy of Sciences, the National Academy of Engineering, and the Institute of Medicine.

The views expressed in this report are those of the authors and do not necessarily reflect the view of the committee, the Transportation Research Board, the National Academy of Sciences, or the sponsors of the project.

Library of Congress Cataloging in Publication Data
National Research Council. Transportation Research Board.
Pavement design, evaluation, and performance.

(Transportation research record; 602)
Includes bibliographical references
1. Pavements–Design and construction–Addresses, essays, lectures. 2. Pavements–Testing–Addresses, essays, lectures. 3. Motor vehicles–Skidding–Addresses, essays, lectures. I. Title. II. Series.
TE7.H5 no. 602 [TE250] 380.5'08s [625.8] 77-4926
ISBN 0-309-025710

Sponsorship of the Papers in This Transportation Research Record

GROUP 2–DESIGN AND CONSTRUCTION OF TRANSPORTATION FACILITIES
W. B. Drake, Kentucky Department of Transportation, chairman

Pavement Design Section
Carl L. Monismith, University of California, Berkeley, chairman

Committee on Rigid Pavement Design
B. F. McCullough, University of Texas at Austin, chairman
Kenneth J. Boedecker, Jr., William E. Brewer, Bert E. Colley, Roman L. Dankbar, Donald K. Emery, Jr., Wade L. Gramling, Yang H. Huang, Ronald L. Hutchinson, Donald M. Jameson, Torbjorn J. Larsen, L. Frank Pace, Robert G. Packard, Frazier Parker, Jr., Thomas J. Pasko, Jr., Surendra K. Saxena, M. D. Shelby, Don L. Spellman, T. C. Paul Teng, William Van Breemen, William A. Yrjanson

Committee on Flexible Pavement Design
Roger V. LeClerc, Washington State Department of Highways, chairman
John W. Hewitt, Federal Highway Administration, secretary
Robert A. Crawford, R. N. Doty, W. B. Drake, Fred N. Finn, Frank B. Hennion, R. G. Hicks, William S. Housel, Michael P. Jones, R. E. Livingston, J. W. Lyon, Jr., Richard A. McComb, Chester McDowell, Carl L. Monismith, William M. Moore, Frank P. Nichols, Jr., Dale E. Peterson, William A. Phang, Donald R. Schwartz, James F. Shook, Eugene L. Skok, Jr., Richard Lonnie Stewart, Paul G. Velz, Stuart Williams

Committee on Design of Composite Pavements and Structural Overlays
Mathew W. Witczak, University of Maryland, chairman
Gordon W. Beecroft, Oregon Department of Transportation, secretary
Ernest J. Barenberg, Walter R. Barker, Richard D. Barksdale, W. G. Davison, William F. Edwards, H. K. Eggleston, Philip F. Frandina, J. H. Havens, R. E. Livingston, Richard A. McComb, Carl L. Monismith, August F. Muller, Leonard T. Norling, Frazier Parker, Jr., John L. Rice, Donald R. Schwartz, George B. Sherman, Lawrence L. Smith, Harvey J. Treybig, William Van Breemen, Loren M. Womack, Eldon J. Yoder

Committee on Surface Properties-Vehicle Interaction
W. E. Meyer, Pennsylvania State University, chairman
Glenn G. Balmer, Frederick E. Behn, Andrius A. Butkunas, A. Y. Casanova III, Michael W. Fitzpatrick, William Gartner, Jr., Ralph C. G. Haas, Douglas I. Hanson, Don L. Ivey, William F. Lins, David C. Mahone, Paul Milliman, Alexander B. Moore, E. W. Myers, Arthur H. Neill, Jr., Bayard E. Quinn, John J. Quinn, Frederick A. Renninger, Rolands L. Rizenbergs, Hollis B. Rushing, Richard K. Shaffer, George B. Sherman, Elson B. Spangler, James C. Wambold, M. Lee Webster, E. A. Whitehurst, Ross G. Wilcox, Dillard D. Woodson

Committee on Pavement Condition Evaluation
Karl H. Dunn, Wisconsin Department of Transportation, chairman
Frederick Roger Allen, Frederick E. Behn, Max P. Brokaw, Edwin J. Dudka, Ralph C. G. Haas, R. G. Hicks, William H. Highter, W. Ronald Hudson, L. B. R. Hunter, David J. Lambiotte, J. W. Lyon, Jr., Alfred W. Maner, K. H. McGhee, William A. Phang, Bayard E. Quinn, Freddy L. Roberts, Lawrence L. Smith, Elson B. Spangler, Robert J. Weaver, Loren M. Womack, Eldon J. Yoder

Committee on Theory of Pavement Design
W. Ronald Hudson, University of Texas at Austin, chairman
James F. Shook, Asphalt Institute, secretary
Richard G. Ahlvin, Richard D. Barksdale, James L. Brown, Santiago Corro Caballero, Michael I. Darter, Fred N. Finn, Ralph C. G. Haas, Eugene Y. Huang, William J. Kenis, Ramesh Kher, Robert L. Lytton, Carl L. Monismith, Robert G. Packard, Dale E. Peterson, G. Y. Sebastyan, James F. Shook, William T. Stapler, Ronald L. Terrel, E. B. Wilkins, Loren M. Womack

Lawrence F. Spaine, Transportation Research Board staff

Sponsorship is indicated by a footnote on the first page of each report. The organizational units and the officers and members are as of December 31, 1975.

Contents

Economic Considerations of Faulting and Cracking in Rigid Pavement Design

John P. Zaniewski, Austin Research Engineers, Inc.

The results of several pavement studies and road tests have been compared to determine the significance and interaction of design variables with respect to distress. The design variables studied are pavement reinforcement, thickness, joint spacing, and subgrade material. The distress modes studied are faulting, transverse cracking, and pumping. To compare faulting between pavement designs with different joint spacings, researchers developed a method for estimating serviceability from faulting and joint spacing data. This method is based on amplitude-wavelength relationships to serviceability that were established in Texas. An extension of this method allows comparisons of reinforced and unreinforced concrete pavements that consider both cracks and joints in concrete pavements to be "faulting opportunities." The expected faulting per length of pavement for various designs is then computed by using the number of joints and cracks and the probability of faulting for each type of joint or crack. Load transfer is used as a criterion for estimating the probability of faulting. A method for considering the relative cost of pavements per vehicle is presented that is based on expected faulting and effect of faulting on serviceability. This method is illustrated by an example problem.

This paper investigates the major problem area of jointed concrete pavements, interactions of problem areas, design parameters that may minimize problems, and economic trade-offs for selecting an optimum pavement design. The use of various design parameters to limit or minimize the effect of pavement distress on serviceability is compared on an economic basis.

TYPES OF PAVEMENT

Jointed concrete pavements (JCPs) consist of any combination of portland cement concrete slabs, reinforcing steel, and load transfer devices. To conveniently describe these combinations, we adopted the following abbreviations for use in this paper:

1. JPCP is jointed plain concrete pavement without load transfer devices at the joints or reinforcing steel,
2. JPCP/D is jointed plain concrete pavement with dowel bars for load transfer at the joints,
3. JRCP is jointed reinforced concrete pavement, and
4. JRCP/D is jointed reinforced concrete pavement with dowel bars for load transfer at the joints.

DISTRESS MODES OF JOINTED CONCRETE PAVEMENTS

The U.S. Army Corps of Engineers (1) lists 18 specific forms of rigid pavement distress. To discuss all of these distress modes in this paper is obviously impossible. Therefore, only 3 major forms of distress have been selected for discussion: (a) faulting, (b) cracking or breakup, and (c) pumping.

Faulting

Faulting, described by Spellman, Stoker, and Neal (2) as the vertical displacement of concrete slabs at joints or cracks, is often considered to be the main weakness of JCP (3) because the vertical dislocation of short pavement sections at transverse joints can lead directly to serviceability loss. Two mechanisms have been identified as being associated with faulting (4). One cause is the loss of slab support, especially under the leave slab (the slab past the joint), which is due to settlement or erosion of the underlying layers. The other cause is the buildup of fine materials under the approach side of the slab (2, 4) when the subbase is very stiff, such as in cement-stabilized subbases. This buildup is a result of the carrying by pressurized water of fine particles of subbase or shoulder material under the approach slab when a heavy axle load passes over a joint (2, 4). For these mechanisms to result in faulting the following conditions must be present:

1. Free water on top of the base,
2. Differential deflection across the joint (inadequate load transfer across the joint), and
3. Heavy axle loads (resulting in high pavement deflections).

Publication of this paper sponsored by Committee on Rigid Pavement Design.

Cracking

Cracking, which may take several forms in JCP, results from a combination of environmental forces (such as thermal contraction forces) and fatigue due to traffic loads. The forms of cracking of interest in this report are corner cracks, transverse cracks, and longitudinal cracks. Cracking associated with construction problems, such as double cracking at joints (4), is not considered in this report.

Corner cracking is usually associated with excessive corner deflections resulting from heavy axle loads, loss of slab support, and inadequate load transfer across the joint. Because one of the primary catalysts of corner cracking is loss of slab support due to pumping of the underlying layers, conditions related to pumping may also be considered to be associated with corner cracking.

Transverse cracks are generally associated with environmental forces, especially thermal contraction resulting from a temperature drop. The amount of force (or stress) generated in this manner is a function of slab thickness, joint spacing, amount and rate of temperature drop, concrete shrinkage and slab-subbase or slab-subgrade interaction (friction). Although environmental effects are usually considered the primary factor for transverse cracking, the effect of traffic loading cannot be ignored. This was discovered at the American Association of State Highway Officials (AASHO) (now American Association of State Highway and Transportation Officials) Road Test (5) where pavement sections on the traffic loops developed cracks and sections on the nontraffic loop had no apparent cracks.

Longitudinal cracks generally occur in a manner similar to that of transverse cracks. The effect of longitudinal cracks on pavement serviceability should be somewhat less than the effect of transverse cracks because longitudinal cracks are parallel with traffic flow and therefore are encountered less often than transverse cracks.

Pumping

Pumping of materials from under a jointed concrete pavement does not directly lead to loss of serviceability, but pumping is such a major contributor to other pavement distress that it should be considered a major design problem. Pumping was defined at the AASHO Road Test (5) as "the ejection of water and subbase material or embankment soil from beneath the pavement surfacing." The result is a loss of slab support. Pumping may occur at the pavement edge, joints, or cracks. In general, more material is ejected during edge pumping than during crack or joint pumping (5). The conditions required for pumping are pumpable material underlying the slab, free water under the slab, and high deflections.

DESIGN PARAMETERS FOR MINIMIZING JCP DISTRESS

The design parameters for jointed concrete pavement are well known; therefore, they will only receive a brief review here. The purpose of this review is to discuss the reasons for applying the various design parameters to minimize the previously discussed problem areas and to introduce the concept of the interactions of the various design parameters.

Pavement Thickness

Pavement thickness is perhaps the most obvious design parameter. Proponents of JRCP support the concept that a pavement of adequate thickness can be designed so that minimum distress will occur during the design life of the pavement (3). Critical stresses in JPCP are a result of corner loading; critical stresses in JRCP are the result of edge loading if there is good load transfer at the joints. Pavements designed to withstand corner loading must be thicker than pavements designed for edge loading.

Reinforcement and Load Transfer Devices

Internal pavement reinforcement, such as is used in JRCP, is not used as a direct measure to increase the pavement strength, but rather is used as a measure to ensure that pavement strength is maintained. The method for maintaining pavement strength is to provide sufficient reinforcement to ensure aggregate interlock across cracks that form in the concrete. Proponents of JRCP claim that the "slightly" greater cost of reinforcement is offset by the need for fewer joints, lower maintenance cost, and higher serviceability during the life of the pavement (6). Load or shear transfer devices at joints are usually in the form of dowel bars.

Subbase and Subgrade

Subbase design varies according to the desired objectives for the design agency. Originally, subbases were placed under concrete pavements to provide drainage and reduce pumping. In the 1940s Hveem recommended the use of treated or chemically stabilized subbase materials to reduce damage to the subbase (2).

Joint Design

Joint design plays an important role in how a pavement will perform. Four basic types of joints are currently being used: construction, expansion, contraction, and warping joints. Joints are necessary for the proper design of jointed concrete pavements because of volume changes in the concrete that are due to shrinkage and temperature changes. Early experiments with long sections of continuous plain concrete pavement proved that joints are necessary. The two most important design considerations are joint spacing and load transfer.

Drainage

The earlier discussion of distress showed that the presence of free water under a pavement is one of the most important catalysts for pavement distress. Therefore, providing proper drainage under the pavement should be an important design parameter, especially in wet climates.

Interactions

Although a discussion of the individual design parameters is useful for understanding the basic concepts of these parameters, an understanding of the interaction of these parameters is equally important. For example, the thickness of the pavement should reflect the subbase design used. A pavement on a strong cement-treated subbase may conceivably be thinner than a pavement placed directly on a weak subgrade if all other design factors are equal. A summary of other important interactions is given in Table 1. In this table, interactions are described as being either primary or secondary. A primary interaction occurs when a change in one variable causes a direct effect on another variable. A secondary interaction is defined as a change in the variable that causes an indirect effect on another variable. This table was used as a guideline for a literature review of

the effectiveness of the various design factors. If the design factor interactions are not recognized, results of the literature survey could be misleading.

OBSERVATIONS OF DISTRESS MODES WITH RESPECT TO DESIGN STRATEGIES

This section summarizes the findings of laboratory studies and field observations about the relative merits of three design strategies used for jointed concrete pavements:

1. Plain concrete pavements without dowel bars for load transfer at joints,
2. Plain concrete pavements with dowel bars, and
3. Jointed reinforced concrete pavements with dowel bars.

The pavement distresses studied were faulting, transverse cracking, and pumping.

Faulting at Joints and Cracks

As mentioned earlier, faulting of JCP leads directly to a loss of serviceability. Therefore, to compare the design concepts of interest, one needs a method to compare the effects of faulting on serviceability. Such a method may be developed based on the results of an amplitude-wavelength-serviceability study reported by Walker and Hudson (8). Figure 1 shows how the amplitude-wavelength data may be used to determine present serviceability ratings (PSR) levels (8). This figure was developed in a manner similar to that used to develop the original present serviceability index (PSI) at the AASHO Road Test (5). A surface dynamic profilometer was used to measure the amplitudes and wavelengths of several pavements throughout Texas. These measurements were then correlated with road users' opinions of pavement serviceability. Use of the amplitude-wavelength measurements provides a good measure of PSI because only amplitude-wavelengths that are highly correlated with PSR are included in the relationship.

This information may be used to estimate PSR levels of pavements given joint spacing and faulting data. If faulting is assumed to equal amplitude and joint spacing is assumed to equal wavelength, the results of faulting studies may be plotted directly on Figure 1 to estimate PSR levels. For example, assume that the amplitude-wavelength measurements for a pavement with 9.14-m (30-ft) slabs are shown by the dashed line in Figure 1. The "hump" in the dashed line would represent the occurrence of faults at the joints. The penetration of the 2.0 to 2.5 PSR line by the faults indicates that this is the critical wavelength for the pavement. The PSR of the pavement then would be governed by faulting; therefore, measurements of faulting and joint spacing are useful for estimating PSR.

Assuming that PSR may be estimated in this manner is somewhat inaccurate because the curves were developed for smooth variation in the road profile and faults are abrupt variations in the profile. This becomes especially critical for the long wavelength or joint spacings. For example, the curve shows that an amplitude of 3.43 cm (1.35 in) and a wavelength of 24.38 m (80 ft) corresponds to a PSR of 4.0 to 4.5. A fault of 3.43 cm (1.35 in) obviously could not be tolerated on a roadway every 24.38 m (80 ft). This problem is offset by two factors. First, the curves are plotted for the 99 percent level of amplitude. Therefore, on the average, the 3.429-cm (1.35-in) amplitude would only occur once every 100 joints, which corresponds to once every 2438 m (8000 ft). Second, the high side of the fault usually occurs on the approach side of the joint (2); therefore, the traffic is dropping off the fault. This is less severe than if the approach slab were lower than the leave slab and the traffic was hitting a "bump."

Faulting criteria cited by Brokaw (3) for JPCP with 4.5 to 6.1-m (15 to 20-ft) slabs have been plotted on Figure 1. It appears that there is good agreement between the faulting criteria and the wavelength-amplitude curve. Unfortunately, similar criteria do not exist for pavement with longer slabs.

Two hypotheses may be developed from Figure 1. First, tolerable faulting levels for a given PSR increase with slab length. Second, minor increases in faulting of a pavement with short slabs result in a significant drop of PSR. This method of analysis allows comparison of faulting in pavements with different slab lengths.

Observations of pavement performance with respect to faulting tend to support these hypotheses. In a 5-year progress report of a New York rigid pavement study (4), faulting of pavement sections with 6.1-m (20-ft) unreinforced and 18.54-m (60-ft, 10-in) reinforced slabs was studied. Because of the limited amount of traffic during the 5-year period, faulting had not developed to a significant degree. All sections except for one had less than 0.16-cm ($\frac{1}{16}$-in) average faulting; therefore, variation between sections was too limited for forming statistically significant conclusions. The following trends were observed from averages of the observations:

1. Sections on granular bases had more faulting than sections on stabilized bases had;
2. The 18.54-m (60-ft, 10-in) slabs had more faulting than the 6.1-m (20-ft) slabs had; and
3. Higher roughnesses were measured on the sections with short slabs.

Because of the limited amount of faulting, plotting results of this study on Figure 1 would not be significant.

De Young (9) reported the results of a joint spacing study of plain concrete pavements in Iowa. Pavements were constructed with joint spacings of 6, 15.2, and 24.4 m (20, 50, and 80 ft). After 8 years of traffic, transverse cracking had reduced the sections to average slab lengths of 5.8, 8.8, and 11.3 m (19, 29, and 37 ft) respectively. Faulting on these sections at the 99 percent level was approximately 0.64, 0.86, and 0.79 cm (0.25, 0.34, and 0.31 in) respectively. As shown on Figure 1, the section with the longest joint spacing would be expected to have the highest PSR. Roughness measurements with the BPR roughometer verified that the sections with the long joint spacings were the smoothest.

Even though these data do not allow definite conclusions to be drawn, they do indicate that there is a trend for pavements with long slabs to be smoother than pavements with short slabs. Regardless of the slab length used, faulting needs to be controlled.

In this paper, load transfer is defined as the leave slab deflection divided by the sum of the approach and leave slab deflections and converted to a percentage. Load transfer by aggregate interlock requires that joints remain very "tight" to maintain contact on the bearing faces. Observations at a Michigan test road (10) verified that, when joints without dowel bars separate, load transfer drops off significantly. For example, average load transfer across 10 joints changed from 46.2 to 36.1 percent when the joint width changed from 0.11 to 0.16 cm (0.045 to 0.064 in) due to temperature changes. A California faulting study (2) found similar results.

Studies of joint openings at the Michigan test road (10) showed that contraction joints opened as much as 0.51 cm

(0.20 in) at -17.78°C (0°F) for 6.1-m (20-ft) joint spacings. Furthermore, all contraction joints were found to sustain permanent openings that gradually increased after 10 to 15 years of service. This means that there is a high probability, especially in colder climates, of loss of load transfer across joints with only aggregate interlock. Average load transfer across nine doweled joints on the Michigan test road was 48.8 percent; average joint width was 0.16 cm (0.063 in).

Load transfer across several joint designs was studied by the Portland Concrete Association (PCA) (11) by using repeated load tests on slabs. Results from these tests are given in Table 2. Note that both the 15.24-cm (6-in) and 20.32-cm (8-in) slabs with dowel bars and 0.635-cm (0.25-in) joint width performed better than the joints without load transfer devices.

It is apparent that dowel bars provide good load transfer at joints and that joints with only aggregate interlock tend to lose their load transfer capability. Several pavement studies confirm this statement.

At the AASHO Road Test (5), all joints had dowel bars. As a result, "faulting at joints was notably absent throughout the project." Observations in Georgia (7) of plain concrete pavements without dowel bars at joints found that "all projects on the Interstate Highway System in Georgia with plain concrete pavements exhibited faulting." Findings at a test pavement in Kentucky (12) were that "sections having load transfer dowels in all joints have shown less faulting of the joints." Similar results were reported at the Michigan test road (10): "Plain concrete pavements with dowels at contraction joints performed better than plain concrete pavements without dowels at contraction joints." Sufficient variation in pavement designs and environmental and traffic conditions exists among these pavement studies to allow the general conclusion that dowel bars are an effective means for limiting faulting.

Subbase design also affects faulting of jointed concrete pavements. Two alternate approaches to subbase design are currently being practiced: (a) use of stabilized subbase to reduce differential deflection or (b) use of free-draining subbases to remove free water.

Findings of the Georgia faulting study (7) with respect to subbase design were that "plain concrete pavements (without dowels at joints) on a cement stabilized subbase tend to have less faulting than those constructed on a bituminous stabilized or soil-cement subbase for the same traffic parameter." At the New York pavement experiment (4), more faulting was observed on granular subbases than on stabilized subbases.

Based on these findings, faulting appears to decrease as subbase stiffness increases. This trend cannot be so firmly established as the conclusions about the effectiveness of load transfer devices can be because of a lack of data.

Part of the problem in comparing results of several road tests is that the design of the experiments generally is aimed at obtaining results for a specified set of design parameters over a fixed range of values. The interactions of design parameters often prevent the specific results determined during one pavement study from being compared to the results of other pavement studies. For example, no faulting was observed at the AASHO Road Test (5) where the rigid pavements were built either directly on the subgrade or on granular subbases. In contrast, the Georgia faulting study showed that faulting does occur on pavements with cement-stabilized subbases. The conclusion that granular subbases are more effective than stabilized subbases for limiting faulting would be incorrect because dowel bars were used in the AASHO pavements but not in the Georgia pavements.

Transverse Cracking

One of the most important factors determining the amount of transverse cracking is the spacing of contraction joints. The Michigan test road results showed that a joint spacing of approximately 3.1 m (10 ft) was necessary to completely prevent transverse slab cracking (10). Joint spacings of 4.5 to 6.1 m (15 to 20 ft) are more commonly used to minimize transverse slab cracking. Figure 2 shows the development of transverse cracking with respect to time as a function of joint spacing in JPCP (9). Transverse cracking developed in JRCP would be similar because the reinforcing steel does not prohibit the formulation of transverse cracks. This was verified at the Michigan test road (10) where the amount of transverse cracking was not significantly different for reinforced and unreinforced test sections whose design was the same in other respects.

A significant factor at the Michigan road test is that the pavements with reinforcement were generally in much better condition than the nonreinforced pavements (10). This occurred because the reinforcement held the cracks close enough that the aggregate interlock was maintained across the crack for load transfer. This is not really a fair comparison of the performance of reinforced versus nonreinforced pavements because of the interaction between reinforcement and joint spacing. Plain concrete pavements are generally designed to have shorter slabs than reinforced pavements.

Because of the shorter slab lengths of plain concrete pavements, much less transverse cracking occurs than with reinforced concrete pavements. In the New York pavement study (4), twice as many transverse cracks formed in the 18.54-m (60-ft, 10-in) reinforced slabs as in the 6.1-m (20-ft) unreinforced slabs. This appears to be an advantage of shorter unreinforced slabs. However, when one considers that the criteria for joint spacings of unreinforced slabs were developed from crack spacing data, one is not surprised that only limited transverse cracking occurs on these sections.

Because slab lengths for reinforced and nonreinforced pavements are considerably different, to compare the number of cracks per slab or per length of pavement for these two design concepts is inappropriate. The most logical comparison that can be made is comparing the number of faulting opportunities per length of pavement and the likelihood of faulting. To make this comparison, one considers joints and transverse cracks to be faulting opportunities. A comparison of this type has been made by using the New York data (4). Figure 3a shows a 36.6-m (120-ft) pavement with 6.1-m (20-ft) slab lengths; Figure 3b shows a 36.6-m (120-ft) pavement with 18.3-m (60-ft) joint spacings. The pavement with 6.1-m (20-ft) slab lengths has five internal joints and two transverse cracks, or a total of seven faulting opportunities. The pavement with 18.3-m (60-ft) slabs has one joint and four transverse cracks, or a total of five faulting opportunities. The ratio of faulting opportunities for the two slab lengths would decrease as pavement length increases, but, for the conditions reported at the New York test road (4), the number of faulting opportunities for the pavement with long slabs will be equal to the number of joints in the pavement with short slabs, as would be expected if the joints in the JPCP are considered to be preformed cracks.

If the concept of faulting opportunity is used, JRCP appears to have an advantage over JPCP if transverse cracks and joints have the same probability of faulting. Unfortunately, there are no data available on the probability of faulting by joints and cracks. Laboratory studies of load transfer of various joints have been performed (11) that can be used to postulate the relative

Table 1. Interactions of pavement design variables.

Design Factor	Design Factor Code	Interaction[a]	
		Primary	Secondary
Pavement thickness	1	2, 3, 4, 5, 6, 7, 8, 9	
Steel load transfer	2	1, 5, 6, 7, 8	4
Steel reinforcement	3	1, 5, 6	4
Subbase thickness	4	1, 2, 3, 5, 6, 8	7, 9
Type of subbase material	5	1, 2, 3, 4, 6, 8, 9	7
Subgrade stabilization	6	1, 2, 3, 4, 5, 7, 8	
Joint spacing	7	1, 2, 3, 5, 6	4, 9
Joint load transfer	8	1, 2, 3, 5, 6, 9	4
Drainage	9	1, 2, 3, 5, 6, 8	4, 7

[a] Numbers refer to design factor codes.

Figure 1. Amplitude-wavelength relationships for two PSR levels.

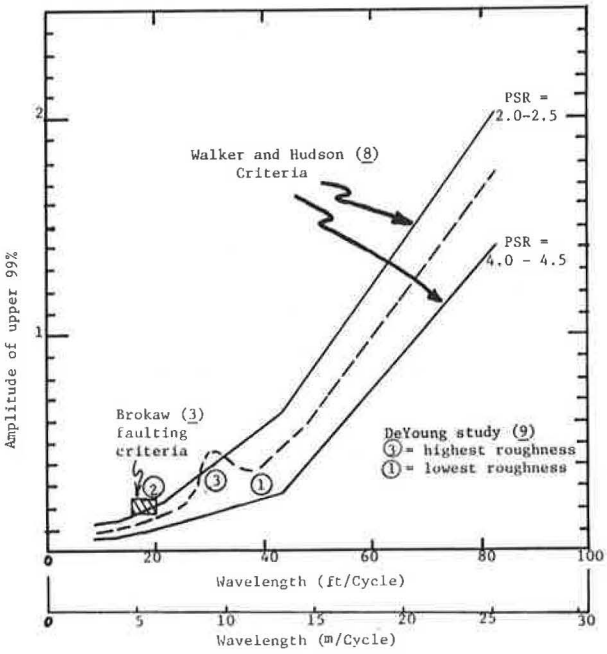

Figure 2. Reduction of slab length over time due to transverse cracking.

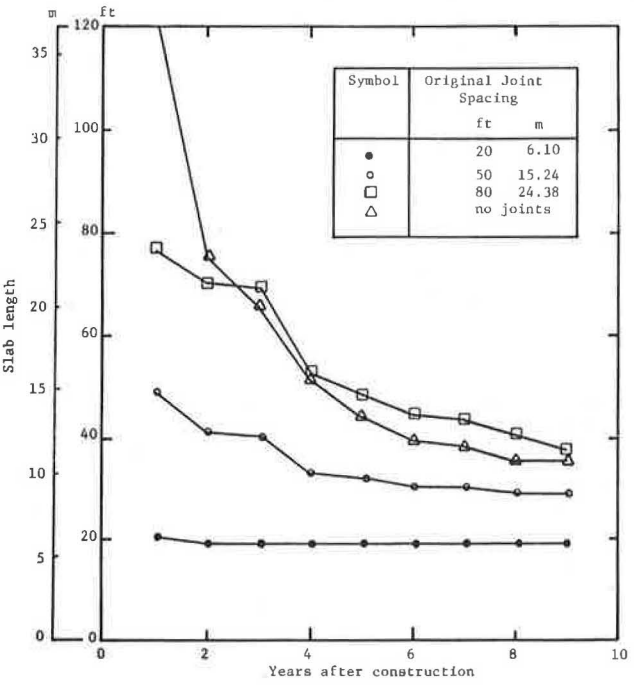

Table 2. Summary of PCA joint study.

Joint Type	Ties	Slab Depth (cm)	Cement-Stabilized Subbase Depth (cm)	Cycles[a] ($\times 10^6$)
Aggregate interlock	None	15.24	0	0.10
	Two 0.635 cm[b]	15.24	0	1.33
Dowel	Two 1.905 cm	15.24	0	2.00
Aggregate interlock	None	15.24	7.62	0.42
Dowel	Two 1.905 cm	15.24	7.62	2.37
Aggregate interlock	None	20.32	0	0.24
Dowel	Two 1.905 cm	20.32	0	0.90
Aggregate interlock	None	15.24	15.24	0.24
	Two 0.635 cm[b]	15.24	15.24	3.98
Dowel	One 2.54 cm	15.24	15.24	1.58

Note: 1 cm = 0.394 cm.

[a] Number of load cycles required for load transfer to drop from initial value to 44 percent. Load transfer decreases with number of applications.
[b] No. 2 size.

Figure 3. Faulting opportunities for (a) JPCP and (b) JRCP.

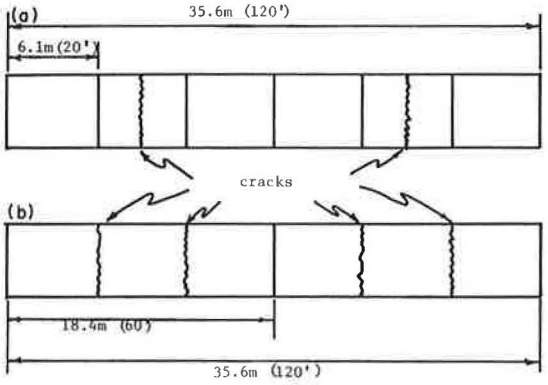

Figure 4. Estimating probability of faulting from load transfer.

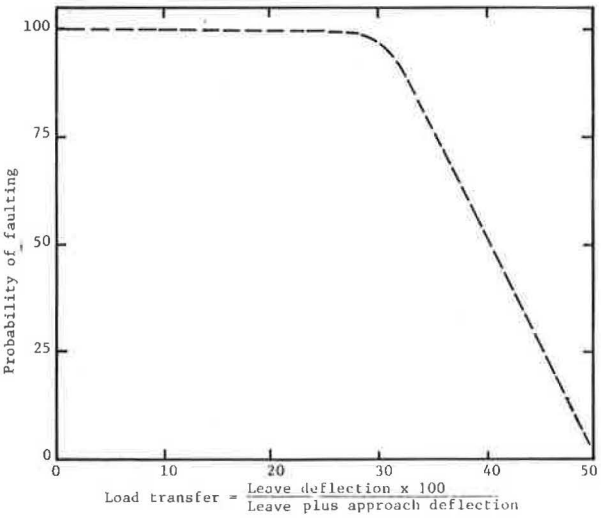

Table 3. Probability of faulting for joints and cracks.

Type A Pavement	Type of Fault	Load Transfer	Probability of Faulting	Number of Joints or Cracks/ Kilometer	Expected Faulting
JRCP/D	Joint	45	0.25	55	22
	Crack	44	0.30	109	53
	Total				75
JPCP/D	Joint	45	0.25	164	66
	Crack	36	0.70	55	62
	Total				128
JPCP	Joint	36	0.70	164	185
	Crack	36	0.70	55	62
	Total				247

Note: 1 joint/km = 1.609 joints/mile.

probabilities of faulting because faulting is largely dependent on load transfer. Use of the PCA data (11) to determine the relative probability of faulting for joints and cracks requires the following assumptions:

1. The laboratory study of joints may be extended, in a relative fashion, to field conditions;
2. The aggregate interlock joint with no tie (11) is representative of cracks in unreinforced pavements and joints that do not have load transfer devices;
3. The dowel joint tested represents a dowel joint in a pavement; and
4. The aggregate interlock joint with tie bars is representative of cracks in reinforced pavement.

An additional factor that should be considered is the fact that the PCA tests were run at joint widths of zero for the aggregate interlock joints with and without reinforcement and 0.635 cm (0.25 in) for the doweled joints. Therefore, the performance of the aggregate interlock joints would probably decrease and the performance of the dowel joints would probably increase. The results of the PCA joint study (11), given in Table 2, indicate that in all cases the unreinforced aggregate interlock joint did not perform as well as the other joints did. Comparison of reinforced aggregate interlock joints and dowel joints is confounded by the change in type of subbase and dowel design.

As an illustration of the concept of considering both the number of faulting opportunities and the probability of faulting, the following example problem was conceived. Graphical relationships and numerical data used in this example were contrived based on limited field data.

Based on some data from the Michigan test road (10), Figure 4 was drawn to show the relationship between load transfer and the probability of faulting. By using this relationship and the number of faulting opportunities occurring for each type of fault or joint, one can calculate the expected faulting on a section of JCP as

$$E(f) = \sum_{i=1}^{k} P(f)_i \cdot n_i \qquad (1)$$

where

E(f) = expected number of faults,
k = number of types of joints and cracks occurring in the pavement,
$P(f)_i$ = probability of the ith type of crack or joint faulting, and
n_i = the number of ith type of cracks or joints.

Equation 1 may be applied to compare expected faulting for the sections in the New York study; three pavement designs are evaluated in the New York study: (a) JPCP with 6.1-m (20-ft) slabs, (b) JPCP/D with 6.1-m (20-ft) slabs, and (c) JPCP/D with 18.3-m (60-ft) slabs. The joints and cracks per length of pavement can be calculated from the data shown in Figure 3; these calculations are given in Table 3.

The probability of faulting for each type of joint or crack was obtained by assuming load transfer values and by using Figure 4. These calculations show that, for the assumed conditions, the jointed reinforced concrete pavement would have considerably less faulting than either of the plain concrete pavements would have and that the plain concrete pavement with doweled joints would have less faulting than the one without dowel bars would have.

Pumping of Rigid Pavements

Concrete pavements were originally placed directly on the subgrade. As axle loads increased (which caused higher pavement deflections), the subgrade material under the pavement began to mix with free water and formed mud. Deflection of the pavement then forced the mud out from under the pavement, or mud pumping, which was a serious problem. To stop the problem, granular subbases were placed under the pavements. These worked well for many years, and it was thought that the granular subbase was not a pumpable material. Then, at the AASHO Road Test, heavy axle loads on the thinner test sections resulted in pumping of the granular subbases (5).

Cement- and asphalt-stabilized subbases have been used for many years as a means of reducing deflections. In general, pumping is not a problem when stabilized subbases are used, but at a New York experimental pavement (4) pumping has occurred on pavement sections with stabilized subbases; however, the water pumped was free of subbase materials.

California has recently started building cement-stabilized subbases that extend 0.3 m (1 ft) beyond the pavement edge (2). This is being done in part to eliminate or reduce edge pumping. Faulting of California pavements has been attributed to erosion of the subbase under the leave side (2); therefore, the possibility of pumping exists. When a stabilized subbase is used, it should be of high quality to resist erosion caused by rapid movement of free water under the pavement.

ECONOMIC CONSIDERATIONS FOR PAVEMENT DESIGN

The previous sections demonstrated that pavements with stabilized subbases, reinforced slabs, and load transfer devices at joints generally perform better than plain concrete pavements. However, the decision to use JRCP or JPCP is based on economic trade-offs. To make this decision, the designer must determine whether the benefits of using a more expensive pavement design are worth the extra expense. By using the concepts presented, we developed an approach for economic trade-off analysis of different designs.

For the three designs considered in the previous example, the expected wavelengths between faults would be [1/E(f)] × 1609 m, or 6.6, 12.6, and 21.5 m (21.5, 41.3, and 70.4 ft) for designs a, b, and c respectively. If the data in Figure 1 are used, the corresponding 99 percentile fault levels would be 0.51, 1.45, and 3.94 cm (0.20, 0.57, and 1.55 in) for a PSR level of 2.0 to 2.5. The average faulting for these designs may now be estimated from Figure 5. This figure was extrapolated, by use of engineering judgment, from the limited amount of data available on the standard deviation of faulting. The average faulting for designs a, b, and c is 0.25, 0.38, and 5.8 cm (0.1, 0.15, and 0.23 in) respectively.

These allowable average faults may be converted to allowable traffic by using Figure 6. The curve for pavements without dowel bars is based on data collected for Georgia pavements (7). The curve for plain concrete pavements with dowel bars was drawn by using the same shape and slope as were used in the Georgia data, but the curve passed through a point estimated from Michigan test road (10) data. The JRCP curve was estimated based on a conservative evaluation of the PCA joint study (2).

The allowable number of truck-semitrailer combinations for the designs is estimated at 11 000 for the plain concrete pavement without dowel bars, 45 000 for the plain concrete pavement with dowel bars, and 190 000

for JRCP. The ratio of allowable traffic for the designs may be used to estimate the cost efficiency of each design. For these designs the ratios are

1. JPCP/D:JPCP = 4.1,
2. JRCP/D:JPCP = 17.3, and
3. JRCP/D:JPCP/D = 4.7.

Figure 5. Determining average faulting from 99 percentile faulting.

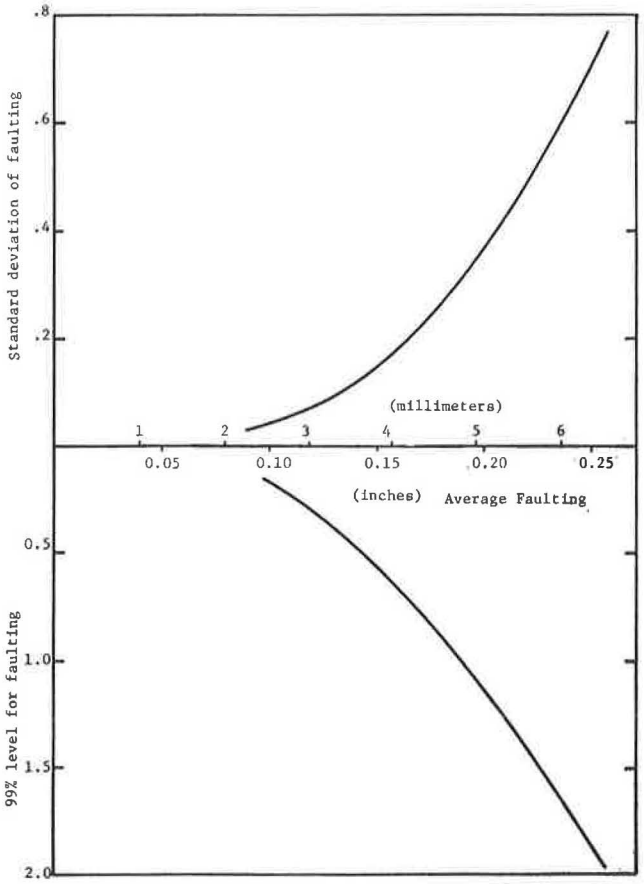

Figure 6. Faulting versus traffic for different load transfer at joints and cracks.

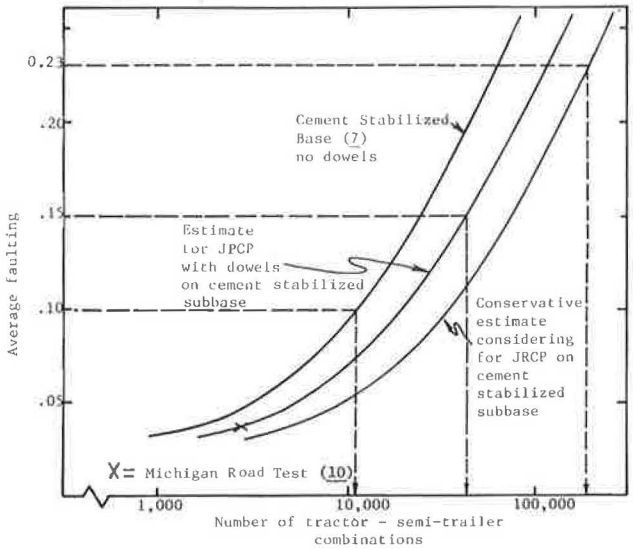

Interpretation of these results indicates that $4.10 could be spent for a plain concrete pavement with dowel bars for every $1.00 spent for plain concrete pavements without dowel bars without changing the cost of the pavement per vehicle served. This analysis is based on initial pavement cost only. If maintenance cost and salvage value were considered, the above ratios would probably be increased. This example was developed from the best available data, which are limited. New data are needed to verify or revise the figures in the paper before this technique can be used for practical pavement economic analysis.

SUMMARY

Research is needed for determining the interaction of design variables and pavement problem areas. Because of the problem of interactions, drawing definite conclusions from a comparison of the pavement studies and road tests is difficult, but several trends have been noted.

1. Dowel bars appear to be an effective means of limiting faulting.
2. Cracks and joints in JRCP tend to occur with the same frequency as do joints in JPCP; therefore, there are fewer faulting opportunities in JRCP.
3. There is a lower probability of faulting at a crack in JRCP than at a crack or unreinforced joint in JPCP.
4. Pavements with long slabs tend to be smoother than pavements with short slabs.
5. Faulting appears to decrease as subbase stiffness increases.
6. High-quality subbases are needed to resist erosion caused by pressurized free water under the pavement slab.

As the cost of pavement materials increases, it is becoming increasingly important for designers to use the most accurate methods available for designing pavements and to make cost comparisons of alternate pavement designs. Design methods used should be based on the best available theories and empirical data.

Analysis of pavement economics should consider not only the cost of the pavement, but also the benefits provided by the pavement. The pavement with the lowest initial cost is not always the most economical pavement.

REFERENCES

1. E. J. Barenberg, C. L. Bartholomew, and M. Herrin. Pavement Distress Identification and Repair. Construction Engineering Research Laboratory, Department of the Army, Champaign, Ill., Technical Rept. P-6, March 1973.
2. D. L. Spellman, J. R. Stoker, and B. F. Neal. California Pavement Faulting Study. Materials and Research Department, California Division of Highways, Sacramento, Research Rept. 635167-1, Jan. 1970.
3. M. P. Brokaw. Effect of Serviceability and Roughness at Transverse Joints on Performance and Design of Plain Concrete Pavement. HRB, Highway Research Record 471, 1973, pp. 91-98.
4. J. E. Bryden and R. G. Phillips. The Catskill-Cairo Experimental Rigid Pavement: A Five Year Progress Report. Engineering Research and Development Bureau, New York State Department of Transportation, Research Rept. 17, Nov. 1973.
5. The AASHO Road Test: Report 5—Pavement Research. HRB, Special Rept. 61E, 1962.
6. L. D. Childs. Jointed Concrete Pavements Reinforced With Welded Wire Fabric. Wire Reinforce-

ment Institute, Inc., McLean, Va., 1975.
7. W. Gulden. Pavement Faulting Study, Extent and Severity of Pavement Faulting in Georgia. Office of Materials and Testing, Georgia Department of Transportation, GHD Research Project 7104, interim rept., Aug. 1972.
8. R. S. Walker and W. R. Hudson. Use of Profile Wave Amplitude Estimates for Pavement Serviceability Measures. HRB, Highway Research Record 471, 1973, pp. 110-117.
9. C. De Young. Spacing of Undoweled Joints in Plain Concrete Pavements. HRB, Highway Research Record 112, 1966, pp. 46-54.
10. E. A. Finney and L. T. Oehler. Final Report on Design Project, Michigan Test Road. Proc., HRB, Vol. 38, 1959, pp. 241-285.
11. C. G. Ball and L. D. Childs. Tests of Joints for Concrete Pavements. Portland Cement Association, Skokie, Ill.
12. M. Evans, Jr., and W. B. Drake. 17-Year Report on the Owensboro-Hartford Cooperative Investigation of Joint Spacing in Concrete Pavements. Proc., HRB, Vol. 38, 1959, pp. 226-240.

Maintenance-Free Life of Heavily Trafficked Flexible Pavements

Michael I. Darter, Ernest J. Barenberg, and Jihad S. Sawan, Department of Civil Engineering, University of Illinois at Urbana-Champaign

Results obtained from a nationwide survey and analysis of the performance of 18 heavily trafficked flexible pavements are presented. The pavements surveyed are located in nine states, and interviews were held with highway engineers at each location. Results show that the major types of distress requiring maintenance for heavily trafficked flexible pavements are fatigue or alligator cracking, transverse cracking, longitudinal cracking, and rutting. The major causes are heavy traffic loadings, inadequate pavement structures, low temperature shrinkage of asphalt concrete, poor lane joint construction, aging of asphalt cement, and disintegration of cement-treated bases from deicing salts and freeze and thaw. The maintenance-free life of conventional flexible pavement depends on several factors including environmental region. For wet regions having significant freeze-thaw cycles, maintenance-free life ranges up to 10 years; for dry freeze-thaw regions, maintenance-free life ranges up to 15 years. In non-freeze-thaw wet or dry regions, maintenance-free life ranges up to 15 years. Several design recommendations are given that were found to improve the maintenance-free life of flexible pavements and whose use may be justified after the high maintenance and user delay costs of heavily trafficked highways are noted.

Many highways in urban and suburban areas are being subjected to high traffic volumes and weights, which cause rapid deterioration and premature failure of pavements. Therefore, considerable maintenance is required to keep the pavements serviceable, but scheduling of remedial and preventive maintenance is almost impossible without closing lanes and producing massive traffic jams, accidents, and delays to the traveling public. Often routine maintenance is completely neglected, thus causing even more accelerated deterioration of pavements.

The purpose of this paper is to determine the maximum maintenance-free life of conventional flexible pavements and to assess the types and causes of distress that require maintenance. This information is required for the eventual development of pavement design procedures to provide zero-maintenance pavements over much longer periods of time than currently exist. The development of design procedures for zero-maintenance pavements is currently under way at the University of Illinois through sponsorship of the Federal Highway Administration. More detailed data are available elsewhere (1). Zero maintenance, as used in this project, is defined as being related only to the structural adequacy of the pavement system. Activities such as mowing, striping, and providing skid resistance are not related to the pavement structure and, therefore, are outside the scope of this study.

The research approach to developing basic data and information from which the zero-maintenance design procedures will be developed relies heavily on information gained from extensive field visits, analytical analyses, and previous research studies.

FIELD SURVEY

A field survey was conducted of 18 heavily trafficked flexible highway pavements currently in service. Attempts were made to select projects in a variety of climatic regions so that the pavements could be evaluated over a variety of climatological conditions. The major climatic categories (wet, dry, freeze, nonfreeze) used in this evaluation are defined as follows:

1. A wet region is one in which the annual precipitation equals or exceeds the potential evapotranspiration of moisture (2) or one in which annual precipitation exceeds 76.2 cm (30 in);
2. A dry region is the opposite of a wet region;
3. A freeze region is one in which significant freezing temperatures result in pavement frost heave or frost damage. Regions that have a freezing index of 100-deg days or greater are categorized as freeze areas; and
4. A nonfreeze region is one that has a freezing index of less than 100 deg.

A project was selected in a given region by using the following guidelines:

1. Age. Longevity was the most important factor, which severely limited the number of available projects. In general, only projects with a service life of greater than 10 years were selected for this study.

Publication of this paper sponsored by Committee on Flexible Pavement Design.

Table 1. Summary of information for Flex projects included in field survey.

Project Number	Location	Route	Date Opened	ADT Average Over Life	ADT 1974	Lanes	8.16-Mg ESAL Applications[a]	Pavement Section Material: Surface	Base	Subbase	Subbase	Subgrade	Maintenance Performed
Flex 1	Manchester, N.H.	I-93	1960	19 800	35 200	4	7.26	7.62-cm AC	6.35-cm AC	30.48-cm GRB	30.48-cm GRB	—	CF
Flex 2	New Jersey	N.J. Turnpike	1951	21 600	32 800	4	12.42	11.43-cm AC	19.05-cm MAC	16.51-cm GRB	13.97-cm SM	30.48-cm SM and S	P and SH
Flex 3	West St. Paul, Minn.	Minn-55, TS 21	1961	9 500	15 600	4	2.01	10.16-cm AC	15.24-cm GRB	31.75-cm GRB	—	A-6 CL	CF and P
Flex 4	West St. Paul, Minn.	Minn-55, TS 22	1961	9 500	15 600	4	1.91	10.16-cm AC	7.62-cm ATB	15.24-cm GRB	40.62-cm GRB	A-4 CL	CF
Flex 5	North St. Paul, Minn.	Minn-36, TS 23	1961	8 000	12 100	4	1.69	13.97-cm AC	3.81-cm ATB	22.86-cm GRB	30.48-cm GRB	A-2-4 SL	CF
Flex 6	South St. Paul, Minn.	Minn-101 TS 109	1966	10 200	14 100	4	5.21	3.81-cm AC	12.70-cm ATB	7.62-cm BTS	—	A-3	CF
Flex 7	Ottawa, Ill.	I-80	1962	11 000	18 900	4	4.70	11.43-cm AC	21.59-cm GRB	58.42-cm GRB	—	A-6	P
Flex 8	Ottawa, Ill.	I-80	1962	11 100	18 900	4	4.82	11.43-cm AC	20.32-cm ATB	10.16-cm GRB	—	A-6	None
Flex 9	Ottawa, Ill.	I-80	1962	11 000	18 900	4	4.72	11.43-cm AC	25.40-cm ATB	10.16-cm GRB	—	A-6	None
Flex 10	Ottawa, Ill.	I-80	1962	11 100	18 900	4	5.59	11.43-cm AC	30.48-cm CTB	10.16-cm GRB	—	A-6	P
Flex 11	Seattle, Wash.	I-90	1960	10 400	13 400	4	1.66	17.78-cm AC	7.62-cm GRB	45.72-cm GRB	—	LST, S and C	None
Flex 12	South San Francisco, Calif.	US-101	1955	21 250	28 000	4	8.81	12.7-cm AC	20.32-cm CTB	20.32-cm GRB	—	—	P and CF
Flex 13	San Francisco, Calif.	Calif-4	1965	19 000	28 000	4	2.27	17.78-cm AC	20.32-cm GRB	38.1-cm GRB	—	—	None
Flex 14	Los Angeles, Calif.	I-405	1965	69 000	138 500	4	3.70	17.78-cm AC	20.32-cm CTB	25.40-cm GRB	—	—	None
Flex 15	Salt Lake City, Utah	I-80	1966	21 000	19 125	4	2.75	11.43-cm AC	12.7-cm CTB	10.16-cm GRB	—	—	None
Flex 16	Phoenix, Ariz.	I-17	1964	11 100	17 000	4	4.27	7.62-cm AC	15.24-cm GRB	25.40-cm SM	—	—	CF and P
Flex 17	Atlanta, Ga.	Ga-78	1951	14 200	11 000	4	4.02	27.94-cm AC	25.40-cm GRB	—	—	C	None
Flex 18	Atlanta, Ga.	Ga-78	1968	14 000	20 000	4	2.38	8.89-cm AC	22.86-cm CTB	19.05-cm GRB	—	C	None

Notes: 1 Mg = 2.205 kips, 1 cm = 0.394 in.
AC = asphalt concrete; ATB = asphalt-treated base; BTS = bitumen-treated sand; C = clay; CF = crack filling; CL = clayey loam; CTB = cement-treated base; GRB = granular base or subbase; LST = laminated silt; MAC = asphalt penetration macadam; P = patching with AC; S = sand; SH = shoulder repair or replacement; SL = sandy loam; SM = select material.
[a]Most heavily traveled lane, one direction.

Table 2. Summary by type of distress and maintenance found on heavily trafficked flexible pavements.

Type of Distress	Projects[a]: Distressed/ Total	Maintained/ Distressed
Longitudinal cracking (lane joint in nearly all cases)	11/18	5/11
Transverse cracking (including reflective cracking)	10/18	7/10
Alligator or fatigue cracking	9/18	5/9
Polished aggregate	8/18	0/8
Rutting	6/18	1/6
Weathering asphalt	4/18	0/4
Depressions	3/18	0/3
Raveling	1/18	0/1

[a]Only the distress rated as moderate to severe as defined by Darter and Barenberg (1) is considered in this tabulation.

2. Maintenance. Only projects that have not been overlayed or seal-coated were selected. Past routine maintenance was not a consideration, and two categories of pavements were selected—those that were maintenance-free and those that received routine maintenance.

3. Traffic. Only pavements that have relatively high traffic volume were considered in the selection. Most of the projects selected were high-volume urban and rural freeways.

The individual projects included in the field survey are denoted Flex 1 through Flex 18. A detailed summary of important data for each project is given in Table 1. The 18 flexible pavements included in the field survey are located in nine states with widely ranging environmental conditions. All the projects have moderate to high traffic volumes; two-directional average daily traffic (ADT) ranged generally from 14 000 to 35 000 (one project, however, had 138 500). The accumulated 8.16-Mg (18-kip) equivalent standard axle load (ESAL) applications in the most heavily traveled lane range up to 12 million. The projects varied in age from 7 to 24 years (the mean was 14 years), and 9 of the 18 projects surveyed showed maintenance-free performance. In addition to the specific projects given in Table 1, other pavements in the various regions visited were also observed, and the general performance characteristics of flexible pavements in the region were discussed with local engineers.

TYPES AND CAUSES OF DISTRESS

Types of Distress

The types and severity of distress occurring on 18 heavily trafficked flexible pavements were determined during the field visits. A summary of types of distress found (rated moderate to severe) and maintenance applied to each flexible pavement is given in Table 2. The distress occurrence data are expressed as the ratio of the number of projects exhibiting a particular distress to the total number of projects surveyed. The maintenance applied to each type of distress is expressed as the ratio of the number of projects having the particular distress that was actually maintained to the total number of projects exhibiting the distress.

Based on data from the field survey and other research studies, including the American Association of State Highway Officials (AASHO) (now the American Association of State Highway and Transportation Officials) Road Test (3), the major types of distress occurring in heavily trafficked flexible pavements that require or receive maintenance and their level of severity are

1. Alligator or fatigue cracking. This type of distress occurs mainly in the wheel path with class 2 and 3 severity levels.
2. Transverse cracking. This type of distress occurs transversely to the longitudinal axis of the roadway and includes low-temperature as well as reflective cracking (resulting from a cement-treated base, for example) with spacing of approximately 3.05 to 9.14 m (10 to 30 ft) and possible spalling.
3. Longitudinal cracking. This type of distress almost always occurs at the lane construction joint and often occurs over more than 25 percent of the length of a project and is spalled.
4. Rutting. This type of distress occurs in the wheel paths and is normally greater than 1.27 cm (½ in) in depth to require maintenance.

Besides four major distresses previously identified on the projects surveyed, there are other types of distress that occur in varying amounts and degrees depending on construction, foundation soil, materials, environment, and the like. These types of distress include surface deterioration (aggregate polishing, bleeding, weathering and studded tire wear), swelling or heaving foundations (4), shoulder distress, depressions, and asphalt stripping (5).

Causes of Major Types of Distress

Based upon field observations and analytical studies, the causes of each of the major types of distress previously listed are given in this section.

Alligator or Fatigue Cracking

The major cause of alligator cracking is repeated traffic loading, which includes tensile stresses and strains in the bottom of the asphalt concrete surface layer if the pavement has a granular base or at the bottom of the base layer if the base course is stabilized by cement, asphalt, or lime and fly ash. If these tensile stresses and strains are of sufficient magnitude and have a sufficient number of applications, fractures will occur at the bottom of the layer and will progress upward with repeated load applications until they eventually reach the surface (6). Eight of the flexible pavements included in the field study showed moderate to severe alligator cracking. Of these eight, four had cement-treated bases and four had granular bases.

For several of the flexible pavements surveyed, an analysis was made by using elastic layered theory and Miner's fatigue damage expression (19) for the purpose of illustrating the cause of alligator cracking by predicting fatigue damage distress. Three assumptions were made in the analysis.

1. The resilient modulus and Poisson's ratio either were determined for each pavement layer and for the subgrade from laboratory tests or were estimated from the results of studies by others such as Robnett and Thompson (7), Southgate and Deen (8), and Monismith and Finn (9). Resilient modulus values for granular and fine-grained soils are stress dependent; therefore, values were selected that closely correspond to the range of expected bulk and deviator stresses in the pavements. The stiffness of asphalt concrete was determined by using the stiffness and temperature data given by Southgate and Deen (8) and was selected as a constant value for given projects corresponding to the mean annual temperature for each region.
2. The traffic loading used in the fatigue analysis is the accumulated 8.16-Mg (18-kip) ESAL applications estimated for the most heavily traveled lane of each project from the time it was opened to traffic through 1974.
3. Fatigue curves of initial tensile strain versus load applications developed by Edwards and Valkering (10) by using the controlled stress mode of testing were used for asphalt concrete. A fatigue curve of strain versus load applications for cement-treated bases (9) was used.

Calculations for three projects (Flex 7, Flex 8, and Flex 18) are discussed to illustrate the analysis. The critical radial tensile strains and stresses were computed under 4.08-Mg (9-kip) wheel load by using the linear elastic layered computer program. These values are given in Table 3 for each project. Fatigue damage was computed by using a 4086-kg (9000-lb) wheel load and the actual estimated 8.16-Mg (18-kip) ESAL applications accumulated over the life of the pavement.

Analysis for Flex 7 shows relatively large radial tensile stresses and strains (1.54×10^{-4} cm/cm) at the bottom of the asphalt concrete surface. By using the fatigue curves for asphalt concrete (constant stress mode), one determines that the number of 4086-kg (9000-pound) wheel load applications to failure is approximately 800 000. The actual estimated 8.16-Mg (18-kip) equivalent single axle load applications were 4.7 million. Hence the analysis indicates a fatigue failure. Actually, Flex 7 has extensive alligator (fatigue) cracking and is currently being overlayed.

Flex 8 is a pavement section adjacent to Flex 7 on I-80 in Illinois but has an asphalt treated base. The maximum computed tensile strain at the bottom of the asphalt-treated base is 7.04×10^{-5} cm/cm, which gives an allowable number of 4086-kg (9000-pound) wheel applications of approximately 13 million compared with 4.82 million equivalent loads actually applied. There is, as expected, no observable fatigue cracking on the surface of this pavement.

Flex 18 had a cement-treated base that showed serious fatigue failure in the field. Computed strains in the cement-treated base confirm the likelihood of this type of distress.

Similar calculations were made for 15 of the 18 flexible pavements surveyed, and the resulting data are given in Table 3. Analysis of the eight projects that have cracking indicated that excessive stresses and strains were present, and the cumulative fatigue damage for each was calculated to be greater than 1.0. In theory, these projects are expected to show fatigue distress, and such distress is apparent in these pavements. The seven projects not showing fatigue damage had cumulative fatigue damage ratios of less than 1.0. Hence the analysis appears to be reasonable (even under the assumptions made) because fatigue or alligator cracking occurred on all projects where analysis indicated potential fatigue. Conversely, for those projects where theoretical analysis did not indicate fatigue distress, such distress was nonexistent.

The cause of fatigue distress can be assumed to be one or more of the following:

1. Inadequate structural thicknesses or support for the stabilized layers to keep the tensile stresses and strains within allowable limits or both;
2. Loss of support of various layers of the pavement and subgrade as a result of excessive moisture, shear failure, and the like, which caused high tensile strains under traffic load in the stabilized layers.
3. Gradual hardening or aging of the asphalt concrete (AC) surface with time resulting in decreased fatigue life of the AC.

A general observation from the field survey is that

Table 3. Summary of fatigue analysis of 15 flexible pavements in field survey.

Project Number	Critical Layer	Critical Stress (kPa)	Critical Strain (cm/cm × 10^{-4})	n or Million Actual 8.16-Mg ESALs	N or Million Allowable 8.16-Mg ESALs[a]	$D = \sum \frac{n}{N}$	Alligator Cracking
Flex 2	APM	455	0.44	12.42	100.00	0.12	No
Flex 3	AC	1696	1.97	2.01	0.31	6.48	Yes
Flex 4	AC	993	0.52	1.91	60.00	0.03	No
Flex 7	AC	1717	1.54	4.70	0.80	5.83	Yes
Flex 8	ATB	476	0.70	4.82	13.00	0.37	No
Flex 9	ATB	372	0.55	4.72	45.00	0.10	No
Flex 10	CTB	331	0.36	5.59	10.27	0.54	—[b]
Flex 11	AC	765	0.70	1.66	13.00	0.13	No
Flex 12	CTB	572	0.50	8.81	1.66	5.31	Yes
Flex 13	AC	862	1.60	2.27	1.00	2.27	Yes
Flex 14	CTB	455	0.40	3.70	6.20	0.60	No
Flex 15	CTB	572	1.20	2.75	0.01	>100.00	Yes
Flex 16	AC	1593	3.00	4.27	0.06	71.20	Yes
Flex 17	AC	483	0.88	4.02	8.00	0.50	No
Flex 18	CTB	483	0.99	2.38	0.17	14.00	Yes

Notes: 1 kPa = 0.145 lbf/in^2, 1 Mg = 2.205 kips, 1 cm = 0.394 in.
AC = asphalt concrete; APM = asphalt penetration macadam base; ATB = asphalt-treated base; CTB = cement-treated base.
[a] According to fatigue considerations.
[b] Severe durability distintegration occurred in this CTB, and ascertaining the cause of distress is difficult.

Table 4. Rut depth data from five projects subjected to same traffic, environment, and subgrade.

Project Number	Pavement Composition			Mean Rut Depth (cm)
	Surface	Base	Subbase	
Flex 7	11.43-cm AC	21.59-cm CS	58.42-cm G	1.68
Flex 8	11.43-cm AC	20.32-cm ATB	10.16-cm G	1.30
Flex 9	11.43-cm AC	25.40-cm ATB	10.16-cm G	1.02
Flex 10	11.43-cm AC	30.48-cm CTB	10.16-cm G	0.96
Comp 5	7.62-cm AC	20.32-cm PCC	15.24-cm G	0.86

Notes: 1 cm = 0.394 in.
AC = asphalt concrete; ATB = asphalt-treated base; CS = crushed stone; CTB = cement-treated base; G = gravel; and PCC = portland cement concrete.

fatigue distress seems to be more prevalent in warmer climates. Let us consider Flex 4 located in Minnesota and Flex 13 located in California. The pavement structures of these two pavements are roughly equal; both have a 17.78-cm (7-in) asphalt-bound upper layer over granular subbase. The applied 8.16-Mg (18-kip) ESAL applications are roughly equal as are their ages (Flex 4 is 13 years old and Flex 13 is 9 years old). Flex 4 shows no signs of load-associated fatigue cracking (but does have temperature transverse cracking) although Flex 13 shows moderate fatigue cracking. The computed fatigue damage indicates fatigue distress for Flex 13 (D = 2.27) and no fatigue distress for Flex 4 (D = 0.03). Thus the computations support the observed distress. The reason for the large shift in the fatigue damage of nearly equal pavements is the reduced E value of the asphalt concrete for the Flex 13 pavement due to a higher average temperature, which results in higher strains and a significantly lower allowable number of loads to failure.

Nonreflective Transverse Cracking

Nonreflective transverse cracking is associated with low temperature shrinkage and occurs most frequently in the northern freeze areas of the United States where crack spacings of 3.05 to 45.72 m (10 to 150 ft) are typical. The areas visited that had this type of distress are New Hampshire (severe), Minnesota (severe), Illinois (major), Michigan (severe), New Jersey (moderate), and Ontario (severe). This distress was not observed (or was observed in minor amounts only) in the areas visited in central and southern Texas, western Washington, western California, southern Arizona, and Georgia.

Although most researchers have attributed the transverse cracking distress to the occurrence of very low temperatures, Shahin and McCullough (11) concluded that transverse cracking can be attributed to both low temperature cracking and thermal fatigue. Thermal fatigue has been shown to occur for AC in the laboratory by thermally cycling restrained beams (12, 13). A considerable amount of research has been performed to determine the causes and cures for this type of distress because it is probably the most predominant type of distress in northern regions of the United States. From the field survey, 6 out of 10 projects located in freeze areas showed transverse cracking as the most severe distress occurrence.

Reflective Transverse Cracking

Five projects containing cement-treated bases are included in the field survey. All projects except one (Flex 15) showed extensive reflective transverse cracking. The cause was definitely attributed to reflective cracking because other flexible pavements in the respective areas did not exhibit transverse cracking. Crack spacing in these sections varies as follows (1 m = 3.28 ft):

Project Number	Spacing (m)
Flex 10	6.1
Flex 12	4.6
Flex 14	15.2
Flex 18	4.6

The probable cause of this type of distress is shrinkage, which in the cement-treated base course cracks and reflects upward through the surface layer. This is a relatively serious distress that has caused maintenance to be performed in several of the projects surveyed. One project in particular (Flex 10), located in a wet freeze-thaw area, was subjected to heavy applications of deicing salts [about 5.64 Mg/lane/km/year (10 tons/lane/mile/year)] and freeze-thaw cycles (approximately 12/year). On this project, the cement-treated base disintegrated at most transverse cracks, which resulted in a depression of the AC surface and serious alligator cracking and spalling of the surface cracks.

Longitudinal Cracking

Longitudinal cracking, which existed on 61 percent of the projects surveyed, almost always occurred at the lane construction joint near the lane paint-strip marking. The basic cause in most cases is attributed to poor joint construction practices.

Rutting

Rutting occurred on 33 percent of the projects surveyed to a moderate to severe level (0.6 to 1.9+ cm) (¼ to ¾+ in). Rutting was severe [>1.9 cm (>¾ in)] on only one

project (Flex 2), where some patching had been performed in the wheel path, and major (1.3 to 1.9+ cm) (½ to ¾+ in) in two projects. Rutting is associated with traffic load and occurs when any of the pavement layers permanently deform under load. Most of the rutting observed at the AASHO Road Test was attributed to changes of thickness of the pavement layers.

The changes in thickness of the pavement layers were concluded to be due primarily to lateral movement of the materials but sometimes to increased density (consolidation). Five projects included in the field study were subjected to the same traffic on I-80 in Illinois. Rut depth data from these pavements are given in Table 4. Flex 7 with crushed stone base has the most rutting, and Comp 5 (a composite pavement) with a portland cement concrete base has the least rutting. These projects are 12 years old and have carried approximately 5 million ESAL applications. A considerable amount of the rutting in Flex 7 appears to have occurred in the crushed stone base or the gravel subbase. Also, by comparing Flex 8 and Flex 9 with Flex 10, one can conclude that some rutting has occurred in the asphalt-treated bases. The rutting of Comp 5 also indicates that a significant amount of rutting is occurring in the AC surface.

MAINTENANCE-FREE LIFE OF CONVENTIONAL FLEXIBLE PAVEMENTS

Conventional flexible pavements are defined according to typical past and current design and construction practice. Pavement compositions vary widely, but typical ranges are as follows: asphalt concrete surface of 7.62 to 15.24 cm (3 to 6 in), a nonstabilized or stabilized granular base of 20.32 to 30.48 cm (8 to 12 in), and a granular subbase ranging from 10.16 to 50.8 cm (4 to 20 in).

Field Performance

Results from the field survey of 18 flexible pavement projects showed 9 with maintenance-free performance. These 9 pavements ranged in age from 8 to 23 years with an average traffic loading of 0.34 million 8.16-Mg (18-kip) ESALs/year in the most heavily traveled lane. Traffic loadings ranged from 0.40 to 0.54 million 8.16-Mg (18-kip) ESALs/year for flexible pavements having average daily traffic ranging from 30 000 to 138 500.

A summary of project data from the field survey grouped by environmental region is given in Table 5. The summary includes the maintenance-free life, major distresses requiring maintenance, and maintenance performed. The following maximum maintenance-free lives are summarized from these data from each environmental region for the actual traffic loading applied:

Environment	Maintenance-Free Life (years)
Wet and freeze	5 to 23+
Wet and nonfreeze	7 to 23+
Dry and freeze	9
Dry and nonfreeze	10 to 11+

Factors Affecting Maintenance-Free Life

The major factors that affect the maintenance-free life of flexible pavements include traffic, environment, materials, construction, and variability. These factors are only briefly discussed in this section to summarize their effect on maintenance-free life.

Traffic

The effect of repeated traffic loadings on maintenance-free life is particularly important for the heavily trafficked flexible pavements. Structural deterioration under repeated loads is, in most cases, the primary factor that limits the life of conventional flexible pavement. Pavement structural distress under repeated traffic loadings is in the form of fatigue (alligator) cracking or permanent deformation of the pavement layers or both. The fatigue analysis presented previously for flexible pavements illustrates the significant effect that traffic loadings have on distress frequency and subsequent maintenance requirements. A plot of accumulated fatigue damage, D, as summarized in Table 3, is shown versus the cracking index for each pavement in Figure 1. Cracking index here includes class 1, 2, and 3 alligator or fatigue cracking. As fatigue damage becomes greater than approximately 0.6, the various projects exhibit a greater incidence of fatigue cracking. Another interesting aspect of this plot is that all projects having accumulated fatigue damage greater than 0.6 have either received maintenance for fatigue cracking or were in need of immediate maintenance at the time of the survey. All projects having fatigue damage of less than the 0.6 (except one) were maintenance free insofar as fatigue distress was concerned. These results illustrate the importance of traffic loading on the maintenance-free life of flexible pavements.

Environment

Several environmental factors affect the maintenance-free life of flexible pavements including freeze and thaw, low temperature shrinkage, cyclic thermal fatigue, excess moisture, and swelling soils. In certain regions of the United States, these environmental factors become the dominant factors in affecting maintenance-free life of flexible pavements. For example, the low temperature cracking of asphalt concrete surfaces is of particular significance in freeze regions in reducing maintenance-free life to less than 5 years, and the swelling soils in portions of Texas and other states limit the maintenance-free life to generally less than 10 years.

Materials

Several material properties affect the maintenance-free life of flexible pavements including factors such as asphalt aging (or hardening and brittleness), asphalt stripping, degradation of aggregates, freeze and thaw, and durability with use of deicing salt of cement-stabilized aggregates. In specific environmental regions and certain localized areas, these factors will control the maintenance-free life of flexible pavements. The factor having the greatest overall affect is asphalt aging. This phenomenon will reduce fatigue life and increase low temperature cracking development in freeze regions. The effect of asphalt aging in reducing the maintenance-free life of a flexible pavement varies depending on type of asphalt, film thickness, voids, climate, and the like. The disintegration of cement-treated aggregate bases in freeze regions due to freeze and thaw and particularly to use of deicing salts is believed to seriously limit maintenance-free life in these regions to less than 10 years (for Flex 10 pavements).

Construction

The major errors or deficiencies that occur during construction and affect maintenance-free life are factors such as built-in roughness of the surface, lack of ma-

terial quality control, inadequate thicknesses of layers, inadequate compaction, and poor construction of the lane paving joint. These have significant effect and greatly reduce the maintenance-free life of flexible pavement. For example, longitudinal joint cracking occurred on more than half of the projects surveyed on multilane pavements. This, by itself, could reduce maintenance-free life to less than 5 years on an otherwise maintenance-free pavement.

Variability

There are many variations and uncertainties associated with load, materials, and climate that can cause local-

Table 5. Maintenance-free life of flexible pavements.

Project Number	Environment	Annual Maintenance-Free Life of Project (years)	Average Million 8.16-Mg ESALs per Year	Distress That Required Maintenance	Maintenance Received
Flex 1	Wet and freeze	5 to 15+[a]	0.52	TC, LC	CF
Flex 3		5 to 10	0.15	TC, ALC, LC	P, CF
Flex 4		5 to 14+	0.15	TC, LC	CF
Flex 5		5 to 14+	0.13	TC	CF
Flex 6		5 to 9+	0.65	TC	CF
Flex 7		5	0.39	ALC	P
Flex 8		13	0.40		
Flex 9		13+	0.39		
Flex 10		8	0.47	TC, ALC	P
Flex 2		23	0.54		P[b]
Flex 11	Wet	15+	0.12		
Flex 17		23+	0.17		
Flex 18		7	0.40	ALC	—[c]
Flex 15	Dry and freeze	9	0.34	ALC	—[c]
Flex 12	Dry	10	0.46	ALC	P, CF
Flex 13		10+	0.25		
Flex 14		10+	0.41		
Flex 16		11	0.43	ALC	P, CF

Notes: 1 Mg = 2,205 kips.
ALC = alligator cracking; CF = crack filling; LC = longitudinal cracking; P = patching; R = rutting; TC = transverse cracking.
[a] Lower value is maximum zero-maintenance life of project due to transverse crack filling.
[b] Received minor amount of maintenance.
[c] Needs immediate maintenance.

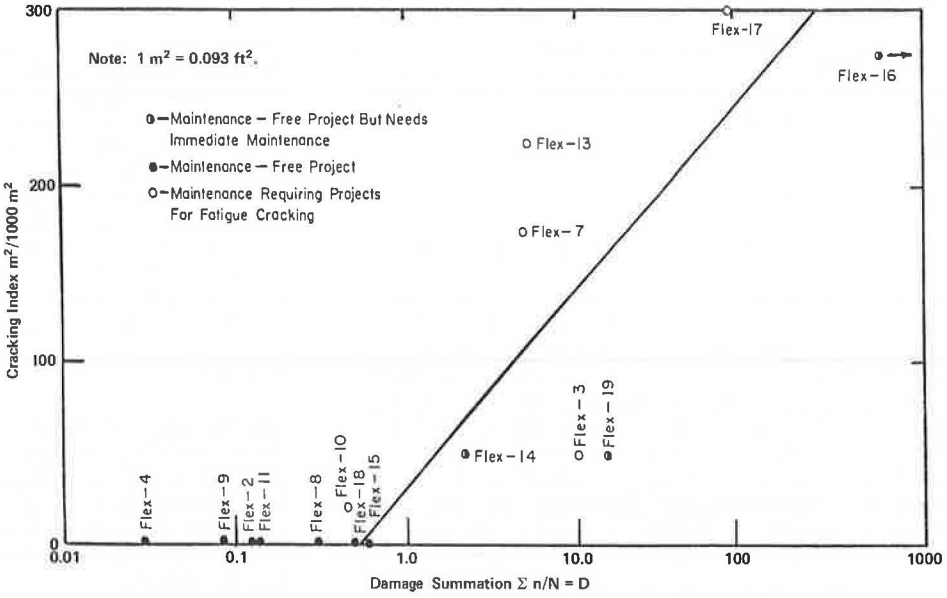

Figure 1. Accumulated fatigue damage versus cracking index for flexible pavements included in field survey.

Table 6. Estimated maximum maintenance-free life of flexible pavements in years.

Environment	Crushed Stone Base			Asphalt-Treated Base			Cement-Treated Base		
	Actual[a]	Computed[b]	Determined by Experience[c]	Actual[a]	Computed[b]	Determined by Experience[c]	Actual[a]	Computed[b]	Determined by Experience[c]
Wet and freeze (regional factor = 1.0)	<5 for Flex 1 <5 for Flex 7	1	<5	7+ for Flex 8 7+ for Flex 9 <5 for Flex 6 18 for Flex 2	14	5 to 15	<5 for Flex 10	4	<5
Wet (regional factor = 0.7)		3	<5	2+ for Flex 11 6+ for Flex 17	20	10 to 15	<4 for Flex 18	6	5 to 10
Dry and freeze (regional factor = 0.9)		1	<5		16	5 to 15	3 for Flex 15	4	<10
Dry (regional factor = 0.5)	3+ for Flex 13 <4 for Flex 16	3	5 to 10		27	10 to 15	<8 for Flex 12 5+ for Flex 14	7	5 to 10

Notes: Layer thicknesses are 12.7 cm (5 in) of AC surface; 25.4 cm (10 in) of base material (either crushed stone, asphalt-treated base, or cement-treated base); and 25.4 cm (10 in) of gravel-sand subbase. Subgrade is similar to that at the AASHO Road Test (AASHO classification = A-6, unified classification = CL, and California bearing ratio = 2 to 4).
[a] Actual project maintenance-free life at 0.7 million 8.16-Mg (18-kip) ESALs/year for those projects where actual traffic is less than 0.7 million/year.
[b] Computed life to serviceability index of 3.5 from AASHO equation C-12 (18).
[c] By field surveys.

ized distress requiring maintenance. These have been identified and analyzed by several researchers (14, 15, 16, 17). These variations include those occurring along a pavement (internal strength, resiliency, durability) and differences between parameter values assumed in design (load, strength, and the like) and those attained "as constructed." These variations can reduce maintenance-free life significantly by causing localized failures.

Expected Maintenance-Free Life

The expected life of conventional flexible pavement was estimated by

1. Use of best available predictive models,
2. Actual project life based on data from the field survey, and
3. Estimate of project staff based on general performance found in the various climatic regions.

The predictive model derived from the results of the AASHO Road Test and included in the AASHO Interim Guide as equation C-12 (18) is used to estimate maintenance-free life of flexible pavement by using the serviceability performance approach. A limiting serviceability value of 3.5 for zero-maintenance conditions is used as recommended elsewhere (1). If this criterion is used along with the AASHO predictive equation, the maintenance-free life may be roughly estimated for certain pavement designs including crushed stone base, asphalt-treated base, and cement-treated base that are located in different environmental regions.

A summary of estimations of the maintenance-free life of various designs is given in Table 6. Two conclusions related to the life estimates given in Table 6 can be drawn.

1. The three sets of estimates in each cell are generally in agreement with each other. For example, consider a flexible pavement with a cement-treated base located in a dry, nonfreeze region. Two projects (Flex 13 and Flex 15) are located in this region with approximately the same structure and provide estimates of actual life of <8 and >5 years respectively. The computed life is 7 years, and the life estimated by the project staff is 5 to 10 years. The relatively short life estimated for the crushed stone and cement-treated bases compares well to the performance of sections of similar composition at the AASHO Road Test. For example, AASHO Road Test section 333 had 15.24 cm (6 in) of AC surface, 2286 cm (9 in) of crushed stone base, and 40.64 cm (16 in) of gravel-sand subbase and lasted only 2 900 000 8.16-Mg (18-kip) ESALs to a serviceability of 3.5. Hence its maintenance-free life would be approximately 4 to 5 years as a major freeway pavement, which is comparable to the estimates given in Table 6.
2. The expected maximum maintenance-free life of conventional flexible pavements located in the four environmental regions is as follows for asphalt-treated base, which provided the best performance:

Environment	Expected Maintenance-Free Life (years)
Wet and freeze	5 to 15
Wet and nonfreeze	10 to 15
Dry and freeze	5 to 15
Dry and nonfreeze	10 to 15

The shorter life of 5 years as indicated for flexible pavements located in freeze regions is due to expected low temperature cracking of the AC surface.

CONCLUSIONS

The conventional design for flexible pavement that has shown the longest maintenance-free life under heavy traffic includes an asphalt concrete surface course of 10.16 to 12.70 cm (4 to 5 in) thickness, an asphalt stabilized base course of 20.32 to 25.40 cm (8 to 10 in) in thickness and a granular subbase. This design, if properly constructed, should provide maintenance-free life ranging from 5 to 15 years in cold regions, and 10 to 15 years in warm regions under heavy traffic [0.7 million 8.16-Mg (18-kip) ESALs/year].

Observations from the field survey and information gained during the interviews indicate several design modifications that would significantly increase the maintenance-free life for flexible pavements.

1. Thickness of the stabilized layers of the pavement structure should be significantly increased to reduce potential fatigue damage.
2. Mix design should be done with the specific environmental region in mind. In the wet and freeze and dry and freeze regions, greater attention should be given to the low temperature ductility of the mix to minimize the cold weather cracking of the AC surface. At the same time, the stability of the AC surface material and the asphalt-treated base must be maintained at a high level to minimize the rutting distress.
3. Only asphalt cement having a low susceptibility to hardening should be used.
4. Construction procedures must be reviewed and modified to eliminate the longitudinal cracking along the lane construction joints. Longitudinal cracking along these cold joints is a potential cause for premature maintenance of flexible pavements.
5. Realistic drainage criteria to minimize the spring damage must be developed and applied.

ACKNOWLEDGMENTS

This study was conducted at the Transportation Research Laboratory of the Department of Civil Engineering, University of Illinois at Urbana-Champaign. The project is sponsored by the Federal Highway Administration.

Much appreciation is extended to Monte Symons, Myra Radoyevich, Huey Shin Yuan, and Paul McNabb for their assistance in conducting this study.

Thanks are also extended to Carol Ewing for typing the manuscript.

REFERENCES

1. M. I. Darter and E. J. Barenberg. Zero-Maintenance Pavement: Results of Field Studies on the Performance Requirements and Capabilities of Conventional Pavement Systems. Univ. of Illinois, interim rept., 1976.
2. R. G. Van Schooneveld. Combined Average Annual Precipitation and Evaporation Map for the United States. Federal Highway Administration, Sept. 1974.
3. The AASHO Road Test: Report 5—Pavement Research. HRB, Special Rept. 61E, 1962.
4. Flexible Pavement Designer's Manual—Part 1. Highway Design Division, Texas Highway Department, Austin, 1972.
5. H. J. Fromm. The Mechanisms of Asphalt Stripping From Aggregate Surfaces. Ontario Ministry of

Transportation and Communications, Canada, Research Rept. 190, 1974.
6. E. Zube and J. Skog. Final Report on the Zaca-Wigmore Asphalt Test Road. Proc., AAPT, Vol. 38, 1969.
7. Q. R. Robnett and M. R. Thompson. Resilient Properties of Subgrade Soils. Univ. of Illinois, Transportation Engineering Series, No. 5, 1973.
8. H. F. Southgate and R. C. Deen. Temperature Distribution Within Asphalt Pavements and Its Relationship to Pavement Deflection. HRB, Highway Research Record 291, 1969, pp. 116-131.
9. C. H. Monismith and F. Finn. Flexible Pavement Design: A State-of-the-Art—1975. ASCE Specialty Conference on Pavement Design for Practicing Engineers, Atlanta, June 1 to 3, 1975.
10. J. M. Edwards and C. P. Valkering. Structural Design of Asphalt Pavements for Heavy Aircraft. Shell International Petroleum Co., Ltd., London, 1970.
11. M. Y. Shahin and B. F. McCullough. Prediction of Low-Temperature and Thermal-Fatigue Cracking in Flexible Pavements. Texas Highway Department, Research Rept. 123-14, 1972.
12. C. M. Jones, M. I. Darter, and G. Littlefield. Thermal-Expansion-Contraction of Asphaltic Concrete. Proc., AAPT, Vol. 37, 1968, pp. 56-102.
13. G. M. Tuckett, G. M. Jones, and G. Littlefield. The Effects of Mixture Variables on Thermally Induced Stresses in Asphalt Concrete. Proc., AAPT, Vol. 39, 1970, pp. 705-744.
14. M. I. Darter and W. R. Hudson. Probabilistic Design Concepts Applied to Flexible Pavement Design System. Texas Highway Department, Austin, Research Rept. 123-18; Texas Transportation Institute, Texas A&M Univ., College Station; and Center for Highway Research, Univ. of Texas at Austin, May 1973.
15. M. I. Darter, W. R. Hudson, and J. L. Brown. Statistical Variation of Flexible Pavement Properties and Their Consideration in Design. Annual Meeting, AAPT, Houston, Feb. 1973.
16. M. I. Darter, B. F. McCullough, and J. L. Brown. Reliability Concepts Applied to the Texas Flexible Pavement System. HRB, Highway Research Record 407, 1972, pp. 146-161.
17. G. B. Sherman. In Situ Materials Variability. In Structural Design of Asphalt Concrete Pavement Systems, HRB, Special Rept. 126, 1971, pp. 180-190.
18. AASHO Interim Guide for Design of Pavement Structures. AASHO, Washington, D.C., 1972.
19. M. A. Miner. Cumulative Damage in Fatigue. Journal of Applied Mechanics, Vol. 4; ASME, Vol. 12, 1945, pp. A159-A164.

Mechanistic Structural Subsystems for Asphalt Concrete Pavement Design and Management

F. N. Finn, Woodward-Clyde Consultants, San Francisco
W. J. Kenis, Federal Highway Administration
H. A. Smith, National Cooperative Highway Research Program, Transportation Research Board

Pavements are extremely complex physical systems involving the interaction of numerous variables. Their performance is influenced by factors such as material properties, environment, traffic loading, and construction practices. Pavement design procedures currently in use depend heavily on empirical relationships based to a large extent on long-term experience and field tests such as the AASHO Road Test. It is generally recognized that such relationships between traffic loading and pavement performance apply only to the conditions under which they were developed. Application of these relationships to other sets of conditions is quite difficult. Considerable research has been conducted over the past 10 to 15 years with the objective of applying mechanistic technology to the structural analysis and design of pavements. This paper discusses realistic approaches to implementation of mechanistic technology resulting from the previous research and two specific studies culminating in usable structural subsystems. The subsystems, in the form of computer programs, are similar in some respects, but each has unique features. After further verification and calibration, they should be useful tools in the fields of asphalt pavement research, analysis, and design.

In recent years, those in the highway field have shown considerable interest in the total cost analysis or system approach to pavement design and management. The concept is essentially that of providing an acceptable level of service (ridability) at the lowest total cost (initial construction, maintenance, rehabilitation, user cost, and interest on investment) over a long-term service life. For a given situation or set of conditions, it permits a realistic total cost analysis (including other than initial construction costs) of strong initial structural designs with no planned rehabilitation actions versus various weaker initial designs with planned rehabilitation. It seems apparent that the structural design of pavements in the future will not be simply a matter of selecting thicknesses of various layers of materials suitable for the indicated traffic and environmental conditions at the lowest initial cost for an anticipated service life of 20 years. This paper explores the application of mechanistic analysis technology to the structural design of asphalt concrete pavements within the context of the evolutionary process of pavement design and management. We hope to clarify terminology and to discuss prospects for practical application of findings from pavement design research of recent years.

Publication of this paper sponsored by Committee on Flexible Pavement Design.

TERMINOLOGY

In recent years, terms such as "theoretical," "rational," "mechanistic," and "empirical" have been used to describe the various pavement design approaches. The term "empirical," described as relying on experience and observations rather than theoretical knowledge, seems quite appropriate for current flexible pavement design methods that are based primarily on local experience with available materials under similar traffic and environmental conditions. "Mechanistic," described as dealing with the laws of mechanics or the action of forces on bodies as related to the determination of stress, strain, and deformation in materials, appears to be the term most applicable to the technology emanating from recent pavement design research. "Theoretical" often has the connotation of not being very practical. "Rational," the general description of which is reasonable or sensible, we hope applies to both current and future design methods. In this paper, the terms "empirical" and "mechanistic" are used to identify the two general approaches to pavement design, those more generally used currently and those being developed for future use.

The results of recent research efforts, which are formulating computer packages and procedures for mechanistic predictive structural subsystems suitable for implementation by highway departments or other pavement design user agencies, are summarized in this paper. The two most notable developments in the United States are the FHWA VESYS IIM structural subsystem and the structural subsystem, PDMAP, currently being assembled by Materials Research and Development for the National Cooperative Highway Research Program (NCHRP) (16).

WORKING HYPOTHESES

In the development of both subsystems observable distress (cracking and rutting) was assumed to be a function

of the state of stress, strain, and deformation (primary response) in the pavement system. The working hypotheses also postulate that material properties are influenced by traffic loading and environmental conditions and that materials can be characterized in relation to primary response behavior as linearly elastic in the case of the NCHRP model and as linearly elastic or linearly viscoelastic or both in the case of the FHWA model. Figure 1 shows a summary of the elements of each of the programs.

The major differences between the two subsystems lie in the distress prediction elements. The NCHRP predictions are developed from observations of cracking and rutting on the American Association of State Highway Officials (AASHO) (now American Association of State Highway and Transportation Officials) Road Test; the FHWA distress predictions are based on the results of laboratory tests and on the hypothesis that material variability contributes to longitudinal roughness. One feature of the FHWA program is the probabilistic treatment of stochastic inputs so that output is presented as means and variances of the distress parameters. The FHWA subsystem also assumes the AASHO serviceability index to be representative of pavement performance and uses the AASHO serviceability index formulation to predict a mean and variance of the expected life of the pavement.

Both subsystems have been developed largely from the findings and results of previous research efforts in the pavement design and materials characterization fields. No new testing procedures are required for use of the subsystems except for the rut depth subsystems. The subsystem models and computer programs are constructed in a modular form so that new or better submodels may be substituted or added with little difficulty. The PDMAP subsystem uses AASHO traffic equivalence factors (17) to determine design traffic; the VESYS IIM subsystem uses the FHWA W-4 tables to express mixed truck traffic volume in terms of a statistical distribution.

VESYS IIM STRUCTURAL SUBSYSTEM

This section provides insight into the formulation of the primary response, distress, and performance elements of the VESYS IIM structural subsystem. A view of the flow of information is shown in Figure 1 except for the performance prediction element that is unique to the VESYS IIM subsystem. The performance or serviceability of the pavement is hypothesized to be represented by the linear accumulation of the distress parameters (cracking, rutting, and roughness) that can be expressed similarly as the AASHO Road Test definition of serviceability index.

Primary Response Analysis

Primary response is defined as the state of stress, strain, or deformation existing in the pavement at any time due to a stationary load applied to the pavement surface. The primary response model represents the pavement system by a three-layer semiinfinite continuum so that the upper two layers are finite in thickness but the third layer is infinite in extent. All layers are infinite in horizontal extent. Each layer can be described by elastic or viscoelastic properties, and the materials in each layer are assumed to be isotropic and locally homogeneous. The model constitutes a closed-form probabilistic solution to the three-layer linear viscoelastic boundary value problem. It is valid for single stationary circular loading at the pavement surface. It assumes complete shear at the interfaces and that the material layers are incompressible.

The viscoelastic model that is used in the VESYS IIM subsystem to compute stress and strain in the pavement structure is identical to an elastic layer theory model except that the material properties may be characterized as time-dependent (viscoelastic). The geometric representations, boundary conditions, and loading functions are the same in the two models. These similarities allow use of the principles of elastic-viscoelastic correspondence to relate the elastic solution to the viscoelastic one. The closed-form probabilistic solutions to the static load response of elastic and viscoelastic three-layer systems, along with the necessary conversions relating the two solutions, are presented elsewhere (1, 2, 3). Figure 2 shows the basic makeup of the primary response model. Stochastic inputs are in terms of the means and variances of the creep compliances for viscoelastic materials. The geometric properties include the thicknesses of the layers. The static load condition includes the magnitude of the applied stress and the area of contact between the load and pavement. Both the geometric and load conditions are deterministic input values. The computer then performs certain mathematical computations involving least squares curve fitting, partial derivitives of the material properties, and evaluation of the Bessel terms, all of which are used in the probabilistic layer theory block. The statistical distributions in terms of mean values and variances of the following seven stress-strain components are computed on command: (a) vertical stress, (b) shear stress, (c) radial stress, (d) vertical displacement, (e) radial displacement, (f) circumferential strain, and (g) radial strain. If any one layer that is used in the analysis has time-dependent properties, the system response will also be represented as a function of time. The values of radial strain at the bottom of the asphalt layer and the vertical displacement at the roadway surface are passed automatically over the distress model.

Distress Analysis

The distress element currently consists of three separate models, each designed to predict distress accumulation of the pavement. The schematic of the element is shown in Figure 3. Static load responses are passed to the appropriate distress model to be operated on for prediction of cracking, rutting, or roughness. Before the static response enters a specific distress model, it is converted to the response that would occur under a load moving at some prescribed speed. The vehicle speed, whether slow or fast, is input to the computer in terms of the time or duration of the stress pulse influence on pavement behavior. Other inputs are shown in Figure 3.

Rut Depth Prediction

The rut depth model is shown in Figure 4. It combines viscoelastic layer theory with a laboratory-based permanent deformation accumulative damage law. The law uses the results of repeated-load laboratory tests to estimate the permanent deformation properties of the layer materials. Computer output from the model is the expected value and variance of rut depth. These values are computed for each incremental analysis period where the Poisson distribution of axle loading rate and temperature are constant. Load amplitude, vehicle speed, and material properties are assumed as stochastic random variables over the analysis period. The mean value and variance of rut depth for each incremental analysis period are summed over the total analysis period. The mean and variance values are printed out by the computer at any time desired and are also automatically passed on

to the roughness model to be used in determining slope variance, the permanent deformation along the longitudinal profile of the pavement. Detailed mathematical solutions of the rut depth model are found elsewhere (4).

Roughness Prediction

Roughness is defined as the variation of permanent deformation along the longitudinal profile of the roadway. The accumulated rut depth R at any time along the wheel path is assumed to vary as a result of material variability and varying construction practices. Roughness is expressed by the AASHO Road Test definition of slope variance; it is computed by using the variance of rut depth, rut depth itself, and the autocorrelation function A(X). A(X) is a measure of the correlation of deflection responses along the wheel path. The variance of rut depth is computed in the rut depth model and is passed automatically to the roughness mode. The roughness model is shown in Figure 5. Detailed mathematical solutions of the model are found elsewhere (1, 2, 3, 5).

Fatigue Cracking Prediction

A phenomenological model, shown in Figure 6, is used for prediction of the extent of cracking based on Miner's hypothesis. The criterion for cracking is based on fatigue resulting from the tensile strain at the bottom of the asphalt concrete layer.

The expected cracking damage E[C] is expressed as a dimensionless index where the crack as initiated appears at the pavement's surface. At this time E[C] = 1. To express cracking in a more meaningful manner, C is assumed to take on a normal distribution at all times, t, with mean E[C] and variance [C]. The expected area of cracking is given by the probability that $C > 1$. The area cracked = 1000 [1 - F(1)] where F(1) = the probability that $C < 1$. The cracking index model is described in greater detail in papers available elsewhere (1, 2, 3) and by Rauhut, Kenis, and Hudson in a paper in this Record.

Performance Analysis

The performance of a pavement in a given environment is considered to be its ability to provide an acceptable level of serviceability with a specified degree of reliability at an assumed level of maintenance. The impairment or loss of ability to provide the necessary services in a given locale may then be considered as the failure of the pavement. When reviewed in this context, failure becomes a loss in performance; it is the extent to which the pavement has failed to render itself serviceable; and it results from an accumulation of distress over a given time period.

In this analysis, the AASHO Road Test definition of present serviceability index (PSI) is expressed as a function of the objective distress components of cracking, roughness, and rutting. The model uses the following general expression:

$$PSI = a_0 + a_1 \log(1 + SV) + a_2 \sqrt{C} + a_3 R^2 \quad (1)$$

where

$a_0 = 5.03$
$a_1 = 1.91$,
$a_2 = 0.01$,
$a_3 = 1.38$,
SV = slope variance (roughness),
C = crack index, and
R = rut depth.

The damage components SV, C, and R are considered as uncorrelated random variables, and mean and variance values are computed. Pavement reliability and expected life are also computed (1, 2, 3).

PDMAP STRUCTURAL SUBSYSTEM

The basic elements of the PDMAP structural subsystem can be divided into three categories: (a) inputs such as material properties, environment, and traffic (fatigue and rutting only); (b) primary response computations such as stress, strain, and deformation; and (c) damage (distress) prediction models. The fatigue cracking and rut depth distress prediction models combine items a and b but use different models for each type of distress.

The mathematics necessary for the probabilistic subroutine were developed by investigators at the University of Utah by Hufferd, under sponsorship of FHWA, and were provided by FHWA for use in NCHRP Project 1-10B (16). The probabilistic aspects with respect to each subsystem are not discussed in this paper. However, one of the objectives of the project is to include in the damage prediction models some indication of the uncertainty of the predictions. Each structural subsystem incorporates concepts that will account for observed variations in material properties, traffic, and environmental factors. Determining the expected value and variance of each distress mode as a function of the expected value and variance of inputs to the structural subsystem will be possible.

The basic features of each of the damage prediction models are summarized in the following sections. It is emphasized that the first step is selection of a specific asphalt concrete pavement structural section. The subsystem then is used to predict fatigue and temperature cracking and permanent deformation (rutting) in relation to the other input variables. General descriptions of the operational procedures are shown in Figures 7 and 8.

Fatigue Cracking Prediction

Material Properties

Materials are characterized in accordance with generally accepted procedures applicable to linear elasticity designed to recognize the temperature, time, and stress susceptibility of asphalt and unbound granular materials. For probabilities to be developed into the prediction model, material properties are input as the average or expected value for a specified time period together with the coefficient of variation. The coefficient of variation should be based on the variations expected in the field and not the laboratory. Hence a rather large coefficient of variation can be expected. Very little information is available regarding what this value should be; however, 50 percent is not considered unrealistic.

Asphalt concrete or asphalt emulsion mixtures are characterized in accordance with procedures applicable to dynamic modulus as described by the Asphalt Institute (6). Testing is to be performed at 10 Hz over a range of temperatures from 37.78° C (100° F) to 4.44° C (40° F). Cement-treated materials are characterized in accordance with ASTM C 469 or its equivalent.

Untreated aggregates are tested in triaxial configuration by procedures reported at the University of California (7). The stress-sensitive expression used to describe the elastic constant is

$$M_R = K_1 \theta^{K_2} \quad (2)$$

where

Figure 1. Mechanistic structural subsystem programs.

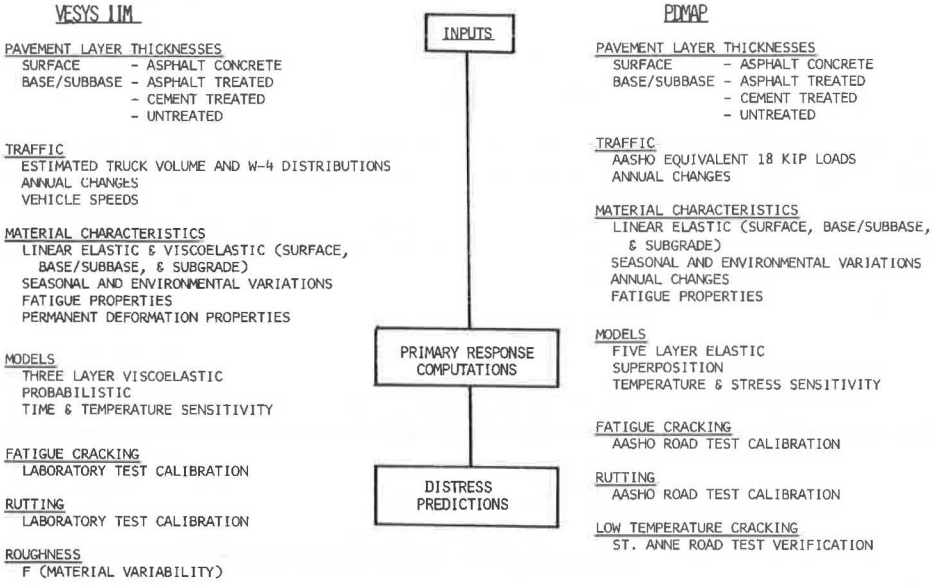

Figure 2. Primary response model.

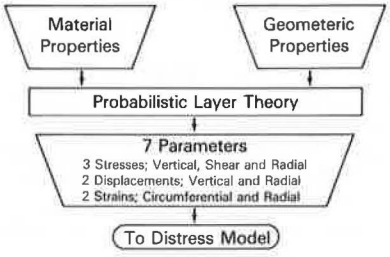

Figure 3. Distress analysis.

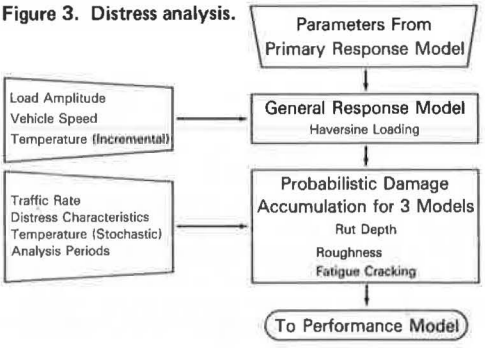

Figure 4. Rut depth model.

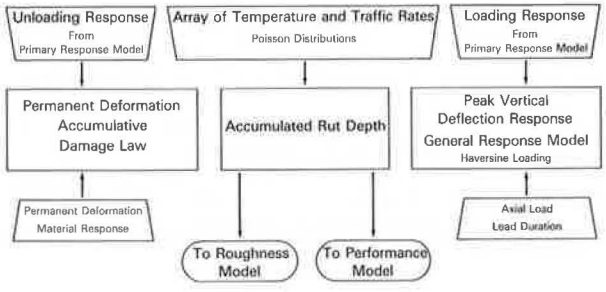

Figure 5. Roughness model.

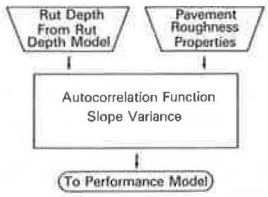

Figure 6. Fatigue cracking model.

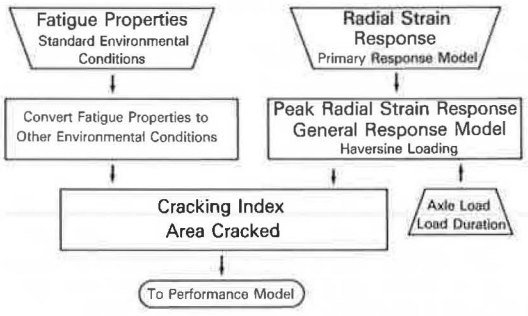

M_R = resilient modulus,
θ = first stress invariant ($\sigma_1 + 2\sigma_3$), and
K_1 and K_2 = fitting coefficients.

Subgrade materials are tested by procedures similar to untreated granular materials and described by an equation of the same form by substituting deviator stress σ_d for the first stress invariant σ.

Traffic

Mixed traffic is converted to 8.16-Mg (18-kip) equivalent single axle loads (ESALs) in accordance with the load equivalency factors determined at the AASHO Road Test. The coefficient of variation for traffic estimates may be included in the program and will influence the reliability for making distress predictions. Traffic growth factors are input on an annual basis. For example, traffic growth can be 10 percent (1.10 times each preceding year) for the first through the third year, 5 percent from the fourth through the tenth year, and zero after the tenth year.

The program is designed to predict damage for each application of an ESAL. Thus the total damage for a single day would be the unit damage multiplied by the number of ESALs for the day. Because air temperatures and asphalt temperature can vary throughout the day (particularly day and night temperatures), the program for fatigue cracking is divided into two 12-h segments for each day. If traffic, for localized reasons, tends to vary between day and night, the program has the capability of reflecting the influence of such systematic variations on fatigue damage.

Temperature and Seasonal Variations

The relationships developed by Barber (8) are used to calculate the temperature in the asphalt layers. The program calculates these temperatures for a typical day during the analysis period. Thus, a considerable amount of averaging will occur, depending on the period for which damage (distress) is being predicted. The program recognizes that damage may vary during the year as a function of seasonal variations. The user must, therefore, decide on how many damage analysis periods are required for each year (for example, one approach would be to divide the year into four seasons).

In a procedure similar to that used for seasonal variations, damage predictions can be adjusted for changes that occur over long periods of time. Thus the user can select one set of material properties for each damage analysis period within a year, as previously described, for a selected number of years (for example, 3 years) and change these for the next set of years and so on for the total number of years under consideration. The major factors influencing long-term change are hardening of asphalt, weathering of base and subbase materials, strength growth of cement-treated materials, and establishment of equilibrium conditions in the subgrade soils.

Primary Response Computations

The purpose of the structural analysis is to compute the mechanistic (primary) responses of the pavement that are required for the damage prediction models. For fatigue cracking predictions, the maximum tensile strain in the treated layer is considered to be the determinant of distress.

A variety of computer programs is available for the solution of a boundary value problem such as multilayered pavement systems. These programs are divided into two major categories: (a) finite element or (b) elastic layered systems.

The computer program selected for NCHRP Project 1-10B (16) structural analysis is $PSAD_2$, an extension of the elastic layered program CHEV5L, with superposition and stress sensitivity for five layers. A subroutine for probability calculations has been appended to this program.

Distress Prediction Model

The purpose of the damage prediction model is to allow the user to estimate the area of cracking that will accumulate under the influence of traffic, the physical state of the pavement components, and the fatigue properties of the treated materials. There is now no purely mechanistic procedure for predicting areal cracking. It has been found useful, therefore, to relate laboratory fatigue results to field observations as a method to take into account crack propagation throughout the paved area. Data from the AASHO Road Test provide for a reasonable determination of such factors for two levels of cracking: (a) up to 10 percent and (b) greater than 50 percent.

The equation developed for predicting cumulative damage of asphalt concrete is

$$\log N_f = -1.234 - 3.291 \log \epsilon \, 0.854 \log [E^*] \quad (3)$$

where

N_f = number of 8.16-Mg (18-kip) ESALs,
ϵ = strain in asphalt concrete, and
$|E^*|$ = dynamic modulus in kilopascals.

This model is considered appropriate for asphalt-aggregate mixtures with 5 percent voids. Other model variations have been developed for asphalt-emulsion-treated bases and for mixtures with different void contents.

Permanent Deformation Prediction

The purpose of the permanent deformation model is to predict wheel-path rutting as a function of traffic and the state of stress in the pavement structure. The method developed under NCHRP Project 1-10B (16) is similar to that developed by Dormon and Metcalf (9) and Finn, Nair, and Monismith (10) except that the magnitude of rutting is predicted rather than a limiting value of the mechanical state of stress and strain. The methodology developed by Morris (11) and by Haas and Meyer (12) was helpful in the prediction models developed under this investigation.

The flow diagram (Figure 7) used for fatigue cracking predictions can be used to illustrate rut depth prediction models with only two exceptions: (a) daily traffic is accumulated on a 24-h basis rather than two 12-h intervals, and (b) the damage prediction model is based on regression fits to field observations with no intervening laboratory evaluation of permanent deformation properties of individual layers.

Data from the AASHO Road Test were used to develop the prediction model. Data from the road test consistently indicated that the rate of rutting $\Delta RD/\Delta N$ was related to the season of the year (spring, summer, fall, winter) and the rate of rutting for the second year decreased compared with the rate of rutting the first year. Figure 9 shows the manner in which permanent deformation occurred on the AASHO Road Test; the figure indicates both seasonal and annual differences. Analysis indicated that the slope of the lines representing the rate of rut depth accumulation per ESAL could be related to various combinations of stress and strain within the pavement section or subgrade.

The final equation developed from the sections at the AASHO Road Test is

$$\log RR = -5.619 + 4.487 \log \Delta - 1.296 \log \sigma - 0.0947 \log N_{18} \quad (4)$$

where

RR = rate of rutting,
Δ = surface deflection $\times 10^{-3}$,
σ = maximum stress in asphalt concrete in kilopascals, and
N_{18} = 8.16-Mg (18-kip) ESALs.

This relationship makes it possible to recognize seasonal variations in the rate of rutting in much the same fashion as for fatigue cracking. Hence new material properties will produce new mechanistic responses, which in turn will produce a revised estimate of the rate of rutting. The rut depth prediction subsystem is designed to divide the year by months or seasons exactly in accordance with the fatigue cracking subsystem. The

Figure 7. Fatigue and rut depth subsystem (PDMAP).

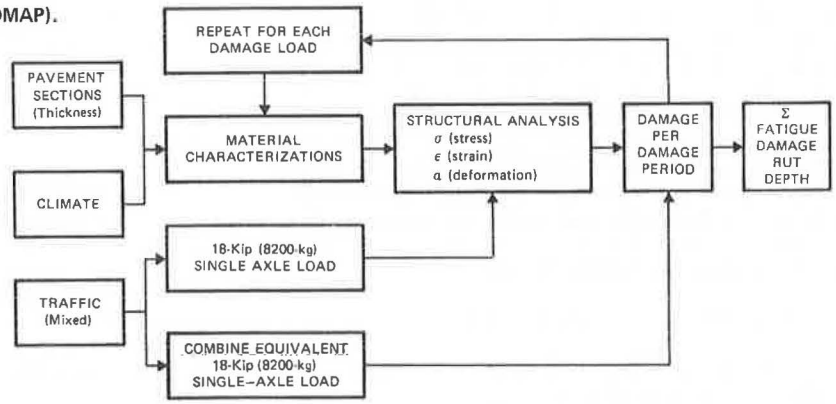

Figure 8. Low-temperature-cracking subsystem (PDMAP).

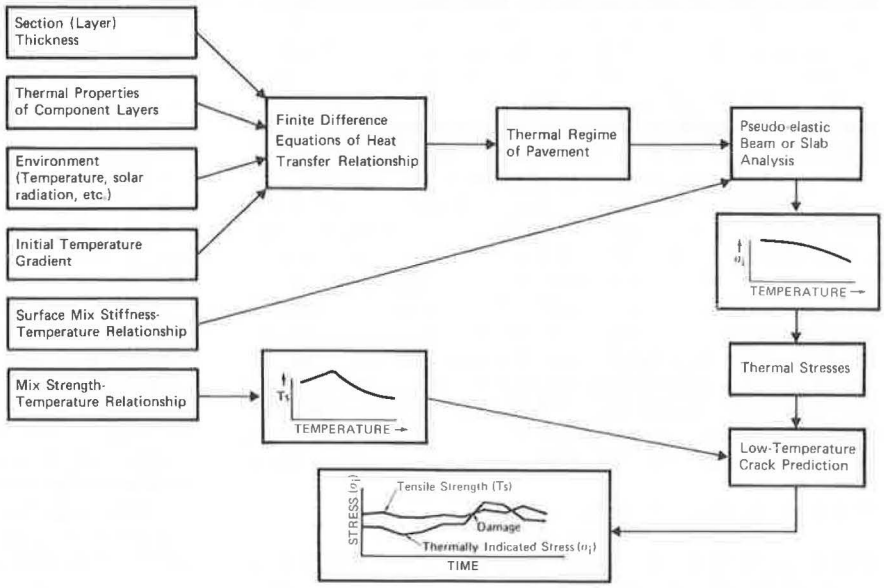

Figure 9. Typical pattern for rutting on AASHO Road Test.

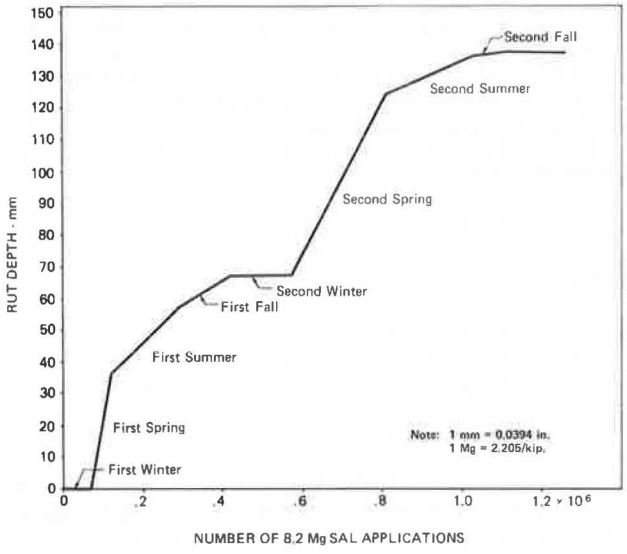

cumulative amount of rutting is obtained by multiplying number of ESALs for any given season times the rate of rutting for that season.

Low-Temperature-Cracking Prediction

The purpose of this subsystem is to estimate the potential for low-temperature cracking of asphalt concrete for a particular asphalt-aggregate pavement structure when placed in a specific environment. The working hypothesis for this subsystem is that low-temperature cracking will occur when the thermally induced tensile stress exceeds the tensile strength. The development work and verification of this hypothesis have been presented by Burgess, Kopvillem, and Young (13) and by Christison and Anderson (14).

To use this prediction model, one must (a) predict the temperature in the surface of the asphalt concrete, (b) calculate the thermally induced tensile stress in the surface of the asphalt concrete, (c) measure the tensile strength of the asphalt concrete, and (d) compare induced stress with strength to determine the potential for cracking. Programs for predicting surface temperature by means of routine climatological data have been included in the program. The basic development of these programs was accomplished by Christison (15) and modified as required by investigators working on NCHRP Project 1-10B (16).

The subsystem provides for both graphical and analytical procedures for the determination of the intersection of thermal stress and tensile strength as shown in Figure 8. Appropriate reliability factors are included to help the user establish confidence levels depending on the functional importance of the facility.

CONCLUSIONS

The programs described in this paper are capable of predicting the amount of distress in terms of cracking and permanent deformation that should be expected in a given asphalt concrete pavement structural section built of a material and located over a soil subgrade of measurable characteristics, and exposed to specific traffic loadings and environmental conditions over a prescribed period of time. The major limitation to this capability is that of verification of the predictions under real-world conditions. It is also recognized that working relationships between pavement distress and pavement performance, in terms of serviceability or ridability, have not been established. As a result, the programs are not capable of designing pavement structures to a specified level of performance for a given set of material, traffic, and environmental conditions. The obvious question that arises is, What advantages or applications do the mechanistic programs offer over currently used empirical pavement design procedures?

In response to this question, let us first consider the advantages and limitations of empirical design procedures. They are simple, not time consuming, and use readily available input data. In addition, the predicted performance is generally adequate when materials, traffic, and environmental conditions are similar to those for which considerable experience is available. However, confidence in predicted performance diminishes as the many combinations of conditions vary from those for which long-term experience is available.

The computer programs based on mechanistic technology, when properly calibrated, will permit the evaluation of pavement structures consisting of a wide variety of materials and exposed to many different sets of traffic and environmental conditions by simulated analytical studies at relatively small investment of time and funds compared with that required for either generally accepted laboratory or field test evaluation procedures. Further verification and calibration of the ability to reasonably predict the amount of distress in a given pavement will certainly be a useful tool to agencies involved in pavement design methodology. The mechanistic pavement design technology will eventually be used to (a) accommodate changing loads, (b) better use existing and new materials, (c) improve reliability of performance estimates, (d) increase ability to consider the influence of environmental factors, and (e) provide for implementation of pavement management systems so essential to best use of available materials and funds for pavement design, construction, and rehabilitation.

ACKNOWLEDGMENTS

The research discussed in this paper is part of current studies being conducted under sponsorship of the Federal Highway Administration and the American Association of State Highway and Transportation Officials. The opinions, findings, and conclusions expressed in the paper are ours and not necessarily those of the sponsors of the projects.

REFERENCES

1. F. Moavenzadeh, H. K. Findakly, and J. E. Soussou. Synthesis for Rational Design of Flexible Pavements. Federal Highway Administration, Vol. 1-3, Rept. 75-30 and 75-31.
2. B. D. Brademeyer. Flexible Pavement Systems: An Analysis of the Structural Subsystem's Deterioration. Massachusetts Institute of Technology, Cambridge, MS thesis, Feb. 1975.
3. W. J. Kenis. Predictive Design Procedures. In Users Manual for the Design of Flexible Pavements Using the VESYS Structural Subsystem, Federal Highway Administration, Project 5C, March 1976.
4. W. J. Kenis and M. J. Sharma. Prediction of Rutting and Development of a Simplified Test Procedure for Permanent Deformation in Asphalt Pavements. Paper presented at 55th Annual Meeting, TRB, 1976.
5. J. B. Rauhut, J. C. O'Quin, and R. W. Hudson. Sensitivity Analysis of FHWA Structural Model VESYS II. Draft of final report submitted to FHWA, 1975.
6. Thickness Design: Full Depth Asphalt Pavements for Highways and Streets. Asphalt Institute, College Park, Md., MS-11.
7. C. C. Monismith and D. B. McLean. Design Considerations for Asphalt Pavements. Institute of Transportation and Traffic Engineering, Univ. of California, Berkeley, Rept. 71-8.
8. E. S. Barber. Calculations of Maximum Pavement Temperatures From Weather Reports. HRB, Bulletin 168, 1957, pp. 1-8.
9. G. M. Dormon and C. T. Metcalf. Design Curves for Flexible Pavements Based on Layered System Theory. HRB, Highway Research Record 71, 1965, pp. 69-84.
10. F. N. Finn, K. Nair, and C. L. Monismith. Applications of Theory in the Design of Asphalt Pavements. Proc., 3rd International Conference on Structural Design of Asphalt Pavements, London, 1972, pp. 392-409.
11. J. Morris. The Prediction of Permanent Deformation in Asphalt Concrete Pavements. Univ. of Waterloo, Ontario, Canada, PhD dissertation, Sept. 1973.
12. R. Haas and F. Meyer. Cyclic Creep of Bituminous Materials Under Transient, High-Volume Loads. TRB, Transportation Research Record 549, 1975, pp. 1-14.
13. R. A. Burgess, O. Kopvillem, and F. D. Young. Ste. Anne Test Road-Flexible Pavement Design to Resist Low Temperature Cracking. Proc., 3rd International Conference on Structural Design of Asphalt Pavements, London, 1972.
14. J. T. Christison and K. O. Anderson. The Response of Asphalt Pavements to Low Temperature Environments. Proc., 3rd International Conference on Structural Design of Asphalt Pavements, London, 1972.
15. J. T. Christison. The Response of Asphaltic Concrete Pavements to Low Temperatures. PhD dissertation, Univ. of Alberta, Edmonton, 1972.
16. Development of Pavement Structural Subsystems. NCHRP, Project 1-10B.
17. AASHO Interim Guide for Design of Pavement Structures. AASHO, Washington, D.C., 1972.

Use of Condition Surveys in Pavement Distress and Performance Relationship

B. Frank McCullough and Phil Smith, Center for Highway Research, University of Texas at Austin

Many people in the field of pavement design have stated that one of the largest deficiencies in a pavement design system is the absence of a good relationship of pavement distress to pavement performance. With this in mind, we decided to explore the meaning of this relationship, examine any past work that had been done in this area, and begin some initial research directed toward establishing a relationship between pavement distress and performance. Four areas were studied: relationship of pavement distress to performance, pavement condition surveys, pavement profiles, and pavement maintenance.

RELATIONSHIP OF PAVEMENT DISTRESS TO PERFORMANCE

Relating distress to performance must be understood before any useful research can be conducted. The data shown in Figure 1 represent an attempt to explain this. Pavement design currently progresses from the inputs (block 1) to performance in the form of accumulated serviceability (block 4) by use of design models (block 5) and the PSI equations (block 6). Doing this overlooks pavement behavior (block 2) and pavement distress (block 3). Accumulated knowledge in these two areas in pavement design should be included in progressing from inputs to performance, but a step in the process is missing. This step involves the progression from distress to performance. Various mechanistic models exist (block 7) that can determine to a fairly accurate degree the pavement behavior given certain inputs; models also exist (block 8) that can determine to a less accurate degree pavement distress given certain pavement behavior. However, no models and very limited knowledge exist that allow the progression from pavement distress (block 3) to pavement performance (block 4). Thus information that will allow this progression, perhaps in the form of a distress weighting function (block 9) used in prediction models, is what is meant by relating distress to performance. By use of a well-designed research plan and by use of continued evaluation of the PSI equation and its terms (block 10), perhaps one can obtain enough information to determine these distress weighting functions and prediction models.

We felt that research conducted toward relating distress to performance should first consist of the determination of the various distress manifestations (cracking, spalling, faulting, scaling, and the like); their magnitudes; and their effect on serviceability and methods of correcting them. This can be done primarily by condition surveys, profile studies, and maintenance studies.

The various distress manifestations, then, need to be associated with distress mechanism. Doing this is more difficult than doing the first step of the research plan but can be done within a detailed work plan. These distress mechanisms, when determined, can be ranked according to priority. Then improvements in the model can be made or new models can be developed for predicting the ultimate goal—the performance of pavements.

PAVEMENT CONDITION SURVEYS

Before a relationship can be established between pavement distress and pavement performance, one must determine the types of distress that actually occur on pavements with information sufficiently detailed to differentiate the various types of distress. Thus we decided to conduct a detailed inspection condition survey to provide information on distress for further use in establishing the distress-performance relationship. The condition surveys included eight different highways and seven counties within Texas Department of Highways and Public Transportation District 14.

The most frequently encountered distress manifestation was patching. Fatigue cracking, mostly in the form of longitudinal and block cracking, was encountered fairly often. The rutting that occurred generally was fairly minor except on some of the secondary road sections. Edge deterioration was somewhat common in pavements with no paved shoulder. Bleeding was encountered often but usually was not severe enough to cause any problems. Raveling was fairly common but

Publication of this paper sponsored by Committee on Flexible Pavement Design.

Figure 1. Distress-performance relationship with use of models.

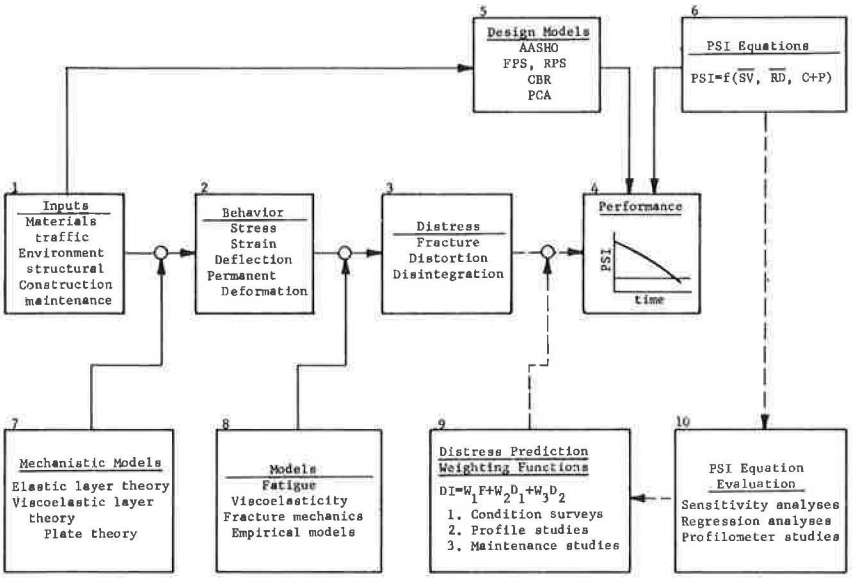

usually not in a severe stage.

In classifying the distress according to the modes (fracture, distortion, and disintegration), we found that the great majority of distress manifestations were fractures. The only distortion to speak of was rutting. No noticeable transverse distortion was present. There was little, if any, swelling or settlement that could be detected visually. The major forms of disintegration were raveling and breakage of the pavement edge.

A meaningful step toward accomplishment of the objectives is the ranking of the distress manifestations according to their contribution of the total distressed area.

Manifestation	Contribution (%)
Patching	59.9
Bleeding	9.4
Rutting	6.1
Longitudinal fatigue cracking	6.0
Edge deterioration	4.9
Raveling	4.8
Block fatigue cracking	4.0
Alligator fatigue cracking	2.6
Edge cracking	0.9
Construction cracking	0.8
Longitudinal cracking	0.7
Shrinkage cracking	0.5
Transverse cracking	0.4
Total	100.0

PAVEMENT PROFILES

After discussions on the uses and capabilities of the surface dynamics profilometer, we decided that there was a good chance that it could be used to collect information about relating pavement distress to pavement performance. Because detailed information on types and locations of distresses was obtained in the condition surveys, profilometer data were collected on some of these sections and the results were compared to the condition survey.

Four 0.32-km (0.2-mile) sections were chosen for profile study. The profilometer was run on these sections at a speed of 32 km/h (20 mph). The strip charts with the profiles of both wheel paths were then analyzed for any profile amplitude or wavelength patterns that occurred. The distress manifestations from the condition survey data sheets were indicated on the profile strip charts by scaling off horizontal distance from the beginning mark of the section. By doing this, we could study the profile pattern for an exact location or a specific distress manifestation. Portions of the strip charts on which this was done are shown in Figure 2.

The profilometer was used to collect serviceability index values for the pavement sections on which condition surveys were performed. It is interesting to note the serviceability index values that were obtained for the sections. The values range from 2.0 to 4.0, and the mean is 2.9. That the mean is as high as 2.9 is somewhat surprising. These values are terminal serviceability values because all of these sections were scheduled for rehabilitation. A mean value of 2.9 for a terminal serviceability is higher than the design terminal serviceability now being used by the Texas Department of Highways and Public Transportation. This indicates that the maintenance personnel who chose these highways for rehabilitation might tend to feel that a highway needs rehabilitation before it reaches design terminal serviceability. Further study in this area might provide useful information on the best design terminal serviceability values to use.

PAVEMENT MAINTENANCE

A study of the maintenance of pavements should be included in research directed toward relating pavement distress to pavement performance. A questionnaire on criteria used to select highways for maintenance was distributed in Texas Department of Highways and Public Transportation District 17 and asked for a rating of decision factors for various maintenance work. The maintenance forces weight the factors of pavement cracking, surface roughness, and type of existing base higher than the highway engineers do. Highway engineers stress raveling of aggregate, visible pavement deformation, skid values, and amount of traffic when considering pavements for maintenance. From results of the questionnaire, we concluded that the selection of pavements for maintenance is still an art the practice of which improves with experience. Collection of information of this type in other districts would be very useful.

Figure 2. Block cracking and patching on section 13, FM 971.

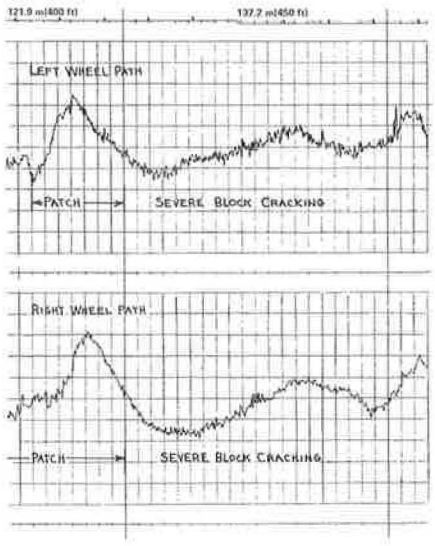

CONCLUSIONS AND RECOMMENDATIONS

We recommend that detailed condition surveys such as the one performed in this research be performed in other districts; each survey may have different distress in both occurrence and prominence. More comparisons of design terminal serviceability with actual terminal serviceability of pavements would also provide interesting and useful information on the proper design value for terminal serviceability. We recommend that a study be made of the history of pavements, including history of design, materials, dimensions, and types of surfaces, for comparison with the distress present on these pavements as an aid for relating distress manifestations and distress mechanisms. These would provide information that would help in determining the cause of certain types of distress.

Each area of study (pavement condition surveys, profile studies, and maintenance studies) can become the basis for a large-scale research project. We believe that detailed information collected in those areas can be combined into a distress-performance relationship that will enable the ultimate goal—the prediction of the performance of pavements—to be reached.

Improved Techniques for Prediction of Fatigue Life for Asphalt Concrete Pavements

J. Brent Rauhut, Austin Research Engineers, Inc.
William J. Kenis, Federal Highway Administration
W. Ronald Hudson, University of Texas at Austin

Predictions for traffic-induced fatigue damage with time for asphalt concrete pavements are usually based on Miner's hypothesis and fatigue characterization of materials obtained from laboratory fatigue tests. In general, considerably greater damage is predicted than actually occurs in the field. This is partly due to inequities between the meaning of fatigue failure in laboratory testing and in a pavement layer in service, differences in stress states between laboratory specimens under test conditions and a pavement layer under wheel loads, and variability in strain and material characteristics in the field. Wheel tracking tests as developed by Shell Laboratories and analytical developments based indirectly on American Association of State Highway Officials (now American Association of State Highway and Transportation Officials) experimental data may be used for establishing much more rational fatigue relationships for asphalt concrete materials than those obtained from standard laboratory fatigue tests. Means for rationally revising the fatigue relationships to consider the effects of changes in temperature on fatigue life are presented. These two improvements allow considerably improved predictions for fatigue damage. Promising concepts for calculating an expected damage index to consider materials variability are discussed. Apparent shortcomings in the current stochastic formulations in VESYS IIM are described along with recommendations for further development.

The classic equation based on Miner's hypotheses for assessing fatigue damage is

$$D_j = \sum_{i=1}^{j} \frac{n_i}{N_i} = \sum_{i=1}^{j} \frac{\epsilon_i^{K_{2_i}}}{K_{1_i}} \lambda_i (t_i - t_{i-1}) \quad (1)$$

where

n_i = number of load cycles during the ith time interval = $\lambda_i(t_i - t_{i-1})$,
N_i = number of cycles to failure under temperature and strain conditions of ith time interval = $K_{1_i}(1/\epsilon_i)^{K_{2_i}}$,
D_j = mean damage index at time t_j,
ϵ_i = mean strain during the ith time interval,
λ_i = traffic rate during the ith time interval,
t_i = the ith element of the time array ($t_0 = 0$),
K_{1_i} = fatigue relation coefficient for ith time interval in terms of temperature, and
K_{2_i} = fatigue relation exponent for ith time interval in terms of temperature.

The fraction of damage or cracking induced during each time interval is accumulated. Cracking failure is considered to occur when $D_j = 1$. Although it is well known that K_{2_i} varies slightly and that K_{1_i} varies radically with temperature, these coefficients used for characterizing the relation between initial strain levels and load cycles to fatigue failure have usually been considered as constants for a material.

MORE RATIONAL FATIGUE RELATIONSHIPS

Values of K_{1_i} and K_{2_i} have been assessed in the United States by a series of uniaxial dynamic beam tests with varying initial strain (or stress) levels and more recently by biaxial dynamic indirect tensile tests. In other countries, biaxial testing through repetitive torsional loads has been used on specimens of various shapes. These tests give somewhat different results, but have one thing in common. Predictions of fatigue life that use test values of K_{1_i} and K_{2_i} generally fall considerably short of actual fatigue lives for the same materials in a pavement slab under service conditions. Although there are several reasons for this, three are considered to be primary.

1. Failure in laboratory tests follows shortly after cracks appear; failure in the field is generally defined in terms of the amount of cracks propagated to the surface of the pavement long after initial cracking at the bottom of the surface layer.
2. Actual stress and strain conditions in a pavement reticulated by cracks in the bottom are considerably different from those estimated by using elastic layer theory.
3. Minor material or test variations in K_{2_i} can cause major variations in fatigue life because of the exponential nature of the relation.

Publication of this paper sponsored by Committee on Flexible Pavement Design.

Two approaches have been taken to obtaining values of K_{1_i} and K_{2_i} that relate to a definition of failure at the surface of a pavement under service conditions. One is the statistical relation of the number of known load applications experienced at the American Association of State Highway Officials (AASHO) (now the American Association of State Highway and Transportation Officials) Road Test to strains estimated through use of elastic layer theory reported by Kingham (7), Witczak (4), and Austin Research Engineers, Inc. (6). The other is use of the Shell Laboratories wheel tracking test (WTT) (5) to test heavily instrumented asphalt concrete (AC) slab sections resting on rubber pads and subjected to two-directional wheel loadings in a fixed path. These relationships are shown as solid lines in Figure 1; typical laboratory test results for essentially the same mixes as used in the WTTs are shown as dashed lines. Note that the slopes of the WTT and AASHO-based curves are quite different but that the curves approach each other out in the range of greatest interest around 5 to 15 million load applications. The laboratory tests would give much smaller predictions of fatigue life.

Figure 2, which is based on Van Dijk's data (5), shows typical strain measurements versus number of load cycles for a WTT on the typical Dutch mix AC-I. Note the stages of crack development at the bottom of the slab and that several times as many loads are required to develop sufficient cracking to represent failure as are required to initiate cracking at the bottom (unlike the standard laboratory tests). Cracks only appeared at the surface near the last stage, designated as the failure stage in Figure 2.

We believe that the fatigue relationships plotted in solid lines in Figure 1 are more rational and may be expected to give more realistic predictions than typical results from standard laboratory tests. Many more of such data are needed.

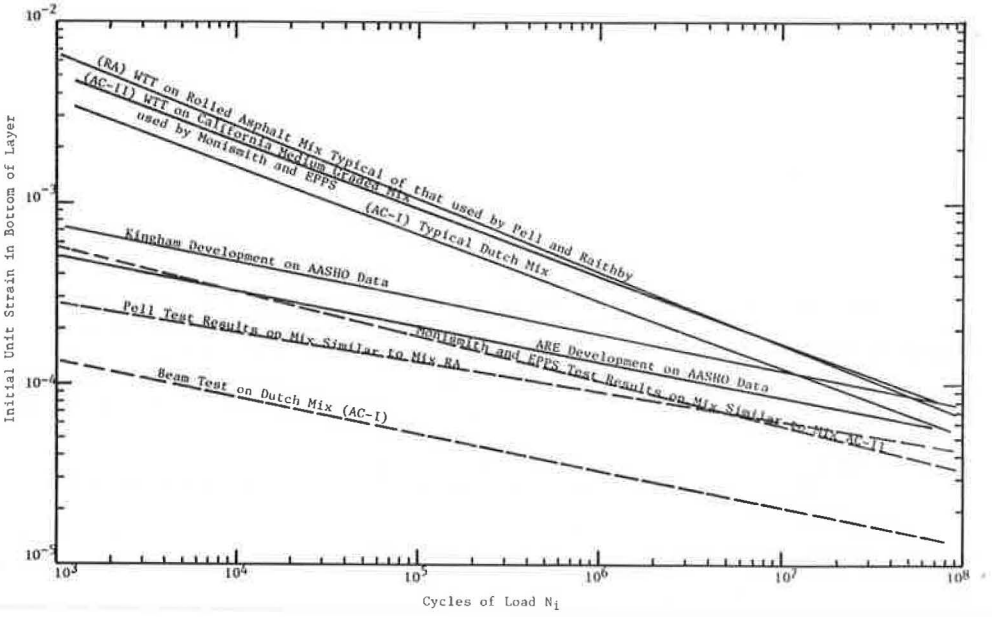

Figure 1. Fatigue relationships from wheel tracking tests, analytical developments based on AASHO test data, and beam tests.

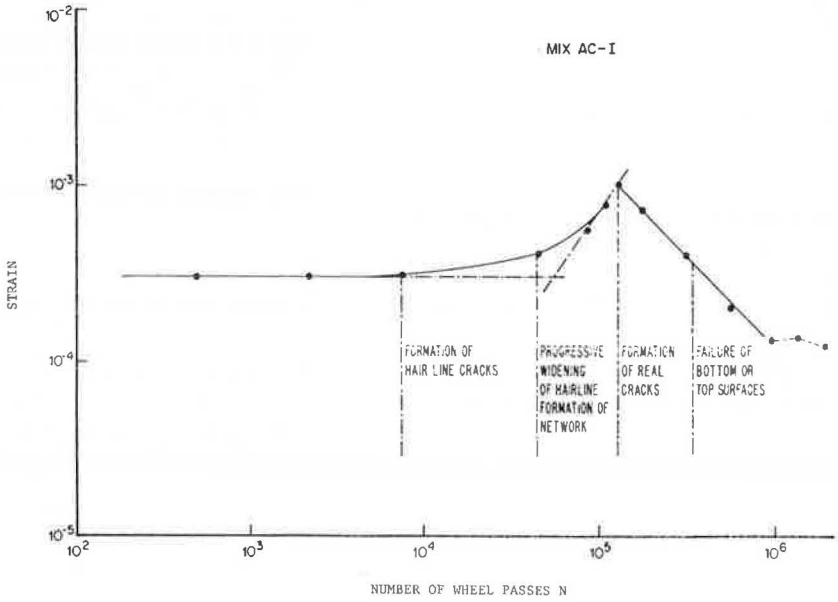

Figure 2. Crack development as a function of strain readings at equivalent number of wheel passes.

Figure 3. Relation between normalized K_1 and temperature.

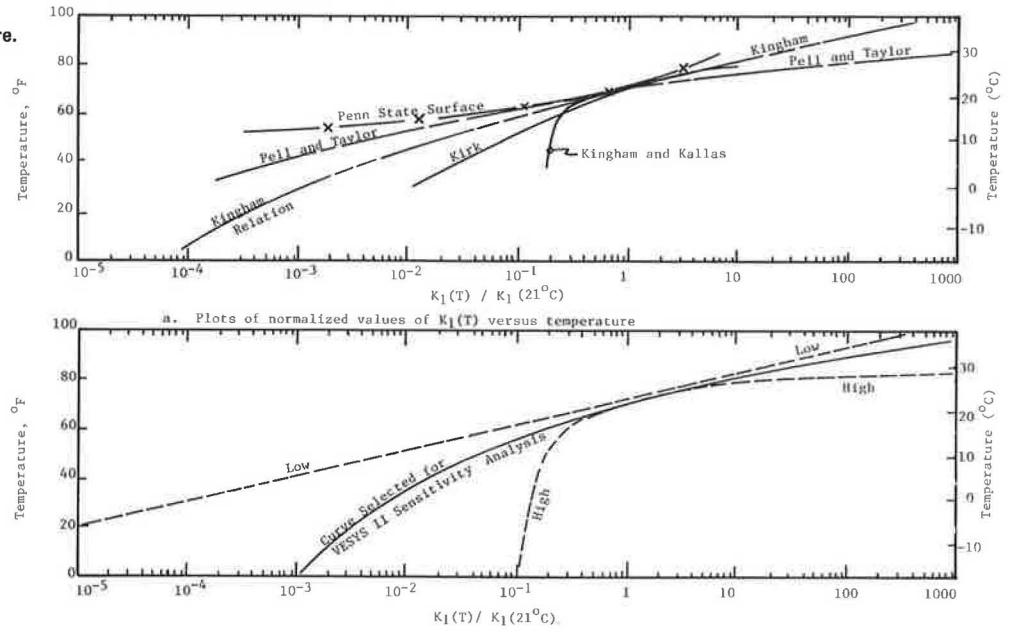

a. Plots of normalized values of $K_1(T)$ versus temperature

b. Plots of normalized values of $K_1(T)$ to use for modifying K_1 (21°C) in VESYS II sensitivity analysis

Figure 4. Relation between normalized K_2 and temperature.

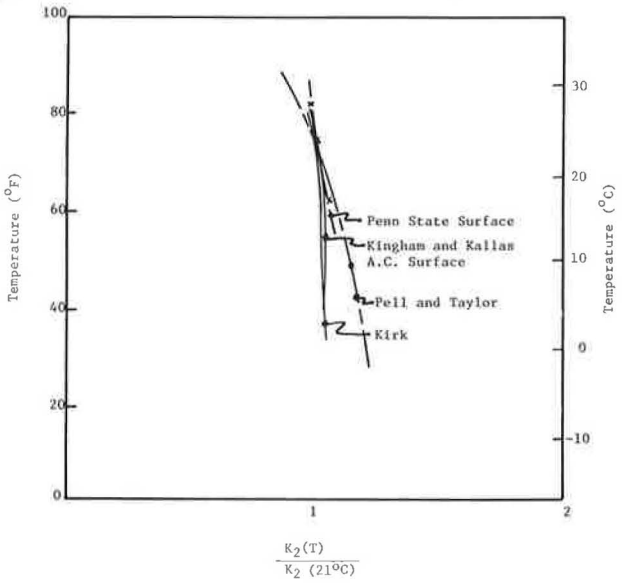

REVISING FATIGUE RELATIONSHIPS FOR DIFFERENT TEMPERATURES

An original computer program called PADS II developed by Moavenzadeh (8) included a capability for considering different values of K_{1_i} and K_{2_i} for different temperatures. This concept was expanded by the Federal Highway Administration (FHWA) to automatically vary K_{1_i} and K_{2_i} as a function of temperature through a parabolic relationship and was tentatively included in VESYS IIM. The relationship was based on laboratory beam tests conducted by the Asphalt Institute (9).

It became apparent while material characterizations were being developed for use in sensitivity analyses for the FHWA VESYS IIM Pavement Analysis and Design System that some better means of revising K_{1_i} and K_{2_i} with temperature was required. As the actual values of data from various sources varied greatly, normalized multipliers $K_1(T)/K_1(21.11°C)$ and $K_2(T)/K_2(21.11°C)$ were used to allow meaningful comparisons of the variation of K_{1_i} and K_{2_i} with temperature (21.11°C = 70° F).

These normalized values from several sources are shown for K_{1_i} in Figure 3a and for K_{2_i} in Figure 4. The sources of data used are available elsewhere (1, 2, 3, 4, 7, 9). The variation for normalized K_{1_i} value was great while that for K_{2_i} was small. However, K_{2_i} is an exponent, and very small variations in K_{2_i} may have much more effect on cracking predictions than relatively greater variations in K_{1_i}.

Figure 3b shows envelopes of the various curves with these boundaries designated as low and high fatigue life. Also shown is a curve selected for modifying K_{1_i} as the temperature varies from 21.11°C (70° F).

The preponderance of data indicate little overall variation in K_{2_i} with temperature (Figure 4), but there is some minor reduction in K_{2_i} with increasing temperature. The following equation was selected to provide a rational minor variation with temperature (21.11°C = 70° F):

$$K_2(T) = K_2\ (21.11°C)\ [1 - 0.001\ (T°C - 21.11)] \qquad (2)$$

By using these relationships, one can make improved fatigue characterizations of the AC surface materials under varying temperature conditions and apply them with equation 1 to accumulate damage with time. Such variations with temperature for a material having a median fatigue life potential are shown in Figure 5. For a particular level of strain ϵ_i, N_i varies radically with changing temperature. Damage due to fatigue predicted by equation 1 for a specific traffic rate λ_i would then accumulate rapidly at low temperatures and very slowly at higher temperatures.

STOCHASTIC FORMULATION TO CONSIDER MATERIAL VARIABILITY

Equation 1 assumes that material properties and pavement thickness are constant, but this is far from true in reality. Variability is present within a project to an extent generally dependent on specifications, quality control, and other factors. Strain predictions are affected by variability in layer thickness and material stiffness;

Figure 5. Variation in fatigue life relationship with temperature.

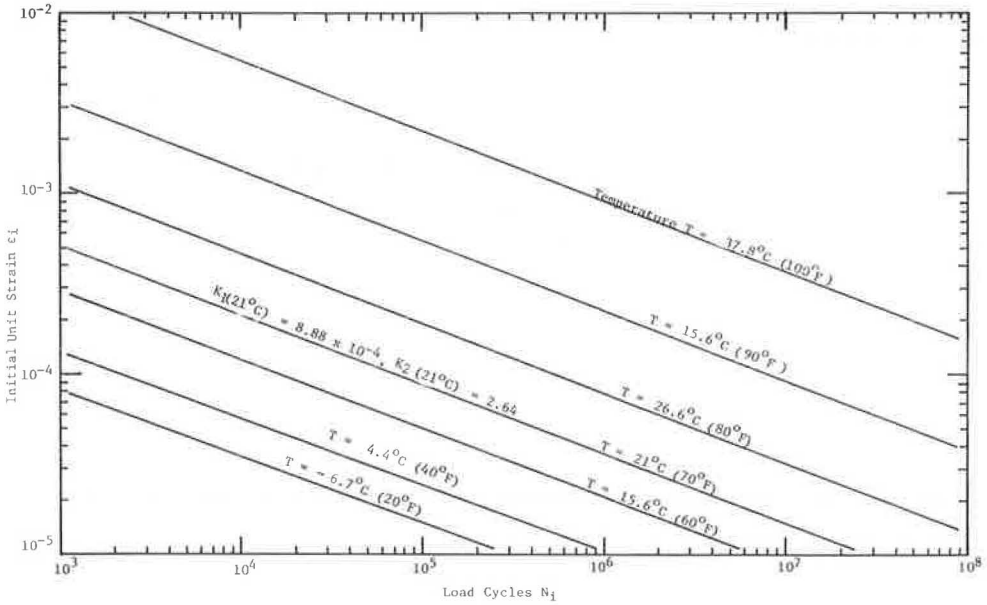

Figure 6. Normal probability density function used to predict area cracked.

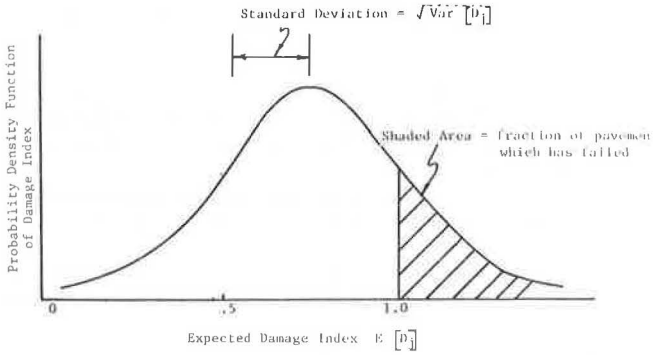

Figure 7. Fatigue life versus coefficients of variation for a material having mean $K_{1_i} = 1.85 \times 10^{-5}$ and $K_{2_i} = 3.04$.

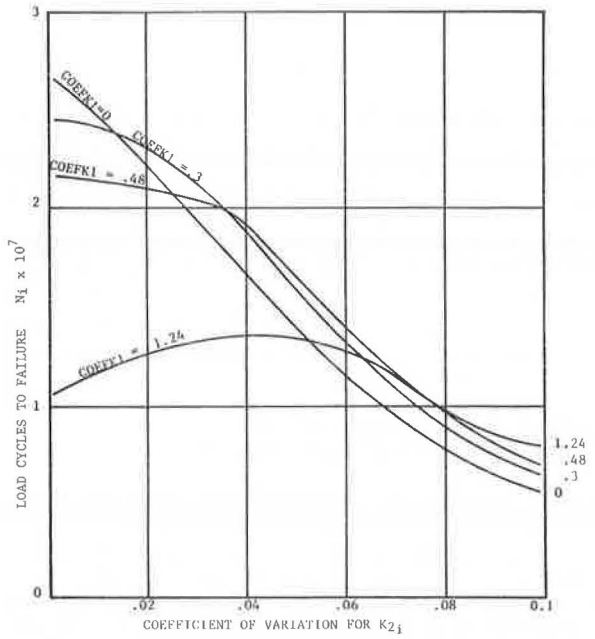

K_{1_i} and K_{2_i} are affected by variations in mix and compaction.

A stochastic formulation was developed by Moavenzadeh (8) and included in VESYS II as follows:

$$E[D_j] = \sum_{i=1}^{j} n_i E\left[\frac{1}{N_i}\right] = \sum_{i=1}^{j} \lambda_i (t_i - t_{i-1}) \left\{ \frac{\epsilon_i^{K_{2_i}}}{K_{1_i}} \left[1 + \frac{Var[K_{1_i}]}{(K_{1_i})^2} - \frac{Cov[K_{1_i}, K_{2_i}] \cdot \ln\epsilon_i}{K_{1_i}} + \frac{Var[K_{2_i}] \cdot (\ln\epsilon_i)^2}{2} \right] + \frac{K_{2_i}(K_{2_i} - 1)\, \epsilon_i^{(K_{2_i}-2)}\, Var[\epsilon_i]}{2K_{1_i}} \right\} \quad (3)$$

where

Var = variance;
Cov = covariance; and
$E[D_j]$ = expected value of the Taylor series expansion for D_j about the means of K_{1_i}, K_{2_i}, and ϵ_i.

The variance of D_j can be obtained in a similar fashion by taking the second moment about the mean of the Taylor series expansion.

D_j is assumed to be the value of a normally distributed random variable with mean $E[D_j]$ and $Var[D_j]$ as shown in Figure 6. The cumulative distribution function (cdf) for this variable at a point D_0 is

$$F(D_0) = \int_{-\infty}^{D_0} f(t)\, dt = (2\pi\, Var[D_j])^{-1/2} \int_{-\infty}^{D_0} \exp\left\{ \left[-\frac{(t - E[D_j])^2}{2\, Var[D_j]} \right] \right\} dt \quad (4)$$

where

$f(t)$ = probability density function of damage at the point t (assumed normal), and
$F(D_0)$ = cdf of damage at the point D_0.

$F(D_0)$ can be interpreted as the probability that the

Figure 8. Function $1/N_i$ and its second-order Taylor series approximation about the means of K_{1_i}, K_{2_i}, and ϵ_i.

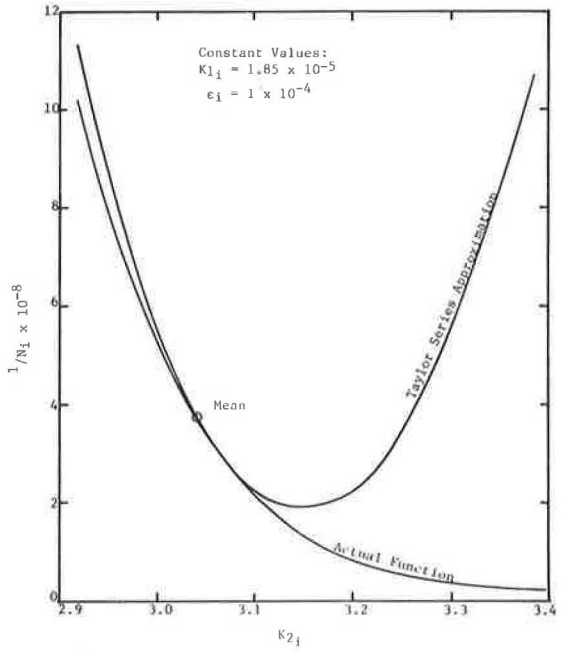

damage index of an arbitrary square meter of the pavement surface is less than or equal to D_0. Hence, under Miner's hypothesis, F(1) is the probability that the specimen has not failed (does not exhibit cracking distress). Therefore,

$$C = 1000 [1 - F(1)] \quad (5)$$

where C = expected area cracked in square meters per m^2 (square yards per 1000 yd^2).

The effects of using equation 3 are shown in Figure 7 in terms of expected load applications at a specific unit strain level of 0.0001 and with a covariance of K_{1_i} and K_{2_i} of -0.86. The degree of variability is shown as coefficients of variation for K_{1_i} and K_{2_i} (called COEFK1 and COEFK2). The ranges shown are considered to be rational based on study of limited data. Note that the range of variation for K_{1_i} is much greater than that for K_{2_i}.

The value of N_i of 26 700 000 load cycles (intercept of COEFK1 = 0 curve at COEFK2 = 0) is the prediction for the mean values of $K_{1_i} = 1.85 \times 10^{-5}$ and $K_{2_i} = 3.04$. The stochastic formulation of equation 3 results in severely decreased fatigue life predictions as the coefficients of variation of K_{1_i} and K_{2_i} increase. Increasing variations in K_{1_i} decrease the expected fatigue life if K_{2_i} is constant but tend to compensate for some of the decrease due to variability in K_{2_i} as that variability increases.

The cause of the surprisingly large decreases in expected fatigue life was investigated, and the Taylor series expansion was found to be a very poor approximation of the function $1/N_i$ except when very near the means of K_{1_i}, K_{2_i}, and ϵ_i. The function $1/N_i$ decreases as an inverse exponential function of K_{2_i} (K_{1_i} and ϵ_i held constant); the value of the Taylor series expansion of the function $1/N_i$ varies as a quadratic function of K_{2_i} (Figure 8).

Estimates of cracking obtained from equations 3, 4, and 5 quite likely are biased by the assumption that damage index D(j) is normally distributed. D_j might be better approximated by a lognormal distribution more typical of fatigue relationships.

Although equation 3 and f(t) in equation 4 appear to require more development, the stochastic concept itself offers considerable improvements in damage predictions and should be pursued vigorously.

CONCLUSIONS

Improved techniques for predicting life have been developed that may be used to obtain more rational predictions of fatigue damage to asphalt concrete pavements. These include (a) fatigue relationships based on tests more simulative of real conditions or analysis based on AASHO experience, (b) a rational procedure for modifying K_{1_i} and K_{2_i} to better consider the effects of temperature on damage accumulation, and (c) stochastic concepts for considering the effects of material and strain variability in fatigue performance.

It appears to us that more rational damage predictions may be obtained by using fatigue relationships within the range of those shown in Figure 1 for the WTT results and the AASHO-based relationships. Such values of K_{1_i} and K_{2_i} can be varied with temperature as discussed by using Figure 3b for K_{1_i} and equation 2 for K_{2_i} for improved consideration of temperature effects.

The stochastic formulation, although sound in concept, cannot as yet be used at a sufficiently high confidence level unless the variation from the mean is slight or considered to be zero. Additional development is required. Rational values for the individual variability of K_{1_i}, K_{2_i}, and ϵ_i and the covariance of K_{1_i} and K_{2_i} are generally unavailable except on a gross basis and the question of applicability of normal distribution versus lognormal or some other distribution is not resolved. The development of a more suitable stochastic formulation and more data on variability of the parameter should significantly improve damage prediction capabilities.

ACKNOWLEDGMENTS

The research was conducted by Austin Research Engineers, Inc. We wish to thank the sponsor, the Federal Highway Administration. The opinions, findings, and conclusions expressed in this publication are ours and not necessarily those of the Federal Highway Administration.

REFERENCES

1. R. I. Kingham and B. F. Kallas. Laboratory Fatigue and Its Relationship to Pavement Performance. Proc., 3rd International Conference on Structural Design of Asphalt Pavements, London, 1972.
2. P. S. Pell and I. F. Taylor. Asphaltic Road Materials in Fatigue. Proc., AAPT, PRPTA Vol. 38, 1969.
3. J. M. Kirk. Results of Fatigue Tests on Different Types of Bituminous Mixtures. Proc., 2nd International Conference on Structural Design of Asphalt Pavements, 1967.
4. M. W. Witczak. Design of Full-Depth Asphalt Airfield Pavements. Proc., 3rd International Conference on Structural Design of Asphalt Pavements, London, 1972.
5. W. Van Dijk. Practical Fatigue Characterization of Bituminous Mixes. Paper presented at 1975 Annual Meeting of AAPT, Phoenix, Feb. 1975.
6. Development of New Design Criteria for Asphalt Concrete Overlays of Flexible Pavements. Austin Research Engineers, Inc., Preliminary Rept. FH2/1, June 1975.
7. R. I. Kingham. Failure Criteria Developed From

AASHO Road Test Data. Proc., 3rd International Conference on the Structural Design of Asphalt Pavements, London, 1972.
8. F. Moavenzadeh. Stochastic Model for Prediction of Pavement Performance. TRB, Transportation Research Record 575, 1976, pp. 56-72.
9. M. G. Sharma and W. J. Kenis. Evaluation of Flexible Pavement Design Methodology. Paper presented at Annual Meeting of AAPT, Phoenix, Feb. 1975.

Pavement Response and Equivalences for Various Truck Axle and Tire Configurations

Ronald L. Terrel and Sveng Rimsritong, Department of Civil Engineering, University of Washington

Many changes in allowable loading and operating procedure for trucks are under consideration in Washington and other states. For example, dual tires and single "flotation" tires for heavy truck loads may have varying damaging effects on pavements. Furthermore, at least for asphalt pavements, time of year and vehicle speed may also influence the analysis for special heavy load permits. This paper is a brief attempt to consider some of these variables on a relative basis. This paper is intended to be a limited approach to answer several pertinent questions from a theoretical study based on hypothetical pavements and loads and also on reasonable material characteristics and pavement behavior from previous research. The computer program was used to compute structural behavior. Maximum allowable numbers of load applications were determined by use of known fatigue and failure design curves. The results are a series of relationships based on pavement life that can be used to determine any number of equivalences. These equivalences can be used to compare the relative destructive effects of various sizes of single and dual tires, axle loads, pavement thicknesses, speeds, and temperatures. The general nature of these relationships provides a wide range of conditions for comparison. Within reason, interpolation is valid. One must keep firmly in mind, however, that these relationships are for assumed conditions (although reasonable) and do not represent actual pavements.

Indications are that many trucks now have front axle loads approaching the maximum allowable for single axles [8.16 Mg (18 kips) in the state of Washington]. That these loads are on single tires increases the potential for pavement damage. In addition, many changes in allowable loading are under consideration in other states. For example, substituting single "flotation" tires for dual tires on heavy truck loads may have varying damaging effects on the pavements. Furthermore, at least for asphalt pavements, time of year and vehicle speed may also influence analysis for special heavy load permits. This paper is a brief attempt to point out the relative effects of some of these variables.

Most of the past studies deal only with relationships between dual-tired single axles and dual-tired tandem axles. Therefore, this study examines relative destructive effect of the single tire versus dual tires and especially the effect of the wide single tire (super single or flotation tire) versus conventional dual tires.

Although this paper is not intended to be a state-of-the-art approach, it is a summary of a larger study (1) based on hypothetical pavements (with reasonable material characteristics and pavement behavior determined from previous research) and loads to answer several pertinent questions by means of current technology. The results are a series of behavior-response relationships based on pavement life. One can use them to determine any number of equivalences of relating variables based on a certain set of conditions.

Basic variables considered in this study include

1. Wheel load,
2. Tire contact pressure and width,
3. Thickness and nature of pavement layers,
4. Speed of vehicle, and
5. Pavement temperature.

A three-layer pavement structure with an asphalt concrete (AC) surface, untreated aggregate base (UTB), and natural soil subgrade was selected for this study. Multilayered elastic theory is used to compute structural response.

The deflections, stresses, and strains are computed by using the Chevron n-layer computer program. The horizontal tensile strain at the bottom of the asphalt-treated layer and the vertical compressive strain at the top of the subgrade are examined in determining the maximum number of load applications to failure (Figure 1). Maximum strains, especially in the thin pavement layers, can occur directly under one of the dual wheels rather than midway between them.

The maximum number of load applications N is determined (a) from criteria developed from laboratory fatigue tests on asphalt to minimize pavement cracking from repeated loading and (b) from criteria developed by Shell Oil Company to minimize surface rutting caused by overstressing the subgrade.

Fatigue and rutting equivalences are established based on the maximum number of standard axle load applications. These equivalences can be used to compare the destructive effects of various sizes of single and dual

Publication of this paper sponsored by Committee on Flexible Pavement Design.

tires and various axle loads.

The effects of changes in the level of temperature and variation in vehicle speeds on fatigue in terms of the maximum number of load applications are also examined.

BACKGROUND INFORMATION

As noted by a number of researchers, the assumption that pavement responds as a layered elastic system appears reasonable at this time. Several computer solutions are available; CHEV 5L was selected for this project to facilitate determination of the stresses. When using such solutions for material response characteristics that depend on stress, one must use an iterative type of solution for pavement sections containing a granular material.

Material Characteristics

In general, asphalt materials are viscoelastic; therefore, their stress-strain characteristics are dependent on both time of loading and temperature. A number of experimental methods have been developed to describe the relationship between stress and strain for asphalt mixes (2). For this study, the resilient modulus for typical Washington mixtures was used and was confirmed by the stiffness concepts of Van der Poel (3) and Heukelom and Klomp (4).

For untreated granular materials and untreated materials such as the subgrade, a measure of stiffness termed the resilient modulus can be determined from

1. The resilient modulus test by using repeated load triaxial apparatus (5),
2. The California bearing ratio test (6), and
3. The repeated plate load test (7).

In this study, data from the Washington State University test track studies (8) and other tests of typical Washington materials (9) were used for the subgrade and base layers. Other materials and localities would require appropriate adjustments.

Distress Criteria

Fatigue has been defined as the phenomenon of fracture under repeated or fluctuating stress and has a maximum value generally less than the tensile strength of the material. Stiffness plays a predominant role in determining the fatigue behavior of asphalt mixes, and maximum principal strain is a major determinant of fatigue crack initiation.

In practice, pavements are subjected to a range of loadings. In accordance with that, a cumulative damage hypothesis is required because fatigue data are usually determined from the results of simple loading tests. One of the simplest of such hypotheses is the linear summation of cycle ratios. Fatigue life prediction under compound loading becomes a determination of the time at which this sum reaches unity.

Numerous studies have been conducted to evaluate the fatigue behavior of AC, and data are available for materials similar to those used in Washington (10). These data were used as the basis for cumulative fatigue damage due to truck traffic.

The other mode of failure considered in this study is permanent deformation, more commonly called rutting. Structural failure due to rutting can occur in one or more pavement layers. Recent research has shown that rutting in the asphalt layers can be predicted reasonably well. This failure mode may be particularly important for thick asphalt sections in hot climates.

A somewhat broader approach to rutting failure is used in the Shell design method (11) as well as in this study. A critical subgrade stress-strain level beyond which the rutting is extended into the subgrade soil appears to exist. For example, if the vertical subgrade strain does not exceed the critical level, ruts due to subgrade failure are not formed. From experience in Washington, rutting failure is not a significant factor, but it was used here to illustrate the different failure modes that the highway engineer must guard against.

Other Factors

Pavement temperatures can be computed from weather data by solving the heat conduction equation by numerical technique, such as finite-difference procedure or finite-element procedure, or by closed form techniques as presented by Barber (12). As an alternative, a representative temperature can be estimated by one of several methods. As indicated, fatigue life is dependent on the asphalt stiffness, and temperature changes throughout the year will affect the analysis of pavement life accordingly. For the limited example in this paper, reasonable pavement temperatures were assigned and computations of pavement life were made to show this relative effect.

In addition to temperature, speed of the moving vehicle has often been considered to affect stresses induced in the pavement and ultimately the pavement life. To illustrate this factor, we considered only the change in stiffness of asphalt as caused by variable rates of loading. For the sake of simplicity, the other pavement layers were assumed to be unaffected.

COMPUTATIONS

Various wheel loads and tire widths to be considered as input variables in the computer analysis were suggested by the Washington Department of Highways. Although the tire-pavement pressure interface is generally known to be somewhat complex and affected by tire design, simplifying assumptions were made to accommodate the CHEV 5L program. These include a circular contact area with tire pressures equal to the contact pressure. Various tire pressure were calculated by dividing the wheel load by a reasonable contact area.

Several thicknesses of pavement structure have been selected: 7.62, 15.24, and 24.13 cm (3, 6, and 9.5 in) of asphalt concrete surface on 20.32 cm (8 in) of untreated base. The subgrade layer is assumed to be semiinfinite.

The types of material in each layer of the pavement structure were selected for this study based on the availability of the laboratory and field test data in combination with whether they were common in Washington. Those chosen are class B wearing course, untreated aggregate base, and the natural undisturbed clay subgrade soil.

The CHEV 5L computer program (13) was used to calculate the stresses, strains, and deflections. The effect of the dual load on any point is then determined by linear superposition of the effects of each of the loads at the point in question. The application of superposition implies linear response; thus use of this principle is an approximation of the dual wheel load.

The computational procedure includes several iterative steps. The summary for a particular computation is made up of seven steps.

1. Select thickness of each layer.
2. Estimate modulus and Poisson's ratio for each layer.

3. Select wheel load and contact area (radius of circular area of contact with pavement).
4. Select points for calculation of stresses, strains, and displacements. These will usually include depths ranging from the surface downward at least into the subgrade. Points are selected radially from the center of load sufficiently far away to include the adjacent dual tire if any. Preliminary calculations indicated that tires at the opposite end of the axle from those under consideration do not contribute significantly.
5. Following computer calculation, select appropriate values from the printout and compare them to the material behavior data. If the required moduli are not within the given range, they are adjusted and the computation repeated until reasonable agreement is attained. When dual tires are used, the additive values are used for this comparison so that maximum values are always considered.
6. When agreement is attained, use the final iteration as representative of that combination of load and pavement response.
7. Repeat steps 1 through 6 for each combination of load, tire width, pavement thickness, and the like.

EQUIVALENCE DETERMINATION

Surface deflection is often a good indicator of pavement behavior changes, but cannot of itself be readily related to performance over a wide range of conditions. Therefore, the main concern here will be with radial tensile strain on the bottom of asphalt concrete layers as it relates to fatigue cracking or failure. In addition, vertical compressive strain on the subgrade is examined with respect to its relationships to limiting rutting in the pavement structure.

By using the computed data, we evolved a series of steps to reduce these data to a form directly applicable to pavement life. This was a relatively straightforward but time-consuming procedure to eventually arrive at the primary relationships shown in Figures 2 and 3.

Fatigue

A complete and reasonably convenient summary of all the data is shown in Figure 2. In this figure, the relative number of applications of a particular load or combination of loads can be determined. As a basis for comparison in establishing Figure 2, a "standard" condition was defined as an 8.16-Mg (18-kip) axle load with 25.4-cm-wide (10-in-wide) dual tires on a pavement with 15.24 cm (6 in) of asphalt concrete. Thus this point on Figure 2 has an equivalence equal to unity. With the data normalized in this manner, any two points can be compared (divided) directly by using the relative equivalences on the vertical scale.

Rutting

In a manner similar to that used for fatigue, Figure 3 has been prepared as a summary of all the combined data for rutting behavior. Use of these data is similar to the use of those for Figure 2. Any two points can be compared in terms of their relative life to failure by their ratio or equivalence.

Climate (Temperature)

For the average case, 20.3°C (68.5° F) was assumed to be the temperature for AC at all depths. However, a range of temperatures is known to be encountered (for example, during the summer and winter months). A profile of temperature within the AC for these pavements was estimated from weather data.

Because of the excessive computations and analysis required, the effect of temperature on pavement behavior is limited to the case for 25.4-cm-wide (10-in-wide) dual tires, 8.16-Mg (18-kip) axle loads, and the usual range in asphalt concrete thickness appropriately adjusted for stiffness by sublayers. By using the same fatigue criteria as before, we determined and plotted the number of load applications to failure in the format shown in Figure 4. These data are for 8.16-Mg (18-kip) axle loads only, but they can be extrapolated to include other axle loads by using the linear nature of curves in Figure 2.

Vehicle Speed

Speed analysis has also been limited to the standard 8.16-Mg (18-kip) axle load with 25.4-cm-wide (10-in-wide) dual tires. Using the 25.4-cm-diameter (10-in-diameter) contact area between tire and pavement as the contributing loaded area, we assumed the wheel to be rolling at a range of speeds. These speeds were converted to load duration. These loading times were used to determine stiffness of the AC based on the principles of Van der Poel (3) and calculated for a particular mix as was done by Monismith, Alexander, and Secor (14) and from data on Washington mixtures (15).

By use of fatigue data, the relative effect of speed on the number of applications of load to failure is shown in Figure 5. Although the basic equivalence relationships shown earlier in Figures 2 and 3 did not indicate a speed, most of the stiffness data were developed for testing load duration of about 0.5 s [about 16 km/h (10 mph)]. The user of these data should be cautioned, however, that only relative values should be compared and not actual load applications to failure, for example.

SUGGESTED USE AND APPLICATIONS

Appropriate use and recognition of the limiting factors in this study are very important. The user must realize that comparisons among the variables considered are only relative and should not be used for actual pavement life predictions, for example. This approach is predicated on the fact that computed data are based on hypothetical pavements, although they are reasonable approximations of typical pavements constructed in Washington.

By means of the key relationships developed herein, one can use Figures 2 through 5 to determine a wide range of equivalences as illustrated in the form of examples or typical situations.

Example 1

Problem

Compare the relative pavement fatigue life expectance of a 7.62-cm (3-in) asphalt pavement when subjected to an 8.16-Mg (18-kip) axle load with 25.4-cm (10-in) dual tires and with 47-cm (18.5-in) single flotation tires.

Solution

From Figure 2, the relative lives for the dual and single cases are 250×10^{-3} and 180×10^{-3} respectively. Therefore, the equivalence of these two is $(250 \times 10^{-3})/(180 \times 10^{-3}) = 1.38$. That is, the single tire would be 38 percent more damaging in terms of fatigue.

One should note that these equivalences are compared for conditions that are constant except for those being compared.

Figure 1. Location of critical strains in pavement.

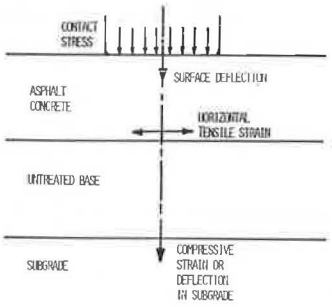

Figure 2. Relative pavement life to failure for a range of loads and pavements based on fatigue of AC layer.

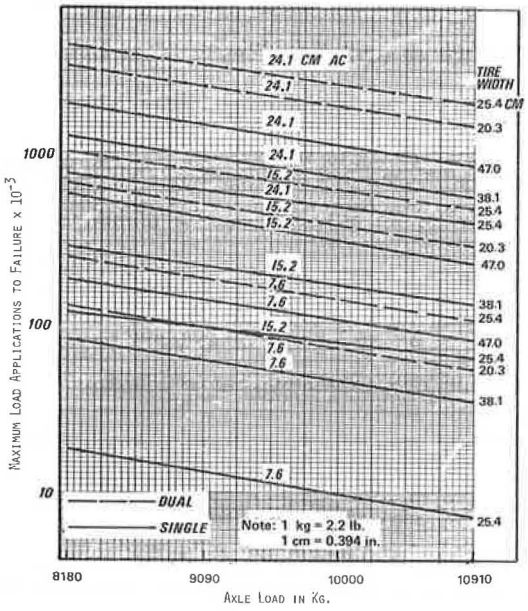

Figure 3. Relative pavement life to failure for a range of loads and pavements based on rutting of subgrade.

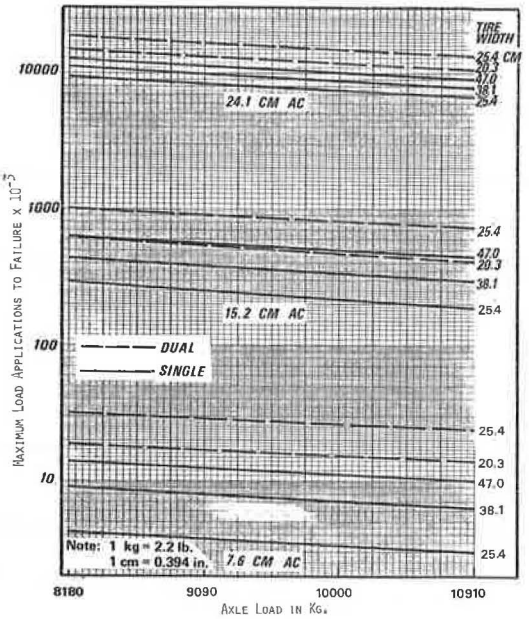

Example 2

Problem

Determine the equivalence for the same loads as in example 1 but in terms of rutting distress.

Solution

From Figure 3, for 7.62-cm (3-in) AC, $N = 32 \times 10^{-3}$ for dual tires and $N = 14 \times 10^{-3}$ for single tires. The equivalence would then be $(32 \times 10^{-3})/(14 \times 10^{-3}) = 2.3$ for rutting damage, which means that the pavement will last 2.3 times longer under dual tires.

Assuming that the pavement was originally designed to preclude failure over a reasonable design life, one can compare the two examples. By changing the 8.16-Mg (18-kip) axle load from dual to single tires as illustrated, the pavement life will be shortened when one considers both fatigue and rutting. From this analysis, one would expect fatigue to be more critical.

Figure 4. Relative pavement life of AC for summer and winter conditions when vehicles have 8.16-Mg (18-kip) axles and 25.4-cm-wide (10-in-wide) dual tires.

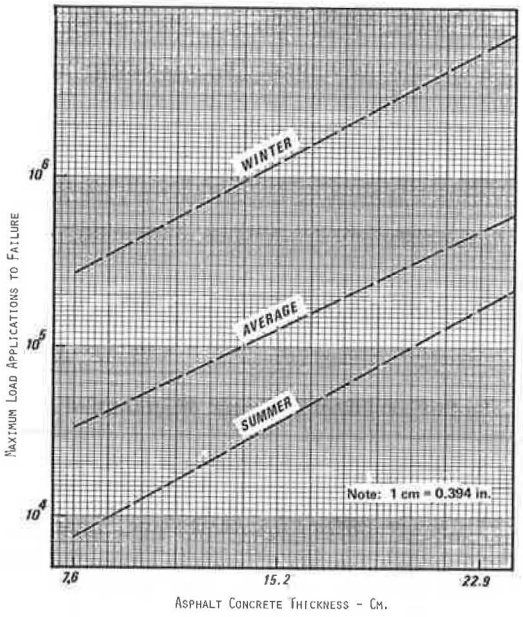

Figure 5. Relative pavement life of AC for range of vehicle speeds when vehicles have 8.16-Mg (18-kip) axles and 25.4-cm-wide (10-in-wide) dual tires.

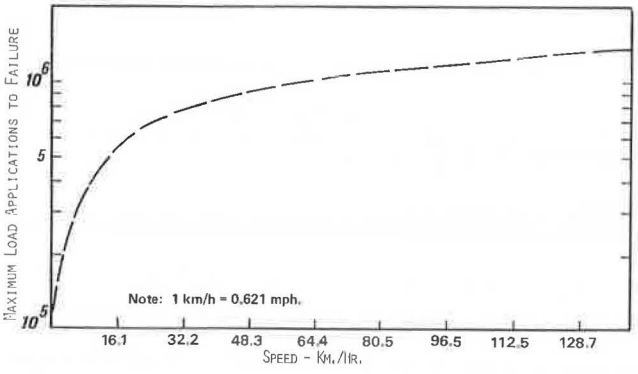

Example 3

Problem

What is the difference for summer and winter conditions as determined by using the results from example 1?

Solution

From example 1, the equivalence was equal to 1.38 and this can be considered the "average" condition in Figure 4. The actual equivalence between 25.4-cm (10-in) dual tires and 47-cm (18.5-in) single tires would remain about the same, but actual life to failure (for a particular case) would need to be adjusted. From Figure 4, summer, average, and winter applications for 7.62-cm (3-in) AC would be 7.4×10^3, 3.3×10^4, and 2.7×10^5 respectively. Therefore, pavement life could be expected to be increased by $(2.7 \times 10^5)/(3.3 \times 10^4) = 8.2$ times in winter and decreased by $(3.3 \times 10^4)/(7.4 \times 10^3) = 4.5$ times in summer.

One must realize, however, that the actual range of winter to summer temperatures are distributed throughout the year, month by month, and a weighted average would be more realistic. The data in Figure 4 are primarily for illustrative purposes and show that because of higher stiffness of AC in winter, it is more resistant to fatigue cracking.

Example 4

Problem

What is the effect of reducing average truck speed from 112.6 to 88.5 km/h (70 to 55 mph) as determined by using the results from example 1?

Solution

The curve in Figure 5, although developed for the "standard" load, can be used for general speed comparisons. At 112.6 km/h (70 mph), load application to fatigue cracking is 1.25×10^6. At 88.5 km/h (55 mph), this value is 1.15×10^6. Therefore, pavement life is reduced by a factor of $(1.15 \times 10^6)/(1.25 \times 10^6) = 0.92$, or 8 percent.

Example 5

Problem

A special highway user requested permission to use a 4.8-km (3-mile) segment of highway for trucks having average single axle loads of 10.89 Mg (24 kips) and 47-cm (18.5-in) single flotation tires. The existing pavement is 7.62 cm (3 in) of AC, and other conditions are similar to those developed in this report. What change in pavement would be required to provide equivalent pavement life compared to the standard 25.4-cm (10-in) dual tire and 8.16-Mg (18-kip) axle load case?

Solution

Provide an AC overlay. Locate the given conditions on Figure 2 [10.89-Mg (24-kip) axle load, 47-cm (18.5-in) single tire, and 7.62 cm (3 in) of AC pavement]. This point is approximately 82×10^{-3} on the vertical equivalence scale. Next, locate the "standard" condition [8.16-Mg (18-kip) axle load, 25.4-cm (10-in) dual tire, and 7.62 cm (3 in) of AC]. This point is approximately 250×10^{-3}. That is, pavement thickness must be increased sufficiently to increase the 82×10^{-3} to 250×10^{-3}.

By examining the family of AC thickness curves [7.62 cm (3 in), 15.24 cm (6 in), and 24.13 cm (9.5 in)], one can interpolate any point in between. Therefore, by moving vertically along the 10.89-Mg (24-kip) axle load line from 82×10^{-3} to 250×10^{-3}, one can interpolate the AC thickness as being approximately midway between the 7.62-cm (3-in) and 24.13-cm (9.5-in) curves or 15.75 cm (6.2 in). This indicates that 15.75 cm (6.2 in) is required and 7.62 cm (3 in) is existing (assuming it is new); therefore, an 8.13-cm (3.2-in) overlay of this 4.8-km (3-mile) section would be required to make it equivalent to the adjoining highway that will receive "standard" traffic.

Additional solutions may be more appropriate depending on the conditions.

1. Add axles to reduce average axle weight.
2. Change to dual tires. [Figure 2 does not include large enough dual tires—27.94 cm (11 in) or 30.48 cm (12 in) would be required by extrapolation but may not be practicable.]
3. Combine solutions 1 and 2.

For larger special loading, the speed may be reduced considerably and this should be considered in the equivalence evaluation. Furthermore, the time of year may be a factor—special hauling may be seasonal and compensation for temperature correction may increase or decrease the equivalency.

SUMMARY AND CONCLUSIONS

This study was initiated in an attempt to examine relative destructive effects of wide single and conventional dual tires on pavements. Basic variables are wheel load, tire width, and AC thickness. Based on available laboratory and field data, three pavement layers consisting of AC surface, untreated aggregate base, and clay subgrade were selected as the materials for this study. The CHEV 5L program was used to compute deflections and critical strains. Prior to determining the fatigue and rutting equivalences, we compared maximum computed deflections and critical strains with other sources. These experimental data seem to agree reasonably well. By using known fatigue and failure design curves, we determined maximum allowable numbers of various axle load applications. Fatigue and rutting equivalence relationships for various axle loads are established by dividing the maximum number of axle load applications by the maximum applications of 8.16-Mg (18-kip) axle loads on an AC thickness of 15.24 cm (6 in) when dual 12.7-cm (5-in) tires are used. These equivalences, shown in Figures 2 and 3, can be used to compare the relative pavement life when subjected to various sizes of single and dual tires and axle loads.

The effects of variation in temperature between summer and winter were also examined. It can be said that, as temperature decreases, pavement structure rigidity increases, thus causing a decrease of vertical stress and thereby permitting a greater number of load applications. As shown in Figure 4, the destructive effect of a vehicle on the pavement during the summer is much greater than in winter, exclusive of spring frost breakup conditions and other soil-moisture variations.

The effect of variation in vehicle speed on the pavements was also briefly considered. In general, slower speed tends to cause longer load duration, resulting in an increase in vertical stress and thereby permitting fewer load applications to failure as shown in Figure 5. This figure can be used to compare the relative pavement life at various speeds as illustrated by the solution to the problem in example 4.

The general nature of Figures 2 through 5 provides a

wide range of conditions for comparison on a relative basis. Within reason, interpolation is valid. One must keep firmly in mind, however, the fact that these relationships are for assumed conditions (although reasonable) and do not represent actual pavements. Comparison must be made on a relative basis and not according to actual pavement life as shown in load applications to failure.

On the basis of this study, several conclusions appear warranted.

1. Single wide flotation tires are generally more destructive than dual tires with equivalent contact area.
2. Wide flotation tires require a thicker asphalt pavement than dual tires do.
3. Pavement requirements for both wide single and dual tires increase at about the same rate as total axle load increases.
4. Pavement life in terms of fatigue is at least an order of magnitude greater in winter than in summer for the conditions of this study.
5. Pavement life is increased directly with speed of the vehicle if all other factors are equal.

ACKNOWLEDGMENT

We wish to thank the Washington Department of Highways and the Federal Highway Administration for their support of this study.

REFERENCES

1. R. L. Terrel and S. Rimsritong. Pavement Response and Equivalencies for Various Truck Axle-Tire Configurations. Washington Department of Highways, Olympia, Research Rept. 17.1, Nov. 1974, 106 pp.
2. R. L. Terrel and I. S. Awad. Symposium on Technology of Thick Lift Construction—Laboratory Considerations. Proc., AAPT, Cleveland, Feb. 1972.
3. C. Van der Poel. A General System Describing the Viscoelastic Properties of Bitumins and Its Relation to Routine Test Data. Journal of Applied Chemistry, May 1954.
4. W. Heukelom and A. J. G. Klomp. Road Design and Dynamic Loading. Proc., AAPT, Dallas, Feb. 1964.
5. Full-Depth Asphalt Pavements for Air Carrier Airports. Asphalt Institute, College Park, Md., Manual Series 11, Jan. 1973.
6. W. Heukelom and C. R. Foster. Dynamic Testing of Pavements. Trans., ASCE, Vol. 127, Part 1, 1962, pp. 425-427.
7. Soils Manual for Design of Asphalt Pavement Structures. Asphalt Institute, College Park, Md., Manual Series 10, May 1964.
8. R. L. Terrel. Analysis of Ring No. 2, WSU Test Track. Asphalt Institute, College Park, Md., Dec. 1968.
9. D. A. Voss and R. L. Terrel. Structural Evaluation of Pavements for Overlay Design. HRB, Special Rept. 116, 1971, pp. 199-211.
10. J. A. Epps and C. L. Monismith. Influence of Mixture Variables on the Flexural Fatigue Properties of Asphalt Concrete. Feb. 10, 1969.
11. J. O. Izatt, J. A. Letter, and C. A. Taylor. The Shell Group Methods for Thickness Design of Asphalt Pavements. Shell Oil Co., Jan. 1-3, 1967.
12. E. S. Barber. Calculation of Maximum Pavement Temperatures from Weather Reports. Bureau of Public Roads.
13. J. Lysmer and J. M. Duncan. Stress and Deflections in Foundations and Pavement. 4th Ed., Univ. of California, Berkeley, 1969.
14. C. L. Monismith, R. L. Alexander, and K. E. Secor. Rheologic Behavior of Asphalt Concrete. Proc., AAPT, Minneapolis, Vol. 35, Feb. 1966.
15. R. L. Terrel and I. S. Awad. Resilient Behavior of Asphalt Treated Base Course Materials. Washington Department of Highways, Research Rept. 6.1, Aug. 1972.

Abridgment

Fatigue Criteria Development for Flexible Pavement Overlay Design

Harvey J. Treybig and Fred N. Finn, Austin Research Engineers, Inc.
B. F. McCullough, University of Texas at Austin

The need for general design criteria for asphalt concrete overlays has existed for many years. The boom in new pavement construction during the late 1950s and the 1960s neglected the existing primary and secondary highway systems in many states. Furthermore, many of the Interstate highways constructed during that time are also now in disrepair. Changes in legal loadings for trucks may have an immediate impact on the serviceability of pavements, which emphasizes the need for rational criteria applicable on a nationwide basis.

METHODOLOGY FOR ESTABLISHING NEW CRITERIA

The procedure for establishing new criteria must be general, flexible, and capable of being updated as research findings evolve that are implementable. In a recent study, an overlay design procedure was developed that is a first generation of this type of necessary analysis model (1). The methodology selected in this study consists of two basic considerations: use of elastic layered theory as an analysis method and use of field studies at the American Association of State Highway Officials (AASHO) (now the American Association of State Highway and Transportation officials) Road Test site as a data base.

Elastic Layered Theory as Analysis Method

To create an overlay procedure with a minimum of empiricism, we selected elastic layered theory as the basic analysis method (2). The use of layered theory offers the best potential for developing a universal design procedure applicable to the many existing conditions. Local conditions may be considered through materials characterization in applying this mechanistic analysis approach.

Publication of this paper sponsored by Committee on Design of Composite Pavements and Structural Overlays.

Field Studies at the AASHO Road Test Site

The AASHO Road Test and its now in-service pavement sections were used to develop updated asphalt concrete overlay design criteria. Many of the test sections were overlaid during the road test and again after the completion of the road test.

Since the completion of the road test in 1962, the Illinois Division of Highways has maintained an inventory of the surface condition and performance of the test sections, which provided a large data base for this study. The field studies included deflection testing, rutting measurements, roughness measurements, condition surveys, and materials sampling, all of which formed the data base for the fatigue criteria development.

CHARACTERIZATION OF AASHO PAVEMENT SECTIONS

The AASHO flexible pavement sections were sampled, and all materials were tested for their quasi-elastic moduli (3). The laboratory modulus values were used together with layered theory to compute deflections, stresses, and strains. Also effective modulus of elasticity values for asphalt concrete were determined for various degrees of cracking through the use of analytical techniques.

Base and Subbase

The base and subbase modulus values were based on laboratory resilient modulus tests of prepared specimens. Based on the testing and the pavement conditions, the values of the base and subbase materials were established as 137 895 and 68 948 kPa (20 000 and 10 000 lbf/in^2) (4, 5).

Subgrade

The overlay modulus for each section was selected by using the average daily temperature on the day the deflection was measured in conjunction with a laboratory curve relating modulus and temperature (3). This value, together with the base and subbase values, was held constant for the computation of deflection.

The subgrade modulus was determined by matching measured and computed Benkleman beam deflections for 99 AASHO pavement sections. The procedure used was a modification of McCullough's earlier work (6) and is as follows:

1. The initial subgrade modulus value used in the comparison, based on laboratory tests, was 27 579 kPa (4000 lbf/in^2);
2. For sections in which the computed deflections were too high, the modulus was increased and, for those in which it was too low, the modulus was reduced; and
3. Step 2 was repeated until the measured and computed deflections matched an acceptable range.

The acceptable range for step 3 was established by using a study of Benkleman beam deflection measurements by the Utah Department of Highways that showed a coefficient of variation of 17.6 percent (7). A range of ±2 standard deviations was selected to provide the desired confidence level for comparison of the measured and computed deflections. The subgrade modulus values resulting from the matching deflections ranged from 103 421 to 62 053 kPa (15 000 to 9000 lbf/in^2). Reasonable values were selected for Poisson's ratio and were held constant in all analyses.

Asphalt Concrete Modulus of Elasticity

The asphalt concrete modulus for the fatigue studies was selected after carefully considering the AASHO Road Test environmental conditions. A temperature of 21.11° C (70° F) was selected, and the overlay modulus should correspond to an asphalt concrete at 21.11° C (70° F). By using a laboratory curve of asphalt modulus versus temperature (1), we selected a modulus of 3 171 588 kPa (460 000 lbf/in^2).

Effective Asphalt Concrete Modulus

An effective modulus of elasticity was evaluated for the asphalt concrete to reflect the condition or degree of cracking present in existing asphalt concrete surfaces. Cracking on flexible pavement sections at the road test was divided into class 2 and class 3 cracking. Class 2 cracking is defined as cracking that has progressed to the point where cracks have connected together to form a grid pattern. Class 3 cracking is when the asphalt concrete segments have become loose (7). For the pavement condition in which class 2 or class 3 or both types of cracking existed, the modulus of the base and subbase layers was reduced because of advanced moisture migration. Depending on the severity of cracking, the modulus was reduced for the surface layer to account for loss in structural support. The explanation and the amount of reduction of the moduli values are described elsewhere (3). For the condition where no cracking existed, the laboratory value was used for the asphalt concrete.

Analyses documented elsewhere (1) yielded the following modulus values for use in computation of strains for the development of the fatigue equation (1 kPa = 0.145 lbf/in^2):

Pavement Condition	Asphalt Concrete Surface Modulus
Uncracked	Same as overlay modulus
Class 2 cracking	482 633 kPa
Class 3 cracking	137 895 kPa

FATIGUE DESIGN CRITERIA DEVELOPMENT

The following paragraphs describe the analyses made on the AASHO Road Test flexible pavement sections and the assumptions made to properly tie together the elastic layer theoretical analysis and the pavement behavior observations.

Strain Computations

The critical strain computed by computer program ELSYM5 (2) was defined as the largest normal transverse tensile strain parallel to the load axle that occurred either between or under two 2041-kg (4500-lb) wheel loads (simulating dual tires). For the uncracked surface, the critical strain was computed at the bottom of the original surface; for the cracked condition, the critical strain occurred at the bottom of the overlay. The strains from the 27 AASHO sections along with other pertinent data are given in Table 1.

Traffic

The traffic to the time when cracks first appeared at the top of the asphalt surface was used in the development of the field fatigue curve and was calculated by using AASHO equation 29 (8, p. 83) as follows:

$$\log W_c = 5.484 + 7.275 \log (0.33\ D_1 + 0.10\ D_2 + 0.08\ D_3 + 1) + 2.947 \log L_2 - 3.136 \log (L_1 + L_2) \quad (1)$$

Because weighted 8165-kg (18-kip) equivalent axle loads were used to develop the field fatigue curve, the above equation was reduced to:

$$\log W_{18} = 1.474 + 7.275 \log (0.33\ D_1 + 0.10\ D_2 + 0.08\ D_3 + 1) \quad (2)$$

where W_{18} = number of weighted 8165-kg (18-kip) axle load applications sustained by the pavement before the appearance of class 2 cracking. The traffic W_{18} for the 27 AASHO sections is also given in Table 1.

Final Fatigue Curve

To develop the field fatigue curve, the strains and traffic given in Table 1 were related and a regression analysis was then used to achieve the best fit line. Figure 1 shows the final field fatigue curve, and the equation is as follows:

$$W_{18} = 9.7255 \times 10^{-15} (1/\epsilon)^{5.16} \quad (3)$$

where ϵ = transverse strain. This regression equation had a standard error for residual of 0.298 and an r^2 of 0.9294.

Comparison of New Curve With Lab Curves

Fatigue in highway pavements is generally less severe than in laboratory conditions because of strain relaxation between loads. A comparison was made of laboratory fatigue curves and the fatigue curve developed from AASHO Road Test field data (Figure 2) to investigate the difference in the rate of strain application between highway and lab conditions.

The relationship between the logarithm of tensile strain and the logarithm of fatigue life is essentially linear, but the slope may vary, which indicates that the relationship is material or project dependent (9). There-

Table 1. AASHO sections used for fatigue curve development.

AASHO Section Number	Thickness of Layers (cm)			Weighted Number of 8165-kg Axle Load Applications Before Class 2 Cracking[a]	ELSYM5-Calculated Unit Strain $\times 10^{-6}$
	Surface	Base	Subbase		
710	5.08	7.62	10.16	4 770	273
717	2.54	7.62	10.16	45	367
727	2.54	0	10.16	3	542
755	2.54	15.24	0	26	366
758	5.08	15.24	0	7 250	249
111	5.08	15.24	20.32	137 700	235
140	10.16	15.24	20.32	200 200	163
145	10.16	7.62	0	13 500	241
161	10.16	15.24	0	24 600	193
575	10.16	7.62	30.48	724 700	175
583	10.16	0	10.16	75 100	268
619	10.16	0	20.32	129 700	233
625	10.16	15.24	33.02	724 700	157
427	12.70	22.86	30.48	1 963 000	125
439	12.70	7.62	10.16	149 600	174
445	12.70	15.24	30.48	1 833 000	134
473	10.16	15.24	10.16	149 600	174
477	10.16	22.86	30.48	1 833 000	148
261	12.70	7.62	30.48	1 122 000	148
297	15.24	7.62	20.32	1 418 000	135
319	12.70	7.62	20.32	672 100	158
333	15.24	22.86	40.64	3 862 000	104
336	15.24	7.62	30.48	1 589 000	127
719	2.54	15.24	10.16	122	371
156	7.62	15.24	20.32	108 500	193
325	15.24	15.24	20.32	1 419 000	120
260	12.70	15.24	20.32	672 000	139

Note: 1 cm = 0.394 in, 1 kg = 0.0022 kip.
[a]Calculated by using the AASHO traffic equation (8, equation 29).

Figure 1. Asphalt concrete fatigue curve developed from AASHO Road Test sections.

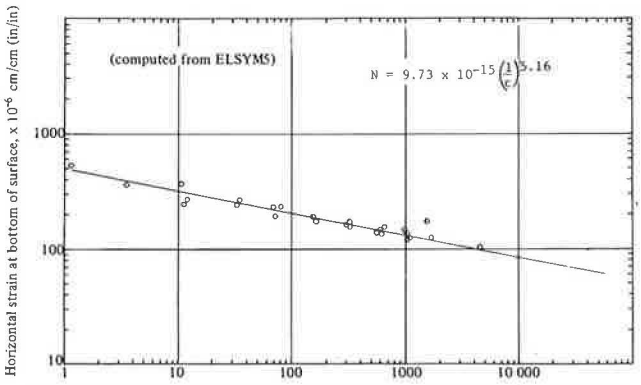

Figure 2. Relationship between bending strain and load applications to failure with varying stiffness.

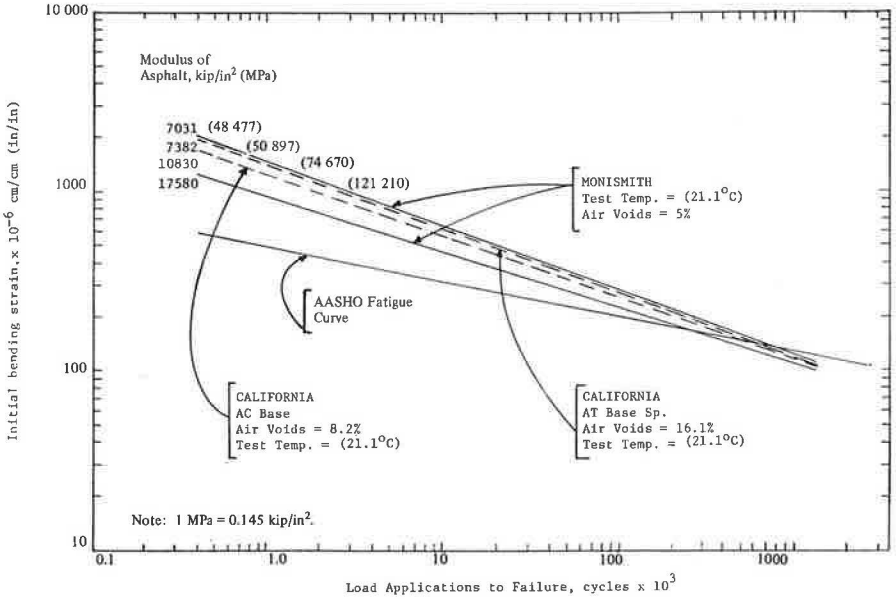

fore, by using AASHO traffic data, a field fatigue curve could be generated that would reduce this dependency or at least tie it more clearly to field conditions.

SUMMARY

A fatigue model based on analyses and observations of numerous different pavement designs has been presented for use in asphalt concrete overlay design. New overlay design procedures are being based on elastic layered theory, and fatigue curve analyses are being based on the analyses mentioned. Thus compatability exists between development and application. The fatigue model presented is based on one asphalt concrete only; therefore, procedures should be investigated to adjust for mix design by using laboratory data.

ACKNOWLEDGMENT

The research was conducted by Austin Research Engineers, Inc. We wish to thank the sponsor, the Federal Highway Administration, U.S. Department of Transportation, for its support in this study.

REFERENCES

1. Design Procedures. In Asphalt Concrete Overlays of Flexible Pavements, Austin Research Engineers, Inc., Vol. 2, Rept. FHWA-RD-75-76, Aug. 1975.
2. G. Ahlborn. Elastic Layered System With Normal Loads. Institute of Transportation and Traffic Engineering, Univ. of California, Berkeley, May 1972.
3. Development of New Design Criteria. In Asphalt Concrete Overlays of Flexible Pavements, Austin Research Engineers, Inc., Vol. 1, Rept. FHWA-RD-75-75, Aug. 1975.
4. G. W. Ring. Drainage and Pavement Rehabilitation. In Pavement Rehabilitation, TRB, Rept. DOT-OS-40022-1, 1974, pp. 171-176.
5. R. G. Hicks. Factors Influencing the Resilient Properties of Granular Materials. Institute of Transportation and Traffic Engineering, Univ. of California, Berkeley, May 1970.
6. B. F. McCullough. A Pavement Overlay Design System Considering Wheel Loads, Temperature Changes, and Performance. Institute of Transporta-

tion and Traffic Engineering, Univ. of California, Berkeley, 1969.
7. G. Peterson and L. W. Shepherd. Deflection Analysis of Flexible Pavements. Materials and Tests Division, Utah Department of Highways, final rept., Jan. 1972.
8. The AASHO Road Test: Report 5—Pavement Research. HRB, Special Rept. 61E, 1962.
9. D. Navarro and T. W. Kennedy. Fatigue and Repeated-Load Elastic Characteristics of In-Service Asphalt-Treated Materials. Center for Highway Research, Univ. of Texas at Austin, Research Rept. 183-2, preliminary review copy, Jan. 1975.

Abridgment

Effect of Pavement Texture on Traffic Noise

Kenneth R. Agent and Charles V. Zegeer, Bureau of Highways, Kentucky Department of Transportation

Noise from highway vehicles primarily comes from engine exhausts, tire-pavement interaction, gears, and rattles. Studies have shown that at high speeds tires become the dominant generators of noise. Measurements on different road surfaces have produced different noise-versus-speed relationships (1). This led to the road surface adjustment used in the noise prediction procedure developed in National Cooperative Highway Research Program (NCHRP) Report 117 (2). This adjustment called for a 5-dBA reduction for smooth surfaces (very smooth, seal-coated asphalt pavement) and a 5-dBA increase for rough surfaces [rough asphalt pavement with voids 12.7 mm (0.5 in) or larger in diameter and grooved concrete]. There was no adjustment for normal surfaces (moderately rough asphalt and concrete pavements).

The surface descriptions are vague, and it is left to the discretion of the user to apply adjustments where applicable. We considered using the term "rough" but abandoned it because it seemed vague and possibly misleading. In addition, various degrees of roughness gave a wide range of noise levels. In fact, the terms "smooth," "normal," and "rough" appear to address only that portion of tire noise generated by drumming or percussion of the tire against knobs in the pavement surface. "Smooth" does not distinguish "smooth and dense" from "smooth and porous." It has been argued that an adjustment of -5 dBA should not be used because some truck tires become excessively noisy on very smooth surfaces and because such surfaces are presumed to be ready for renewal because of their inherent low friction characteristics (3). Minimum noise is believed to be associated with smoothness and optimum porosity. In this report, surfaces are identified according to Kentucky specifications.

Noise data were taken on all major types of surfaces currently used in Kentucky. A reference automobile was used to determine any difference in noise. Strip-chart records were made to evaluate the effect type of road surface had on the noise of the entire traffic stream.

PROCEDURE

Noise data were taken on the 8 types of surfaces, which are given in Table 1. All data were taken at locations having zero grade; the observer was level with the roadway and had no shielding. The distance from the center of the lane tested to the noise-level meter was 50 ft (15 m). The locations were selected to give as great a range in traffic exposure as possible. A precision sound-level meter was used for all measurements; measurements were recorded on a strip-chart recorder.

Two reference cars were used for single-vehicle tests. Care was taken to ensure that no error was introduced in using two different cars. Data were taken at 48, 72, and 97 km/h (30, 45, and 60 mph) at each location when possible. The data taken at 72 km/h (45 mph) were used for direct comparisons because 48- and 97-km/h (30- and 60-mph) tests at all locations could not be obtained. The meter readings were noted by the operator as the reference vehicle passed. Measurements were taken only when the noise from the reference cars could be clearly isolated from the traffic stream. Test runs were made at each speed and until representative measurements were obtained. In all cases, the ground cover between the roadway and observer was short grass. Noise levels were also taken inside the cars at 72 km/h (45 mph). A reference truck was used at one location.

To evaluate the effect of type of surface on the noise of the traffic stream, we compared strip-chart records with predicted values. The measured L_{10} noise level (level exceeded 10 percent of the time) was determined from a 10-min chart record. Noise levels on the chart were read at slightly greater than 1-s intervals in the laboratory by using a digitizing data reduction system and computer cards. The L_{10} noise level was computed. The predicted noise level was determined by the method developed in NCHRP Report 117 (2) but then corrected according to the nomograph developed for Kentucky data (4). No adjustment for type of surface was used in the

Publication of this paper sponsored by Committee on Surface Properties-Vehicle Interaction.

noise prediction. The measured L_{10} noise level was then compared with the predicted level.

RESULTS

Reference Car Noise Measurements

After preliminary testing of several locations in which each type of pavement was involved, a relationship was found between noise level and cumulative traffic. A plot of noise level versus cumulative traffic volume was made for each type of pavement by using the noise level found at 72 km/h (45 mph). A summary of data on noise level versus cumulative traffic for all types of pavement surfaces (except chip seals) is shown in Figure 1. A total of 87 tests at 63 locations were conducted.

Sand asphalt and Kentucky rock asphalt surfaces are the only surfaces that maintained a low noise level (about 66 dBA) with increased cumulative traffic. Class 1, type A (modified) bituminous, chip seal, and open-graded plant-mix surfaces all were relatively quiet sometime during their service life, but the noise level of each increased to between 69 to 70 dBA as the cumulative traffic increased. Class 1, type A (modified) bituminous surfaces were smooth and dense when placed but became noticeably polished after the cumulative traffic reached about one million vehicle passes. Also noise levels increased on open-graded plant-mix surfaces with time. On new chip seal surfaces, the exposed aggregate produced high levels, but noise levels dropped as the aggregate wore and the surface bled. Finally, the older surfaces began to crack and break up, and the noise level again rose. Chip seal surfaces are not included in Figure 1 because they are placed only on low-volume roads and are expected to endure for a limited time. Portland cement concrete and class 1, type A bituminous surfaces maintained a relatively constant noise level (69.5 dBA). Tests on transversely grooved portland cement concrete surfaces yielded a noise level of about 73 dBA.

A few readings were obtained for surfaces that were unusually cracked and bumpy. These surfaces might be classified as rough and were not included in any of the preceding types of surfaces. These rough surfaces had an average noise level of about 72 dBA.

To ensure that the reference car noise data were representative of the average car, we compared results from a previous vehicle noise survey (5) to the reference car data. The survey was conducted on class 1, type A bituminous and portland cement concrete surfaces for various speed-limit locations. The data at 72-km/h (45-mph) and 97-km/h (60-mph) speed limit locations were compared to the reference car data for the corresponding speeds. The survey vehicles were not traveling at exactly the speed limit, but the large number of vehicles in the survey should make the comparisons valid. The median automobile noise level was 68 and 74 dBA for 72 and 97-km/h (45 and 60-mph) speed limit locations respectively. This compares to reference car noise levels of 69.5 and 74 dBA at the corresponding speeds. From this comparison, one can see that the reference car was representative of the average car.

Table 1. Recommended noise level adjustments for various types of surfaces.

Surface Description	Car (dBA)	Truck (dBA)
Grooved portland cement concrete	+4	0
Normal surfaces		
Class 1, type A bituminous concrete	0	0
Class 1, type A (modified), bituminous concrete	0	0
Portland cement concrete	0	0
Open-graded, plant-mix seal	0	0
Chip seals	0	0
Smooth surfaces		
Kentucky rock asphalt	-3	0
Sand asphalts	-3	0

Figure 1. Effects of cumulative traffic on noise levels of various pavement surfaces.

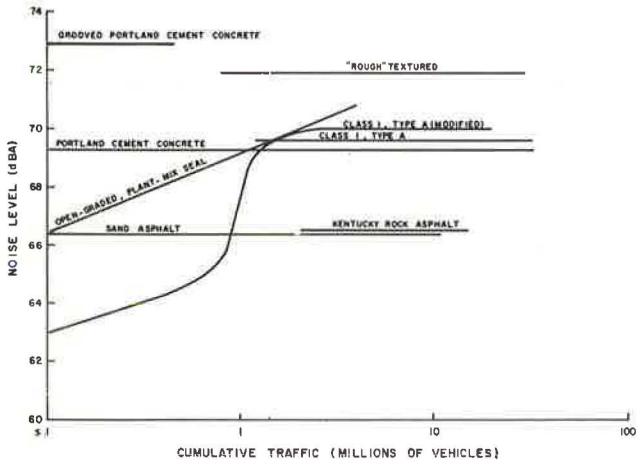

Noise Measurements Inside the Reference Car

To determine the differences in noise levels for occupants of vehicles driving on various surfaces, we took measurements inside the reference car. In all cases, the vehicle speed was 72 km/h (45 mph). The sound-level meter was held about 150 mm (6 in) above the backrest of the front seat, which closely corresponds to ear level. The slow response of the sound-level meter was used so that variations in the noise could be minimized. The average noise level over a uniform stretch of highway was tabulated for each type of pavement. From 3 to 14 locations were tested for each type of surface. The readings were averaged. The sand asphalt and Kentucky rock asphalt surfaces gave the lowest noise levels (65.3 dBA). The other types of surfaces were ordered in the same way as the data obtained from outside the reference car (Figure 1).

Noise measurements were also made inside the car on some bridge decks. Two bridge decks that had been grooved were compared to one ordinary deck. The average readings for the grooved decks were identical to the average of grooved concrete pavements. Grooved decks gave readings approximately 3 dBA higher than ordinary decks.

Noise Recordings

A total of 260 noise recordings taken on various surface types were compared to predicted values. The predicted L_{10} noise levels [based on NCHRP Report 117 (3) with Kentucky correction nomograph] were compared with measured values. The actual and predicted L_{10} values for class 1, type A bituminous concrete; worn class 1, type A (modified) bituminous concrete; portland cement concrete; sand asphalt; open-graded, plant-mix seal; and Kentucky rock asphalt surfaces were within ±1 dBA. New class 1, type A (modified) surfaces were nearly 5 dBA under the predicted levels. This, however, is not indicative of the long-term noise level. Also, at these locations, there were a large number of smaller, quieter

trucks, which resulted in actual noise levels below the predicted levels. Reliable noise recordings for the grooved concrete surface could not be obtained because the only section that had been opened to traffic was two lanes of a four-lane highway. The very low traffic volumes on the chip-seal surfaces made noise recordings unreliable. Some recordings were also taken on some surfaces that were very cracked and bumpy and may be classified as rough. These rough surfaces had actual L_{10} noise levels that were approximately 5 dBA above the predicted values.

Reference Truck Noise Measurements

The truck used was a single-unit, two-axle, six-tire truck. It was loaded to approximately 8165 kg (18 000 lb) on the rear axle. Measurements were taken on a new, unopened section of Interstate Highway. There were two sections of grooved concrete and one section of ordinary concrete. The data were taken 15 m (50 ft) from the center of the lane tested. At 72 km/h (45 mph), the truck gave readings of 80.7 dBA and 81.9 dBA on the two sections of grooved concrete and 81.2 dBA on one section of ordinary concrete. The grooved concrete did not cause additional noise to be emitted by the truck.

SUMMARY AND CONCLUSIONS

To develop adjustment factors for noise levels on various types of pavement, we considered the individual vehicle readings and the traffic stream recordings. The individual vehicle noise readings showed that, after a traffic exposure of 10 million vehicle passes, only Kentucky rock asphalt and sand asphalt surfaces give consistently low values (about 66 dBA). Grooved concrete exhibits noise levels of about 73 dBA. All other surfaces show normal noise levels of 69 to 70 dBA. Thus, the car adjustment was considered to be +4 dBA for the grooved concrete surfaces. An adjustment of -3 dBA was considered appropriate for cars on Kentucky rock asphalt and sand asphalt surfaces.

The truck adjustments were determined from noise recordings on the different types of surfaces as well as the reference truck data on grooved concrete. By comparing predicted with measured noise recordings, several conclusions were reached. Actual values on new class 1, type A (modified) surfaces were quieter than predicted, but worn class 1, type A (modified) surfaces showed noise levels similar to those predicted. The other types of surfaces showed very little differences between predicted and measured levels. Thus no adjustment was considered necessary for trucks on the surfaces for which noise recordings were taken. The reference truck data indicated that no adjustment for trucks was necessary for grooved concrete surfaces.

There is a definite advantage in considering adjustments separately for cars and trucks. In most cases, the L_{10} noise level for trucks predominates in the traffic stream. However, when car noise predominates, a separate adjustment for cars would make predicted levels more accurate. The recommended adjustments for car and truck noise levels are given in Table 1.

REFERENCES

1. W. J. Galloway, W. E. Clark, and J. S. Kerrick. Highway Noise: Measurement, Simulation, and Mixed Reactions. NCHRP, Rept. 78, 1969.
2. C. G. Gordon, W. J. Galloway, B. A. Kugler, and D. L. Nelson. Highway Noise: A Design Guide for Highway Engineers. NCHRP, Rept. 117, 1971.
3. Fundamentals and Abatement of Highway Traffic Noise. U.S. Department of Transportation, Rept. FHWA-HN1, HEV-73-7976-1, June 1973.
4. K. R. Agent and C. V. Zegeer. Evaluation of the Traffic Noise Prediction Procedure. Bureau of Highways, Kentucky Department of Transportation, Frankfort, Nov. 1973.
5. K. R. Agent and R. L. Rizenbergs. Vehicle Noise Survey in Kentucky. Bureau of Highways, Kentucky Department of Transportation, Frankfort, Sept. 1973.

Differential Friction: A Potential Skid Hazard

John C. Burns, Arizona Department of Transportation

Differential wheel-path friction, or differential friction, is a term derived to describe the condition that exists when the individual wheel paths on which a vehicle rides have different or unequal coefficients of friction. The problems associated with differential friction may be minor or extremely serious depending on the magnitude of the frictional difference and its relation to the average coefficient of friction. This problem may occur on surfaces with high as well as low coefficients of friction. For this reason, a frictional inventory made in only one wheel track may not detect such a problem. Although the coefficient of friction may be good to excellent in both wheel paths, the difference might cause a vehicle to spin out of control when braking if the wheel paths are unequal. Therefore, this concept should be given major consideration in any pavement friction evaluation. The paper describes the research performed to evaluate the effects of differential friction on a skidding car. It also describes the magnitude of the problem as well as some of the causes and possible solutions. The results of this research indicate that differential friction should be given major consideration in any pavement friction analysis. There are also strong indications that differential friction may be as important a cause of wet pavement accidents as low friction level. If this is the case, a major reevaluation of pavement friction evaluation, design, and corrective techniques may be necessary.

A thorough evaluation of the phenomenon of differential friction was made as part of the federally sponsored research project. This paper describes the work that was performed during this research, which evaluated the effects that differential friction has on a skidding car. It also describes the magnitude of the problem as well as some of the causes and possible solutions. This subject is covered in greater detail in the final report (1).

DIFFERENTIAL FRICTION

Differential wheel-path friction is a term I have derived to describe the condition that occurs when the individual wheel paths on which a vehicle rides have different or unequal coefficients of friction. Although this phenomenon is usually not considered in a pavement friction evaluation, it can have a significant effect on a braking vehicle.

Several years ago, during stopping distance tests with a skidding car, some pavements caused the car to spin uncontrollably (2). Under normal conditions, the car was designed to stop in a straight line and not rotate. This rotation was found to be caused by unequal friction levels in each of the wheel paths. Because the tires on the left side of the car were exposed to a different pavement friction level than those on the right side were exposed to, a turning movement was caused, and the vehicle rotated toward the higher friction side. As the car spun, the front wheels moved onto the higher friction surface and the rear wheels moved onto the lower friction surface. Thus the car was still unstable, and the spin continued until the vehicle stopped. An example of this is shown in Figure 1, where the left wheel track was bleeding and the right wheel track had been chip sealed. The right wheel path had a wet stopping distance number (SDN_{40}) of 67 and the left wheel path had a wet SDN_{40} of 41, which is a 26 SDN, or 39 percent, difference. In Figure 1a, the car skidded at 64.4 km/h (40 mph) and rotated 90 deg clockwise. In Figure 1b, the car skidded at 80.5 km/h (50 mph) and rotated 270 deg clockwise. Again the direction of skidding was reversed, and the same values were recorded with the car rotating counterclockwise.

Figure 1 is a case used to portray what might happen if one wheel path was flushing and the other was not. Although both wheel paths have a satisfactory level of friction, a hazardous condition exists because of their difference. As the speed increases, the effects of differential friction increase dramatically. The problem is serious because the average driver tends to remove his or her foot from the brake as the car begins to rotate. When this is done, the car is propelled in the direction that the vehicle is facing. This could be off the road or into oncoming traffic. Because of national concern about the potential hazard that this condition might cause, a special research project was initiated to study this and other frictional problems (1). The remainder of this paper will discuss some of the findings of the research project.

Publication of this paper sponsored by Committee on Surface Properties-Vehicle Interaction.

LOCKED-WHEEL SKID

Tests

To fully evaluate the effects of differential friction, numerous locations had to be evaluated to obtain test sites that would have a wide range of differential friction numbers and types of surfaces. From 30 potential sites, 16 were selected for detailed testing. The tests were performed with a 1969 Plymouth Fury and a 1973 AMC Matador. Detailed testing included

1. Measurement of the wet SDN by ASTM E 445-71T (3) for each individual side at 32.2 and 64.4 km/h (20 and 40 mph) with the locked-wheel skid car. The value recorded for each side was used to represent an individual wheel path when the surfaces were tested simultaneously.
2. Measurement of each individual side with the Mu-Meter at 32.2 and 64.4 km/h (20 and 40 mph) after which the mu number was recorded.
3. Measurement of the wet SDN on both surfaces simultaneously at 32.2, 48.3, 64.4, and 80.5 km/h (20, 30, 40, and 50 mph). In addition to stopping distance, degree of rotation was also measured at each speed.
4. Measurement of skidding in the reverse direction to ensure that rotation was due to differential friction and not the mechanics of the vehicle or any possible driver bias.

When the differential stopping distance tests were performed, special care was taken to keep the tests uniform. When the desired test speed was reached, the driver would lock the brakes and hold the steering wheel to prevent it from rotating. This kept the wheels pointed straight ahead in relation to the vehicle. It was decided to use the straight wheel method because it was found that, when all the brakes were locked, rotating the wheel had no effect on reducing the spin of the car. The only effect it did have was to possibly cause the driver to lose his or her concentration and not keep the brakes fully locked. If this had happened when the driver was in a spin, a major accident might have occurred.

When the car stopped, the stopping distance and the rotation in degrees were measured. The rotation was measured in reference to a large protractor fastened to the trunk of the vehicle and a 4.57-m (15-ft) length of string that was extended from the center of the protractor and aligned parallel to the centerline of the highway. This method proved very accurate and reliable.

Results

Several of the actual test results are shown in Figures 2 through 5. From these diagrams, it can be seen that, as the differential friction level increases, the amount of rotation in degrees per meter of skid also increases. This indicates that good but unequal coefficients of friction in both wheel paths, may cause a more hazardous condition than low but uniform coefficients of friction. Similar findings were reported by Zuk (4). In the bottom right corner of these figures is the SDN recorded for the individual wheel paths at 32.2 and 64.4 km/h (20 and 40 mph). The differential friction at 64.4 km/h (40 mph) is obtained by calculating the absolute difference between the SDN for each wheel path recorded at 64.4 km/h (40 mph). To calculate the rotation in degrees per meter, divide the actual rotation at a particular speed (center of the figure) by the stopping distance (bottom left) recorded at that speed. The rotation shown in the right corner is for 64.4 km/h (40 mph).

A complete listing of the test results recorded for all 16 sites is given in Table 1. These data were used to derive equations relating the rotation of a car to SDN, differential friction number (DFN), and vehicle speed. DFN is defined as the absolute difference between the wet SDNs of each wheel path recorded at the same speed and subscripted by that speed if other than 64.4 km/h (40 mph).

Equations for 48.3, 64.4, and 80.5 km/h (30, 40, and 50 mph) were obtained by relating the degrees per meter rotation to the DFN recorded at 64.4 km/h (40 mph). Correlation coefficients ranged between 0.93 and 0.94, and reliable equations were derived as can be seen in Figure 6. Figure 7 shows all three equations plotted on the same graph. Site 6 was not used in the derivation of these equations because it contained a portland cement concrete (PCC) and asphalt concrete (AC) surface differential. The degree of rotation was high, but lower than expected. This may have been due to the longitudinal burlap drag texture on the PCC pavement, which would impart a higher side force and thus inhibit rotation. If this is the case, grooving or grinding might be used to correct a differential friction problem.

From these three equations, a new equation was derived for use with any speed. The equation is as follows:

$$\text{Deg/m} = \left\{0.148 - 0.0049(V) + [0.00263 + 0.0009(V)]\ \text{DFN}\right\} \times 3.28 \quad (1)$$

where

Deg/m = degrees per meter rotation for given velocity and
V = velocity of vehicle when the brakes are locked.

From this equation, it can be seen that the rotation in degrees per meter can be determined easily for any desired speed by simply knowing the SDN for each wheel path.

When this value is multiplied by the stopping distance for the given surface, the total number of degrees that the vehicle will spin can be calculated. Our experiments have shown that the actual stopping distance on the differential surface is approximately equal to the average of the two stopping distances on the individual surfaces at the same speed. For example, if at 64.4 km/h (40 mph) a car stopped in 30.48 m (100 ft) (SDN = 53) in the left wheel path and 60.96 m (200 ft) (SDN = 27) in the right wheel path, then the vehicle would stop in 45.72 m (150 ft) (SDN = 36, DFN = 26) when braking on both surfaces simultaneously. If the degrees of rotation are desired, the 45.72 m (150 ft) would be multiplied by the deg/m rotation value. At 64.4 km/h (40 mph), this would be 3.61 deg/m (1.1 deg/ft) (from the equation) for an estimated total of 165.5-deg total rotation.

VEHICLE CONTROL

Tests

The second part of the evaluation was concerned with the maneuvering problems associated with the differential friction surface. A driver tends to release the brake after he or she begins to spin; at the same time, the driver tries to regain control of the vehicle. Therefore, a similar condition was reconstructed in two phases. The first phase was an experiment to determine how many degrees a car could rotate before it could not be safely corrected by the driver. Figure 8 shows the schematic of the system that was used in the test. The premise of the test was that a vehicle would have a 3.7-m-wide (12-ft-wide) lane in which it could safely maneuver. If the vehicle moved out of its lane for a distance

Figure 1. Effects of differential friction.

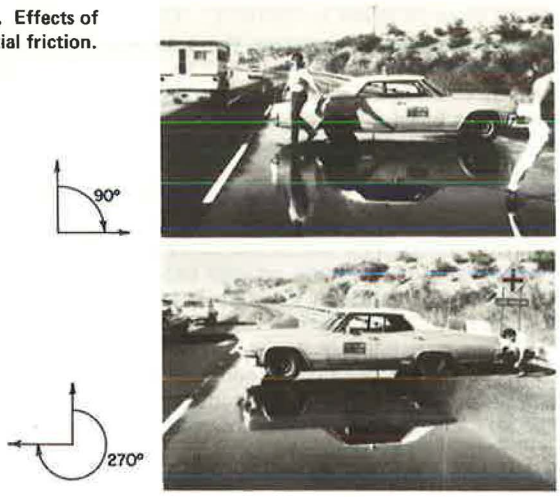

Figure 2. Rotation test, site 12.

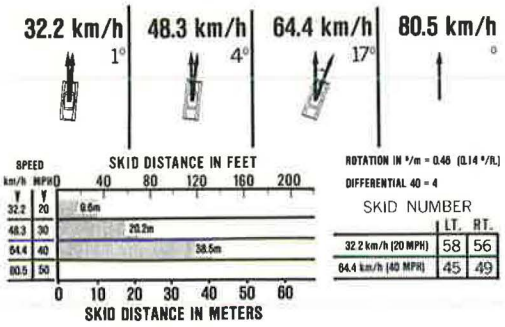

Figure 3. Rotation test, site 4.

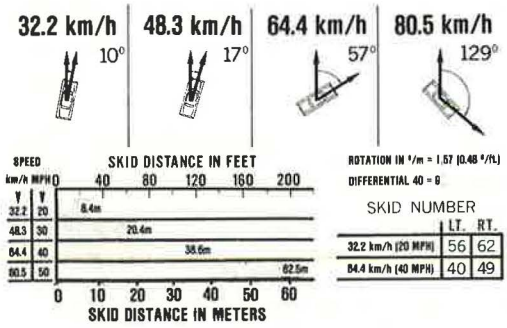

Figure 4. Rotation test, site 15.

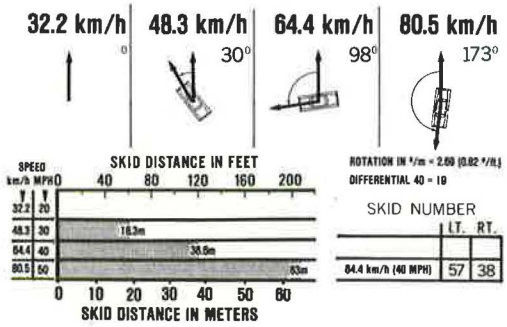

Figure 5. Rotation test, site 9.

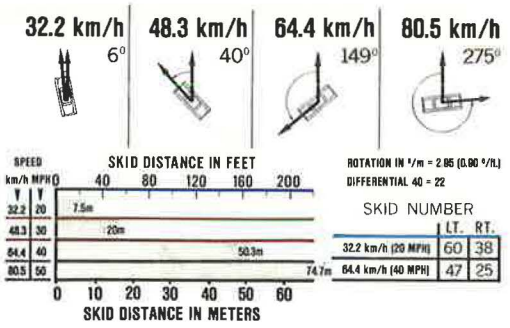

Figure 6. Rotation at 64.4 km/h (40 mph) versus SDN_{40} differential.

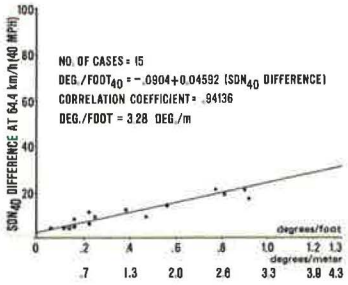

Figure 7. Rotation versus SDN_{40} differential.

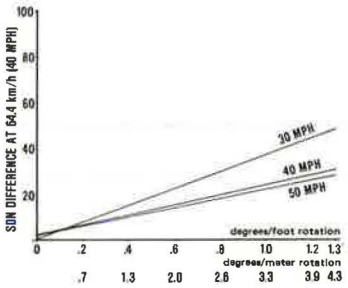

Figure 8. Vehicle control tests.

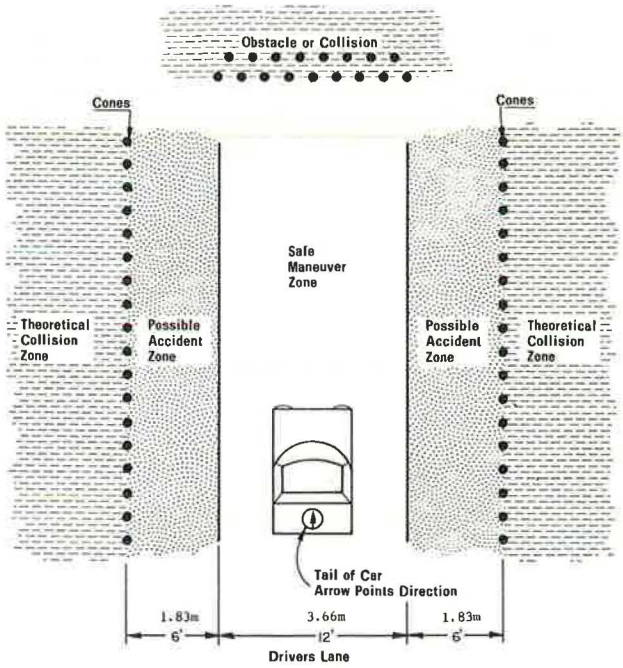

of up to 1.8 m (6 ft) on either side, it was considered to be in another lane and thus in a potential accident zone for oncoming or parallel traffic. The test vehicle was given additional maneuvering space because other traffic was assumed to be able to move 1.8 m (6 ft) and avoid the spinning car. If the car moved any further into another lane, a collision with other traffic was assumed to occur because an oncoming vehicle would not be able to avoid the spinning car. Traffic cones were placed along the imaginary collision zone, which allowed our vehicle a width of 7.3 m (24 ft) in which to maneuver. During each test, the driver was instructed to avoid these cones because they represented oncoming cars.

The second phase of the experiment evaluated the control problems associated with stopping when the brakes were not locked and the driver was allowed to freely maneuver the vehicle. In this case, cones were also set at various distances from a beginning braking point. The distance was 3.05 m (10 ft) further than the maximum braking distance recorded at any particular speed. The driver was then directed to stop in the given distance without hitting the side cones (theoretical collision) or the cones at the end of the distance (obstacle).

Films were made of all tests. Figures 9 through 11 show the trajectory of the vehicle recorded on film for various test speeds. In these figures, a circle was used

Table 1. Differential wheel-path friction test results.

	Separate Wheel-Path Test Data				Differential Test Data				
		Average SDN					Degrees Rotation		
Site Number	Test Speed (km/h)	Left Wheel Track	Right Wheel Track	DFN	Test Speed (km/h)	Stopping Distance (m)	Clockwise	Counter-clockwise	Degrees per Meter Rotation
1	32.2	64	70	6	35.4	7.8	—		—
	64.4	57	62	5	48.3	14.8	—		—
					64.4	29.4	16		0.545
					80.5	45.6	12		0.262
2	32.2	44	64	20	33.8	7.2	15		2.093
	64.4	36	57	21	49.9	16.9	27		1.598
					67.6	37.2	95		2.556
					77.2	58.1	142		2.444
3	32.2	41	56	15	32.2	8.4	5		0.597
	64.4	31	45	14	51.5	22.4	30		1.338
					66.0	44.2	82		1.857
					77.2	63.4	137		2.162
4	32.2	56	62	6	32.2	8.4	10		1.194
	64.4	40	49	9	48.3	20.4	17		0.833
					64.4	36.6	57		1.558
					78.8	62.5	129		2.064
5	32.2	61	63	2	32.2	6.2	6		0.961
	64.4	52	61	9	49.9	17.0	14		0.820
					64.4	29.7	25		0.840
					80.5	49.7	37		0.745
6	32.2	51	76	25	32.2	6.4	14		2.188
	64.4	47	73	26	49.9	15.7	34		2.146
					64.4	28.2	57		2.008
					82.1	47.9	119		2.487
7	32.2	42	44	2	32.2	8.9	6		0.672
	64.4	42	48	6	48.3	20.4	16		0.781
					64.4	35.8	27		0.754
					78.8	53.1	42		0.791
8	32.2	49	61	12	51.5	23.0	22		0.955
	64.4	36	44	8	64.4	43.6	24		0.551
					72.4	47.9	28		0.584
9	32.2	60	38	22	33.8	7.5		6	0.804
	64.4	47	25	22	48.3	20.0		40	2.004
					66.0	50.3		149	2.963
					80.5	74.7		275	3.681
10	32.2	58	40	18	33.8	9.1		9	0.991
	64.4	49	32	17	51.5	25.1		50	1.995
					66.0	45.8		139	3.031
					80.5	74.6		209	2.802
						46.4		—	—
11	64.4	53	57	4	48.3	15.5	5		0.322
					64.4	29.9	12		0.400
					80.5	56.4	35		0.620
12	32.2	58	56	2	33.8	9.6	1		0.105
	64.2	45	49	4	48.3	20.2	4		0.197
					64.4	38.5	17		0.443
13	64.4	60	49	11	64.4	30.6		23	0.751
14	64.4	58	46	12	48.3	17.1		26	1.522
					64.4	29.0		37	1.276
					80.5	50.9		81	1.591
15	64.4	57	38	19	49.9	18.3		30	1.640
					66.0	36.6		98	2.677
					82.1	63.0		173	2.746
16	64.4	51	55	4	48.3	15.5	0		0
					64.4	29.0	6		0.207
					80.5	47.9	12		0.249

Note: 1 km/h = 0.621 mph. 1 m = 3.28 ft. 1 deg/m = 0.305 deg/ft.

to represent the position of the rear end of the vehicle. The arrow inside the circle indicates the direction that the front of the car was facing at that moment.

Results

Figure 9 shows the trajectory of the vehicle during tests at 48.3 km/h (30 mph). When the vehicle was allowed to rotate 20 deg before releasing the brake, the vehicle moved into the possible accident zone, but did not enter the collision zone. In these tests, the vehicle had almost come to a complete halt before the brakes were released. When an obstacle was placed in the highway, the driver was able to stay in his or her lane but unable to stop before reaching the object.

Figure 10 shows the results of the 64.4-km/h (40-mph) tests. The figure shows that the only case in which the vehicle did not move into the collision zone was the 20-deg rotation test. In this case it only moved into the

Figure 9. Vehicle control tests at 48.3 km/h (30 mph) where DFN = 17.

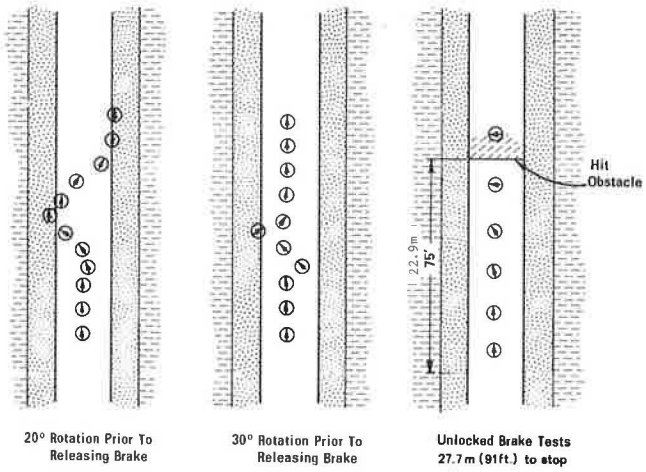

Figure 10. Vehicle control tests at 64.4 km/h (40 mph) where DFN = 17.

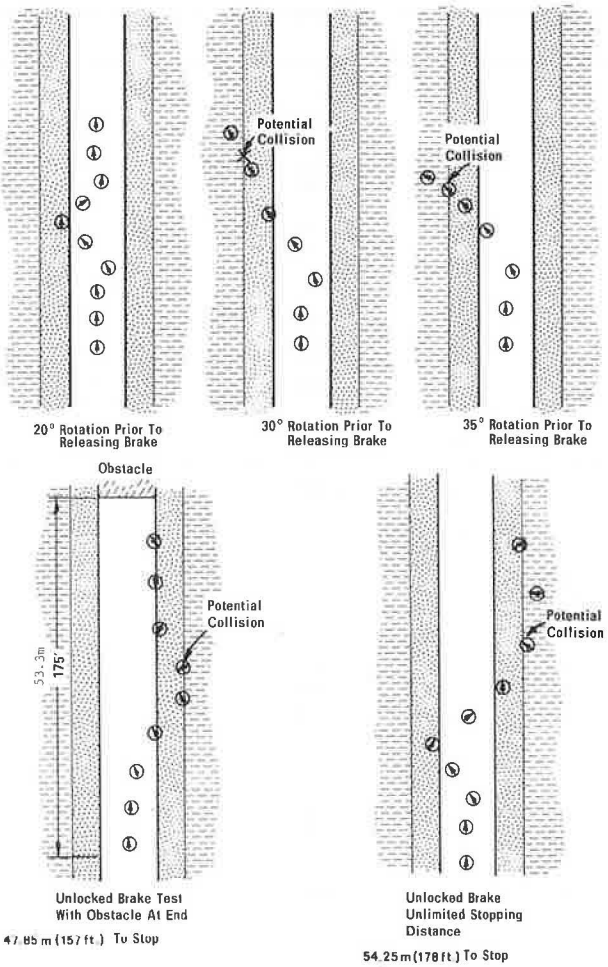

Figure 11. Vehicle control tests at 80.5 km/h (50 mph) where DFN = 17.

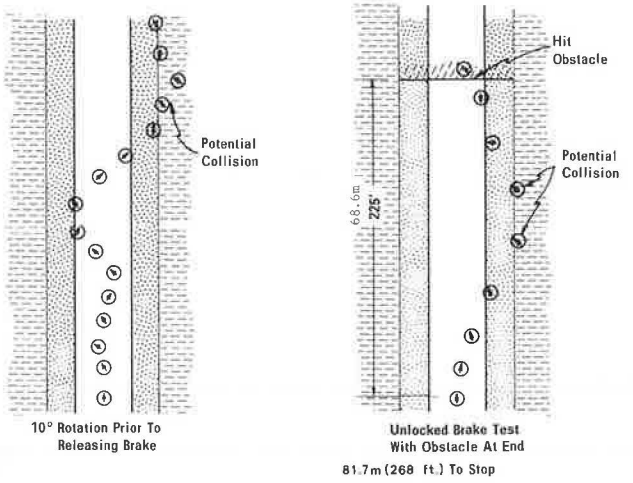

Figure 12. Differential flushing or bleeding.

Figure 13. Chip or slurry seal occupying only a portion of a lane.

possible accident zone. The car was basically uncontrollable after rotating 30 deg or more. When an obstacle was placed in the road, the driver avoided it at 64.4 km/h (40 mph); however, to do this, the car moved into the collision zone and spun out of control. When the obstacle was removed and the driver was given unlimited stopping distance, the driver was still unable to prevent the car from spinning out of control and entering the collision zone.

Figure 11 shows the results of the 80.5-km/h (50-mph) tests. In this case, the driver was unable to control the vehicle after 10-deg rotation and moved into the collision zone. When an obstacle was placed in the road, the vehicle not only moved into the collision zone but also spun into the obstacle.

From the results of these speed tests, it is obvious that differential friction can significantly affect the control of a braking vehicle and produce a potentially hazardous condition that the driver may not be able to correct.

The greatest problem arises when the driver releases the brake after the car has begun to spin. When this is done, the vehicle is propelled in the direction it is facing, whether it be off the road or into oncoming traffic. The greater the rotation is, the more uncontrollable the vehicle is. After passing 90 deg, the car will actually be propelled rearward if the brakes are released.

If the driver keeps the brakes locked, the car will slide straight ahead and spin about its center of gravity or front wheels. Unfortunately, the average driver is not conditioned to do this. It is the tendency of the average driver to be confused by the rotation and possibly release the brake after spinning approximately 30 deg. If the vehicle is still moving, this is an extremely dangerous thing to do.

From our tests, it can be generally concluded that, if the differential friction causes a vehicle to rotate more than approximately 25 deg while it is still sliding at a speed greater than 24.14 km/h (15 mph), the driver may not be able to prevent the vehicle from entering the collision zone if the brakes are unlocked. Because there are numerous combinations of speeds and differential friction levels that will produce this condition, it is evident that differential friction can indeed be a potential hazard to the driving public. It is estimated that, when braking, a major loss of control may occur if the differential friction surface produces total rotations greater than those listed in the following tabulation (1 km/h = 0.621 mph):

Speed at Which Wheels Are Locked (km/h)	Total Rotation After Car Has Stopped (deg)
48.3	30
64.4	50
80.5	70

As the total rotation increases above these values, the potential loss of control is drastically increased.

Our tests were performed under theoretically controlled conditions in which the driver was familiar with the surface. Even under these conditions, the tests were hazardous at speeds in excess of 48.3 km/h (30 mph), and thus only one site was thoroughly investigated. Spot testing at other locations confirmed that this site was representative of the results that could be expected. It is unfortunate that at some locations the driving public may be faced with such conditions at speeds of 88.5 km h (55 mph) or more. There is a strong indication that differential friction may be as important as low friction level in causing wet pavement accidents. If so, a major reevaluation of current pavement friction evaluation, design, and corrective techniques may be necessary.

CAUSES OF DIFFERENTIAL FRICTION

There are numerous causes of differential friction. Some are created or induced by construction practices, others by maintenance techniques. Most are initiated or compounded by exposure to traffic.

It should be remembered that friction is a force generated at the tire-pavement interface. For this reason, both the pavement and the tires, as well as the vehicle dynamics, greatly affect the coefficient of friction. It follows that vehicle dynamics and tires may cause differential friction even though the pavement may have a uniform friction level. Because this report is primarily interested in the effects of highway surfaces, only differential friction caused by the pavement surface will be considered here.

The following sections give information on the most commonly found differential wheel-path friction conditions. There are numerous other causes of differential friction that will not be mentioned here. Most of the causes of differential friction need not occur and can be avoided if proper consideration is given to this phenomenon.

Differential Flushing or Bleeding

Differential flushing or bleeding (Figure 12) is created when a portion of the lane is flushing or bleeding while the rest is not. Such a condition can also occur when full-lane-width repairs are not made.

Unequal Wear or Flushing

Unequal wear or flushing, like differential flushing or bleeding, may be caused when the contact of two asphalt ribbons falls inside one travel lane. Unlike the cause of differential flushing or bleeding, however, the main contributor to the condition is traffic. If the two ribbons are not alike or are polished at different rates, vehicles riding in the lane will experience differential friction. An unequal transverse distribution of traffic in very wide lanes can also cause this problem because truck and passenger car traffic may ride on different portions of the lane and cause differential wear.

Chip or Slurry Seals

When a chip or slurry seal is placed across only a portion of the lane width (Figure 13) a major differential friction condition may exist. Maintenance forces may create such a problem while attempting to reduce costs; however, it only creates a more expensive and hazardous condition. This problem is greatly magnified if the seal bleeds.

Dissimilar Shoulder Surfacing

When a distress or shoulder lane has a dissimilar surface texture different from the travel lane (Figure 14), a differential friction condition may exist. An example of this may be the use of a chip seal shoulder and an AC travel lane or an AC shoulder and a concrete travel lane. A recent preliminary report (5) has shown that 65 percent of truck traffic may ride with one wheel on the shoulder. This indicates that differential friction should be of concern.

Maintenance Crack Patching

Maintenance crack patching can be a major problem when the rate of crack patching in one wheel track is much greater than in the other (Figure 15). When this problem

exists, it is almost impossible to cure without major corrective action.

Unequal Drainage Properties

When surface drainage characteristics are different, a differential friction condition may exist (Figure 16). An example of this might be a chip seal in combination with an AC surface.

Unequal Water Layer Thickness

Unequal water layer thickness or ponding can be caused by improper geometrics or low spots in a highway. Because this situation may cause only one side of a car to hydroplane, an extreme differential friction may be created even though there is uniformity in the surface. This condition can also occur when only a portion of the pavement is wet, as in the case of roadside sprinklers that spray onto the highway.

Figure 14. PCC pavement travel lane with AC distress lane.

Figure 15. Maintenance crack patching.

Figure 16. Unequal drainage properties.

PREVENTION OF DIFFERENTIAL FRICTION

Differential friction can be avoided if the problem is considered during construction and maintenance operations.

During construction, ribbons should be placed so that all longitudinal joints fall on the outside of the lane at or very near the location of the lane stripe. The shoulder and distress lanes should also be of the same type of surface as that used for the travel lanes. The use of a chip seal shoulder with an AC travel lane or an AC shoulder with PCC pavement travel lane may cause differential friction and should be avoided if possible.

During maintenance operations, it is imperative that most operations be uniform across the full width of the lane. The application of any corrective action for only a portion of the lane width should be avoided when possible. Heavy crack patching or maintenance operations in only one wheel track will cause a differential friction condition that is not easily corrected.

The problem of differential friction is corrected when both wheel paths have similar coefficients of friction. This is not difficult to achieve if the underlying variables are understood. If they are not, then there is little hope for correcting or eliminating the differential friction problem. In fact, there is a good chance that such problems will be inadvertently created by many highway operations.

CONCLUSIONS AND RECOMMENDATIONS

Differential friction can cause an extremely hazardous condition for a braking vehicle. Because the problem can occur at high as well as low friction levels, it should be given major consideration in any pavement friction evaluation.

There is a strong indication that differential friction may be as important as low friction in causing wet pavement accidents. If this is the case, a major reevaluation of current pavement friction evaluation, design, and corrective techniques may be necessary.

For any particular combination of differential friction number and speed, the number of degrees of rotation can be calculated by equations given in this paper. Thus the magnitude of the problem can be predicted by means of normal skid testing techniques without the hazards of actual vehicle rotation tests.

When riding on a differential friction surface, the greatest problem arises when the driver releases the brakes after the car has begun to spin. When this is done, the vehicle is propelled in the direction that it is facing. This could be off the road or into oncoming traffic. The greater the degree of rotation is, the more uncontrollable the vehicle is.

Surface friction inventories made in only one wheel track may not detect this problem unless visual observations are recorded. Although one or both wheel paths may have a high friction level, a hazardous condition for a braking vehicle may be caused if they are unequal.

There are numerous causes of differential friction, most of which can be avoided during construction, design, and maintenance operations. Because maintenance operations may be the largest contributor to this problem, it is hoped that, in the future, the maintenance engineer as well as other highway engineers will give more consideration to this problem and its correction. This paper outlines some of the major causes and corrective techniques that need to be considered with this problem.

ACKNOWLEDGMENT

The contents of this paper reflect my views. I am responsible for the facts and accuracy of the data presented herein. The contents do not necessarily reflect the official views or policies of the Arizona Department of Transportation.

REFERENCES

1. J. C. Burns. Frictional Properties of Highway Surfaces. Arizona Department of Transportation, Phoenix, HPR 1-12 (146), Aug. 1975, 123 pp.
2. J. C. Burns and R. J. Peters. Surface Friction Study of Arizona Highways. Arizona Department of Transportation, Phoenix, HPR 1-9 (162), Aug. 1972, 75 pp.
3. Stopping Distance on Paved Surfaces Using a Passenger Automobile Equipped With Full-Scale Tires. ASTM, Philadelphia, Tentative Method E 445-71T, 1974.
4. W. Zuk. The Dynamics of Vehicle Skid Deviation as Caused by Road Conditions. International Skid Prevention Conference, Sept. 1958.
5. D. K. Emery, Jr. Paved Shoulder Encroachment and Transverse Lane Displacement for Design Trucks on Rural Freeways. Georgia Department of Transportation, Atlanta, preliminary rept., Jan. 1974.

Abridgment

Effects of Abrasive Size, Polishing Effort, and Other Variables on Aggregate Polishing

S. H. Dahir and W. E. Meyer, Pennsylvania State University

Although pavement skid resistance is subject to cyclic changes, there is a gradually diminishing overall decrease and an eventual leveling off of the minimum, which depends on the surface aggregate, traffic, and the like (1). Because the skid resistance level is primarily a function of the reduction of the microtexture of the surface aggregate, six typical rock samples were polished in a reciprocating polishing machine (2) to equilibrium (6000 passes). To eliminate the effects of aggregate shape, size, gradation, and edge effects, 100 by 150-mm (4 by 6-in) flat surfaces of rock were employed. Friction was measured with the British portable tester according to ASTM E303. Eight grades of silica abrasive (Mohs hardness 7) were used. Thin sections were made to identify the rock properties (Figure 1).

Figure 2 shows the results obtained. With the Valentine limestone, the polish becomes smoother as finer abrasive is applied; this occurs independently of the order in which the abrasive grade is applied. The Hummelstown-Myerstown limestone performance is quite similar, but the friction level is lower. This is surprising because the Hummelstown stone contains 15 percent dolomite with a Mohs hardness of 3.5 to 4, and the basic calcite of both limestones has a hardness of 3. The micrographs provide the likely explanation—30 percent of the Valentine limestone consists of large crystals of sparry calcite embedded in very fine micrite and the Hummelstown stone has uniform and small grain size.

The diabase samples came from Fairfax County, Virginia, and are representative of triassic diabase, commonly known as traprock. In this case, a finding that had already been made with the limestones was confirmed—no specific abrasive size produces the highest polish of a particular type of rock. It became clearly evident that, for a given rock and prevailing conditions, the polish depends primarily not only on abrasive size but also on polishing effort (number of passes and the contact pressure between polishing pad and specimen). When a ground surface was polished with 5-μm abrasive, no change occurred, but, when a 10-μm abrasive was used, the BPN dropped significantly. Further increase of the abrasive size caused only minor changes. When the process was reversed, a large drop in BPN occurred with the 53-μm abrasive. A partial explanation of such behavior may be that the initial natural coarseness of the texture must first be destroyed before actual polishing can take place and that, depending on polishing effort and rock structure, discontinuities occur in the polishing process.

With the lithic sandstone, similar behavior was noted except that a higher friction level prevailed. Because this rock has a rough natural texture 80 percent of which consists of large quartz grains that are held together by sericite and quartz fragments, this is not surprising. Arkosic sandstone performs no differently in principle, except that it does so at a still higher friction level. Although similar in composition and structure to the lithic sandstone, it is more friable because of a softer matrix. This causes a continuous release of particles during polishing, which results in high friction.

The quartzite behavior is not basically different from that of other hard rocks, but, next to the Valentine limestone, it is the most polish-susceptible rock of this series probably because it consists of uniform mineral grains.

These observations lead us to four conclusions.

1. The level of polish attainable depends on type of rock and petrography. Rocks composed of minerals having different hardness and loose bonding, such as the sandstones, will not polish to the low friction levels of fine-grained or uniform minerals, such as limestones and quartzites.
2. Coarse-grained rocks require greater polishing effort than fine-grained ones. The grains apparently must first be flattened or rounded off before polishing begins.
3. In general, the finer the abrasive is, the finer the ultimate polish will be, regardless of type of rock.
4. The coarser abrasives tend to scratch and roughen polished surfaces of soft rocks, such as lime-

Publication of this paper sponsored by Committee on Surface Properties-Vehicle Interaction.

Figure 1. Thin-section photomicrographs.

Lithic Sandstone

Quartzite

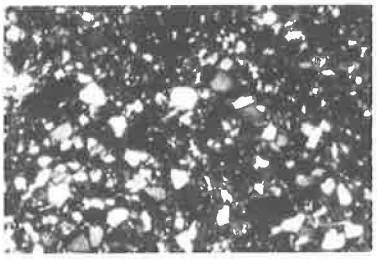

Arkosic Sandstone

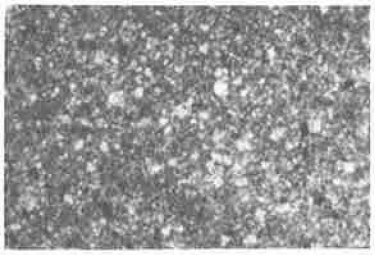

Hummelstown-Myerstown Limestone

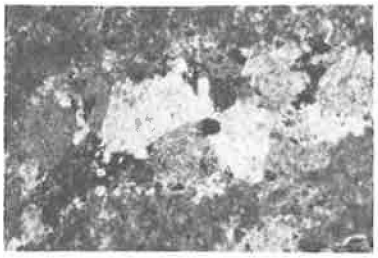

Valentine Limestone

Diabase

Figure 2. BPNs of polished rock surface.

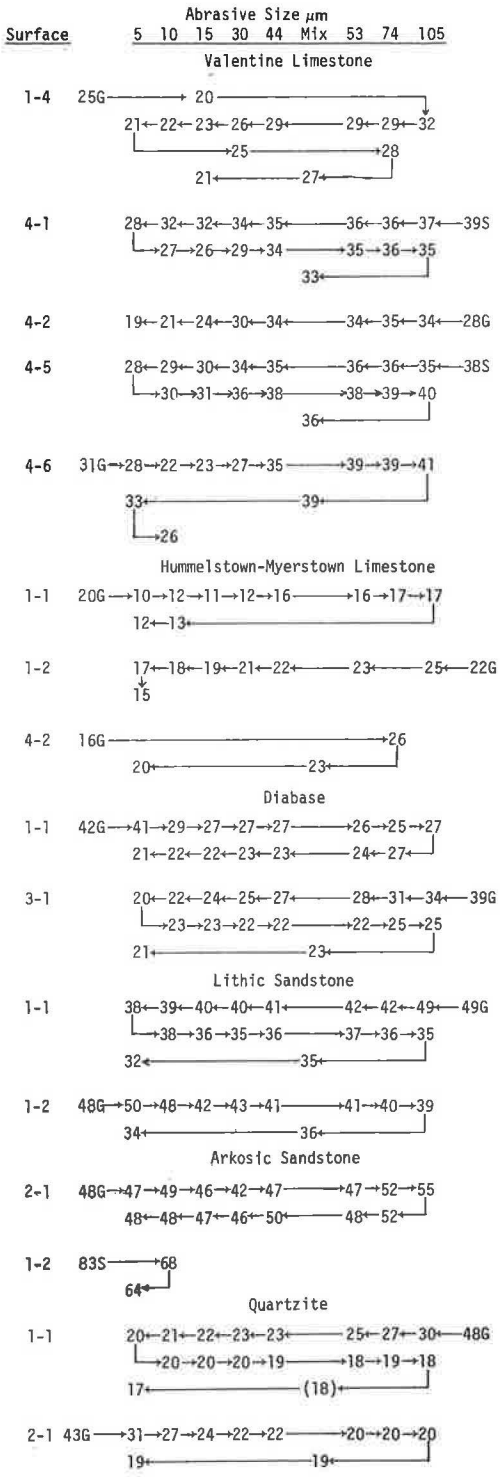

Note: G = ground; S = sawed surface.

stone, but have little or no effect on hard-mineral rocks, such as diabase, sandstone, and quartzite.

ACKNOWLEDGMENTS

This work was performed in cooperation with the Pennsylvania Department of Transportation and the Federal Highway Administration. The opinions, findings, and conclusions expressed are ours and not necessarily those of the sponsors.

REFERENCES

1. S. H. Dahir and W. E. Meyer. Bituminous Pavement Polishing. Pennsylvania State Univ., University Park, Pennsylvania Department of Transportation Project 67-11, Automotive Research Report S66, final report., 1974, 217 pp.
2. S. H. Dahir, W. E. Meyer, and R. R. Hegmon. Laboratory and Field Investigation of Bituminous Pavement and Aggregate Polishing. TRB, Transportation Research Record 584, 1976, pp. 1-14.

Automation of the Schonfeld Method for Highway Surface Texture Classification

E. D. Howerter and T. J. Rudd, ENSCO, Inc., Springfield, Virginia

The research reported here concerned the development of a system for measurement and automatic classification of pavement surface texture properties in accordance with the Schonfeld method. Electronic stereophotogrammetric techniques, previously used in the field of aerial mapping, were first adapted to obtain digital height data from stereophotographs of the pavement surface. Algorithms were then developed to process these data on a computer and automatically classify the surface texture in accordance with the Schonfeld method, properly accounting for such effects as tire-pavement interaction and deep voids in the surface. Application of the computer algorithms was demonstrated to yield Schonfeld parameter values that correlated reasonably well with those obtained by the manual method, thereby proving the feasibility of an automated approach to the Schonfeld classification process. Preliminary designs of camera systems that could be mounted on highway vehicles and could collect the required photographic data were also developed and shown to be feasible. The automated procedure allows a much more comprehensive investigation of surface texture to be carried out than that allowed by the manual method. The detailed information obtained on pavement texture can provide valuable data for understanding the mechanics of skid resistance and the generation of noise due to vehicle tires. It can also be effective in the specification and control of pavement construction and for monitoring wear and polishing of pavements.

A considerable amount of research has been performed in recent years to identify those pavement surface texture properties that affect skid resistance. Typical parameters of the pavement texture that are studied include average texture depth, mean void width, profile ratios (ratio of length of actual profile to length of horizontal baseline), average number of peaks per unit length, and maximum height variation (1, 2, 3, 4).

Robert Schonfeld of the Ontario Ministry of Transportation and Communications is a researcher who has extensively investigated this problem and has developed a classification system that is more comprehensive than those used previously. In his system, the pavement texture characteristics are visually examined and classified into six categories. These category values can be combined so that they correlate well with the skid number of the pavement as measured by a locked-wheel skid trailer (5).

The particular application with which this study is concerned is the automatic classification of pavement texture in a manner consistent with this Schonfeld system. The existing Schonfeld method uses visual stereointerpretation as a means of classifying the texture of the pavement sample. Automation of this procedure will have the effect of removing the human subjectivity associated with visual stereointerpretation and lead to more efficient implementation of the Schonfeld method of pavement texture classification. Furthermore, the automated technique, by using a much larger data base, has the potential for allowing much more effective classification techniques to be identified.

Stereophotography has been used for many years as a means of recording three-dimensional information. It has been used for scientific investigation and in commercial enterprises since the time Abbé Moigne equipped a stereoscope with early stereophotographs (daguerreotypes) in 1849. The original technique for measurement of the depth information depended on the stereoscopic visual acuity of the particular human observer. Not until the 1950s, when the first contours were automatically produced from an instrument developed by Bausch and Lomb, was the practicality of automatic stereoscopic measurement demonstrated (6). Now modern stereoscopic equipment has shifted the dependence from human judgment to mechanical devices under computer control. These stereocompilers are capable of rapidly deriving accurate information from stereopairs and recording the data directly on computer-compatible magnetic tape.

The primary emphasis for stereophotography, particularly in recent years, has been in the field of aerial mapping and reconnaissance. To our knowledge, it was first used only for classifying pavement structure texture by the British in 1967. At that time, the depth information contained in the stereophotographs was obtained mechanically by laboriously measuring the parallax information through the use of a stereocomparator (4). The work reported here couples the use of the Schonfeld texture classification procedure with the techniques of high-speed electronic stereocompilation to

Publication of this paper sponsored by Committee on Surface Properties-Vehicle Interaction.

yield an efficient tool for pavement texture characterization.

TECHNICAL APPROACH

To develop and validate the automatic classification scheme, we first selected a number of stereophotographs that covered a wide range of pavement textures. These pavement texture samples were obtained from the Ontario Ministry of Transportation and Communications, and had previously been manually analyzed by Schonfeld.

The selected stereophotographs were electronically digitized to convert the texture information contained in the stereophotographs to digital data. Algorithms were then developed for yielding information on particle width, height, angularity, and density in accordance with the Schonfeld method. These algorithms were then applied to the digital pavement data and comprehensive statistical data obtained for the macrotexture and microtexture on the pavement surfaces. This information was then condensed to yield the six Schonfeld parameters for the surfaces and compared with the manually obtained parameters for validating the automated technique.

Electronic Stereocompilation of Pavement Samples

The process of converting the light-intensity and parallax information in the stereophotographs into digital form can be performed efficiently and accurately by using commercially available photomappers. For the purpose of this study, the digitizing services of Gestalt International Limited were procured. The equipment used for automatic stereocompilation was the second generation Gestalt Photomapper (GPM-2). During stereocompilation, the GPM-2 creates an orthophotograph (essentially a projection viewed from infinity) of the information contained in the stereopair. An example of an orthophotograph for one of the texture samples analyzed is shown in Figure 1. The reference wedge and ruler used in the Schonfeld procedure are visible in the upper portion of the figure. The pavement texture that was analyzed by the computer algorithms is contained within the white border in the lower half of the photograph.

In addition to the orthophotograph, a contour sheet is produced by the GPM-2. This sheet is a graphical display of the relief information contained in the stereophotographs. The contour sheet corresponding to the texture sample of Figure 1 is shown in Figure 2. The reference wedge and ruler are again visible in the upper portion.

The GPM-2 produces the orthophotographs, contour sheets, and the digital information for the pavement samples in a patchlike but systematic manner (7). The digital data associated with these patches is stored on computer-compatible magnetic tape. It is this digital information that is eventually used to classify the pavement texture through the use of a comprehensive set of computer algorithms. Based on studies performed at Gestalt International Limited, the GPM-2 is capable of digitizing the data within root-mean-square (rms) errors of 20 μm (787 μin), 25 μm (984 μin), and 38 μm (1496 μin) in the X, Y, and vertical Z directions respectively, provided the stereophotographs are of sufficient quality. In this study, the resolution required was only 180 μm (0.007 in) because of the limitations of the original stereophotographs.

Schonfeld Method of Pavement Texture Classification

The Schonfeld method of pavement texture classification assigns six parameters to the surface. Three of the parameters relate to the average widths, heights, and angularities of the macroparticles. The fourth parameter describes their density on the surface. A fifth parameter is used for characterizing the texture between the macroparticles (background microtexture), and the sixth parameter characterizes the microtexture on top of the macroparticles. These are characteristics of the pavement surface that are known to affect skid resistance.

In the original Schonfeld method, to obtain the parameter value for a given pavement sample, an operator performs the texture code assignment on 10 randomly selected square centimeters. The location of the 10 square centimeters is determined by placing a transparent grid over one of the photographs during stereointerpretation. The results obtained from classifying the 10 random square centimeters are then combined to yield the six texture code parameters for the pavement sample under investigation.

Automatic Classification Scheme

The computer algorithms developed for the automatic classification of pavement texture are divided into two sets.

The first set consists of algorithms that prepare the digitized stereophotographic data for processing in the computer. Here one algorithm takes the patchlike data obtained from the stereophotographs and links them together into profile form. A second algorithm is then used to produce a computer plot of the resulting profiles for visual verification of the data.

The second set of algorithms analyzes the appropriately formatted data to obtain the Schonfeld numbers. Here the first algorithm assigns to each of the individual particles on the surface (macroparticles and background microparticles) a width, height, and angularity consistent with the Schonfeld definition. It also measures the base area of each macroparticle for determining the Schonfeld density parameter. The microtexture on top of the macroparticles is then extracted and classified in a similar manner. A summary statistical algorithm next takes the individual particle statistics to form a complete width, height, and angularity distribution for all the particles on the surface. The six Schonfeld parameters for the surface are then obtained by taking appropriate averages of this particle statistical data.

It should be noted that the computer algorithms analyze the stereophotographs much faster and more completely than the manual method. Furthermore, because the whole photograph is analyzed (rather than 10 randomly selected square centimeters), the computer algorithm yields much more representative results for the Schonfeld parameters than the manual method does. In addition, other valuable information (topographic distributions, orientation of particles, and the like) is available from the computerized approach.

Details of Computer Algorithms

The algorithms employed to characterize each particle on the surface are briefly described in this section. [More complete details can be found in the final report for phase 1 of this research project (9).]

The digital data describing the pavement surface contain long wavelength undulations introduced from variations in both the average level of the texture and from

the electronic stereocompilation. (The undulations introduced by the electronic processing are caused by the stereophotographic alignment procedure.) These undulations are effectively removed by applying a two-dimensional filter to the data that is implemented recursively in the computer to save processing time. A CalComp plot of the filtered data for half of the pavement sample of Figure 1 is shown in Figure 3. (To reduce the plot density, only alternate profiles were plotted.) The same two-dimensional digital filter is used to separate the microtexture from the top of the macroparticles when classifying these particles and to obtain other texture-interaction surfaces as will be described.

Figure 1. Orthophotograph of pavement texture sample 1.

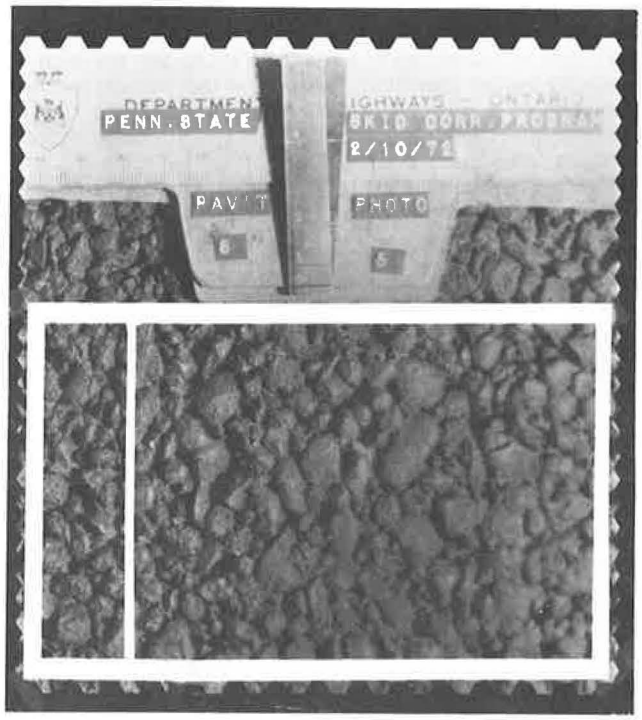

Figure 2. Contour map of pavement texture sample 1.

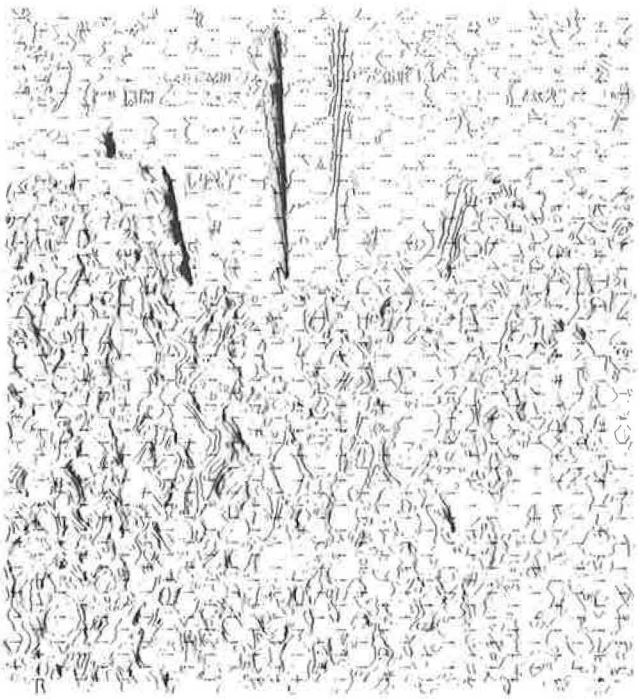

In the Schonfeld classification scheme, regions on the pavement surface with sparsely spaced macroparticles are treated differently from regions with densely packed macroparticles because dense macroparticles, when they are sufficiently high, can reduce the effective tire-pavement interaction area. Also regions where there are deep cavities or cracks must be specially treated and the cavities must be "removed" before the Schonfeld analysis. In both cases, this is done by using a threshold analysis. After identifying the regions of tire-pavement interaction and deep cavities, a reference texture-interaction surface is generated that is stored in the computer to account for these effects.

Before the width, height, angularity, and density contributions of individual particles can be obtained, the boundaries of the particles on the surface have to be identified. To accomplish this, each of the profiles that make up the surface is divided into a set of intervals. The end points of the intervals are determined (based on relative heights and slopes of critical points occurring in the profiles) so that the interval represents a probable cross section of a particle. Each of these intervals in a profile is then compared to intervals in adjacent profiles for identifying the boundaries of the particle bases.

After the base of the particle has been identified, the height of the particle is taken as the distance from the apex of the particle to the average height of the boundary points that define the base of the particle. The width of each particle is taken as the length of the minor axis of an ellipse that is fitted to the boundary points of the particle. The angularity of a particle is taken as the smallest radius of curvature over the surface of the particle and is determined by fitting a parabola to each joint on the particle surface. (The curvature in two orthogonal directions is considered.) The density contribution of a particle is defined as the ratio of its base area to the total surface area of the sample. The base area is determined by carrying out an integration over the particle base points.

The individual statistics for all macroparticles and background microtexture on the surface are calculated by the above procedure and are stored on magnetic tape. After completion of this first phase of the classification process, the algorithm extracts the microtexture from the top of the macroparticles. This extracted microtexture is then classified by a procedure similar to that for the macroparticles.

At this stage, complete information is available on the width, height, angularity, and density contributions for the macrotexture, background microtexture, and asperity microtexture. This comprehensive information on all the macroparticles and microparticles on the surface is subsequently condensed into Schonfeld form, yielding the six texture code parameters.

Stereocamera System Designs

Two camera systems were designed that are capable of taking the necessary pavement texture stereophotographs. [Detail designs of these two systems are given in the final report (9).] One system that uses a high-speed strobe is designed to be operable from on board a moving vehicle at speeds up to 64 km/h (40 mph). This would enable stereophotographs of the pavement surface to be taken with negligible interruption of road traffic. The second system is a higher resolution portable sys-

tem designed for stationary picture-taking. With this system, the assembly would be placed directly on the road surface to be analyzed and the picture would be taken. Although this could be completed in less than a minute, there would naturally be a short interruption of road traffic when this system is in use. However, the advantages of this stationary system (higher resolution and lower cost) may make it preferable to the moving system.

VALIDATION OF AUTOMATIC TECHNIQUE

The results obtained from the automatic classification procedure for the four texture samples analyzed in this study are given in this section and are compared to the results obtained manually by Schonfeld. (Clearly, a larger number of texture samples is required to completely validate the computer classification algorithms. As a consequence, in a subsequent phase of this research project, a further 14 pavement samples are being processed.)

Two computer analysis runs were made for each sample under investigation. The first one involved a small portion of the texture sample corresponding to the smaller of the two rectangular areas shown in Figure 1. The second run classified the entire texture sample shown enclosed by the larger rectangle. As can be seen in the data given in Table 1, the agreement between the automatic and manually obtained results is reasonably good when one considers the differences in sampling and the subjectivity associated with the manual method. Furthermore, in the automatic scheme, use of the smaller sample seems adequate to obtain representative results for the pavement characteristics.

For texture sample 1, the average width of the macroparticles obtained by the automatic technique was consistently higher than that obtained by the manual method. Based on observations of the orthophotograph for the texture sample, the value obtained by the automatic scheme appears to be more representative for the surface. Furthermore, in the manual technique, it was reported that there was no background microtexture present on this

Figure 3. Computer plot of portion of pavement texture sample 1.

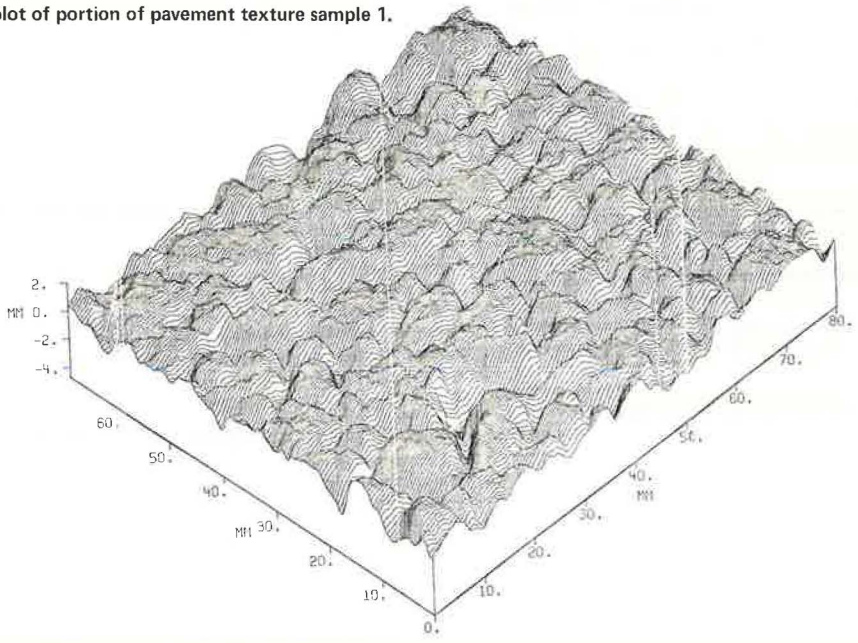

Table 1. Comparison of manual and automatic results for pavement samples 1, 2, 3, and 4.

Texture Sample	Method	Average Macrotexture Height		Average Macrotexture Width		Average Macrotexture Angularity		Macrotexture Density		Asperity Microtexture Harshness		Background Microtexture Harshness		Area Analyzed (mm^2)
		Category	Value (mm)	Category	Value (mm)	Category	Value (mm)	Category	Value (%)	Category	Value	Category	Value	
1	Manual	3.6	1.61	2.1	2.89	2.1	—[a]	3.4	85	3.2	—[a]	0.0	—[a]	1 000
	Automatic	3.5	1.477	1.3	5.131	1.6	1.050	2.3	57	2.3	—[a]	4.4	—[a]	1 440
		3.6	1.600	1.3	5.184	1.8	0.924	2.3	57	2.3	—[a]	4.1	—[a]	10 979
2	Manual	3.0	1.00	2.3	2.70	2.0	—[a]	0.2	5	3.7	—[a]	3.2	—[a]	1 000
	Automatic	1.3	0.324	1.0	3.301	1.1	1.428	1.1	27.5	2.1	—[a]	2.5	—[a]	1 440
		1.4	0.349	1.8	3.629	1.0	1.550	1.1	26.9	2.0	—[a]	2.5	—[a]	10 979
3	Manual	3.5	1.49	2.0	3.00	2.1	—[a]	0.8	19	2.8	—[a]	2.8	—[a]	1 000
	Automatic	2.1	0.571	1.9	3.357	1.4	1.200	1.1	26.1	2.1	—[a]	2.6	—[a]	1 440
		2.1	0.566	1.6	4.275	1.4	1.203	1.0	24.9	—[a]	—[a]	2.7	—[a]	10 455
4	Manual	3.5	1.54	2.4	2.65	2.4	—[a]	0.7	18	3.2	—[a]	4.0	—[a]	1 000
	Automatic	1.5	0.366	2.0	3.000	0.9	1.583	0.5	11.1	2.0	—[a]	2.5	—[a]	1 440
		2.0	0.490	1.7	3.808	1.5	1.56	0.8	20.1	2.3	—[a]	2.6	—[a]	1 817
		1.8	0.453	1.6	4.119	0.9	1.702	0.6	15.2	2.0	—[a]	2.5	—[a]	9 932

Notes: 1 mm = 0.0394 in.
Category numbers correspond to Schonfeld category numbers. Values correspond to actual physical measurements where applicable.
[a]Not applicable.

surface. The orthophotograph revealed that microparticles do indeed exist between macroparticles of the pavement sample, and, therefore, there should be a nonzero value for background microtexture. Because the manually obtained results categorized all of this microtexture with the macrotexture, it is not surprising that a larger final macrotexture density was obtained.

The second pavement texture sample that was analyzed corresponded to a concrete road surface with small aggregates. The automatic classification technique is only sensitive to height and does not discriminate between material composition; it was expected to identify more macrotexture than actually existed on the pavement because clusters of concrete, which are greater than 2 mm (0.08 in) in width, are classified as macroparticles by the automatic technique. This accounts for the increased macrotexture density in the automatic results compared with the macrotexture density in the manual results. Similarly, the height, width, and angularity parameters obtained automatically have a reduced value because concrete clusters that are comparable in size to aggregates are being included in the automatic method.

The correlation between manual and automatic results for texture samples 3 and 4 is very good; the only major discrepancy is in the macrotexture height parameter. The manually obtained results indicated that the average heights of the macrotexture present on texture samples 1, 3, and 4 were approximately equal and on the order of 1.5 mm (0.059 in). Visual observation of the individual stereophotographs revealed that the macrotexture in sample 1 was, in fact, considerably higher than that in samples 3 and 4, indicating a possible error. The difference in the two height values for the automatic and manual technique was therefore expected.

CONCLUSIONS AND RECOMMENDATIONS

It was demonstrated that pavement texture can be automatically classified in accordance with the Schonfeld scheme through use of electronic stereophotogrammetric techniques coupled with computer processing. Camera systems for taking the required stereophotographs of the pavement samples from either a moving vehicle or a stationary position were designed and shown to be feasible.

The computer algorithms that were developed are capable of yielding the widths, heights, angularities, and density contributions of all the macroparticles and microtexture on the surface. This is much more information than that given by the current Schonfeld manual method, which is based on average pavement properties of 10 randomly selected square centimeters. On further investigation, this comprehensive information could lead to the establishment of definitive relationships between pavement surface texture parameters and performance factors such as skid resistance and tire noise generation. To develop such relationships, a large sample of stereophotographs should be obtained simultaneously with the measurements of skid resistance and, possibly, tire noise. The connection between the texture characteristics and the skid resistance and noise performance could then be effectively pinned down by using the computerized approach developed in this contract.

Although the automatic classification scheme developed in this study is an excellent research tool for understanding the significance of pavement texture for pavement performance, it may not be effective as an operational tool for large-scale inventory of pavement surface texture because of the off-line requirement for the digitization of the stereophotographs and the high cost associated with the digitizing of the stereophotographs and required computer processing. For surveying large numbers of road surfaces on a long-term basis, a more cost-effective approach should be developed. Such an approach should be based on use of fewer data and ideally should avoid the need for stereophotographic digitization. (The stability of the results obtained in this project between small and large data samples indicates that use of a smaller data base is indeed feasible.) One method for obtaining the required data might be to use a profile scanning instrument similar to the laser proximity measurement device developed by the Transport and Road Research Laboratory (8). Simpler computer algorithms could then be used to process the data obtained from this instrument to yield pavement surface texture equivalent to the comprehensive approach.

ACKNOWLEDGMENTS

This research was carried out under the direction of S. Kinney and S. Parrish of the Bureau of Research, Maryland Highway Administration, under administrative contract AW-076-111-046 [HP&R 1(11), Part 2]. We are grateful to R. Hegmon of the Office of Research, Federal Highway Administration, for valuable suggestions during this project; to Robert Schonfeld of the Ontario Ministry of Transportation and Communications for lending us selected stereophotographs of pavement samples; and to Robert Orth of Gestalt International Limited, Vancouver, Canada, for setting up the photogrammetric equipment to digitize the pavement stereophotographs.

The opinions, findings, and conclusions expressed in this paper are ours and not necessarily those of the sponsor or other individuals involved in the project.

REFERENCES

1. H. A. Goodman. Pavement Texture Measurement from a Moving Vehicle. Joint Road Friction Program, Pennsylvania Department of Highways and Pennsylvania State Univ., Rept. 19, March 1970.
2. B. M. Gallaway and H. Tomita. Microtexture Measurements of Pavement Surfaces. Texas Transportation Institute, Texas A&M Univ., College Station, Research Rept. 139-1, Feb. 1970.
3. K. D. Hankins. Pavement Surface Texture as Related to Skid Resistance. Texas Transportation Institute, Texas A&M Univ., College Station, Rept. 45-4, Aug. 1967.
4. B. E. Sabey and G. N. Lupton. Measurement of Road Surface Texture Using Photogrammetry. Road Research Laboratory, Crowthorne, Berkshire, England, Rept. LR 57, 1967.
5. R. Schonfeld. Skid Numbers from Stereophotographs. Ontario Ministry of Transportation and Communications, Rept. RR-155, Jan. 1970.
6. M. M. Thompson. Manual of Photogrammetry. American Society of Photogrammetry, Falls Church, Va., 3rd Ed., 1965.
7. B. G. Crawley. Gestalt Contours. Gestalt International Limited, Vancouver, British Columbia, Canada, April 1974.
8. D. R. C. Cooper. Measurement of Road Surface Texture by a Contactless Sensor. Transport and Road Research Laboratory, Crowthorne, Berkshire, England, TRRL Rept. 639, 1974.
9. E. D. Howerter and T. J. Rudd. Automation of the Schonfeld Method for Highway Surface Texture Classification: Three Dimensional Classification Technique. ENSCO, Inc., Springfield, Va., Rept. FHWA-MD-R-76-8, Aug. 1975.

Wear and Skid Resistance of Full-Scale Experimental Concrete Highway Finishes

W. B. Ledbetter and A. H. Meyer, Texas Transportation Institute, Texas A&M University

Results on an evaluation of two sets of full-scale experimental concrete test sections are summarized. Eighteen experimental concrete finishes were evaluated in terms of skid resistance under standard trailer water conditions and under simulated rainfall conditions. In addition the changes in texture depths and skid values with time were measured. Results indicate that (a) texture depths of 0.15 cm (0.06 in) or greater can be constructed easily and economically with 0.32-cm (1/8-in) metal tines spaced closer than 1.27 cm (½ in) apart; (b) under normal traffic conditions, all concrete textures can be expected to wear down approximately 25 to 35 percent during the first half year and then remain relatively unchanged for a prolonged period; (c) skid measurements made under standard trailer water conditions may not be indicative of real-life conditions in wet weather; (d) low skid values could be obtained in almost any rainfall in which the pavement is completely wetted regardless of texture; and (e) under simulated rain condition, deep transverse texturing will result in the greatest improvement in skid values.

The purpose of this investigation was to determine the effects of various experimental concrete surface finishes on the skid resistance and durability of portland cement concrete (PCC) pavement.

The scope of this paper is to report on the changes in skid resistance under various simulated rainfall conditions on two sets of full-scale experimental test section surfaces constructed on concrete pavements in different parts of the state of Texas. Also reported are the changes in texture depths and skid resistances as the pavements wore down under traffic.

BACKGROUND

The safety and durability of concrete pavement surfaces have long been of importance to highway engineers. Concrete pavements are often selected because they are supposed to last a long time and their surfaces are supposed to provide high skid resistances. At the time of this study the Texas Department of Highways and Public Transportation required the use of a longitudinal burlap drag finish with an initial minimum texture depth of 0.064 cm (0.025 in). During this time, three questions were raised.

1. Should deeper textures be required, and, if so, will these deeper textures result in less durable surfaces or have any other undesirable effects?
2. Are there better types of textures than the burlap drag?
3. Does the direction of texturing—longitudinal or transverse—influence safety or durability?

In attempting to answer these questions, we examined the literature. Currently, a number of excellent reports have been prepared on PCC surface textures. Among them are the state-of-the-art summaries by Ray and Norling (2) and Rose and Ledbetter (3). They point to the need for deeper textures and attest to the fact that durable concrete surfaces can be easily constructed.

A survey of 69 PCC pavements in 27 states has been conducted (4). The data on the change in average texture depth (ATD) were limited, but, for those reporting initial and present values of ATD, they did show a drop of about 30 to 40 percent in 3 to 4 years. In terms of skid values, an average loss of 20 percent was observed in 5 years.

An excellent summary of the research work done in England is reported by Murphy and Maynard (5). This report shows that transverse grooves provide the highest resistance to skidding at high speeds, and England now requires transverse grooving of their highways. Concerning tire wear they state that "the rate of wear depends upon the harshness, or microtexture, of the surface, the macrotexture being of little importance."

From the evidence reported, it appears that deeper textures would be advantageous from a safety standpoint, provided that there were no undesirable effects created. Undesirable effects could include increased noise, increased cost, decreased life, adverse driver effect, and increased tire wear.

The possibility of increased noise was investigated by the Texas Transportation Institute (6), and only one texture (the transverse plastic broom) appeared to generate objectionable noises.

The possibility of increased construction cost and de-

Publication of this paper sponsored by Committee on Surface Properties-Vehicle Interaction.

creased pavement life were investigated in this study and are discussed in this paper. Driver effects and tire wear are beyond the scope of this study.

TEST SECTION CONSTRUCTION

Seven test sections, each 244 m (800 ft) long, were constructed on Tex-6 in College Station, Texas, in November 1971 (Table 1, sections F-1 through F-7). A complete description and discussion of the construction of these 7 test sections are given elsewhere (6). Traffic on these sections averaged 868 vehicle passes/day (VPD) in June 1972, 1483 vehicle passes/day in January 1973, and 1530 vehicle passes/day in July 1974.

Eleven test sections were constructed in September 1973, on I-10 near Van Horn, Texas. The average length of each section was 183 m (600 ft) and was prepared by using a granite gravel and granite sand, type II portland cement, and an air entrainment admixture. A description of construction conditions, mix design constraints, control tests, and original batch data is given elsewhere (7).

A burlap drag finish was accomplished by passing a wet burlap cloth, with approximately 0.5 m (2 ft) of burlap in contact with the surface until the desired texture was obtained. The brush finish was accomplished by passing a natural-bristle (strawlike) brush over the slab surface, which slightly grooved the concrete. The broom was inclined at an angle of approximately 30 deg to the surface. The tine finish was accomplished by passing a series of thin metal strips (tines), 0.32 by 12.7 cm (⅛ by 5 in) long, over the section surface, which produced grooves that were approximately 0.32 cm (⅛ in) in depth in the concrete. The tine spacing was varied from 0.32 to 0.64 cm (⅛ to ¼ in) (clear distance between tines). The burlap-drag-plus-tine finish was accomplished by first passing the burlap drag over the section surface, followed by one pass of the tines as previously described. The tine spacing was varied from 0.64 to 2.54 cm (¼ to 1.0 in) (clear distance between tines).

RESULTS TO DATE

Texture Depth

The texture of a pavement surface is the character of the surface profile consisting of a series of abrupt changes in elevation. Variations in texture can result from the different sizes of aggregates on the surface and from various pavement finishing operations. The textures resulting from construction can be altered by the effects of traffic, wear, and environment.

One major finding of this study was that all of the experimental textures were easily constructed. No increase in construction cost would be expected if any of the experimental textures were specified.

Texture measurements were initially made by using the putty impression method (8) and later by using the sand patch method as well (Tex 436-A) (9). To develop the correlation between these two tests, we made a linear regression analysis of 276 observations on the Tex-6 test sections, 124 observations on the I-10 test sections, and 44 observations on laboratory blocks of various finishes (10). The resulting equation is

$$TXD_s = 0.8185\ TXD_p \quad (1)$$

where

TXD_s = sand patch value and
TXD_p = putty impression value.

The square of the correlation coefficient for equation 1 = 0.96.

For Tex-6, texture depth measurements were taken at various intervals between December 1971 and July 1974. The test surfaces evaluated in December 1971 had little or no traffic on them. Conversely, the same surfaces, tested in July 1974, had been subjected to 8 months of construction traffic and 23 months of public use. The texture depths decrease rapidly at first and then appear to level off.

Evaluation of each surface finish on I-10 was conducted in essentially the same manner. The initial textures were measured in December 1973 before any traffic movement. The second measurements were made in July 1974 after the 11 different textures had been subjected to approximately 3 months of construction traffic and 5 months of public traffic.

The average wearing down for the Tex-6 textures was 32 percent, which is in substantial agreement with data taken from accelerated wear testing of 98 laboratory-constructed concrete finishes on the Texas Department of Highways and Public Transportation circular test track. The average wearing down of these 98 surfaces was 24 percent with a standard deviation of 13 percent (10). The average wearing down for the I-10 textures was 34 percent. Therefore, it can be concluded that concrete pavement textures, regardless of type, may be expected to wear down a minimum of 25 to 35 percent under normal southern United States traffic conditions, based on initial texture depth.

Skid Measurements Under Standard Conditions

For the outer lane of the Tex-6 test sections, the variations in skid resistance at 64 km/h (40 mph) with time are shown in Figure 1. Following an initial period of anomalous behavior, all sections appear to be exhibiting lower skid resistances with time. However, every experimental texture exhibited a higher initial skid resistance than that for the burlap control.

On I-10, only two sets of skid resistance measurements have been made to date. The longer term behavior of the I-10 test sections is unknown at this time.

Skid Measurements Under Simulated Rainfall

Skid measurements under light simulated rainfall conditions on the Tex-6 test sections are summarized in Figure 2. The data are given in Table 2. Under rainfall intensities of approximately 3.8 cm/h (1.5 in/h) (Figure 2), all of the experimental textures exhibited higher skid resistances [10 to 20 skid numbers (SNs)] than the burlap control, although skid gradients were similar [about 0.97 SN drop per km/h (0.6 SN drop per mph)]. Under rainfall intensities of approximately 15 cm/h (6 in/h), the beneficial skid effects of the deeper textures were somewhat masked, especially at higher speeds. A more complete discussion of these conditions can be found elsewhere (6).

For the I-10 test sections, skid measurements under simulated rainfall are shown in Figures 3 and 4 for selected test sections on I-10. The data are given in Table 3. For comparison purposes, skid values that use standard trailer water are also shown. These data and figures again show that, at elevated speeds [64 and 97 km/h (40 and 60 mph)], skid measurements under standard trailer water were significantly higher than under simulated rainfall.

Before discussing these results in detail, it should be pointed out that all the simulated rainfall data were

gathered on relatively new pavement surfaces that had neither been worn nor contaminated by road films and the like. If worn pavements had been used, lower skid values would be expected.

In general, as vehicle speed increases, SN decreases. The entrapment of water between a sliding tire and a wet pavement surface is responsible for the development of hydrostatic pressure. This pressure decreases tire pavement friction in direct proportion to its magnitude. If this pressure develops to the extent that the tire is supported almost entirely by the water film, hydroplaning results (11).

At the different test speeds, the tire-pavement interface becomes wet to various degrees. This fact, in part, may account for some of the anomalies that occur during the testing of pavement surfaces, as can be seen by comparing skid values for standard trailer water with skid values for various depths of water on the pavement surface.

These data seem to indicate that skid measurements under standard trailer water conditions may not be indicative of real-life conditions in rainy weather. If we assume that the simulated rainfall conditions represent more closely real-life conditions, then the lack of skid resistance under these rainfall conditions is alarming at speeds in excess of about 64 to 80 km/h (40 to 50 mph), regardless of texture.

Table 1. Test section surface treatments.

Test Section Number	Surface Treatment
F-1	Transverse broom
F-2	0.32-cm transverse tines
F-3	Longitudinal broom
F-4	0.32-cm longitudinal tines
F-5	Burlap drag + 0.32-cm longitudinal tines
F-6	Burlap drag (control)
F-7	Transverse brush
F-11	Burlap + 0.64-cm longitudinal tines
F-12	Burlap + 1.27-cm longitudinal tines
F-13	Burlap + 2.54-cm longitudinal tines
F-14	Burlap + 1.91-cm longitudinal tines
F-15	0.64-cm longitudinal tines
F-16	0.32-cm longitudinal tines
F-17	Burlap drag (control)
F-18	0.32-cm transverse tines
F-19	0.64-cm transverse tines
F-20	Transverse brush
F-21	Burlap + 2.54-cm transverse tines

Note: 1 cm = 0.394 in.

Figure 1. Skid measurement results at 64 km/h (40 mph) on the outside lane of Tex-6 in College Station.

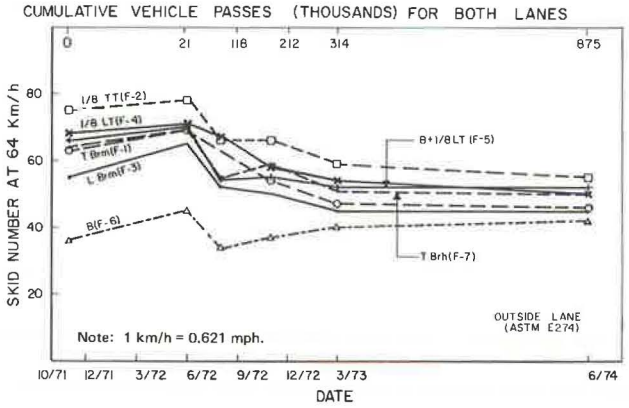

Table 2. Skid measurements under simulated rainfall on Tex-6 in College Station, August 1972.

Test Section Number	Description	Bald Tire				Treaded Tire			
		Water Depth (cm)	32-km/h SN	64-km/h SN	97-km/h SN	Water Depth (cm)	32-km/h SN	64-km/h SN	97-km/h SN
F-1	Transverse broom (TXD_t = 0.084 cm, TXD_p = 0.109 cm)	-0.051	64	40	28	-0.051	69	56	41
		0.010	67	36	23	0.010	75	54	37
		0.061	57	39	24	0.061	74	55	25
		0.122	58	28	16	0.122	74	55	25
F-2	Transverse tines (TXD_t = 0.145 cm, TXD_p = 0.163 cm)	-0.150	72	48	36	-0.150	77	59	45
		-0.089	77	47	32	-0.089	82	62	47
		0.000	72	56	43	0.000	74	62	49
		0.061	84	47	28	0.061	84	59	34
F-3	Longitudinal broom (TXD_t = 0.038 cm, TXD_p = 0.071 cm)	-0.020	53	32	19	-0.020	71	49	33
		0.051	61	29	22	0.051	75	53	28
		0.079	54	29	19	0.079	71	51	33
		0.107	55	26	19	0.107	75	53	36
		0.130	66	28	21	0.130	74	51	27
		0.155	58	25	19	0.155	75	62	29
F-4	Longitudinal tines (TXD_t = 0.140 cm, TXD_p = 0.157 cm)	-0.066	75	50	29	-0.066	80	61	35
		0.020	76	47	23	0.020	84	67	28
		0.071	69	35	20	0.071	75	64	28
		0.150	74	30	18	0.150	75	63	24
F-5	Burlap + longitudinal tines (TXD_t = 0.150 cm, TXD_p = 0.165 cm)	-0.036	69	40	23	-0.036	67	59	42
		0.030	68	42	20	0.030	72	58	34
		0.130	72	46	20	0.130	73	56	23
		0.180	74	46	18	0.180	76	55	18
F-6	Burlap drag (control) (TXD_t = 0.051 cm, TXD_p = 0.081 cm)	-0.025	46	26	16	-0.025	57	41	26
		0.010	50	28	16	0.010	61	45	21
		0.041	54	26	16	0.041	62	41	26
		0.140	60	31	16	0.140	64	47	20
F-7	Transverse natural brush (TXD_t = 0.053 cm, TXD_p = 0.084 cm)	0.000	64	35	25	0.000	83	63	43
		0.051	56	30	25	0.051	78	55	38
		0.079	66	32	23	0.079	85	65	36
		0.127	49	29	23	0.127	70	56	26

Note: 1 cm = 0.394 in. 1 km/h = 0.621 mph.

Figure 2. Effect of vehicle speed on skid values of Tex-6 test sections under simulated light rainfall.

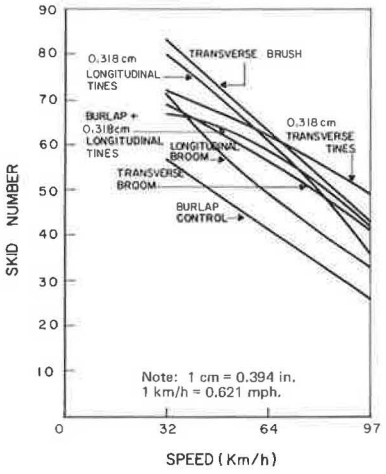

Figure 3. Effect of vehicle speed on skid values of section F-11 on I-10 under simulated rainfall.

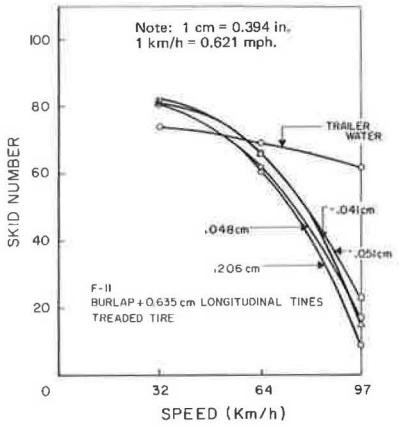

Figure 4. Effect of vehicle speed on skid values of section F-19 on I-10 under simulated rainfall.

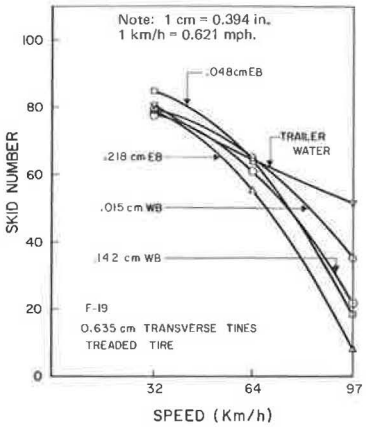

Table 3. Skid measurements under simulated rainfall on I-10 near Van Horn, October 1973.

Test Section Number	Description	Bald Tire				Treaded Tire			
		Water Depth (cm)	32-km/h SN	64-km/h SN	97-km/h SN	Water Depth (cm)	32-km/h SN	64-km/h SN	97-km/h SN
F-11	Burlap + 0.64-cm longitudinal tines	-0.135	78	51	16	-0.051	82	66	23
	(TXD_s = 0.178 cm,	-0.117	77	56	26	-0.041	81	66	15
	TXD_p = 0.206 cm)	-0.018	78	46	12	0.048	81	62	17
		0.165	80	52	9	0.206	81	61	9
F-12	Burlap + 1.27-cm longitudinal tines	-0.018	79	46	18	-0.033	80	61	34
	(TXD_s = 0.155 cm,	0.005	81	45	12	-0.023	79	59	16
	TXD_p = 0.191 cm)	0.074	78	40	7	0.028	83	61	14
		0.160	78	38	3	0.132	79	59	9
F-13	Burlap + 2.54-cm longitudinal tines	-0.030	66	33	13	-0.041	71	52	18
	(TXD_s = 0.114 cm,	0.163	60	32	11	0.025	69	51	18
	TXD_p = 0.157 cm)	0.036	70	30	5	0.061	70	48	8
		0.107	68	27	4	0.127	71	46	8
F-14	Burlap + 1.91-cm longitudinal tines	0.036	73	33	11	0.061	81	63	14
	(TXD_s = 0.132 cm,	0.069	74	29	6	0.089	78	54	8
	TXD_p = 0.163 cm)	0.132	75	33	6	0.142	78	50	7
		0.135	69	22	3	0.183	82	60	11
F-16	0.32-cm longitudinal tines	0.046	75	43	13	0.033	81	66	25
	(TXD_s = 0.165 cm,	0.051	75	36	4	0.058	82	65	17
	TXD_p = 0.173 cm)	0.114	79	44	11	0.102	84	65	20
		0.175	77	42	4	0.165	85	68	10
F-17	Burlap drag (control)	-0.028	65	31	10	-0.023	77	57	16
	(TXD_s = 0.069 cm,	-0.005	62	25	4	-0.008	71	52	16
	TXD_p + 0.086 cm)	0.081	67	28	8	0.076	78	49	14
		0.135	65	21	4	0.165	77	48	9
F-18	0.32-cm transverse tines	-0.015	73	33	21	0.156	88	64	22
	(TXD_s = 0.132 cm,	0.145	73	25	7	0.137	94	65	9
	TXD_p = 0.127 cm)	0.0005	79	32	20	0.023	89	65	28
		0.013	78	34	15	0.041	88	65	17
F-19	0.64-cm transverse tines	0.188	65	23	9	0.218	79	55	8
	(TXD_s = 0.079 cm,	0.137	63	21	9	0.142	78	61	22
	TXD_p = 0.079 cm)	0.048	61	24	13	0.048	85	64	18
		0.015	60	25	14	0.015	79	65	35
F-20	Transverse brush	0.114	59	20	5	0.114	76	51	16
	(TXD_s = 0.059 cm,	0.099	60	20	5	0.099	74	49	15
	TXD_p = 0.053 cm)	0.081	56	24	10	0.081	85	56	19
		0.013	58	29	16	0.013	85	62	31
F-21	Burlap + 2.54-cm transverse tines	0.112	67	22	10	0.112	77	55	14
	(TXD_s = 0.079 cm,	0.117	67	19	7	0.117	75	50	9
	TXD_p + 0.076 cm)	0.033	61	28	13	0.030	73	49	16
		0.015	62	23	11	0.013	78	60	21

Note: 1 cm = 0.394 in. 1 km/h = 0.621 mph.

Statistical Analysis of Skid Measurements Under Simulated Rain Conditions

All the data (Tables 2 and 3) from the test sections on Tex-6 and I-10, including the bald tire data, were statistically analyzed by using a two-step select regression analysis technique where best fit models of the following form were developed (these models are designed for U.S. customary units only; therefore, values are not given in SI units):

$$SN = \frac{C_1}{MPH^{C_2}}\left[C_3(TD+1)^{C_4}\ TXD^{C_5} + \frac{1}{(WD+0.1)^{C_6}}\right] \quad (2)$$

Table 4. Regression models.

Texture Direction	Equation Number	Regression Model	Number of Data Points	Square of Correlation Coefficient	Standard Error[a]
Transverse	24	$SN = \frac{205}{MPH^{1.15}}\left[17.92\ (TD+1)^{0.18}\ TXD^{0.29} + \frac{1}{(WD+0.1)^{0.53}}\right]$	168	0.79	11.88
Longitudinal	25	$SN = \frac{910}{MPH^{1.37}}\left[3.06\ (TD+1)^{0.14}\ TXD^{0.04} + \frac{1}{(WD+0.1)^{0.31}}\right]$	252	0.76	13.56

Note: TD is measured in 32nds of an inch; TXD and WD are measured in inches.
[a]In terms of skid number.

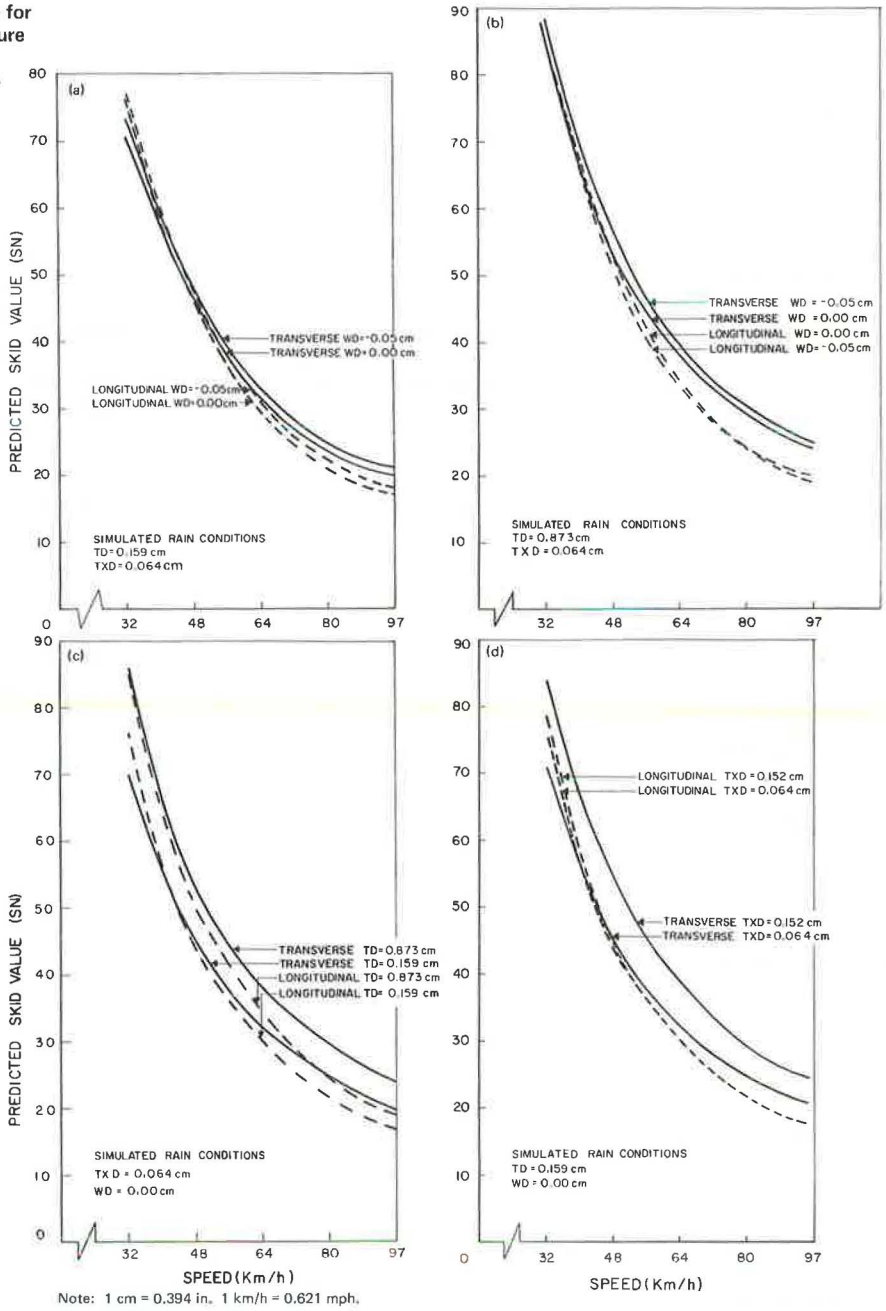

Note: 1 cm = 0.394 in. 1 km/h = 0.621 mph.

Figure 5. Effect of vehicle speed on skid value for (a) tread depth of 0.159 cm (0.06 in) and texture depth of 0.064 cm (¼ in), (b) tread depth of 0.873 cm (0.33 in) and texture depth of 0.064 cm (¼ in), (c) water depth of 0.00 cm (0.00 in) and texture depth of 0.064 cm (¼ in), and (d) tread depth of 0.159 cm (0.06 in) and water depth of 0.00 cm (0.00 in).

where

SN = skid number,
MPH = vehicle speed in miles per hour,
TD = skid tire tread depth in 32nds of an inch,
TXD = pavement texture depth in inches,
WD = water depth on the pavement surface in inches measured from the top of the pavement asperities, and
$C_1, \ldots, C_6$ = constants.

A complete description of this technique is given elsewhere (12, 13). The regression analyses yielded two equations—one for transverse textures and one for longitudinal textures—that are summarized in Table 4. The correlation coefficients obtained through the use of this statistical technique are satisfactory. However, the standard errors in terms of SN are somewhat high. There is considerable data scatter because many variables, such as type of finish, location of test section, and type of aggregate, were not considered in this analysis. Therefore, at best, these models for the prediction of SN must be used with engineering judgment because considerable variability may be expected. The results have been plotted in Figures 5, 6, 7, and 8 by using the models.

Figure 5a shows the effect of increasing speed on skid value, of both transverse and longitudinal texturing, assuming a tread depth of 0.16 cm ($^1/_{16}$ in) (the legal minimum in Texas) and a texture depth of 0.064 cm (0.025 in) (the specified as-constructed minimum in Texas) (1) for two water depths: -0.05 cm and 0.00 cm (-0.02 in and 0.00 in) as measured from the top of the pavement asperities. The significant influence of vehicle speed on available friction (SN) can be immediately seen because the SN value drops very rapidly as speed is increased. At low speeds very high SN values are obtained, but, at high speeds [above 64 km/h (40 mph)], the SN values drop below 30 and here transverse texturing results in higher skid values regardless of water depth. This becomes very important at speeds of 97 km/h (60 mph) because the SNs are very low (around 20) and even small increases in skid values become significant on a relative basis.

Figure 5b shows the same type of plot but for a tire depth of 0.87 cm ($^{11}/_{32}$ in), which represents a new tire. From this figure, it can be seen that, even for a deep tread, the loss in skid value becomes alarmingly high as vehicle speed is increased. Here again, at speeds in excess of 48 km/h (30 mph), the transverse textures exhibit higher skid values than longitudinal textures exhibit. For example, at 97 km/h (60 mph) and -0.05-cm (-0.02-in) water depth, there is a 24 percent greater skid value for transverse texturing over longitudinal texturing (24 versus 20 SN). Another interesting finding shown in Figure 5b is the relatively small influence of water depth on measured skid value, only 1 SN difference for a change in water depth from 10.05 cm to 0.00 cm (-0.02 in to 0.0 in). Examination of all the data reveals that, for the range of conditions evaluated, this is a general finding regardless of texture direction, tread depth, water depth, and vehicle speed. If it were carried further, it would seem to indicate that low skid values could be obtained in almost any rainfall in which the pavement surface was completely wet.

The effect of tread depth on skid values for a water depth of 0.00 cm (0.00 in) and a texture depth of 0.064 cm (0.025 in) is shown in Figure 5c. At speeds approaching 97 km/h (60 mph), the relative differences in SN values between full tread, 0.87 cm ($^{11}/_{32}$ in), and minimum tread, 0.16 cm ($^1/_{16}$ in), become very significant. Full tread results in 20 percent more available skid resistance than minimum tread does (SN values of 24 versus 20).

The effects of texture depth and texture direction are shown in Figure 5d for a tread depth of 0.16 cm ($^1/_{16}$ in) and a water depth of 0.00 cm (0.00 in). For this water depth, at 97 km/h (60 mph), transverse texturing is again significantly better than longitudinal texturing, and a 0.15-cm (0.06-in) texture depth is significantly better than 0.064-cm (0.025-in) texture depth (20 percent for transverse texturing—24 versus 20). Figure 5d summarizes the effects of vehicle speed on skid value for conditions that may reasonably be expected to exist on Texas highways in almost any rainfall in which the pavement is completely wet.

CONCLUSIONS

Six conclusions relate to the findings of this study and are subject to the limitations involved in the study. Generalizations beyond the parameters investigated may not be warranted.

1. Texture depths of 0.15 cm (0.06 in) or greater were easily and economically constructed in PCC pavement in either the longitudinal or transverse direction by using 0.32-cm-wide ($^1/_8$-in-wide) metal tines spaced closer than 1.27 cm ($^1/_2$ in) apart.
2. Based on initial texture depth, all textures wore down between 25 and 35 percent under traffic and appeared to have leveled off.
3. At speeds of 64 and 97 km/h (40 and 60 mph), locked-wheel skid measurements using trailer water were significantly different from the same measurements made under simulated rain conditions. The simulated rain conditions indicated much lower skid values regardless of measured water depths. This indicates that skid measurements made under standard trailer water conditions may not be indicative of real-life conditions in wet weather.
4. Statistical analysis of the skid measurements under simulated rainfall conditions indicate that, for the rainfall conditions evaluated, extremely low skid values occurred at speeds greater than 64 km/h (40 mph) regardless of water depths. This means that low skid values could be obtained in almost any rainfall in which the pavement was completely wet.
5. Under simulated rain conditions, deep transverse texturing will result in the greatest improvement in skid values.
6. Statistical analysis is needed of the data required in regression models that can predict skid values for a selected vehicle speed, tire tread depth, pavement texture depth (with an appropriate factor for expected wearing down) and texture direction, and pavement water depth.

RECOMMENDATION

Transverse tine textures, with the tines spaced less than 1.27 cm ($^1/_2$ in) apart, should be required for concrete pavements. These textures should be significantly deeper than now required. Furthermore, any required initial texture depth should consider expected wearing down and subsequent loss of texture, and the regression models should be used to determine required texture depths. This recommendation has been successfully applied by the Texas Department of Highways and Public Transportation on two recent construction projects and will be the standard practice for current projects.

ACKNOWLEDGMENTS

The information contained here was developed in Research Study 2-6-70-141, Quality of Portland Cement Concrete Pavement as Related to Environmental Factors and Handling Practices During Construction, in a cooperative research program with the Texas Department of Highways and Public Transportation and the Federal Highway Administration.

The contents of this paper reflect our views, and we are responsible for the facts and the accuracy of the data presented. The contents do not necessarily reflect the official views or policies of the Federal Highway Administration.

REFERENCES

1. 1972 Standard Specifications. Texas Highway Department, Austin, Item 360.8.
2. G. K. Ray and L. T. Norling. More Microtexture in Concrete Pavement for Greater, Longer-Lasting Skid Resistance. Portland Cement Association, Skokie, Ill., 1974, 18 pp.
3. J. G. Rose and W. B. Ledbetter. Summary of Surface Factors Influencing the Friction Properties of Concrete Pavements. HRB, Highway Research Record 357, 1971, pp. 53-63.
4. Surface Wear of Portland Cement Concrete Pavements. TRB, Transportation Research Circular 170, Sept. 1975.
5. W. E. Murphy and D. P. Maynard. Surface Texture of British Concrete Pavements. Journal of Highway Division, Proc., ASCE, Vol. 101, No. TE1, Feb. 1975, p. 115.
6. J. L. Davis, W. B. Ledbetter, and A. H. Meyer. First Progress Report on Concrete Experimental Test Sections in Brazos County, Texas. Texas Transportation Institute, Texas A&M Univ., College Station, Research Rept. 141-2, Aug. 1973, 63 pp.
7. W. B. Ledbetter, A. H. Meyer, and D. E. Ballard. Evaluation of Full-Scale Experimental Concrete Highway Finishes. Texas Transportation Institute, Texas A&M Univ., College Station, Research Rept. 141-4F, Sept. 1974, 81 pp.
8. J. G. Rose and others. Summary and Analysis of the Attributes of Methods of Surface Texture Measurement. In Skid Resistance of Highway Pavements, ASTM, Philadelphia, STP 530, 1973, pp. 60-77.
9. Manual of Testing Procedures. Texas Highway Department, Austin.
10. K. D. Hankins, J. P. Underwood, O. Darnaby, and W. B. Ledbetter. Pavement Surface Polishing Characteristics: A Circular Track Test. Texas Transportation Institute, Texas A&M Univ., College Station, Research Rept. 126-3F, June 1974, 118 pp.
11. R. W. Yeager. Tire Hydroplaning: Testing, Analysis, and Design. In The Physics of Tire Traction, Plenum Press, New York, 1974, pp. 25-63.
12. R. R. Hocking and R. N. Leslie. Selection of the Best Subset in Regression. Technometrics, Vol. 9, 1967, pp. 531-540.
13. L. R. Lamotte and R. R. Hocking. Computational Efficiency in Selection of Regression Variables. Technometrics, Vol. 12, 1970, pp. 83-93.

Abridgment

Skid Number and Speed Gradients on Highway Surfaces

David C. Mahone, Virginia Highway and Transportation Research Council

In the project from which this paper was derived, three major factors that influence the skid number (SN) and speed gradient (G) were studied: tire tread depth, water film, and pavement surface texture (1). However, only the effect of pavement surface is discussed here; the measurement of texture is not considered. The 31 sites that were included in the study are given in Table 1.

In the study, tread depths of 0.87 cm, 0.71 cm, 0.56 cm, 0.40 cm, 0.24 cm, and bald ($^{11}/_{32}$ in, $^{9}/_{32}$ in, $^{7}/_{32}$ in, $^{5}/_{32}$ in, $^{3}/_{32}$ in, and bald) and water film thicknesses of 0.04, 0.05, 0.08, and 0.10 cm (0.015, 0.020, 0.030, and 0.040 in) were tested at speeds of 48.3, 64.4, 80.5, 96.6, and 112.6 km/h (30, 40, 50, 60, and 70 mph). For each combination of test conditions, 5 skid resistance measurements were made at each site for each speed, which totaled more than 13 000 tests. The data reported here have been combined and averaged from all tread depths, excluding bald, and all water film thicknesses for each test speed. Detailed descriptions of the testing method and the procedures used in combining the data can be found elsewhere (1). However, I feel that the data show the same general trends that would be expected with treaded tires and the normal water output required by ASTM E 274-70 (2).

RESULTS

In the analysis of the test data, the pavements generally fit into three groups: steep gradients—0.50 G or greater, intermediate gradients—0.28 to 0.40 G, and flat gradients—0.20 G or less. The curves for the three groups are shown in Figure 1.

Five of the 31 sites provided G values of 0.50 or greater. They consisted of smooth concrete, a sand asphalt, and a well-worn S-5 bituminous concrete. Table 2 gives the average SNs for the various test speeds, the average G for each of these sites, and the total accumulated traffic.

Twenty of the 31 sites fit in the intermediate speed gradient group. Table 3 gives the summary data for these sites. The sites consisted of various aged S-5 bituminous concrete surfaces; a special urban bituminous mix (3); a surface treatment; and several types of portland cement concrete textures including single burlap-dragged, longitudinally tined, grooved, and bush-hammered textures (4).

Table 4 gives the summary data for the sites in the flat gradient group. These sites consisted of bituminous concrete surfaces, open-graded (popcorn mix) bituminous surfaces, and surface treatments.

Basically, the textures for the pavements represented by the three curves in Figure 1 are

1. Steep gradient, which is for surfaces with smooth macrotexture but gritty or smooth microtexture.
2. Intermediate gradient, which is for all of those surfaces with a good combined microtexture and macrotexture. In addition, some well-worn surfaces that would originally have been found in the steep gradient group fell into this group when they lost their microtexture. Also included are some well-worn surfaces that originally would have been in the flat gradient group. These two exceptions can usually be identified by a lower than expected SN_{40} value combined with knowledge concerning the accumulated traffic passes and the material from which the surface was fabricated.
3. Flat gradient, which is for surfaces with excellent microtexture and macrotexture.

The estimated slopes for the curves are as follows for various speed ranges (1 km/h = 0.621 mph):

Group	48 to 80 km/h	64 to 96 km/h	80 to 112 km/h	48 to 112 km/h
Steep	0.73	0.61	0.47	0.60
Intermediate	0.42	0.33	0.25	0.33
Flat	0.23	0.17	0.08	0.15

It should be noted that the gradient decreased as the test speed increased and that the gradient between 64.4 and 96.6 km/h (40 and 60 mph) was quite similar to the gradient between 48.3 and 112.6 km/h (60 and 70 mph). On

Publication of this paper sponsored by Committee on Surface Properties-Vehicle Interaction.

Table 1. Site information.

Site Number	Type of Surface	Year Placed	Lane	Accumulated Traffic (vehicles)
1	Portland cement concrete	1970	EBTL	4 028 870
2	Portland cement concrete	1970	WBPL	1 007 218
3	S-5 bituminous concrete[a]	1970	EBTL	4 028 870
4	S-5 bituminous concrete[a]	1970	WBPL	1 007 218
5	S-1 sand asphalt[a]	1968	N&SBTL	3 149 950
6	Portland cement concrete	1959	SBTL	17 212 962
7	Portland cement concrete	1959	SBPL	4 303 240
8	Mechanically chipped concrete	1974	SBTL	0
9	Mechanically chipped concrete	1974	SBPL	0
10	S-5 bituminous concrete[a]	1969	EBTL	4 411 755
11	S-5 bituminous concrete[a]	1969	WBTL	4 411 755
12	S-5 bituminous concrete[a]	1969	EBPL	1 102 939
13	S-5 bituminous concrete[a]	1969	WBPL	1 102 939
14	Bituminous urban mix[a]	1971	SBTL	3 255 800
15	Bituminous urban mix[a]	1971	SBPL	3 255 800
16	Popcorn bituminous mix	1973	NBTL	2 285 630
17	Popcorn bituminous mix	1973	SBPL	571 408
18	S-5 bituminous concrete[a]	1968	NBTL	9 187 050
19	S-5 bituminous concrete[a]	1968	SBPL	2 296 762
20	Portland cement concrete	1973	EBTL	2 106 780
21	Portland cement concrete	1973	EBTL	526 695
22	Portland cement concrete	1968	EBTL	13 430 175
23	Portland cement concrete	1968	EBPL	7 815 106
24	Grooved portland cement concrete	1968	EBTL	13 430 175
25	Grooved portland cement concrete	1968	EBPL	7 815 106
26	Surface treatment	1969	NBPL	534 542
27	Surface treatment	1969	SBTL	2 138 170
28	Surface treatment	1970	NBPL	449 680
29	Surface treatment	1970	SBTL	1 798 720
30	S-5 bituminous concrete[a]	1965	WBPL	2 342 388
31	S-5 bituminous concrete[a]	1965	EBTL	9 360 550

Note: EB = eastbound; WB = westbound; NB = northbound; SB = southbound; TL = through lane; and PL = passing lane.

[a]Specifications can be found in Road and Bridge Specifications (5).

the other hand, the gradient between 48.3 and 80.5 km/h (30 and 50 mph) bears little resemblance to that between 80.5 and 112.6 km/h (50 and 70 mph). Therefore, great care should be taken in selecting test speeds to establish gradients.

There is no question that the average G value decreased with increased macrotexture. Exceptions to this were the grooved concrete pavements on which the grooves or macrotexture provided ample water escape routes but no microharshness; therefore, the gradient was rather steep. This finding indicates that, in addition to a provision for the escape of water, a pronounced

Figure 1. Speed gradients for three groups of pavements.

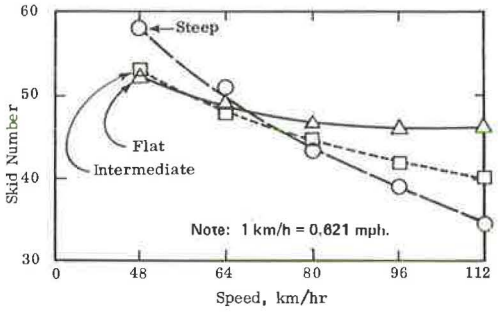

Table 2. Summary data for steep gradient group.

Site Number	Skid Number 48 km/h	64 km/h	80 km/h	96 km/h	112 km/h	Slope (SN/km/h)	Accumulated Traffic (millions of vehicle passes)
1	58	50	43	39	35	0.58	4.0
2	67	60	52	47	41	0.65	1.0
5	62	54	46	39	33	0.73	3.1
23	57	52	45	42	37	0.50	7.8
31	47	40	32	28	25	0.55	9.4
Average	58	51	43	39	34	0.60	

Note: 1 km/h = 0.621 mph.

Table 3. Summary data for intermediate gradient group.

Site Number	Skid Number 32 km/h	48 km/h	64 km/h	80 km/h	96 km/h	112 km/h	Slope (SN/km/h)	Accumulated Traffic (millions of vehicle passes)
3	–	54	45	45	51	39	0.38	4
4	–	56	53	49	47	44	0.28	1
6	–	37	32	29	25	23	0.35	17
7	–	47	42	37	33	31	0.40	4
8	–	42	37	33	31	30	0.30	0
9	–	50	45	41	37	36	0.35	0
10	–	53	49	45	42	40	0.33	4.3
11	–	52	49	45	44	42	0.25	4.3
14[a]	61	56	46	50	48	–	0.33	3.25
15[a]	65	59	55	51	49	–	0.40	3.25
18	–	53	50	46	42	39	0.35	9
19	–	56	53	50	46	44	0.30	2.5
20	–	60	58	56	53	48	0.30	2
21	–	72	66	63	59	57	0.38	2.5
22	–	50	44	39	36	38	0.30	13.5
24	–	49	48	43	41	39	0.25	13.5
25	–	56	52	49	45	40	0.40	7.7
27	–	42	38	35	33	31	0.28	2
29	–	45	41	37	36	34	0.28	1.75
30	–	55	48	47	41	41	0.35	2.3
Average		53	48	44	42	40	0.33	

Note: 1 km/h = 0.621 mph.

[a]Only 0.05-cm (0.020-in) film of water tested with speeds 32.2 to 96.6 km/h (20 to 60 mph).

Table 4. Summary data for flat gradient group.

Site Number	Skid Number 48 km/h	64 km/h	80 km/h	96 km/h	112 km/h	Slope (SN/km/h)	Accumulated Traffic (millions of vehicle passes)
12	53	50	48	46	46	0.18	1
13	53	50	47	46	48	0.18	1
16	50	50	48	47	45	0.13	2.3
17	50	47	46	46	46	0.10	0.5
26	51	48	46	42	43	0.23	0.5
28	53	49	48	47	46	0.18	0.5
Average	52	49	47	46	46	0.15	

Note: 1 km/h = 0.621 mph.

microtexture is needed to provide a flat gradient. By the same token, if an open-graded bituminous mix is manufactured with aggregate that is highly polish susceptible, it probably will develop a rather steep gradient in addition to becoming slippery.

The data, then, point to the following: High G values are common to pavements that do not have a relatively high degree of macrotexture. Although this fact merely substantiates previous research on the subject, if the surface has a sharp microtexture, as is the case for all locations except site 31 in the steep gradient group, its skid resistance can be excellent at all legal speeds with legal tread tires.

The highest skid numbers recorded in the study were at low speeds in the steep gradient group, which means that a low macrotexture and a high microtexture provide the best skid-resistance surface at low speeds [64.4 km/h (40 mph) and lower]. Cities and counties should take this into account when they are paving streets with low speed limits. On the other hand, the open-graded mixes, which provide flat gradients, provide a very desirable surface for high-speed traffic. Grooving does not improve the skid resistance or the G value for treaded tires. Thus, because grooving does not decrease the G value, I suggest that the mere provision for water escape does not guarantee that the pavement surface will have a flat gradient.

REFERENCES

1. D. C. Mahone. An Evaluation of the Effects of Tread Depth, Pavement Texture, and Water Film Thickness on Skid Number-Speed Gradient. Virginia Highway and Transportation Research Council, Charlottesville, March 1975.
2. Standard Method of Test for Skid Resistance of Paved Surfaces Using a Full-Scale Tire. ASTM, Philadelphia, E 274-70, April 1971.
3. D. C. Mahone, C. S. Hughes, and G. W. Maupin. Skid Resistance of Dense-Graded Asphalt Concrete. TRB, Transportation Research Record 523, 1974, pp. 134-140.
4. M. F. Creech. Mechanical Alteration of the Texture of Old Concrete Pavement With the Klarcrete Machine. TRB, Transportation Research Record 484, 1974, pp. 9-23.
5. Road and Bridge Specifications. Virginia Department of Highways and Transportation, Richmond, July 1974.

Correlation of Data From Tests With Skid-Resistant Tires

S. Weiner, L. J. Runt, and R. R. Hegmon, Federal Highway Administration
A. J. Stocker, Texas Transportation Institute, Texas A&M University

A standard test tire is generally used for skid resistance testing. The American Society for Testing and Materials (ASTM) Committee on Skid Resistance has recently adopted a new standard tire (ASTM E 501) to replace the first standard tire (ASTM E 249). The new tire is somewhat larger than the first tire and has a bias-belted construction instead of the bias-ply construction of the first tire. The Federal Highway Administration has conducted a test program to establish a correlation between skid resistance measurements of these two tires. A large-scale field test program was held at the Texas Transportation Institute and was supplemented by a small laboratory study at the Tire Research Facility of CALSPAN Corporation. A range of values for the major variables in skid-resistance testing was used. These included four different pavements, three speeds, two water film thicknesses plus some dry tests, maximum and minimum tire groove depths, and, to the degree possible, low and high temperatures during testing. The results show that both tires respond in a similar way to changing test conditions but that tire ASTM E 501 is expected to measure about 4 percent higher than tire ASTM E 249 under standard test conditions at 64 km/h (40 mph). Similar conclusions hold for dry pavements although the difference is somewhat greater. Effect of groove width, which was too narrow in the first production batch but was rectified, has been found to be insignificant under the stated test conditions.

As a result of the First International Skid Prevention Conference in 1958 (1) and the associated program at Tappahannock, Virginia, in 1962 (2), the American Society for Testing and Materials (ASTM) Standard Tire for Pavement Tests (E 249) (3) came into general use for measuring skid resistance. This was probably the most important step in standardizing the measurement of skid resistance. Indeed, subsequent studies (4) have shown that good agreement can be obtained between skid testers of different designs when the standard test tire is used. However, tire and vehicle design did not remain static, and, by 1970, the standard test tire was no longer representative of current tires either in size or in construction. A revised standard for a test tire was prepared by ASTM and was approved in 1974 under the designation E 501 (5). The essential specifications of the two tires are given in Table 1.

During more than 10 years of use, a large amount of test data with the E 249 tire has been accumulated. With the changeover to tire E 501, the skid resistance data of the E 501 tire must be correlated with the accumulated data taken with tire E 249. Past experience has shown that attempts to correlate skid resistance measurements can be frustrating because of the large variability in skid testing. The only way to overcome this problem is by a large-scale test program under controlled conditions.

Exploratory tests were conducted in July 1974, and the full program was executed between September and December of the same year at the Texas Transportation Institute. Some additional field tests were run in May 1975. At the same time as the main test program, laboratory tests were run at the CALSPAN Tire Research Facility. These have been documented in the full report (6) and will not be discussed here. The results of field and laboratory tests were in good agreement.

TEST CONDITIONS

Both tires were tested under equal conditions, some of which were varied according to the test plan. The data given in Table 2 show the various test conditions.

TEST METHOD

Skid tests were conducted according to ASTM E 274 except that the surfaces were continually wet during testing. However, between tests there was sufficient time for the water to drain from the surface; therefore, no puddling occurred. Before the first locked-wheel skid in each test sequence, two watering passes were made, without locking the test wheel, to prewet the surface.

Random sequencing, as far as practical, was used in the design of the test plan. In any one day, tests were made at all three speeds in the morning and afternoon with each of the two types of tires. Each test sequence consisted of eight consecutive skids for a total of 192 skids/test day. Types of tires were switched after one or at most two of such sequences. The same tire was used throughout the test day although provisions had been

Publication of this paper sponsored by Committee on Surface Properties-Vehicle Interaction.

made for replacement in case of failure.

Any test day program was repeated three times with new tires for a total of 384 skids/type of tire under identical conditions, at least as far as conditions could be controlled. During the program, 8448 individual skid measurements were made.

During testing, a number of factors were recorded. Tire, pavement, and ambient air temperatures were measured and recorded. Tire pressure was measured but not readjusted unless a loss of pressure was found. Mean tire groove depth was measured and recorded. Tires were inspected visually for excessive or irregular wear.

The grooves in the first production batch of E 501 tires were narrower than specified. This has now been rectified. To determine whether this difference in groove width of 4.4 instead of 5.1 mm (0.175 instead of 0.200 in) affects the measurement, we added a few days of testing at the end of the first program with tires of narrow and correct groove width. Conditions were the same as those in the full test program although limited in extent. No significant differences could be found.

EXPERIMENTAL DESIGN AND ANALYSIS PLAN

For each type of tire, the experiment is structured as a $2 \times 3 \times 4 \times 8$ complete factorial design with 16 replications and two covariates. The factors are water depth (two levels), speeds (three levels), pavements (four levels), and order of run (eight levels). The two covariates are grooved depth x_1 and temperature x_2.

The objective was to establish a correlation between the two test tires and to determine the effect of the design factors and covariates on each tire. The analysis was conducted in three stages.

Within-Mean Analysis

The purpose of the within-mean analysis is twofold. The first is to examine order-of-run effect on each tire under every design combination and overall replications; the second is to compute means and variances for each set of eight skids.

The following linear order-of-run model is assumed for each group of eight runs:

$$y = a + bx \tag{1}$$

where

y = skid number (SN) value for an individual test run;
a and b = regression coefficients to be estimated; and
x = order of run = 1, 2, . . . , 8.

For this model to realistically hold true, all other effects (water depth, speed, pavement, groove depth, and temperature) must be constant while quadratic and higher order-of-run effects are assumed to be zero.

For each group, we calculate the following quantities:

$$\hat{b} = \left[\sum (x - \bar{x})(y - \bar{y})\right] \Big/ \left[\sum (x - \bar{x})^2\right] \tag{2}$$

$$E = \left[\sum (y - \bar{y})^2\right] - (\hat{b}\ \text{num}\ \hat{b}) \tag{3}$$

where

$\hat{b}$ = unbiased estimate of b,
E = error sum of squares (constituting the sum of the squares of the deviations of the eight observations about the least squares fit), and
num $\hat{b}$ = numerator of b.

If we assume that each observation is identically and independently normally distributed, a formal consolidated F-test on all data groups can be made. This was done at the 5 percent level of significance to test the null hypothesis that the linear order-of-run effect was nonexistent.

For each tire type, the test statistic is

$$F_{m,n} = \left(6 \sum \hat{b}\ \text{num}\ \hat{b}\right) \Big/ \left(\sum E\right) \tag{4}$$

where

m = 384 and
n = 6 × 384 = 2604.

The summations in equation 4 are taken over 384 groups. From this test, the order-of-run effect was concluded to be not significant; therefore, no adjustment was necessary to conduct the between-mean analysis.

Between-Mean Analysis

The results of the within-mean analysis permitted us to disregard the order-of-run effect. Now all analyses involve the group means of eight runs (784 in all). The experiment can now be regarded as a $2 \times 3 \times 4$ factorial design with two covariates and 16 replicates for each of the type of tire means. An analysis of covariance was performed to answer five questions.

1. Is the E 249 or the E 501 standard test tire more variable?
2. Are there significant interactions between variable factor effects?
3. Are the error variances the same at different speeds on different pavements?
4. Does the increase of water depth from the standard of 0.51 to 0.84 mm (0.020 to 0.033 in) have a significant effect on the skid measurement? If such an effect exists, is it the same for both tires?
5. Do groove depth and temperature have significant effects?

Table 3 gives a summary of the analysis of variance conducted on each tire. The mean squares are seen to be comparable between types of tires for all main effects, interactions, and error terms. All effects have been adjusted by the two covariates (groove depth and temperature), which thereby reduces the number of degrees of freedom in the error mean square estimate by two. If a random components model is assumed to exist (7, Chapter 22), a simple statistical test procedure is employed for testing the significance of each error source in Table 3. This procedure develops individual F-tests on the mean squares for the main effects and interactions. Computed F-values are given in the table and are compared to the critical F-test value provided in the last column. Those that exceed the corresponding test values are considered to be significant. It is seen that only the H × P and H × V source effects are not significant.

A regression analysis was performed to determine the effect of increasing water depth. The results show that the skid number decreases by $H_1 - H_2$, which, according to the following, are equal and opposite:

Tire	H	σ	df
E 249	0.735	0.157	364
E 501	0.831	0.149	364

Thus, for tires E 249 and E 501, average respective SN decreases of 1.47 and 1.66 can be expected. This difference between the two tires was determined to be insignificant.

The data given in Table 4 show the effects of groove depth and temperature. The standard deviations (σ's) are obtained by the relation $t = b/(\sigma_b)$. All t-values are significant, which indicates that groove depth and temperature do affect the skid resistance measurement. To test for equality of this effect for both tires, we assumed approximate normality and applied the following test statistic:

$$u = (z_1 - z_2)/[(\text{var } z_1 - \text{var } z_2)^{0.5}] \quad (5)$$

where z's = slopes of regression. At the 5 percent level, the tests show that groove depth and temperature effects are about the same for both tires.

A comparison of the within-mean variances and between-mean variances from Table 3 is given in Table 5. From the data given in Table 5, the following pooled within-mean and between-mean information is determined:

Pooled Data	E 249	E 501	Pooled Data	E 249	E 501
Within mean Variance	4.46	4.80	Between mean Variance	3.38	2.97
σ	2.11	2.19	σ	1.84	1.72

First, there is a reversal in the relative magnitude of the variances. The E 501 tire exhibits a larger within-mean variance but a smaller between-mean variance than the E 249 tire. The variances, however, are of the same order of magnitude. Second, the between-mean variances, although somewhat smaller than the within-mean variances, are not smaller by a factor of eight as might be expected. Our data tell us that the between-mean variance is based on means of eight observations and, if the model is correct, should have a smaller expected value than the within-mean variance based on individual observation. Thus an error source was probably introduced by the transverse and longitudinal variability of the pavements although efforts were made to maintain the same path in each run. Some seasonal variations in the surfaces due to environmental effects also probably occurred because the tests extended over a period of 3.5 months (September to December 1974).

Furthermore, it can be seen in Table 5 that the error variances are highest at the 32-km/h (20-mph) speed condition and much lower at the two higher speeds (except on pavement section 1, which is portland cement concrete). This has been attributed to the usually greater skid resistance and speed gradients at low speeds. Therefore, for the same deviation from the desired test speed, the spread of measured skid resistance will be greatest at the lowest speed.

Tire-Calibration Analysis

In this, the third part of the analysis, various sets of equations are derived relating SN values of E 249 and E 501 tires. Thus, when skid resistance is measured with the new test tire, the equivalent skid resistance for the E 249 tire can be computed by using the given appropriate equation. These equations were tested for their predictability, and the recommendations given in this paper are based on these tests.

The full calibration model is

$$SNY = a_0 + a_1 SNX + a_2 D + a_3 T \quad (6)$$

where

SNY = predicted skid resistance for tire E 249;
SNX = measured skid resistance for tire E 501;
$D = 25.4[(x_1)_{249} - (x_1)_{501}]$ in millimeters;
$T = \{[(x_2)_{249} - (x_2)_{501}] - 32\}/1.8$ in degrees Celsius;
x_1 = mean groove depth of designated tire;
x_2 = pavement temperature of the wet pavements; and
a_i = the ith fitted constant in equation 4 (i = 0, 1, 2, 3).

Prediction of skid resistance presumes the same speed, pavement, and water depth for both tires. Therefore, these factors do not appear in equation 6. Groove depth and temperature, however, are uncontrolled variables, and the equation provides a correction for these.

In the preliminary analysis, variability was found to decrease with increasing speed (Table 5). The analysis of variance showed strong pavement and speed interactions. The failure of between-mean variances to be appreciably less than the within-mean variances was also surmised to be due to pavement variability. All this indicated the need to examine in the calibration various pavement and speed combinations as well as each of the major factors.

Calibrations were made separately for each speed and pavement, each pavement pooled over the three speeds, each speed pooled over the four pavements, and all pooled data. Thus an increasingly larger sample was included in the calibrations. Calibrations were also made without forcing the regression equation to go through zero by the constant term a_0, the intercept. The coefficients in the equations became increasingly consistent as the sample size increased and as the constant term was dropped. Figure 1 shows the coefficients for the composite data, with and without the intercept, while consecutively omitting the terms in T and D. Omission has little effect on the a_i terms, which indicates that their inclusion is only of secondary importance.

PREDICTABILITY OF CALIBRATIONS

The predictability of a calibration can be thought of as the variance of a predicted response. The calibration models examined so far were of the general form

$$y = \sum_{1}^{k} a_i x_i \quad (7)$$

where

y = response;
a_i = computed coefficient with covariance matrix W (i = 0, 1, . . . , k); and
x_i = independent or controlled variable.

For $x_0 = 1$, this model contains a constant term or intercept; for $x_0 = 0$, the model does not involve the intercept. For every regression equation as given in equation 7, a residual or error variance is also obtained, which we label s_e^2. This model may be used as a predictor at a given set of values $x' = (x_0, x_1, \ldots, x_k)$ or $(x_1, x_2, \ldots, x_k)$. If the prediction is to be used for estimating the mean of the population corresponding to x', then the variance of the predicted response is estimated by

$$s_p^2 = x'Wx \quad (8)$$

where x = transpose of row vector x′. However, if equation 8 is to be used to estimate the response to an individual observation at x′, then the predicted variance is estimated by

$$s_y^2 = x'Wx + s_e^2 \quad (9)$$

In practice, equation 9 is used to compute the prediction variance and will serve here as the criterion of the predictability of an equation. The criterion for selection of the appropriate prediction model has been the subject of considerable research in recent years. Some of the accepted ranking criteria are relatively complex, and the required set of computations has to be done by computer. Also, for any particular experiment, such criteria would not agree on the same ranking order. However,

Table 1. Pavement friction test tire specifications.

Item	E 249 Tire	E 501 Tire
Size designation	7.50-14	678-15
Rim designation	14 × 5J	15 × 6JJ
Tread width, mm	118	149
Number of ribs	5	7
Number of 5.1-mm grooves	4	6
Groove depth, mm	8.89	9.09
Minimum groove depth[a], mm	0.381	0.419
Inflation pressure, kPa	165.5	165.5
Test load, kg	492	492
Construction	Bias ply	Bias belted

Note: 1 mm = 0.0394 in. 1 kPa = 0.145 lbf/in². 1 kg = 2.205 lb.
[a]Wear indicator.

Table 2. Test conditions.

Item	Test Conditions
Tire description	New and shaved to wear indicator
Water film thickness[a], mm	0.51 and 0.84
Speed, km/h	32, 64, and 97
Wheel load, kg	492
Inflation pressure, kPa	165.5
Time[b]	Morning and afternoon
Surface[c]	
Skid number range	20 to 60
Texture range, mm	0.3 to 1.25

Note: 1 mm = 0.0394 in. 1 km/h = 0.621 mph. 1 kg = 2.205 lb. 1 kPa = 0.145 lbf/in².
[a]Some dry tests were also conducted.
[b]Two test series were run—one in the morning and one in the afternoon—to cover as wide a temperature range as possible.
[c]Four surfaces were tested.

Table 3. Summary of analysis of variance between means.

Source	df	Mean Squares			
		E 249 Tire	E 501 Tire[a]	Average[a]	Both Tires
Water depth (H)	1	119.79	146.71	133.25	133.00
Pavement (P)	3	12 682.78	11 796.92	12 239.85	12 237.30
Speed (V)	2	4 349.23	3 859.99	4 104.61	4 101.08
H×P	3	30.18	22.51	26.34	25.10
H×V	2	10.83	1.33	6.08	4.73
P×V	6	128.34	104.28	116.31	113.01
H×P×V	6	13.11	18.38	16.05	15.72
Error variance	358	3.38	2.97	3.17	3.18[b]

Note: df = degrees of freedom.
[a]Two tires.

Table 4. Linear regression coefficients for covariates groove depth and temperature.

Tire	Groove Depth			Wet Pavement Temperature		
	Slope b	σ	t	Slope b	σ	t
E 249	8.700	0.909	9.568	-0.025	0.0106	-2.342
E 501	10.402	0.720	14.457	-0.023	0.0099	-2.303
Both	9.694	0.568	17.056	-0.024	0.0073	-3.286

Table 5. Error variances.

Pavement Type	E 249 Tire			E 501 Tire		
	32 km/h	64 km/h	97 km/h	32 km/h	64 km/h	97 km/h
2	5.80	1.99	1.54	6.35	2.52	1.54
11	4.21	2.00	1.40	5.09	1.92	1.67
1	5.19	4.35	5.80	5.23	5.07	6.45
6	12.60	5.15	3.54	11.71	5.95	4.12
Mean	6.94	3.37	3.07	7.09	3.87	3.45

Figure 1. Calibrations for composite data (384 observations).

MODEL SNŶ =	COEFFICIENTS			
$a_0 + a_1SNX + a_2D + a_3T$	-1.49	1.018	13.32	-0.087
$b_0 + b_1SNX + b_2D$	-1.41	1.015	13.66	
$c_0 + c_1SNX$	-1.59	1.011		
$a'_1 SNX + a'_2 D + a'_3 T$		0.977	18.52	-0.067
$b'_1 SNX + b'_2 D$		0.976	18.55	
$c'_1 SNX$		0.963		

Figure 2. Skid resistance and speed gradients versus texture depth by putty method.

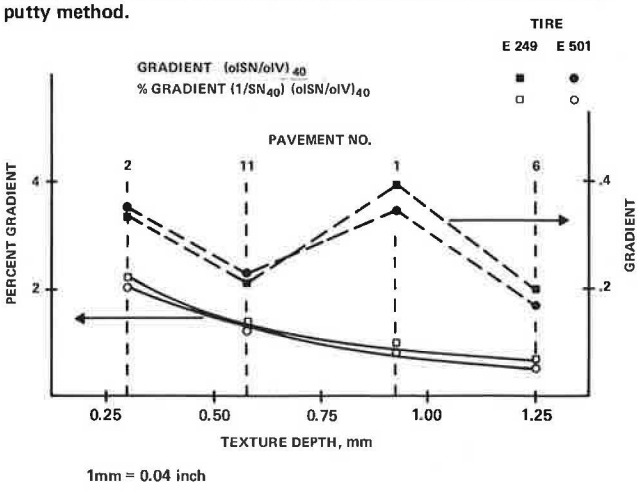

1mm = 0.04 inch

Table 6. Predictions for composite data models.

Nominal SNX	Prediction Model a			Prediction Model a′			Prediction Model c			Prediction Model c′		
	SNŶ	Variance	σ	SNŶ	Variance	σ	SNŶ	Variance	σ	SNŶ	Variance	σ
10	8.69	2.9412	1.72	9.77	3.2047	1.79	8.52	3.0928	1.76	9.63	3.4171	1.85
30	29.05	2.9255	1.71	29.30	3.2183	1.79	28.74	3.0722	1.75	28.89	3.4243	1.85
50	49.41	2.9570	1.72	48.83	3.2455	1.80	48.96	3.0988	1.76	48.16	3.4387	1.85
70	69.78	3.0447	1.75	68.37	3.2863	1.81	69.18	3.1726	1.78	67.42	3.4603	1.86

a useful and simple criterion that gives similar results to those for equation 9 is the average estimated variance (AEV) (8). In effect, the AEV criterion tends to give higher preferred ranking to simpler models. Four values of SNX were selected for predictability testing. Table 6 gives predictions for the full and truncated intercept and nonintercept models together with the standard deviations of the predictions. The intercept models give somewhat closer predictions in the high SN range; the nonintercept models give better predictability in the low SN range, which is more critical. The standard deviations are of the same order of magnitude for all composite prediction equations. Similar analyses were made for each pavement, each speed, and each pavement and speed combination.

ADDITIONAL ANALYSES

To determine the dependence of skid resistance on speed, we fitted to the data quadratic regression equations of the form

$$SN = a + bV + cV^2 \quad (10)$$

All linear coefficients were negative, and all quadratic coefficients were positive. The resulting equations represent decreasing slopes with higher speeds, which is in agreement with experience.

Skid resistance and speed gradients were computed and plotted against the texture depth (Figure 2). Smooth curves were obtained for percentage gradients, that is, the gradient divided by the skid resistance at the same speed.

Regression equations of skid resistance versus temperature were also computed but were inconclusive despite the large amount of data and the wide temperature spread of 5 to 45° C (41 to 113° F). The effects of the other conditions were probably dominant. All that can be concluded from this analysis is that a 5° C (9° F) temperature increase may cause a drop of at most 2 SN.

ORDER-OF-RUN EFFECT PROGRAM

The analysis procedure was performed in three steps: determination of order-of-run effect within each group of eight runs, covariance analysis on the resulting tire means, and evaluation of calibration equations from regression lines. Because the latter two steps employed standard statistical packages (9, 10), this discussion concentrates on the order-of-run effect program.

As previously noted, the test procedure included a pavement prewetting run before each of the eight skid runs. This step introduces a possible cumulative error within the eight runs. The error appears as a trend in the SN that is positively correlated with the run order. The magnitude and statistical significance of this trend can be measured by means of techniques of linear regression, and a special program was developed for this purpose.

The program actually served three functions in the initial analysis scheme: data summary, order-of-run effect determination, and significance testing of overall order-of-run effect for each test series. By measuring and compensating for this trend, one can compress the data by a factor of eight to one without loss of significance in later analyses.

The program is written in FORTRAN IV for an IBM 360 model 65 and executes in 76 000 bytes of core. One execution of the program processes the data from one test series (3072 points). Data are numerically coded to identify test series, type of tire, water depth, surface, and so forth. Each pass of the main program loop reads two sets of eight runs (one set per card). The loop accumulates statistics for each eight-run series and computes the slope coefficient and the associated F-statistic for the eight skid numbers. The sample output from this loop is shown in Figure 3. Punched output consisting of the mean SN, groove depth, and pavement temperature was generated for later input to the covariance analysis programs. Following the eight-run trend analysis, table summaries of the mean SNs were printed as shown in Figure 4. Similar tables were constructed for variances and covariates for groove depth and pavement temperature. The final step in the program is the calculation of the overall F-statistic to test the slope coefficient for each type of tire over all 3072 data points.

SUMMARY

After more than 4000 field skid tests with each of the two types of tires and additional laboratory tests, we believe that findings presented here provide as reliable a set of correlations as possible when one considers the large variability in skid testing.

Table 7 gives a summary of the recommended correlation equations that give the expected skid resistance of the E 249 tire (SNY) as a function of the skid resistance measured with the E 501 tire (SNX); two additional terms account for any difference in groove depth and difference in pavement temperature. (Calculations for D are based on use of inches and calculations for T are based on use of degrees Fahrenheit. SI units are not given inasmuch as operation of this model requires U.S. customary units.) All other test conditions, such as speed, wheel load, and water depth, are the same for both tires. In most cases, differences between groove depths and temperatures either will not be known or will be neglected. In this case, the terms involving D and T drop out and there remains a simple relation between the skid numbers of the two tires, namely, SNY = kSNX where k represents the appropriate coefficient in Table 7.

Equations A to D in Table 7 have been obtained by averaging over the four pavements used in this program and should therefore be valid for any type of pavement normally found on public highways. Equation A may be used at any speed between 16 and 112 km/h (10 and 70 mph), and equations B to D apply only at the indicated speeds. Equations E to H are valid only for pavements that are similar in every respect to the corresponding pavement in this program. These equations may also be used over the speed range 16 to 112 km/h (10 to 70 mph).

The coefficients for D and T in Table 7 vary over a wide range. These differences have no physical meaning but are caused by the uncertainty in the measurements. This is especially true for temperature measurements, where the coefficients vary by a factor of 20 or greater. Whenever the terms involving D and T are to be included, equation A should be used because the coefficients are based on a larger sample (384 data pairs of mean SNs) and therefore have more validity. However, for skid resistance data at the standard test speed of 64 km/h (40 mph), equation C is recommended, provided that the terms in D and T are neglected. The prediction variance at this speed has been found to be smaller than at the other test speeds and also smaller than with the composite model (equation A).

Table 7 also gives the prediction variances for each of the eight equations. The given values have been computed for the simple case of equal groove depth and equal temperature (D = O and T = O) and are based on the sample size used in this correlation, namely eight skids. For a different sample of size n, the first term in the variance equations should be multiplied by 8/n. Thus

Figure 3. Order-of-run analysis output.

```
REGRESSION ANALYSIS OF TEST TIRE CALIBRATION DATA
          (RUN DATA  VS  RUN ORDER)

      TIRE          :   E501

      TEST SERIES   :  40-2

      TIME          :   PM

      REPLICATION   :   4

      CONDITION     :   NEW

      SPEED         :   40

      SURFACE       :    6

      WATER DEPTH   :   .033

      ROAD TEMP     :    60 F

      GROOVE DEPTH  :  0.364 IN.
STATISTICAL ANALYSIS :

      MEAN SKID RESISTANCE =    30.80

      VARIANCE             =     1.43

      STD. DEV.            =     1.19

      NUMBIJ  SS(X,Y)      =   -12.00

      DENBIJ  SS(X,X)      =    42.00

      BIJ                  =    -0.29

      BIJ X NUMBIJ         =     3.43

      ERROR S.S.           =     6.57

      WITHIN VARIANCE      =     1.09

      F (H:BWO)            =     3.13
```

```
REGRESSION ANALYSIS OF TEST TIRE CALIBRATION DATA
          (RUN DATA  VS  RUN ORDER)

      TIRE          :   E501

      TEST SERIES   :  40-2

      TIME          :   PM

      REPLICATION   :   4

      CONDITION     :   NEW

      SPEED         :   60

      SURFACE       :    6

      WATER DEPTH   :   .033

      ROAD TEMP     :    61 F

      GROOVE DEPTH  :  0.364 IN.
STATISTICAL ANALYSIS :

      MEAN SKID RESISTANCE =    29.80

      VARIANCE             =     5.71

      STD. DEV.            =     2.39

      NUMBIJ  SS(X,Y)      =    23.00

      DENBIJ  SS(X,X)      =    42.00

      BIJ                  =     0.55

      BIJ X NUMBIJ         =    12.60

      ERROR S.S.           =    27.40

      WITHIN VARIANCE      =     4.57

      F (H:BWO)            =     2.76
```

Note: SI units are not given for the variables of this model inasmuch as its operation requires that they be in U.S. customary units.

Figure 4. Typical summary printout by mean skid number.

UPPER ROW -MORNING, LOWER ROW - AFTERNOON

SITE	SPEED	REPS	TIRE E249 1	2	3	4	MEAN	TIRE E501 1	2	3	4	MEAN
	20		24.300	23.562	21.800	22.587	23.062	24.300	24.800	23.175	23.950	24.056
			25.925	22.587	22.950	22.275	23.434	25.437	20.850	25.200	24.450	23.984
2	40		12.687	15.700	14.275	13.950	14.153	15.800	17.100	15.525	13.950	15.594
			14.250	15.425	14.600	14.362	14.659	15.787	15.900	16.150	15.300	15.784
	60		10.987	11.262	9.862	10.800	10.728	11.500	10.925	11.225	12.012	11.416
			11.500	11.950	10.637	10.800	11.222	11.712	12.575	11.725	11.262	11.819
	20		23.350	19.412	21.175	21.662	21.400	26.312	20.887	21.800	22.125	22.781
			21.487	20.737	22.112	20.425	21.191	22.600	22.812	26.800	21.525	23.434
11	40		15.437	15.200	15.525	16.050	15.553	17.000	16.400	17.237	16.500	16.784
			15.787	15.787	16.262	15.500	15.834	16.275	16.400	18.937	17.550	17.291
	60		12.562	11.750	11.962	11.400	11.919	12.212	11.862	12.800	13.200	12.519
			11.837	12.550	11.350	10.875	11.653	12.812	12.575	13.537	11.100	12.506
	20		51.012	49.437	48.650	50.987	50.022	48.012	49.437	48.387	48.062	48.475
			51.612	49.575	49.437	47.900	49.631	52.562	51.937	49.437	48.387	50.581
1	40		38.662	38.500	38.562	37.087	38.203	40.075	39.712	37.512	39.800	39.275
			39.637	38.725	37.575	37.087	38.256	39.025	40.500	37.562	38.300	38.847
	60		32.050	30.250	29.425	27.950	29.919	35.925	31.487	27.550	30.875	31.459
			33.525	32.550	30.675	30.300	31.762	32.687	35.337	28.800	31.887	32.178
	20		37.437	43.562	32.675	35.987	37.416	33.437	38.375	33.425	35.512	35.187
			33.112	36.962	33.550	33.550	34.294	33.500	36.825	34.425	37.525	35.569
6	40		28.675	32.462	30.050	30.000	30.297	29.775	31.800	30.987	30.612	30.794
			29.512	32.175	28.925	28.600	29.803	30.425	32.300	29.175	29.862	30.441
	60		30.175	27.062	27.925	26.412	27.894	29.550	28.150	27.300	27.000	28.000
			25.425	27.800	27.925	28.300	27.362	27.612	30.300	27.800	26.462	28.044

BY SPEED	20	40	60
	32.782	25.098	20.650

BY SITE	2	11	1	6
E249	16.210	16.258	39.632	31.178
E501	17.109	17.553	40.136	31.339

BY TIRE	
E249	25.919
E501	26.534

Note: SI units are not given for the variables of this model inasmuch as its operation requires that they be in U.S. customary units.

Table 7. Summary of correlation equation and associated variances.

Equation	Prediction: SNY =	Variance for D = T = O	Application
A	0.977 SNX + 18.52 D - 0.067 T	3.2030 + (0.0041 SNX)^2	General
B	0.991 SNX + 15.07 D - 0.177 T	4.9700 + (0.0075 SNX)^2	32 km/h
C	0.957 SNX + 12.31 D - 0.006 T	1.6434 + (0.0053 SNX)^2	64 km/h
D	0.964 SNX + 22.71 D - 0.002 T	2.2213 + (0.0072 SNX)^2	97 km/h
E	0.986 SNX + 29.62 D - 0.125 T	3.6735 + (0.0067 SNX)^2	Pavement type 1
F	0.924 SNX + 12.82 D - 0.073 T	2.0914 + (0.0097 SNX)^2	Pavement type 2
G	0.997 SNX + 14.29 D - 0.106 T	3.6853 + (0.0091 SNX)^2	Pavement type 6
H	0.918 SNX - 3.84 D - 0.054 T	1.2766 + (0.0084 SNX)^2	Pavement type 11

Note: 1 km/h = 0.621 mph.

Figure 5. Mean skid number of ASTM E 249 (14-in) tire versus mean skid number of ASTM E 501 (15-in) tire.

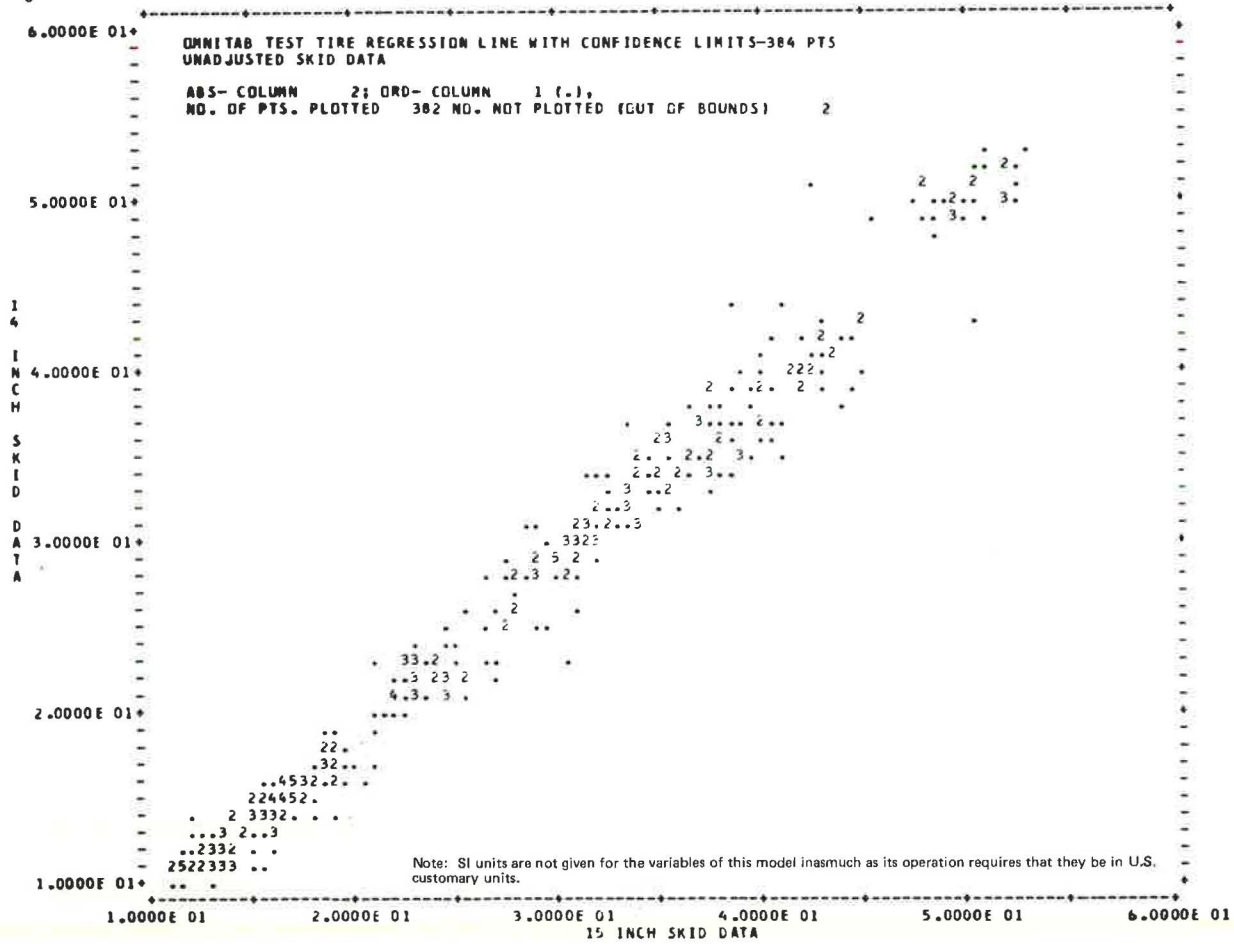

the prediction variance (or standard deviation, which is the square root of the variance) increases as the number of skids per test site decreases.

The correlation between the two tires over all conditions is shown in Figure 5. The computer prints a number whenever two or more points fall on the same coordinates (at the given resolution). The best fit line (from Figure 1) is

$$SNY = -1.49 + 1.018\ SNX \quad (11)$$

which is different from the recommended nonintercept prediction equation in Table 7 (equation A)

$$SNY = 0.977\ SNX \quad (12)$$

Dropping the constant term is justified because it simplifies the conversion and may improve the prediction. In any case, the difference between the two equations is about 1 to 2 percent in the critical skid resistance range of 30 to 40 SN. This is much less than the percentage standard deviation caused by pavement nonuniformity.

Some tests were conducted on dry surfaces, both in the field and in the laboratory. These were limited tests, and the data are insufficient for computing a correlation equation. The results show, however, that skid resistance measurements with the E 501 tire may be expected to be 5 to 10 percent higher than with the E 249 tire. There are six other important findings.

1. The within-mean variances (variance among the eight repeat skids within each sample) as well as the between-mean variances (variance among the mean skid numbers) are about the same for both types of tires. The variance at 32 km/h (20 mph) is, however, more than twice that at the two higher speeds; therefore, low-speed skid testing is not recommended unless prevailing conditions make this necessary.
2. The effect of increased water depth is the same for both tires and may drop about 2 SN when the standard water film thickness of 0.5 mm (0.02 in) is doubled.
3. Tire wear has a somewhat stronger effect on the

E 501 tire than on the E 249 tire. The drop in measured skid resistance is most pronounced during the initial wear. The difference in wear effects between the two tires may vanish when the groove width of the E 501 tire is corrected to meet the specifications. This groove width was, in the first production run, 4.4 instead of 5 mm (0.175 instead of 0.200 in). This has now been corrected. A brief test program was conducted to determine the effect of this change. Under the prevailing test conditions, no systematic difference that came about as a result of the different groove widths could be found.

4. The effect of temperature on skid resistance is confirmed. For a temperature increase of 5° C (9° F), a decrease in SN of at most 2 percent may be expected. However, temperature effects are frequently submerged in other effects, and, at present, no reliable correction method is known.
5. Based on an analysis of four replications with different tires in which all other conditions held constant, tires of the same type and same production run do not differ significantly with respect to skid resistance measurement.
6. The decrease of skid resistance with speed depends on pavement macrotexture. Good correlation can be obtained between macrotexture and percentage gradients (the skid resistance and speed gradient divided by the skid resistance at the same speed).

In general, both tires respond similarly to changing test conditions; therefore, skid testing with the E 501 tire is not expected to present more problems than were experienced with the E 249 tire. This statement does not, however, apply to tire wear, which will have to be judged from experience.

In summary, the equations given in the stub of Table 7 may be used to relate skid resistance measurements taken with one type of tire to those of the other type of tire. The corresponding variances are given for SNX (when skid resistance is measured with the new test tire). If, however, SNX is to be computed from a measured SNY, the latter can be used in the variance equation, without introducing significant errors.

REFERENCES

1. Proceedings. First International Skid Prevention Conference, Univ. of Virginia, Charlottesville, 1969.
2. J. H. Dillard and D. C. Mahone. Measuring Road Surface Slipperiness. ASTM, Philadelphia, Special Technical Publication 366, 1963.
3. Standard Tire for Pavement Test. ASTM, Philadelphia, E 249-66, 1966.
4. W. E. Hegmon and T. D. Gillespie. Locked-Wheel Pavement Skid Tester Correlation and Calibration Techniques. NCHRP, Rept. 151, 1974.
5. Standard Tire for Pavement Skid Resistance Tests. ASTM, Philadelphia, E 501-73, 1973.
6. R. R. Hegmon, S. Weiner, and L. J. Runt. Pavement Friction Test Tire Correlation. Federal Highway Administration, Rept. FHWA-RD-75-88; NTIS, Springfield, Va., PB 252 032.
7. R. L. Anderson and T. A. Bancroft. Statistical Theory for Research. McGraw-Hill, New York, 1952.
8. R. W. Helms. The Average Estimated Variance Criterion for the Selection of Variables Problem in General Linear Models. Techometrics, Vol. 16, No. 2, 1974, pp. 261-273.
9. Biomedical Computer Programs. Univ. of California, Los Angeles, 1970.
10. Omnitab Computing System. National Bureau of Standards, 1971.

Abridgment

Field Test and Evaluation Center Program and Skid Trailer Standardization

E. A. Whitehurst and M. W. Gallogly, Ohio State University

Efforts to measure the skid resistance of highway pavement surfaces through the use of some form of towed vehicle have been reported for at least 50 years. The towed vehicle began to take the form of a two-wheel trailer at least 40 years ago. A sharp increase in interest in and concern over pavement skid resistence began in the 1950s, and during the ensuing years there has been considerable proliferation of two-wheel trailers and some one-wheel trailers operating under generally similar principles. Early reports by developers and users of such equipment quickly revealed that, in spite of the best efforts of investigators, different skid trailers could not be expected to give similar results when used in testing the same pavement under the same conditions within the same time framework. This observation has led to several efforts during the years to effect a correlation between trailers.

The first effort of significance occurred in 1958 as a preliminary to the first International Conference on Skid Resistance. This correlation study, performed on five typical pavements in the Virginia highway system, revealed that, when a number of skid trailers were used to evaluate the condition of these pavements (with the tests performed under identical watering conditions at speeds as nearly identical as possible and within a few minutes of each other), the various units tended to rate the pavements in the same relative order of performance but reported widely differing values of coefficient of friction. Subsequent correlations held in Tappahannock, Virginia, in 1962 and in Okala, Florida, in 1967 revealed that there had been little change in this circumstance. These results were disappointing in view of the efforts of various investigators during the intervals between the correlations to identify and eliminate or minimize the causes of the variations in performance among similar skid measurement systems.

The most recent major correlation, conducted at the Pennsylvania State University in 1972, revealed that significantly different results were still being obtained on the same pavements under the same test conditions by different skid measurement systems all of which were presumed to be measuring the same phenomenon. The data collected during this correlation study were analyzed in far greater depth than those collected during any previous study in an effort to identify the causes for differences in the performance of different skid measurement systems and to assess the magnitude of difference that might be expected between systems because of specific variations in system design or operation.

The broadest effort yet undertaken toward eliminating variations and establishing correlation among skid measurement systems is that which constitutes the field test and evaluation center program at the Federal Highway Administration (FHWA). The fundamental purpose and form of that program have been described by Watson and Cook and will not be elaborated on here. In brief, the program involves FHWA contracts that have resulted in the creation and operation of three field test and evaluation centers having as their purpose the evaluation and correlation of skid measurement systems owned and operated by state departments of transportation and other agencies and a contract with the National Bureau of Standards to provide for calibration and correlation of the equipment used at the centers with a national standard system.

Although this paper deals with the facilities and operation of the Field Test and Evaluation Center for Eastern States (EFTC), operated by the Ohio State University, the facilities available and the procedures employed are identical or substantially identical to those at the Field Test and Evaluation Center for Central States, operated by the Texas Transportation Institute at College Station, Texas, and the Field Test and Evaluation Center for Western States, operated by the Ford Motor Company at its Desert Proving Ground near Kingman, Arizona.

FACILITIES AND PROCEDURES

EFTC is located about 72 km (45 miles) northeast of Columbus, Ohio, at East Liberty, Ohio, among the facilities of the Transportation Research Center of Ohio. In addition to support facilities such as offices, a conference room, a maintenance shop, and tire storage and

Publication of this paper sponsored by Committee on Surface Properties-Vehicle Interaction.

tire mounting and balancing facilities, the principal facilities at EFTC fall into three catagories: facilities involved with water calibration and evaluation, facilities involved with force measurement calibration, and facilities involved with dynamic correlation. Facilities are also available for speed calibration and calibration of tire pressure gauges.

Before water subsystem calibration and evaluation, the angle and location of the nozzle with respect to the pavement and wheel must be determined to fall within the requirements of ASTM E 274. If they do not, appropriate adjustments are made if it is reasonably possible to do so.

The calibration of water delivery subsystems, as well as most of the evaluation of the performance of such subsystems, is accomplished while the trailer sits over a specially constructed pit located in the garage area. Movable ramps permit the trailer to be positioned over the pit and provide a support for associated test equipment. When the trailer is properly positioned on the ramps, the towing vehicle is sitting with its rear wheels on a set of dynamometer rollers that permit it to be operated with the transmission engaged to simulate speeds of 32, 64, and 97 km/h (20, 40, and 60 mph). The trailer wheel for which the water delivery subsystem is being evaluated (usually the left wheel) is removed, and the axle height is adjusted to be at the same height above the ramp as if the wheel were still in place. Water is then pumped through the nozzle into the pit at simulated speeds of 32, 64, and 97 km/h (20, 40, and 60 mph) while the resulting trace widths are measured. The policy at the centers is to measure the trace width at the elevation at which the water would normally strike the pavement but with the water in free-fall into the pit. This does not take into effect any spreading action of the water during the brief period of time between its contacting the pavement and reaching the test tire, but, on the basis of considerable experimentation, this was the only trace width that could be measured with reliably repeatable results.

After trace widths have been determined for the three test speeds, water flow is calibrated. This is accomplished by pumping water through the nozzle at the three simulated speeds and collecting the discharge for a measured period of time in a Q-tank. This tank is calibrated so that the collected discharge may be measured to the nearest 0.4 liter (0.1 gallon). If, on the basis of the previously measured trace widths, the water delivery rate does not fall within the specification limits of ASTM E 274, an attempt is made to bring it into compliance with that specification. This attempt may involve replacement of drive shaft or water pump pulleys, addition of gate valves, or repair or replacement of the water pump, or all of these things. If adjustments of flow rate are required, trace widths are rechecked and changes in the subsystem are accomplished until the combination of trace width and flow provides the most acceptable results throughout the speed range involved.

After the flow rate has been appropriately calibrated, and adjusted if required, the delivery of water in front of the test wheel is evaluated for uniformity and lateral positioning on the static distribution gauge (SDG). The SDG consists of a segmented receiver that splits the water in sections of equal width at the level of the roadway surface. The water from each segment of the container is collected in a separate reservoir, and each reservoir is connected to a sight tube. The sight tubes for all reservoirs are mounted in a rack so that the heights of the columns of water in the adjacent sight tubes represent, in effect, a histogram of the water delivery at the roadway surface. The test is performed at simulated speeds of 32, 64, and 97 km/h (20, 40, and 60 mph), and a photograph is taken of the sight tubes containing water at the end of each test. Adjustable tabs at the bottom of the tubes define the position of the outer edges of the test tire. If the delivered water is not laterally centered on the test tire, the nozzle position is adjusted to correct this problem.

The force measurement subsystems of visiting skid measurement systems are evaluated through the use of an air-bearing force plate. This force plate, calibrated by the National Bureau of Standards, is recessed in the garage floor so that its height is even with that of the floor, thus eliminating any need for blocking up the trailer and towing vehicle. The test wheel to be calibrated is positioned on the force plate; the brake is applied to lock the test wheel; and horizontal force is induced through a chain and air cylinder. The output from the force plate and the conditioned signal output of the system being calibrated are fed into an X-Y plotter, and the resulting plot is evaluated for linearity and hysteresis. In addition, both signals are read on a digital voltmeter, and the results are given to the visiting organization in a form usable for constructing a calibration curve if necessary or desired. If the system being calibrated has the capability of measuring dynamic vertical load, the vertical load transducer is also calibrated on the force plate by jacking up on the trailer to reduce the load below static and by loading the trailer with bags of lead shot to increase the load. As a portion of the force plate calibration procedure, the test wheel is weighed, as is the load on the tongue, and adjustments are made if necessary.

Throughout the horizontal force calibration, the actual vertical load on the test wheel is measured. Thus the incrementally observed load transfer can be used to determine an effective value of h/l. This value rarely agrees perfectly with the value based on individual physical measurements of h and l. The effective value is reported to each state together with a recommendation that it be used in calculating skid numbers (SNs).

The third principle area of investigation involves dynamic correlations between the inventory system under examination and the center's area reference system (ARS). Two such correlations are performed: An initial correlation is performed at the beginning of the inventory system visit before any changes are made in the system, and a final correlation is performed after all appropriate modifications and adjustments have been completed.

Correlations are performed on the center's primary reference surfaces. Five such surfaces were built at each of the three centers. Every effort was made to achieve the same surfaces at each center, including the use of an epoxy binder produced in one lot and shipped to all three centers and construction by the same commercial crew using the same equipment at all three centers. The original objective was to achieve five surfaces that would have a range of SN_{40} of approximately 20 to 70; two of these five surfaces were to have similar SN values but different speed gradients. The objective was partially achieved, but after final construction it was found that all five pads had SN values approximately 10 higher than those originally desired. Pad 5 was found to have an SN of about 85 and to be extremely damaging to tires. After some period of use, it was decided that pad 5 should be eliminated and that an additional pad (pad 0) constructed of Jennite should be placed on the existing base. Approximate current SN_{40} values for EFTC pads are as follows:

Pad	Value	Pad	Value
0	20	3	51
1	35	4	63
2	53		

On the basis of the two correlations just described, each visiting organization is provided with two sets of correlation equations: (a) one relating their system to the center's ARS in the as-arrived condition, which may be used to adjust SN values measured prior to the visit to the center, and (b) one relating inventory values to those of the center's ARS after calibration, modification, and adjustment, which may be used to relate values measured in the future to the ARS level.

OBSERVATIONS AND ACCOMPLISHMENTS

In the course of the evaluations of 23 systems at the Eastern Center to date, some circumstances have arisen frequently enough to indicate inherent problems associated with certain types of skid measurement systems. The most common has been in achieving required water delivery from the nozzle or nozzles.

Center personnel have yet to find on any skid measurement system nozzles that adequately deliver a proper amount of water at all speeds to the test wheel. Typically, nozzles are fundamentally too narrow for use with the ASTM E 501 38-cm (15-in) test tire [which is approximately 2.54 cm (1 in) wider in tread width than the discontinued ASTM E 249 36-cm (14-in) tire]. Some nozzles deliver water in such a manner that the flow tends to converge, producing a trace width narrower than the nozzle orifice width. Some diverge so rapidly that attempts to pump the required amount of water through the nozzle result in trace widths on the order of 46 cm (18 in).

In an effort to standardize nozzles and minimize variations attributable to them, the centers often replace the existing system nozzle with a Penn State type of nozzle. One of the problems associated with nozzles of the Penn State type is the divergent flow of water that produces trace widths (as measured at the center) that do not remain constant as flow rate is increased but increase with increased flow. This causes some difficulty in adjusting flow rate per wetted centimeter to be within the ASTM E 274 specifications for those units in which the pump is driven by the vehicle drive shaft because the tendency of such systems is to deliver a gross flow rate that is essentially proportional with respect to speed. As a consequence, a flow rate per wetted centimeter is delivered that is not essentially proportional with respect to speed. Therefore, if the flow rate per wetted centimeter is properly trimmed at 64 km/h (40 mph) for such nozzles and water delivery systems, a slightly excessive flow is usually found to be produced at the lower speeds, and a somewhat inadequate flow is usually found to be produced at higher speeds.

A number of skid measurement systems make use of a flow control concept in which some of the pumped flow is recirculated back to pump suction. In such a case, the pump may be drive-shaft-driven and the gross pump output is proportional to speed, but the nozzle output becomes very nonlinear with speed. An additional problem with this type of system is that the flow diverted back to the tank is typically adjusted by use of a relief valve that is not designed as a continuously operating flow-control valve and accordingly is a poor performer in this mode.

Calibration of force (and load) transducers to date has shown most to be remarkably linear and free from significant hysteresis. However, the calibration pulse value commonly represents force different from that which the inventory crew believes it to represent.

Although speed calibrations have generally shown the inventory systems to be measuring and recording speed within 0.8 km/h (0.5 mph) of true ground speed, some instances have been noted in which the measured and recorded speed differed from true speed by as much as 10 percent. Although it may be a matter of small importance, very few visiting crews have been found to have tire pressure gauges that accurately measure gauge pressure at 165 kPa (24 lbf/in^2); the difference in one case was as great as 27.6 kPa (4 lbf/in^2). In work with a number of state skid measurement systems, it has become evident that in some cases the procedures used in data reduction (defined as conversion of transducer output signal to SN) can cause some difficulty through the recording of erroneous SN values. The most common such procedure is an attempt to relate chart lines on the system recorder directly to SN.

The relationship between horizontal measured force and SN is clearly not a linear relationship because of the unloading of the test wheel. For those systems in which both the horizontal force and the vertical load are measured and the force is divided by the load electronically to obtain SN, a linear relationship between chart lines and SN results. For those systems in which only the horizontal force (or something representing this force) is measured, the linear relationship does not exist and an effort to force it results in error. In some cases, the users of the system involved have acknowledged the lack of linearity in the fundamental relationship and have attempted to minimize the error throughout the range of SNs in which they are most interested, perhaps 35 to 45, by such techniques as setting artificial zero values. In other cases, the users have simply assumed that the load on the test wheel remains constant and have scaled their recorder chart directly in SN values. In each case, the center gives the user sufficient information to permit development and use of a true calibration curve if desired as well as an indication of the magnitude of error introduced in the user's reported values of SN through failing to do so.

During operation, a principal problem that is being observed in many units is the difficulty of setting or confirming the zero signal. It is becoming increasingly popular to use disk brakes on skid measurement system test wheels. Typically, such brakes do not fully retract when released, and some drag remains on the disk. This makes it essentially impossible to confirm the zero setting of the instrumentation without stopping the vehicle and jacking up the test wheel. In a few cases, the residual drag has been observed to be sufficient to cause highly excessive heat buildup in the test wheel system (perhaps sufficient to affect transducer calibration and readout). A solution to this problem, which involves replacement of two valves, appears to be at hand.

The center operations are currently felt to be accomplishing two functions that are expected to have a primary effect on skid measurement system operation:

1. Standardization of water subsystem delivery rates and distribution and
2. Calibration on an air-bearing force plate relatable to the National Bureau of Standards.

If these and other procedures are, in fact, affecting the results of inventory skid measurement system testing, the effect should be apparent as differences between the as-arrived performance of the system and that when the systems are ready to depart from the center.

One such demonstration is seen in the elimination of speed effect on calibration. Typically the as-arrived correlation will result in a distinct correlation equation for each of the three speeds, and the departing correlation will result in no significant difference and a slope of essential unity in the three equations [that is, SN_{ALL} (REF) = -2.21 + 1.011 SN_{ALL} (Inventory)].

Another possible measure of the effectiveness of the calibration and correlation procedures is the standard

deviation of the visiting inventory system during the initial and final correlations. Of the 16 systems for which such data are now available, 11 showed reductions in standard deviation of SN between the two correlations; the average reduction in standard deviation for the 11 systems was 1.0 SN. In the case of the poorest performance noted to date, one system had an initial standard deviation of 6.8 SN that was reduced to 3.8 SN on the final correlation (a replacement brake hydraulic valve has since been found that should make a further step improvement in this system). The average standard deviation for all 16 systems was 3.2 SN as they arrived at the center and 2.6 SN as they departed the center.

SUMMARY

On the basis of one and a half seasons of operation involving 23 skid measurement systems, we believe that the procedures followed at the field test and evaluation centers result in significantly improved uniformity of operations among a variety of skid measurement systems and provide a procedure through which skid numbers measured over a wide area may be transformed to reference values. Operation of the centers to date has clearly shown the need for certain system improvements, notably the need for development of a nondivergent nozzle of suitable dimensions that will deliver an adequately uniform flow of water, adherence in system design to pump systems that deliver flow at the nozzle proportional to speed, development of fully retracting brakes to make possible frequent checks and adjustments to signal zero levels, and refinements in data reduction procedures.

ACKNOWLEDGMENT

We gratefully acknowledge the sponsorship by the Federal Highway Administration of the work reported here. The report, however, expresses our views, and we are responsible for the collection and the accuracy of the data presented. The views expressed do not necessarily reflect the official views or policies of the Federal Highway Administration.

Impulse Index as a Measure of Pavement Condition

Frank W. Brands and John C. Cook, Washington State University

A rapid method of measurement of pavement structural condition has been developed that is adaptable to automatic data acquisition from a moving vehicle and yields numerical data suitable for computer manipulation. A hand-carried version has been developed that measures parameters indicative of structural condition and computes an evaluating number called the impulse index. To determine the impulse index, an impulse of energy is delivered to the pavement with a hammer blow. Two transducers are used to monitor the acceleration of the pavement very close to the impact point and the attenuation of the energy as it propagates through the pavement. The outputs of the accelerometers are manipulated electronically to compute the impulse index. Comparisons of Benkelman beam deflections and impulse index measurements for the same locations on a wide variety of types of pavement and pavement conditions are presented in graphical form for easy comparison. A high degree of correlation was found between the impulse index and Benkelman beam deflections. This impulse index is much faster to obtain and requires only lightweight, highly portable equipment.

This project was initiated to develop a method of nondestructive testing of highway pavements that would be more economical and faster than existing methods. A system was desired that would ultimately be adaptable to operation from a moving vehicle and in which the data would automatically be acquired and recorded in computer-compatible format such as on magnetic tape. If the system can be made to operate fast enough, the pavement condition of the entire highway system can be logged at planned intervals, yielding the state of deterioration as well as the rate of deterioration of every increment of highway pavement. Such a log would be a valuable aid in highway management and in documenting budgetary requirements and establishing priorities of maintenance.

PAVEMENT STRUCTURAL LINEARITY

Earlier tests performed at Washington State University indicated that the structural parameters of pavement are sufficiently linear over a broad enough range so that the energy or force used in deflection or impulse testing need not be as great as in previously accepted methods. These findings are consistent with those of other investigators (1, 2). The direct consequence of this reasonable linearity is that nondestructive pavement testing equipment need not be large and heavy. The impulse index results reported in this paper were acquired by using a driving function of approximately 9 J (6.5 ft·lbf). The total weight of the impulse index equipment is currently about 25 kg (55 lb), and it can be made even lighter.

IMPULSE DRIVING FUNCTION

The advantages of using an impulse driving function rather than a steady-state sinusoid were also explored. Textbooks on linear circuit theory (3, 4, 5) present the theoretical background that shows the necessity of using a broad range of frequencies when system response is investigated. Use of single frequency excitation carries the risk that response will be very dependent on the locations of the S-plane poles of the system transfer function with respect to the poles of the single frequency driving function. A unit impulse, on the other hand, contains an equal amount of all frequencies, and the response of a system to a unit impulse is determined only by the parameters of the system under test and not by a response to a specific single frequency selected for a driving function that may or may not coincide with self-resonant frequencies of the system under test.

A true unit impulse is, of course, not actually attainable, but a pulse of finite height and width can be substituted provided that the width is much narrower than the period of the highest frequencies of interest.

IMPULSE INDEX

Tests were conducted on various pavements by using an impulse of energy for system excitation. Various characteristics of the response of the pavement to such excitation were examined for correlation of parameters with known pavement condition. The result of the research was the development of a system that uses a hammer blow for excitation and two accelerometers on the pavement surface. One accelerometer is placed as

Publication of this paper sponsored by Committee on Pavement Condition Evaluation.

near to the point of impact as possible and the second accelerometer is positioned a fixed distance away [46 cm (18 in) was found to be a convenient and suitable distance]. The output from each accelerometer is electronically processed so that its absolute magnitude is determined and then integrated with respect to time. If we designate the resulting quantity as R and the unprocessed output of the accelerometer as a, then

$$R = \int |a| \, dt \quad (1)$$

This quantity R from each accelerometer can be used for plotting a profile of the pavement response basin, which is loosely referred to as a deflection profile under impulse loading.

For convenience, the quantity from the accelerometer nearest the hammer has been designated R_1 and the quantity from the second accelerometer is designated R_2. A relation was developed that reduces the profile information into a single number, designated impulse index.

Experiments on flexible pavements indicated that the attenuation of energy propagated through better pavements was less than that for poorer pavements. The ratio of R_1/R_2 provides a form of measure of this attenuation. Poorer pavements also yielded higher values of R_1 than did better pavements. If we take both of these observations into consideration, the impulse index is generated as follows:

$$\text{Impulse index} = (R_1/R_2) \times R_1 = R_1^2/R_2 \quad (2)$$

High values of impulse index correspond to weakened pavement, and low values correspond to sound pavement. Further details on impulse index are available elsewhere (6).

VEHICLE OPERATION

The total time required for an impulse index measurement is a fraction of a second. To acquire the data from a moving vehicle is therefore feasible. A test vehicle that demonstrates one possible approach to mechanizing the automatic acquisition of impulse index data has been constructed (7). The transducers and a hammer pin are mounted in a continuous belt that contacts the pavement in a manner similar to that of the tread of a tracked vehicle. The end support wheels for the belt are approximately 6 m (20 ft) apart. As the vehicle travels down the highway, the belt lays the transducers and hammer pin on the pavement where they are stationary with respect to the pavement until the vehicle advances far enough so that the belt travels up and over the near support wheel. At 50 km/h (30 mph), the transducers would be on the pavement for nearly 0.5 s, ample time to make an impulse index measurement. A measurement is made with each complete revolution of the belt. Two belts side by side could be used, if desired, to monitor both wheel tracks of the lane.

Additional development is required to make the operation of the vehicle smooth and satisfactory at highway speeds. Before proceeding with further development of the vehicle, it was determined that a thorough evaluation of the validity of the impulse index as a measure of pavement condition would be required.

HAND-CARRIED IMPULSE INDEX COMPUTER

To acquire sufficient data for a thorough evaluation of the validity of the impulse index as a measure of pavement condition, demonstrate the system, and perform spot checks, a suitcase-sized hand-carried version of the impulse index computer was assembled. The device includes the hammer, two transducers, and the necessary electronics, batteries, and readout meters. A block diagram of the device is shown in Figure 1. Figure 2 shows the device in operation. In use, the device rests on the pavement, the hammer is raised to its limit and dropped, and the meters give R_1, R_2, and impulse index values. The results in the remainder of this paper were acquired by using the hand-carried impulse index computer.

COMPARATIVE DATA FOR PAVEMENT SECTIONS WITH KNOWN HISTORY

Some interesting locations on I-90 were examined. At milepost 122 in the eastbound lane east of Ellensburg is a joint in the top lift. The top lift west of the joint had been laid only 2 weeks before these tests were conducted. The top lift east of the joint had been laid 2 years earlier. Both of these regions would have the same traffic history. The impulse index was measured about 30 m (100 ft) on each side of the joint in the top lift. Measurements were made in the outside wheel track, lane center, and inside wheel track in the extreme right hand lane of both areas. Figure 3 shows a graph of the data. In Figure 3, the lower impulse index values were obtained where the top lift had been in place for only about 1 week. The higher values of impulse index were obtained about 60 m (200 ft) to the east where the top lift had been placed several years ago.

A low reading of impulse index signifies better pavement condition than a higher reading does. Several things can be noted from Figure 3. The region with the brand new overlay registered the lower value of impulse index. Note that the wheel track registers the highest (most distress).

I-90 AND YAKIMA FREEWAY INTERCHANGE RAMP

Tests were made on the ramp from eastbound I-90 to southbound Yakima Freeway. This ramp has been in service for several years although the top lift had not been previously applied. The paving project was under way while the tests reported here were made. The top lift had just been applied in the passing lane a few hours earlier and had not yet been applied in the extreme right lane. Measurements were made after one lane had just received the top lift and the other lane had not. Figure 4 shows a graph of the impulse index measurements from the usual six places. The lane that had the top lift applied had lower impulse index values.

IMPULSE INDEX AND BENKELMAN BEAM COMPARISONS

District 1 Sites

Nine sites located in Skagit and Snohomish Counties in the western part of the state of Washington were selected for tests to compare impulse index measurements with Benkelman beam measurements (7). These particular sites were selected because the district 1 personnel were already scheduled to make Benkelman beam tests at those sites under a program designed to determine future load limits under freeze-thaw conditions. The sites are identified in Table 1.

At each test site, nine positions were marked off at 7.5-m (25-ft) intervals. One Benkelman beam set was used and it was operated by the crew from district 1. The pointer of the beam was projected through the space

between the dual wheels of the truck to a point 1.2 m (4 ft) ahead of the axle centerline. The truck was driven slowly ahead and the maximum deflection was recorded. The position on the pavement of the pointer of the Benkelman beam was marked before the beam was moved. The truck provided a rear axle load of 6800 kg (15 000 lb).

Eight impulse index measurements were made at each test position. The instrument was rotated 45 deg between each measurement and positioned so that the hammer would impact at the point where the tip of the Benkelman beam had rested.

Figures 5 through 13 show comparisons for each of the nine positions. The eight impulse index readings taken at each test position are averaged and graphed along with the Benkelman beam reading for each position. A separate graph is presented for each test site, but the scale is identical for all graphs. One unit of impulse index corresponds rather consistently with 0.08 cm (0.03 in) of Benkelman beam deflection for the region of operation examined. It can be observed from these graphs that the Benkelman beam measurement and the

Figure 1. Block diagram of impulse index computer.

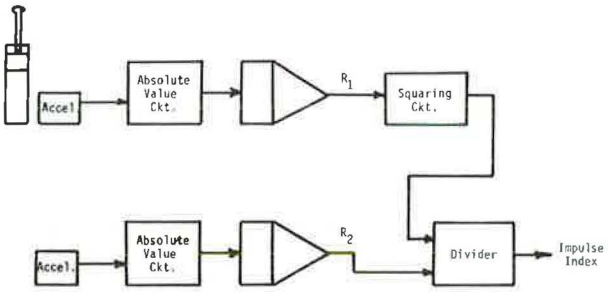

Figure 2. Impulse index computer in operation on Wash-270.

Figure 3. Impulse index profile of I-90 at milepost 122.

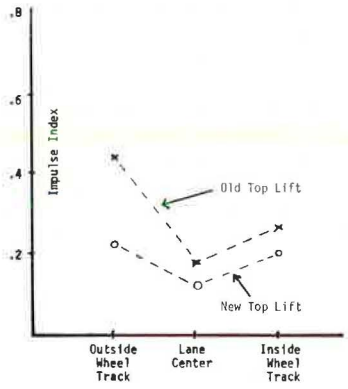

Figure 4. Impulse index profile for I-90 and Yakima Freeway.

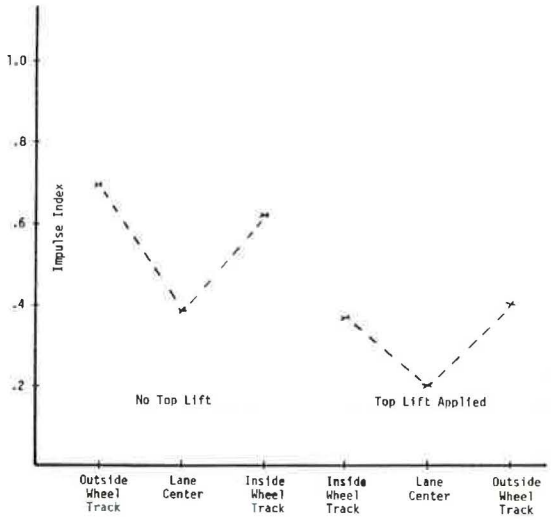

Figure 5. Benkelman beam and impulse index of district 1, test site 1.

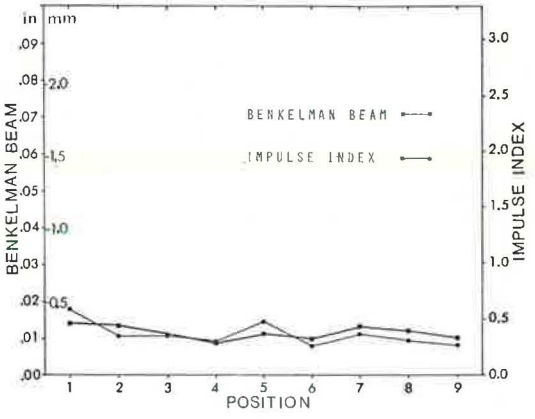

Table 1. District 1 sites.

Site	Route	Milepost	Direction	Location	Surface
1	Wash-20	6	Eastbound	South of Anacortes	0.11-m AC, 0.12-m CTB, 0.08-m sand
3	Wash-20	18.6	Westbound	West of Lyman	0.11-m RS, 0.09-m AC, 0.11-m SRB, 0.24-m SSGB
4	Wash-20	21	Westbound	East of Lyman	0.15-m RS, 0.11-m AC, 0.198-m SRB, 0.15-m SSGB
6	Wash-9	27	Southbound	South of Arlington	0.08-m AC, 0.08-m CSTC, 0.18-m GB, 0.21-m SSGB
7	Wash-9	17	Southbound	South of Marysville Jct.	0.12-m AC, 0.06-m CSTC, 0.27-m SSGB, 0.21-m SSB
8	Wash-204	1.1	Westbound	East of Everett	0.12-m AC, 0.18-m SG, 0.24-m SSB
9	Wash-9	13	Southbound	South of Wash-204 Jct.	0.14-m AC, 0.05-m CSTC, 0.15-m SGB, 0.21-m SG
10	Wash-2	10	Eastbound	East of Snohomish	0.12-m AC, 0.03-m CSTC, 0.3-m SGB, 0.15-m SSG
11	Wash-2	19	Eastbound	West of Sultan	0.27-m AC (5 layers), 0.03-m CSTC, 0.06-m SSGB, 0.3-m SG

Notes: 1 m = 3.28 ft.
AC = asphalt concrete; CSTC = crushed surfacing top course; CTB = cement-treated base; GB = gravel borrow; RS = resurfacing; SG = sand and gravel; SBG = sand and gravel borrow; SRB = selected roadway borrow; SSB = silty sand borrow; SSGB = silty sand and gravel borrow.

impulse index correlate fairly well on a point-by-point basis.

Pullman Area Sites

It can be observed from the Benkelman beam deflection as well as from the impulse index that the district 1 sites yielded fairly low deflections. In an effort to obtain comparisons over a wider range of pavement condition, some additional sites were selected in the vicinity of Pullman (8). The locations and pavement profiles of Pullman sites are given in Table 2. The procedure for obtaining the impulse index for these sites was modified. Only four readings were taken at each position at 90-deg rotations instead of eight readings at 45-deg rotations as with the district 1 tests.

The Benkelman beam technique was also slightly modified. The pointer of the beam was placed between dual wheels for the reference. The truck was then driven ahead 6 m (20 ft), and the pavement rebound was re-

Figure 6. Benkelman beam and impulse index of district 1, test site 3.

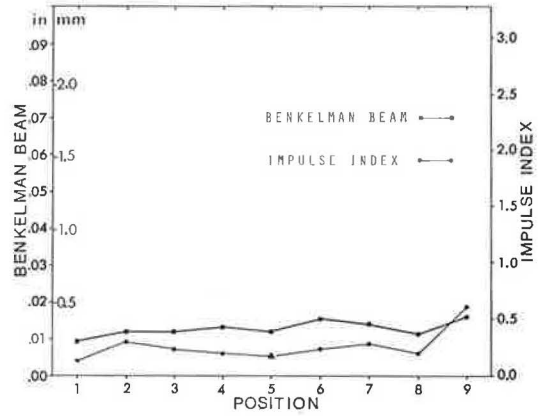

Figure 7. Benkelman beam and impulse index of district 1, test site 4.

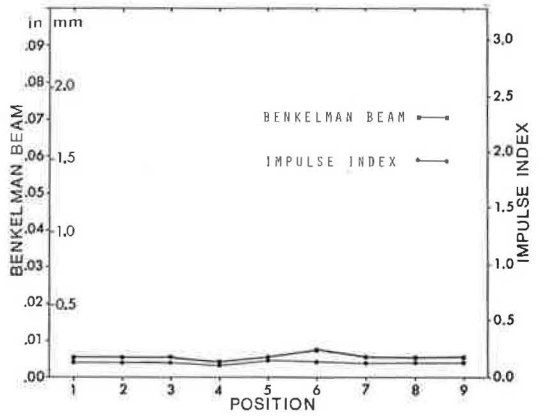

Figure 8. Benkelman beam and impulse index of district 1, test site 6.

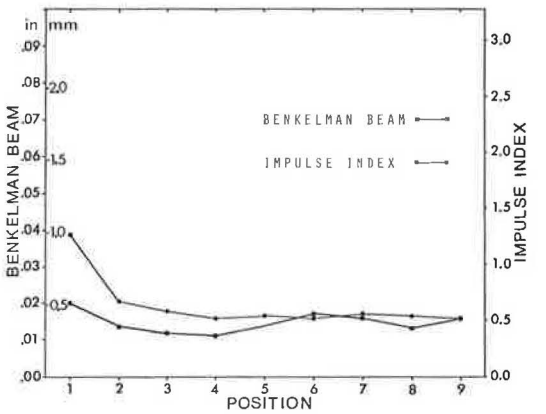

Figure 9. Benkelman beam and impulse index of district 1, test site 7.

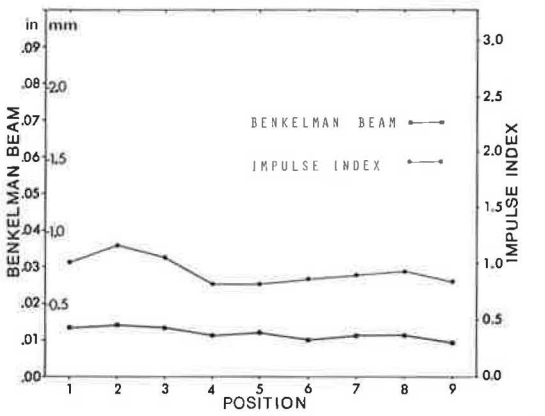

Figure 10. Benkelman beam and impulse index of district 1, test site 8.

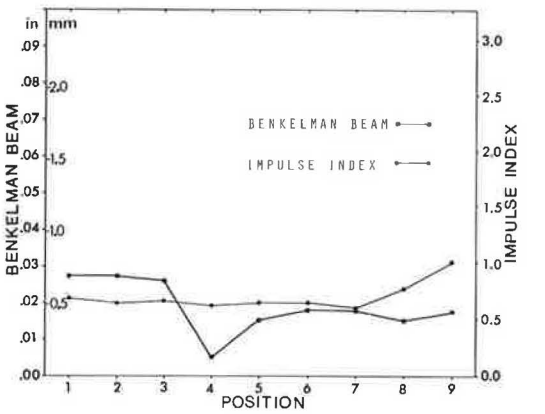

Figure 11. Benkelman beam and impulse index of district 1, test site 9.

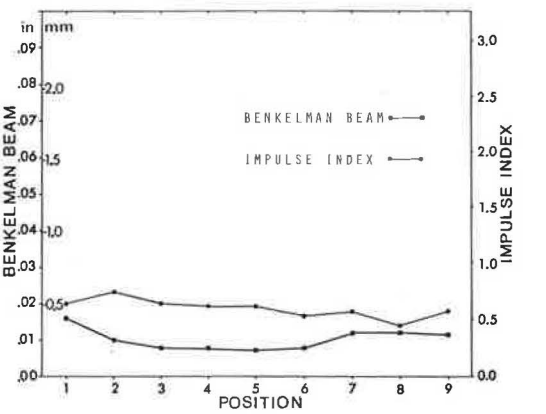

Figure 12. Benkelman beam and impulse index of district 1, test site 10.

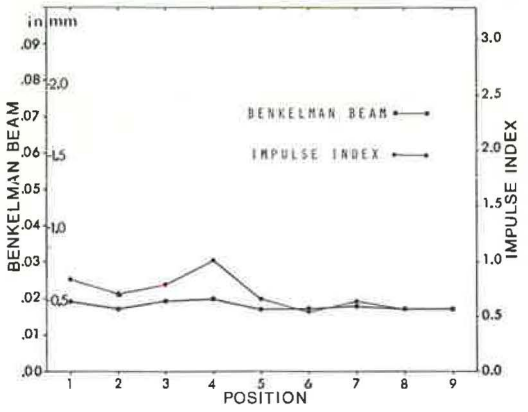

Figure 13. Benkelman beam and impulse index of district 1, test site 11.

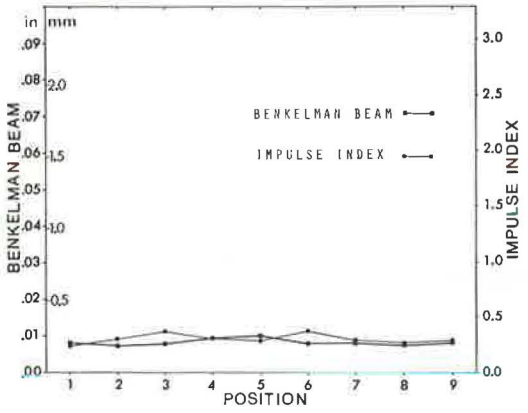

Figure 14. Benkelman beam and impulse index of Pullman area, test site A.

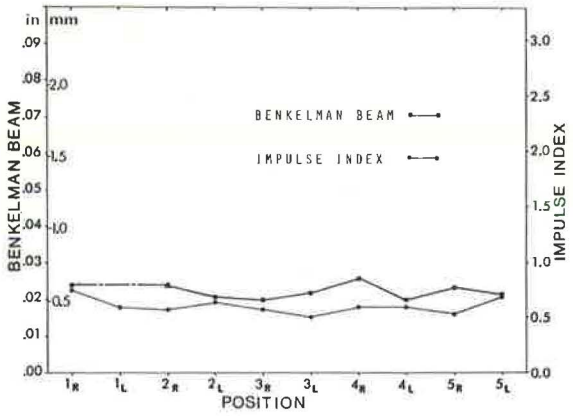

Figure 15. Benkelman beam and impulse index of Pullman area, test site B.

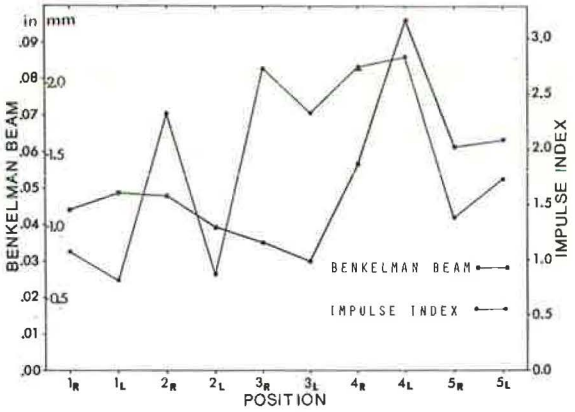

Figure 16. Benkelman beam and impulse index of Pullman area, test sites C and D.

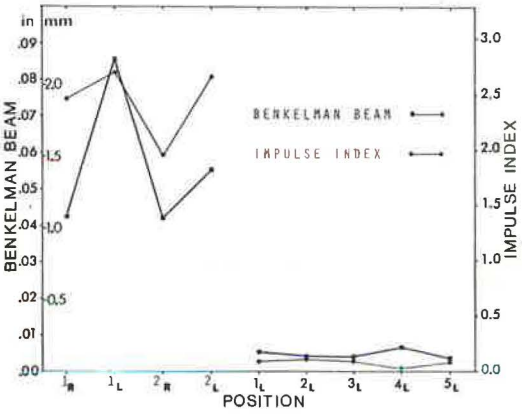

Figure 17. Benkelman beam and impulse index summary.

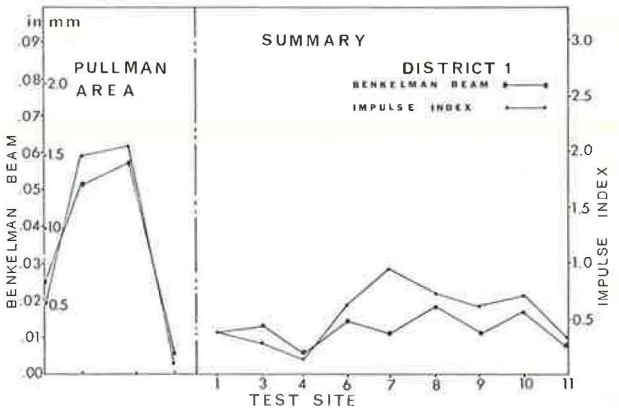

Table 2. Pullman area sites.

Site	Location	Surface
A	Westbound lane, southwest Crestview, 130 m west of Grand Avenue, Pullman	0.08-m AC, 0.08-m CSTC, 0.2-m GB
B	Intersection of parking lot entrance with approach road to new Pullman high school	0.08-m permanent vertical deformation, 0.05-m AC, 0.15-m GB
C	Larry Street extension, main access road to high school	0.05-m AC, 0.15-m GB
D	1000 block of North Grand, Pullman	0.15-m nonreinforced PCC, 0.3-m GB

Notes: 1 m = 3.28 ft.
AC = asphalt concrete; CSTC = crushed surfacing top course; GB = gravel base; PCC = portland cement concrete.

corded from the Benkelman beam.

The four impulse index readings obtained at each position were averaged and are shown in Figures 14, 15, and 16 along with Benkelman beam deflections at each point.

SUMMARY AND CONCLUSIONS

Because of anomalies in pavement structure, monitoring of a single point on a pavement does not give an adequate measure of pavement condition. Many points must be monitored to compensate for these variations. To compare the overall results of the Benkelman beam deflections with impulse index measurements, we averaged all of the Benkelman beam measurements made at each test site and all of the impulse index measurements obtained for each test site. The resulting data, shown in Figure 17, indicate the correlation between the impulse index and Benkelman beam deflections.

The advantage of the impulse index technique is the very small amount of time required for the tests and the light weight and portability of the equipment.

ACKNOWLEDGMENTS

The impulse index as a measure of pavement condition has been under development for the last 5 years at Washington State University in cooperation with the Washington Highway Commission and the U.S. Department of Transportation. This work was made possible by support from the Washington Department of Highways in cooperation with the Federal Highway Administration.

REFERENCES

1. J. M. Phelps and T. R. Cantor. Detection of Concrete Deterioration Under Asphalt Overlays by Microseismic Refraction. HRB, Highway Research Record 146, 1966, pp.
2. M. E. Szendrei and C. R. Freeme. Road Response to Vibration Tests. Journal of Soil Mechanics and Foundations Division, Proc., ASCE, Vol. 15, No. 6, Nov. 1970, pp. 7709-2124.
3. R. Bracewell. The Fourier Transform and Its Applications. McGraw-Hill, New York, 1965.
4. E. J. Craig. Laplace and Fourier Transforms for Electrical Engineers. Holt, Rhinehart, New York, 1964.
5. D. K. Cheng. Analysis of Linear Systems. Addison-Wesley, Reading, Mass., May 1961.
6. F. Brands and J. C. Cook. Pavement Deflection Measurement—Dynamic—A Feasibility Study. Highway Research Section, Washington State Univ., Pullman, Publication H-32, June 1970.
7. F. W. Brands and J. C. Cook. Pavement Deflection Measurement—Dynamic, Phase IV, Final Report. Highway Research Section, Washington State Univ., Pullman, Publication H-38, Aug. 1972.

Condition Surveys for Pavement Structural Evaluation

Robert L. Lytton and Joe P. Mahoney, Texas Transportation Institute, Texas A&M University

Two types of condition surveys for pavement structural evaluation, decision surveys and design surveys, are defined. The decision survey is examined further by using the results of a recent survey conducted among state and other selected highway agencies. Emphasis is placed on the amount and types of distress mechanisms that influence maintenance decisions. The criteria that nondestructive equipment should meet to assist in conducting such surveys are stated, and the effectiveness of the two methods used to collect pavement condition information is compared. A related statistical sampling study that uses Dynaflect is shown, and promising developmental techniques for measuring stiffness and cracking of pavements are presented.

The decision to rehabilitate a pavement is usually made well in advance of the time when that pavement becomes functionally distressed. The functional performance of a pavement is defined by its riding and safety quality (1), which are indicated more or less reliably by various profilometer and skid resistance measurements (2). Deterioration of the functional condition of a pavement is preceded by or occurs at the same time as a deterioration in its structural condition (3), its loss of strength and stiffness, its cracking, and other measures of distress. This known relation between structural distress and functional decline is used by many highway agencies to determine which segments of a highway network must have maintenance or rehabilitation work.

There are two major purposes for evaluating the structural condition of pavements: to furnish information for design and to provide data for rehabilitation decisions. The first of these purposes required detailed information either for the design of new construction or for determining the amount of rehabilitation (overlays, seal coats, reconstruction) that will be required. Data for the second of these purposes, rehabilitation decisions, will not need to be so detailed but they should be consistent in ranking the distressed condition of all pavement sections in a highway network.

The two main purposes of pavement structural evaluation require two kinds of condition survey: a detailed survey for design data and a rapid survey for decision data. Because each of these surveys has its own unique objectives, it is not surprising that each should also have its own criteria for what determines an acceptable survey. In general, the decision survey is interested in a quick but comprehensive view of everything that is going wrong with the pavement. It is primarily interested in the distressed condition of a whole section of pavement, and its objectives are better served if its assessments of the level of distress are consistent from one section to the next. As such, the decision survey forms only a part of what is called the sufficiency survey in current highway practice. A sufficiency survey also may consider factors such as safety, geometry, traffic, and obstructions (4).

The design survey is concerned with the structural adequacy of the pavement section to carry future anticipated loads. It is an attempt to gather data on thickness, stiffness of layers, material properties, and crack spacing to determine the thickness of planned overlays or the depth of a pavement to be reconstructed. The design survey is intended to be broader in scope than the structural evaluation commonly used in current highway practice. The structural evaluation is usually associated with deflections and pavement layer moduli. In addition to these data, a design survey may gather other kinds of data such as those on crack spacing, which are required in some overlay design procedures (5).

In an ideal case, there should be some correlation between the results of these two surveys. The decision survey should indicate reliably which sections need work, and the design survey should tell how much work is needed. The common tie between these two survey systems is distress. The greater the distress is, the more urgently the pavement needs attention and, in general, the more extensive the rehabilitation will be.

Although both types of surveys are important, this paper will be primarily concerned with the decision survey because of its importance in making maintenance and rehabilitation decisions. Several aspects of these surveys will be investigated:

1. Importance of the decision survey in making

Publication of this paper sponsored by Committee on Pavement Condition Evaluation.

rehabilitation decisions;

2. Relative weights given to various forms of distress and thus the most important forms of distress to measure;
3. The most effective ways to apply measurement equipment in determining the current pavement structural condition; and
4. Promising development methods of measuring stiffness and cracking, which are shown to be the most important indicators of pavement structural condition.

PAVEMENT CONDITION SURVEYS

A letter was sent to the highway departments in most states and territories and selected Canadian provinces requesting information on their pavement condition rating system currently in use or projected for use in the immediate future. Fifty-eight agencies were contacted, and 44 responses were received or had previously been made available. The agencies included not only those in the states and selected Canadian provinces but also one in a county in Washington and two in cities in Texas.

Most of the agencies contacted responded by furnishing extensive information on their rating methods. However, some agencies cannot be treated adequately because of one of the following reasons: (a) sufficient information was not sent to permit a complete examination of the rating system; (b) development efforts were under way for a new system; or (c) the agency did not reply to the questionnaire. As a consequence, whatever information provided was used to the greatest extent possible.

Five general items were derived from the replies.

1. Thirty-four agencies are using or are adopting rating systems.
2. Twenty-four agencies are using a composite numerical rating score.
3. Twenty agencies are using ratings or rating scores in maintenance decisions.
4. Thirty agencies are using rating systems for flexible pavements.
5. Eighteen agencies are using rating systems for rigid pavements.

Of the states and agencies for which information was available, a total of 16 either currently use or plan to use mechanical devices to assist in obtaining pavement ratings.

1. Sixteen use roughness measuring devices.
2. Eight use skid measuring devices.
3. Three measure deflections by Dynaflect.
4. One measures deflections by Benkelman beam.

These types and amounts of mechanical devices are used for decision surveys and should not be confused with the number of mechanical devices used in design survey procedures. Many agencies use the types of devices shown but do not necessarily use them in a rating system.

CHARACTERISTICS OF PAVEMENT CONDITION SURVEYS

These condition survey methods represent valuable experience in determining the most important kinds of distress. As a consequence, they were analyzed in detail from the following points of view:

1. Percentage of pavement condition rating determined by various types of distress, as opposed to traffic, safety, skid, geometry, obstructions, and other nondistress items and
2. Percentage of the condition rating determined by each form of distress, such as cracking, rutting, raveling, patching, and the like.

Item 1 shows how important the maintaining agencies consider distress, and item 2 determines the forms of distress considered most important in these rating scores.

Distress Versus Nondistress Items

The approximate percentage of the pavement condition rating score that is determined by distress is given in Table 1. Of the 24 agencies using numerical ratings, only 18 can be listed because of available data. The percentages range from 17 percent (Arizona) to 100 percent (Maine). No geographical pattern is evident from the distribution of the percentages. On the average, 49 percent of the rating score for flexible pavements and 40 percent for rigid pavements is accounted for by distress. Because the remaining percentages account for such items as roughness, traffic, geometry, and the like, it is readily apparent that distress considerations are a significant, though highly variable, part of the individual rating systems.

Importance of Various Kinds of Distress

Figure 1 shows the percentage of the pavement rating score that is represented by each of the forms of distress. The types of distress listed are self-explanatory except for the type listed as general. This category is used to group those forms of distress listed by the various agencies under generalized headings such as structural adequacy.

The amount that individual types of distress influence the overall rating can be examined in two ways: (a) by determining the average for those agencies that actually use the type of distress and (b) by averaging over all agencies. The latter is considered the most informative because, if an agency does not include a given type of distress, it indicates that the distress is considered unimportant.

Based on the latter averaging procedure, the general category accounts for an average of 13 percent of the overall pavement rating score for flexible pavements and 17 percent of the overall pavement rating score for rigid pavements. Of all of the specific types of distress, cracking is the most heavily weighted (17 percent for flexible pavements and 7 percent for rigid pavements). The next most important forms of distress for flexible pavements are rutting (5 percent) and patching (3 percent). The next most important forms of distress for rigid pavements are spalling (5 percent) and faulting (3 percent). Deflections average 3 percent for flexible pavements but are not considered as distress in this analysis.

It is apparent from this study that cracking is the major distress variable used in making maintenance and rehabilitation decisions. Deflections, roughness, and skid number are being measured, but the most heavily weighted type of distress (cracking) is not being measured by mechanical devices or instruments. Visual methods are the main techniques used currently but, in the future, as larger percentages of the highway budget are spent on maintenance and rehabilitation activities, it is anticipated that there will be a corresponding need for an increased use of measuring equipment to achieve faster and more consistent measurement on a larger percentage of the nation's highways. This need can be

met by some existing equipment and some that are still in the conceptual stage, the most promising of which use nondestructive testing techniques. In the next section of this paper, the criteria that must be met by this equipment, the most efficient ways of using it, and some promising developmental techniques for measuring stiffness and cracking will be discussed. As noted previously, stiffness (or structural adequacy) and cracking are the most heavily weighted factors in making maintenance and rehabilitation decisions.

EQUIPMENT CRITERIA FOR MEASURING PAVEMENT STRUCTURAL CONDITION

Highway technology has produced a significant number of nondestructive pavement evaluation techniques. Some of these are production models that are used daily by various highway agencies. Others are still in the development stage and, although their principles of operation are known and the data they produce can be used in several ways, few of them produce data that can be analyzed to produce material properties of the pavement layers. A detailed description of this survey of equipment, their principles of operation, their capabilities of producing analyzable data, and their advantages and disadvantages for applications in pavement evaluation is available elsewhere (6).

The kinds of data that must be collected in the two kinds of surveys are different, a reflection of their different purposes. Decision surveys are concerned with distress, and design surveys are concerned with material properties, crack spacing and severity, and the response of a pavement structure to imposed loads or environmentally induced stresses. The types of data that each of the surveys may assemble can be broken down. A decision survey may assemble data on

1. Deflections,
2. Stiffness,
3. Cracking,
4. Rutting,
5. Roughness, and
6. Skid resistance.

A design survey may assemble data on

1. Deflections,
2. Cracking, and
3. Layer moduli.

The measurements made in a decision survey are of major interest because the results of a decision survey are a major factor in maintenance and rehabilitation decisions.

USE OF MEASUREMENTS IN A DECISION SURVEY

There are two methods of conducting a decision survey, a mass inventory or a statistical sampling study, and each has its own merits. In a mass inventory, one makes many measurements along the pavement to discover the location of the weak points most in need of repair. The pavement section with the greatest density of weak points in the roadway network presumably would receive maintenance attention earlier than one with a lower density. In a statistical sampling study, one makes sufficient measurements to determine a reliable statistical distribution of the pavement variable being measured. The pavement sections with the poorest average and greatest spread (as measured by the standard deviation) presumably would receive the earliest rehabilitation efforts. In either method, the objective is to establish rehabilitation priorities among several candidate sections in a roadway network.

The merits of the mass inventory methods as opposed to statistical sampling methods will be discussed as they are applied to deflection or stiffness or both and to cracking.

Decision Surveys of Pavement Stiffness

The California traveling deflectometer and the Lacroix deflectograph are the best known mass inventory devices for measuring pavement stiffness. They are capable of making between 1000 and 4000 measurements/day while covering approximately 17.7 to 22.5 km (11 to 14 miles) of road. The data that are produced are a collection of stiffness numbers that may or may not be well correlated with Benkelman beam data and may not mean the same thing on one pavement section as they do on another. What these devices give is an estimate of how stiff the pavement is at one location relative to the pavement at adjacent locations along the same length of road. This approach can pinpoint places for spot patching.

In the statistical sampling study, the emphasis shifts toward collecting data that can be analyzed to determine elastic moduli, coefficients of subgrade reaction, or other similar material properties of the pavement while obtaining a reasonably reliable statistical distribution of pavement stiffness numbers. These numbers may or may not represent material properties. In some cases, various measurements taken within a Dynaflect basin, such as surface curvature index (SCI), base curvature index (BCI), and Dynaflect maximum deflection (DMD), are used as a measure of pavement stiffness (7). In other cases, elastic moduli may be calculated from the measurements of surface deflections (8). Because this approach is slower and makes fewer measurements per day, it loses the detail that can be achieved with the mass inventory methods. Nevertheless, the statistical sampling approach still achieves the major objective of the survey, which is to collect data from which rehabilitation decisions can be made. Furthermore, it has the advantage that the data can be analyzed to determine the distribution of material properties along the length of a pavement.

In net balance, the adaptability of the statistical approach that uses slower equipment with analyzable data is expected to demonstrate more cost-effective long-range benefits.

Statistical Sampling Study Using Dynaflect

A study of the statistical approach was conducted by using Dynaflect data, which were measured every 0.8 km (0.5 mile) over a 161-km (100-mile) length of rigid pavement on I-45 between Houston and Dallas. A series of two computer programs were written to analyze the data. The first is the analysis program that used Westergaard's equations for the deflections of a point load on a rigid pavement resting on a liquid subgrade (9) to determine the elastic modulus E of the concrete and the subgrade modulus k of the subgrade. The equation for surface deflections w is of the form

$$w = (P/kl^2)\, f(x/l) \qquad (1)$$

where

P = size of point load,
x = distance away from point load,
l = radius of relative stiffness = $[Eh^3/12k(1 - \mu^2)]^{1/4}$,

Table 1. Percentage of pavement condition rating score determined by distress.

Agency	Flexible Pavements	Rigid Pavements	Agency	Flexible Pavements	Rigid Pavements
Arizona	17.0	17.0	Nebraska	40.0	0.0
California	73.2	—	New Mexico	40.0	40.0
Florida	50.0	—	North Dakota	75.5	—
Georgia	37.5	—	Tennessee	50.0	50.0
Indiana	22.0	22.0	Texas	80.4	88.5
Kansas	44.0	50.0	Virginia	48.0	42.0
Louisiana	30.0	30.0	Washington	50.0	50.0
Maine	100.0	—	King County, Washington	37.5	—
Maryland	40.0	40.0			
Minnesota	50.0	50.0			

Note: In general, distress measured by ride meters is not used in the computation of percentages.

Figure 1. Breakdown of Table 1 data.

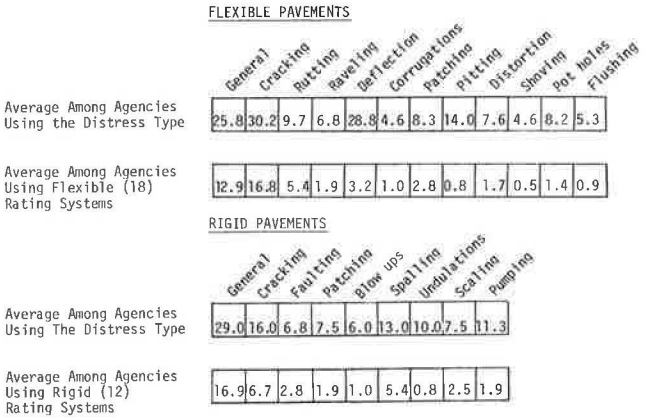

Figure 2. Variation of concrete elastic modulus along 40 km (25 miles) of I-45 between Houston and Dallas.

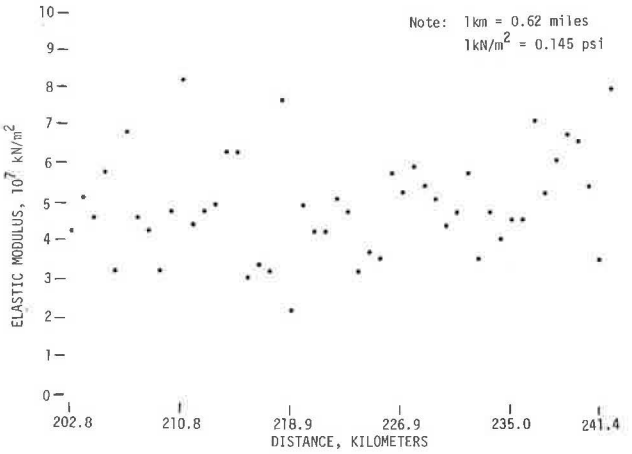

μ = Poisson's ratio of the concrete, and
f = a decreasing function of x/l.

The technique used chooses E and k by trial and error to minimize the sum of the squared errors between predicted and observed deflections. The second program determines the statistical properties of the calculated E and k value along the road. This program then drops out data in a specified pattern so that 90 percent, 80 percent, 70 percent, and smaller size samples can be used to calculate the same statistical properties, which include the mean, standard deviation, skewness, and kurtosis of the distribution. By finding the smallest size of sample that produces about the same statistical properties, one locates the minimum sampling rate for a pavement survey.

Figure 3. Variation of subgrade modulus along 40 km (25 miles) of I-45 between Houston and Dallas.

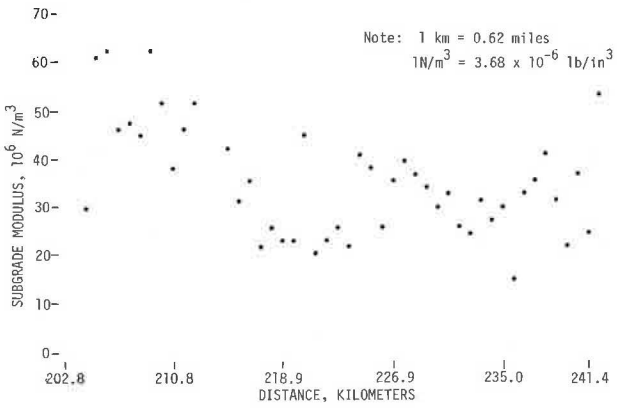

Table 2. Statistical properties of elastic modulus distribution.

Sample Size (%)	Mean (GN/m²)	Standard Deviation (GN/m²)	Skewness (GN/m²)	Kurtosis (GN/m²)
100	47.2	11.1	-1.05	-5.4
80	46.6	11.2	-1.06	-5.8
50	46.6	11.4	-2.07	-4.8
30	46.5	11.9	-1.33	-3.2
10	46.2	12.1	-1.93	-6.7

Note: 1 N/m² = 0.00145 lbf/in².

Figure 2 shows a typical distribution of the elastic modulus of the concrete pavement over a 40-km (25-mile) length of pavement. The values of E range between about 21 and 83 GN/m² (3 and 12 million lbf/in²). The higher values are undoubtedly in error probably because of an underestimate of the thickness of the pavement or because of the presence of a stiff subbase material that has the same effect on the analysis as underestimating the thickness of the concrete. This is confirmed, to some extent, by Figure 3, which shows the values of the subgrade modulus over the same length of road. The larger values of E are in roughly the same location as the larger values of k, which indicates the possible presence of a three-layer pavement that is insufficiently well modeled by the two-layer Westergaard equation.

The statistical program then sampled the calculated data and produced the statistical measures of elastic modulus given in Table 2. The total number of samples considered was 180. Skewness measures the distribution of the data around the mean, and kurtosis measures how peaked the distribution is. A value of zero in each case is a property of the normal distribution curve.

The 50 percent sample, representing a measurement every 1.6 km (1 mile), gives values that are nearly identical with those of the 100 percent sample. Even the 10

percent sample, computed from only 18 measurements, gives acceptably close values of the mean and standard deviation. This 10 percent sample represents a measurement made every 8.0 km (5 miles). A similar determination was made for the subgrade modulus distribution. Although this is not suggested to be standard practice, it does show that relatively infrequent measurements can produce acceptable statistical measures of pavement properties. Furthermore, it indicates that a study such as this can sometimes greatly reduce the amount of data required for making decisions on rehabilitation and at the same time produce data that are sufficiently accurate for the design of overlays and other forms of pavement rehabilitation.

These considerations demonstrate that the speed of operation of deflection or stiffness measuring devices, or in fact any kind of device, is relatively unimportant as long as the equipment can be used effectively as part of a statistical sampling survey.

Impulse and Impedance Methods

Among the methods of determining pavement stiffness are the Phoenix falling weight deflectometer (PFWD) and the impulse testing techniques developed at the Cornell Aeronautical Laboratory (CAL) and the Washington State University (WSU) as well as the vibration testing impedance technique developed in South Africa at the National Institute for Road Research (NIRR). All of these devices are capable of making measurements that can be analyzed provided that both input force and output response are measured as a function of time. The WSU device measures vertical accelerations as the pavement output response with time; the NIRR device measures vertical velocities as the output response; and the CAL and PFWD devices measure displacements with time. Because of the way they operate, these devices are well suited to a statistical sampling survey. The vehicle-mounted WSU device is even capable of collecting data on a mass inventory basis. Szendrei and Freeme (10), referring to the NIRR device, define the pavement impedance function $Z(\omega)$ as the ratio of the Fourier transforms of the input force and the output velocity response.

$$Z(\omega) = \left[\int_{t=-\infty}^{t=\infty} f(t) \exp(-j\omega t)dt \Big/ \int_{t=-\infty}^{t=\infty} v(t) \exp(-j\omega t)dt \right] \quad (2)$$

where

$f(t)$ = input force as function of time,
$v(t)$ = output velocity response as function of time, and
ω = frequency in radians per second.

By using the derived impedance function $Z(\omega)$ and other such derived data, namely, the exponential rate of saturation and the phase retardation with distance, one can calculate the deflection response of a pavement surface to a moving load. As long as the pavement deflects reasonably linearly overall, which it does even for fairly heavy highway loads (10, 11), the calculated response can be expected to be reasonably accurate. The same impedance function could be derived from the WSU measurements by means of the following relation at every point where acceleration a(t) is measured:

$$Z(\omega)/j\omega = \left[\int_{t=-\infty}^{t=\infty} f(t) \exp(-j\omega t)dt \Big/ \int_{t=-\infty}^{t=\infty} a(t) \exp(-j\omega t)dt \right] \quad (3)$$

Thus approximately the same analysis techniques developed in South Africa could be used to analyze data

Figure 4. Typical GM profilometer data showing a cracked pavement profile.

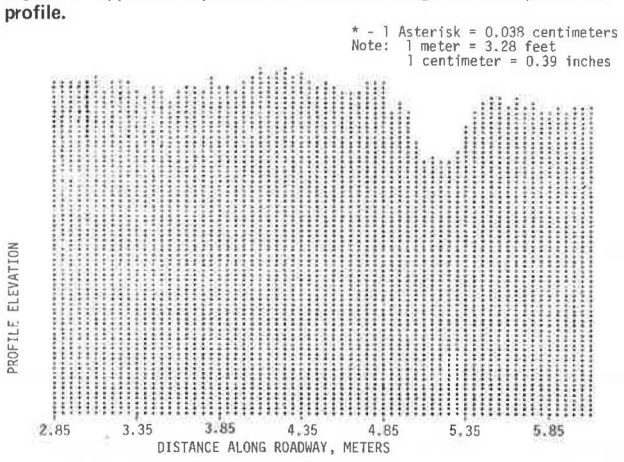

Figure 5. Frequency distribution of crack depths along I-20 between Midland and Odessa, Texas.

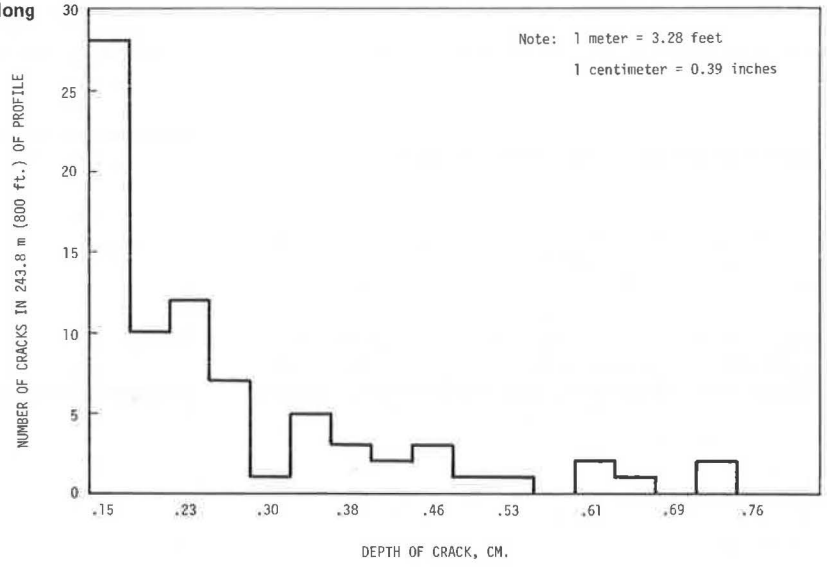

from the WSU device. This would permit a calculation of the deflection response of a pavement to any selected moving load.

Both the CAL and the PFWD measure output displacement response at only one point immediately beneath the load. Therefore, use of their data to make moving load predictions would be impossible. However, as shown by Szendrei and Freeme (10), these measurements are sufficient to predict the deflection response of a pavement to an impulse load, which, in itself, is a reasonable indication of the overall stiffness of a pavement.

The results of these measurements, data reduction, and Fourier transformation is an analytical measure of overall pavement stiffness that can be determined quickly and can be expected to be sensitive to changes in pavement stiffness, either with time or with distance. This makes this device potentially useful in a statistical sampling survey.

Crack Counting With GM Profilometer

The General Motors (GM) profilometer is capable of making very accurate detailed measurements of pavement profile in the right and left wheel paths. Usually the analogue measurements made by the profilometer are converted to digital data, and a profile elevation is given every 5.149 cm (2.027 in) along the roadway. The entire process is described in detail elsewhere (12, 13). A computer plot of typical profilometer data is shown in Figure 4 where each asterisk represents an elevation change of about 0.038 cm (0.015 in). The numbers marked at the bottom of the figure are the distances in meters from the beginning of the profile, which was measured along a test section of badly cracked flexible pavement on I-20 in Texas Department of Highways and Public Transportation District 6. The cracking along this length of pavement is apparently caused by thermal shrinkage of the base course.

The large dip centered on distance 5.25 m (17.22 ft) is a crack that is about 0.71 cm (0.28 in) deep. The really significant feature of this crack is the depression on each side of it. As expected from analysis (14), a shrinkage crack in the base course will draw down the pavement on each side of it for a considerable distance, which in this case is about 0.46 m (1.5 ft). The characteristic V shape of a crack makes it a visually distinctive feature in a profile of a flexible pavement. A crack in a rigid pavement where the surface course is a brittle material will be much more abrupt. In either case, the crack may become accentuated with time as fines are pumped out of the base course. Distortion around the crack will always point toward the most active layer—the layer that has caused the crack.

The observation of the V shape around a crack led to the development of a special profile filter that distinguishes a V shape and stores in computer memory the location of the center of the crack. The profile filter first smooths the profile by averaging the 5 points centered around a given point and then manufactures an even smoother profile by averaging 30 points around the given point. A crack is defined by a difference in elevation between the 5-point averaged and the 30-point averaged profiles. The 30-point averaged profile provides a relatively smooth datum with which to compare the 5-point profile while following the general slope of the pavement fairly faithfully. The 5-point averaging was done to eliminate extraneous material from the profile.

The crack-counting filter found that there are two cracks in the space shown in Figure 4:

1. A crack of severity 4 [0.15 cm (0.06 in)] at 3.50 m (11.48 ft) and
2. A crack of severity 19 [0.71 cm (0.28 in)] at 5.25 m (17.22 ft).

A frequency distribution of the cracks found within a 243.8-m (800-ft) distance is shown in Figure 5. A total of 78 cracks were found with this filter, which gives an average crack spacing of just over 3 m (10 ft). A field survey of this same section of pavement indicated that the visible cracks occur on the average of 3.7 m (12 ft), a reasonably close match.

Although the difference between a 3-m (10-ft) and a 3.7-m (12-ft) crack spacing may be only a statistical error, it does suggest that the crack-counting filter found some 11 out of 78 surface profile features that resembled cracks but may not have been.

There are two possible interpretations of this finding.

1. The crack-counting filter is in error and should use a greater difference in elevation as a crack criterion. An elevation difference of 0.20 cm (0.08 in) would give an average crack spacing of about 4.9 m (16 ft).
2. The crack-counting filter has found some cracks that are as yet invisible.

It is impossible at this stage to say which of these interpretations is correct. This determination will require further field investigation. Analytical results such as those of George (14) show clearly the mechanism of pavement depressions forming above where cracks in the base course have not yet broken through the surface. Whether such a depression will always indicate the presence of an invisible crack is another question that remains to be determined.

That the crack-counting filter is a convenient, automatic, and rapid method of determining cracks from GM profilometer data can certainly be concluded. The filter may have a hidden potential for detecting invisible transverse cracks and may be very useful in statistical sampling surveys.

SUMMARY AND CONCLUSIONS

Pavement structural evaluation is a major consideration in pavement condition surveys that are widely used in making maintenance and rehabilitation decisions. Although each highway agency has developed its own rating system independently, there is broad agreement on the most significant indicators of pavement condition. Equipment to measure some of these indicators is being used routinely but there is some controversy about the best way to use the equipment in sampling the condition of the roadway and a lack of development of equipment that can reliably measure cracks. Several innovative ways of using existing equipment have been tried, and the results are presented in this paper. The major conclusions of this study are as follows:

1. Most highway agencies are conducting pavement condition surveys for flexible and rigid pavements;
2. Most agencies with pavement condition rating methods use these systems in making maintenance decisions;
3. Car ride meters are now the most widely used methods of measuring riding quality;
4. Cracking is the most heavily weighted distress indicator in the rating systems and as yet is not measured by instrumentation, and general structural adequacy is also a major factor in the rating systems;
5. The GM profilometer combined with a crack-counting filter shows promise as a possible crack-measurement device;
6. The most rapid, reliable method of gathering

data for a decision survey will use a statistical sampling technique; and

7. Impulse and impedance methods of measuring pavement stiffness must have further development in data reduction and analysis techniques, but they show promise of being a rapid, reliable indicator of pavement stiffness; currently used devices for measuring pavement deflections can produce reliable measures of pavement stiffness but also can be analyzed to give material properties of the pavement layers.

ACKNOWLEDGMENT

We wish to acknowledge the assistance of the Federal Highway Administration for their sponsorship of phase 1 of FHWA Contract DOT-FH-11-8264, Pavement Evaluation. That report served as the basis for this paper.

REFERENCES

1. State of the Art: Rigid Pavement Design, Research on Skid Resistance, Pavement Condition Evaluation. HRB, Special Rept. 95, 1968.
2. M. Y. Shahin and M. I. Darter. Pavement Functional Condition Indicators. Construction Engineering Research Laboratory, U.S. Army Corps of Engineers, Champaign, Ill., Technical Rept. C-15, Feb. 1975.
3. R. Haas. Surface Evaluation of Pavements: State of the Art. Workshop on Pavement Rehabilitation, Federal Highway Administration and Highway Research Board, San Francisco, unpublished rept., Sept. 1973.
4. W. E. Willey. Arizona's Experience With Sufficiency Ratings. HRB, Bulletin 53, 1952, pp. 3-6.
5. B. F. McCullough. A Pavement Overlay Design System Considering Wheel Loads, Temperature Changes, and Performance. Univ. of California, Berkeley, PhD dissertation, July 1969.
6. R. L. Lytton, W. M. Moore, and J. P. Mahoney. Pavement Evaluation. Federal Highway Administration, Final Rept., Phase 1, FHWA-RD-75-78, March 1975.
7. G. Peterson and L. W. Shepherd. Deflection Analysis of Flexible Pavements. Materials and Tests Division, Utah Department of Highways, final rept., Jan. 1972.
8. F. H. Scrivner, C. H. Michalak, and W. M. Moore. Calculation of the Elastic Moduli of a Two-Layer Pavement System From Measured Surface Deflections. HRB, Highway Research Record 431, 1973, pp. 12-24.
9. H. M. Westergaard. Stresses in Concrete Pavements Computed by Theoretical Analysis. Public Roads, Vol. 7, No. 2, April 1926, pp. 25-35.
10. M. L. Szendrei and C. R. Freeme. Road Response to Vibration Tests. Proc., ASCE, Vol. 96, No. SM6, Nov. 1970, pp. 2099-2124.
11. F. H. Scrivner and C. H. Michalak. Linear Elastic Layer Theory as a Model of Displacements Measured Within and Beneath Flexible Pavement Structures Loaded by the Dynaflect. Texas Transportation Institute, Texas A&M Univ., College Station, Research Rept. 123-25, Aug. 1974.
12. R. S. Walker, F. L. Roberts, and W. R. Hudson. A Profile Measuring, Recording, and Processing System. Center for Highway Research, Univ. of Texas at Austin, Research Rept. 73-2, April 1970.
13. R. S. Walker and W. R. Hudson. Analog-to-Digital System. Center for Highway Research, Univ. of Texas at Austin, Research Rept. 73-3, April 1970.
14. K. P. George. Mechanism of Shrinkage Cracking of Soil-Cement Base. HRB, Highway Research Record 442, 1973, pp. 1-10.

Abridgment

Study of Rutting in Flexible Highway Pavements in Oklahoma

Samuel Oteng-Seifah and Phillip G. Manke, Oklahoma State University

Field and laboratory observations indicate three major modes of rutting in flexible pavements. For the bituminous materials of a pavement, these are (a) post-construction differential densification of one or more of the pavement layers (4; 7, pp. 58-80), (b) shear failure or lateral displacement of material in one or more layers from beneath the wheel paths (2; 8, pp. 21-39), and (c) surface wear or erosion of surface material under traffic (5, 6). In addition, densification (consolidation) or shear failures or both in the nonbituminous base and subgrade materials will influence the total amount of rutting. In a specific case, each of these factors may act singularly or in various combinations.

The primary objective of this research was to investigate rutting on high-quality flexible pavements and to detect if possible evidence of contribution of bituminous-bound pavement materials to this type of failure. This research did not deal directly with the influence or contributions to rutting of the subgrade soils and non-asphalt-bound base materials.

A transverse profile gauge was developed to plot the profile of the pavement surface perpendicular to the centerline. Rut depths could be scaled directly, and humps outside the wheel-path locations could be detected from the transverse profile tracings. Heaving or humping adjacent to ruts was considered an indication of outward or lateral creep of material from beneath the wheel paths.

Cores of the asphalt-bound pavement materials, 10.16 cm (4.00 in) in diameter, were recovered at selected points across the pavement. The core samples were subdivided into surface course; leveling course; and upper third, middle third, and bottom third of the base course. The percentage density values of the respective subdivisions of the core samples were determined and compared. Significant differences in the percentage density values between materials in the wheel-path locations and those outside the wheel paths were considered as evidence of differential densification.

Stereo photography (6) was employed to obtain quantitative estimates of differential wear in the wheel-path locations. Also a visual rating of the pavement surface condition was made at each test site to provide additional data for the study of these locations.

Sixteen test sites were selected on two Interstate Highway systems (I-35 and I-40) in Oklahoma. Performance of four test sites on flexible pavements constructed on each of the following types of base course materials was studied: (a) hot-mix sand asphalt (HMSA), (b) soil-cement base (SCB), (c) stabilized aggregate base course (SABC), and (d) black base (BB).

Although a limited number of test sites were studied, classical statistical methods that use the statistical analysis system (SAS) computer program (1) were employed in the analysis of test data to detect possible performance trends.

TRANSVERSE PROFILE GAUGE

The transverse profile gauge was developed to provide a portable and accurate apparatus for making a continuous profile tracing of the pavement surface. With these profile tracings, the shape of the pavement surface in and adjacent to the wheel-path depressions could be ascertained and the rut depth could be measured to the nearest 0.025 cm (0.01 in). In essence, this apparatus consisted of a supported guide rail, a trolley system, and an X-Y recorder (Figure 1).

The guide rail had a total length of 3.96 m (13.00 ft) and was made from two magnesium alloy carpenter's framing levels. The rail was supported at the center point and at the ends with adjustable height supports and was oriented to span a traffic lane perpendicular to the centerline of the roadway. The two end supports were adjusted to set the rail at a given height above the pavement surface at these points, and the center support was adjusted to remove any midspan deflection. Thus, the rail became a planar surface and served as a guide for the trolley system and as the datum for the measurements.

The trolley system consisted of an aluminum suspension plate with four nylon rail-track wheels machined to

Publication of this paper sponsored by Committee on Pavement Condition Evaluation.

fit the top and bottom flanges of the guide rail. A 12.70-cm-diameter (5.00-in-diameter) rubber-rimmed actuating wheel made of Teflon was attached to a short pivot arm hinged to the bottom of the suspension plate. The pivot arm also supported a helical potentiometer, whose shaft was connected to the axle of the actuating wheel, and a bracket connection for one end of a linear potentiometer. The other end of this linear potentiometer was attached to the suspension plate.

The actuating wheel contacted and rolled along the pavement surface as the trolley system traversed the guide rail. The helical potentiometer scaled the horizontal displacement, and the linear potentiometer scaled the vertical displacement of the actuating wheel. These displacements were recorded as a continuous transverse profile trace of the pavement surface by an X-Y recorder. A more complete description of the construction and operation of the profile gauge has been reported by Manke and Oteng-Seifah (3).

PROFILE MEASUREMENTS

Lack of an original profile tracing of the pavement surface at a test site made it difficult to determine the total subsidence or upheaval that the surfaces had undergone since the roadway was opened to traffic. For this reason, the observed profile measurements were based on defined datums. That is, rut depth was measured as the maximum vertical displacement of the surface in the wheel path from a straight line whose ends formed tangents to the transverse profile curve at the adjacent points of maximum elevation.

It was known from design records that the pavement surface at the test sites had been designed with uniform cross slope for lanes in the same traffic direction. A straight line joining the end support points on a tracing was assumed to be the original surface, and significant upward displacements of the surface above this line were scaled from the profile tracings. The maximum upward displacement was considered as probable heave resulting from lateral displacement of materials.

Figure 1. Transverse profile gauge.

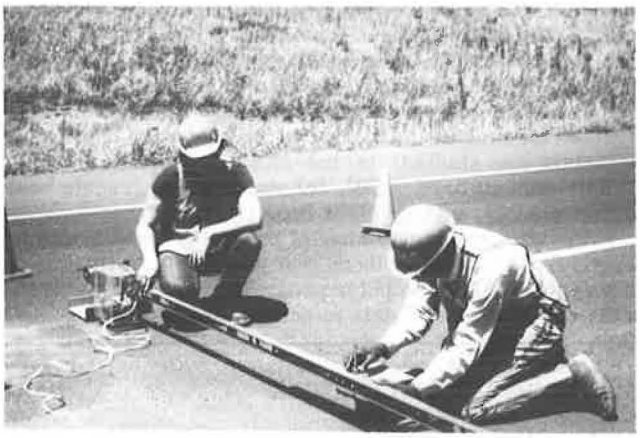

STEREOPHOTOGRAPHIC INTERPRETATION

Estimates of differential wear in the wheel paths at the test sites were based on the relative projections of the surface aggregates above the matrix. The pairs of photographs were viewed stereoscopically under six power magnification on a fluorescent light table. The aggregate projections were compared with the projection of a wedge-shaped scale placed on the pavement surface when the photographs were taken to obtain the heights of the aggregate projections. Comparison of the surface aggregate projections in the wheel paths with those at locations receiving less wheel coverage was considered a reasonable approach to determining the amount of surface attrition that had occurred.

LABORATORY DENSITY DETERMINATIONS

Core samples of full thicknesses of the asphalt-bound materials were cut from wheel-path and non-wheel-path locations at the selected test sites. As previously stated, these cores were cut into segments corresponding to the respective pavement layers with a concrete saw. Specific gravities of the individual layers could then be determined and differences in density detected. Bulk specific gravities of the core segments were determined by using ASTM method D1188. The maximum specific gravities of the mixtures were determined by using ASTM method D2041.

SUMMARY OF RESULTS

Table 1 gives the contributions of the various modes of

Table 1. Modal contributions to rutting.

Site Number	Type of Base Course	Age (months)	Maximum Rut Depth (cm)	Approximate Contribution to Rutting			
				Densification (%)	Surface Wear (%)	Lateral Creep (%)	Base or Subgrade Deformation (%)
10	HMSA	36	2.515	28	2	70	—[a]
60	HMSA	169	1.090	40	5	55	—[a]
70	HMSA	169	1.458	40	5	55	—[a]
120	HMSA	105	0.965	42	8	50	—[a]
20	BB	82	1.450	58	12	30	—[a]
30	BB	56	1.542	25	2	—[a]	73
40	BB	56	1.633	22	2	—[a]	76
50	BB	86	1.996	8	2	—[a]	90
80	SABC	165	1.450	9	5	—[a]	86
90	SABC	165	1.588	9	13	—[a]	78
100	SABC	156	1.542	18	5	—[a]	77
110	SABC	156	1.224	20	6	—[a]	74
130	SCB	148	0.556	43	8	49	
140	SCB	148	0.734	30	5	65	
170	SCB	169	1.270	14	8	78	—[a]
180	SCB	169	1.214	25	6	69	—[a]

Note: 1 cm = 0.394 in.

[a]Not a major factor; some contribution indicated.

rutting at the test sites. The measurements of rut depth, heave, surface wear, and differential density determined in this study were subject to many inaccuracies primarily because of the lack of initial data on the pavement sections. Thus the tabulated values should be regarded only as indications of the component contributions. Despite this, however, the data from this study consistently showed that the bituminous mixes were responsible for a significant amount of the rutting that occurred on these flexible pavements.

CONCLUSIONS

Based on the test procedures employed and the pavement sections studied, six conclusions are drawn.

1. The transverse profile gauge provides a portable and accurate means of obtaining continuous transverse profile tracings of a pavement surface.
2. In addition to measurements of surface deformations, profile graphs can provide permanent records of these conditions at a specific time in the service life of a pavement and can be used for future studies.
3. Densification contributed a significant amount to the total surface rut depth. On the thicker pavements (sections employing black base or sand-asphalt base), the amount of rut depth ascribed to densification ranged from 8 to 58 percent in the outer lane.
4. Evidence of lateral creep or instability in the bituminous material layers was found at 11 of the 16 test sites. This occurred in high- as well as low-density materials and contributed from 30 to 78 percent of the rutting at these locations. More prominent surface heaves were noticed at sites where the material layers had low densities.
5. Surface wear or attrition in the wheel paths on heavily traveled lanes was an important contributing factor to rutting. Proper consideration should be given to this factor in the design of surface mixtures.
6. Base and subgrade deformations influenced the magnitude of rutting at many of the test sites. Extensive surface cracking and indications of surface subsidence were found at these sites. Consolidation and shear failure in these layers conceal the effects of lateral creep in the bitumen-bound materials.

REFERENCES

1. A. J. Barr and others. A User's Guide to the Statistical Analysis System. North Carolina State Univ., Raleigh, Aug. 1972.
2. C. R. Foster. Dominant Effect of Fine Aggregate on Strength of Dense-Grade Asphalt Mixes. HRB, Special Rept. 109, 1968, pp. 1-3.
3. P. G. Manke and S. Oteng-Seifah. Characteristics of Rutting on High Quality Bituminous Highway Pavements. Oklahoma Department of Highways, Oklahoma City, Research Project 72-03-3, Interim Report 2, Dec. 1975.
4. N. W. McLeod. Influence of Viscosity of Asphalt Cements on Compaction of Paving Mixtures in the Field. HRB, Highway Research Record 158, 1967, pp. 76-115.
5. C. K. Preus. Studded Tire Effects on Pavements and Traffic Safety in Minnesota. HRB, Highway Research Record 418, 1972, pp. 44-54.
6. R. Schonfeld. Photo-Interpretation of Skid Resistance. HRB, Highway Research Record 311, 1970, pp. 11-25.
7. The AASHO Road Test: Report 5—Pavement Research. HRB, Special Rept. 61E, 1962.
8. E. J. Yoder. Principles of Pavement Design. Wiley, New York, 1959.

Application of Waterways Experiment Station 7257-kg Vibrator to Airport Pavement Engineering

A. F. Sanborn, SITE Engineers, Inc.
J. W. Hall, Jr., U.S. Army Engineer Waterways Experiment Station, Vicksburg, Mississippi

For many years the airfield pavement industry has been searching for a suitable nondestructive method that would eliminate the necessity for borings and test pits. This paper describes the use of the Waterways Experiment Station 7257-kg (16-kip) vibrator for the evaluation of load-carrying capacity and the design of bituminous concrete overlays for highly variable flexible pavements at commercial airports. The primary purpose of using dynamic testing was to provide a rapid, nondestructive, and independent system of measurement of existing pavement strength. The vibrator is electrohydraulic and can apply loads up to 66.7 kN (15 000 lbf) on a 45.7-cm-diameter (18-in-diameter) plate at frequencies of 5 to 100 Hz. Primary measurements included dynamic stiffness testing, borings with California bearing ratio tests, and condition surveys. Dynamic stiffness was correlated with physical condition and types and thicknesses of pavement and subgrade to determine allowable gross loads and overlay thicknesses. The study shows that the stiffness concept in which a large vibratory load is used relates well to conventional (California bearing ratio) methods provided that sufficient conventional data are available at a limited number of locations representing the range of conditions. The immediate potential values of this method are speed of field operation, unexpected ranges of strength, and convenience of a single parameter expression of overall pavement and subgrade strength. Potential improvements in dynamic nondestructive methodology include use of deflection basin data and relation of stiffness to a theoretical basis.

Dynamic nondestructive testing of pavements has been undergoing considerable development since the 1950s. This paper describes the use in an actual design project of the third generation U.S. Army Engineer Waterways Experiment Station (WES) equipment as developed under U.S. Air Force and Army research (1) and used in the Federal Aviation Administration (FAA) research in the early 1970s (2). Most of the data and methodology given here are from investigations by SITE Engineers, Inc., at Philadelphia International Airport in 1973. Reference is also made to information obtained from WES studies for the FAA and to investigations by SITE Engineers, Inc., at Albany County, New York, Airport and Oakland-Pontiac, Michigan, Airport. Most of the pavements involved were flexible or semiflexible.

Publication of this paper sponsored by Committee on Pavement Condition Evaluation.

The purpose of the investigations was to evaluate the existing strength and to design bituminous concrete (BC) overlays for expected increases in aircraft size and frequency.

Specific objectives of the dynamic testing were to

1. Determine a single number parameter at individual locations that would express the relative strength of the highly variable existing systems involving pavement, base, and subgrade in depth;
2. Determine the existing strength and overlay requirements by a semiindependent system of measurements;
3. Obtain better (more closely spaced) coverage by actual tests than was practicable with conventional destructive tests; and
4. Expedite the investigations by minimizing shutdown times to aircraft operations and reduce the cost of the study.

EXISTING CONDITIONS

Philadelphia International Airport is built in the floodplain of the tidal Delaware River and has been under development since the 1920s. The original surficial soil was alluvial organic silt having California bearing ratios (CBRs) on the order of 1 to 5 percent and thicknesses ranging from 3.05 to 15.24 m (10 to 50 ft). Underlying this soil are very strong granular and cohesive soils. Overlying the organic silts are random fills of granular material; loose, hydraulically deposited sandy silts; and cinders.

The airport was built in stages above the random fills during a 40-year period. It was built to various criteria and with a number of different types of pavement sections and overlay thicknesses. Within the project area, the existing pavements were composed of materials as given in Table 1. Figure 1 shows a plan of the project area and the location of the types of pavement.

The physical condition of the flexible pavements varied from very good (no major defects) to very poor (continuous deep alligator cracking or significant rutting in the wheel-path areas or both). Previous traffic on

Figure 1. Project plan.

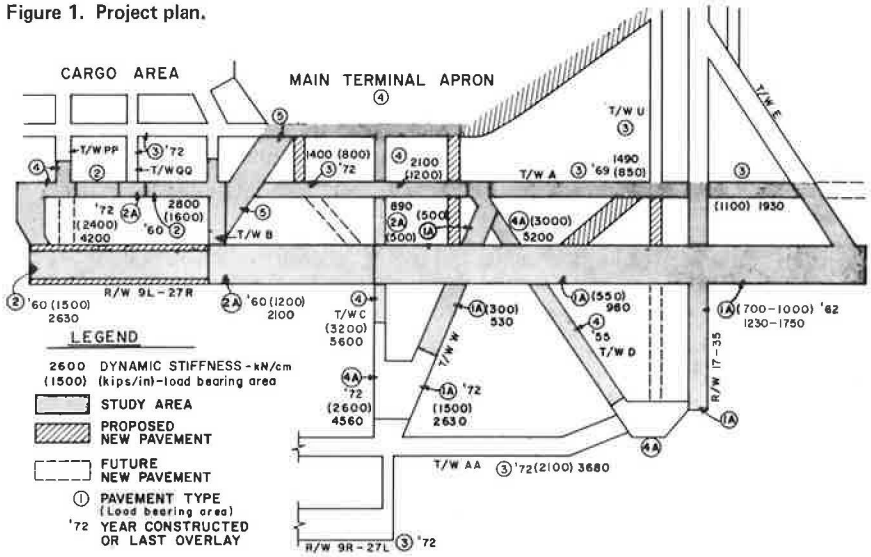

Table 1. Pavement composition.

Pavement	Surface	Stone Base	Select Fill	Random Fill	Overlay
1	5-cm BC	13 to 25-cm CM	0.7 to 0.9-m C	0.9 to 2.4-m S or SL + CL or both	
1A	5-cm BC	13 to 25-cm CM	0.7 to 0.9-m C	0.9 to 2.4-m S or SL + CL or both	5 to 33-cm BC
2	10-cm BC	25 to 30-cm M	1.5 to 3.0-m GS	0 to 1.5-m S or SL + CL or both	
2A	10-cm BC	25 to 30-cm M	1.5 to 3.0-m GS	0 to 1.5-m S or SL + CL or both	5 to 15-cm BC
3	28 to 33-cm BC	8 to 15-cm WGM	0.7 to 1.5-m G or G + S	0.7 to 1.2-m S or SL + CL or both	
4	30-cm PCC	0	0.9 to 1.5 G or G + S	0.7 to 0.9-m S or SL + CL or both	
4A	30-cm PCC	0	0.9 to 1.5 G or G + S	0.7 to 0.9-m S or SL + CL or both	5 to 20-cm BC

Notes: 1 cm = 0.394 in, 1 m = 3.28 ft.
BC = bituminous concrete; C = cinders; CL = coal; CM = coarse material; G = gravel; GS = gravelly sand; M = macadam; PCC = portland cement concrete; S = sand; SL = silt; WGM = well-graded material.

Figure 2. Nondestructive testing equipment.

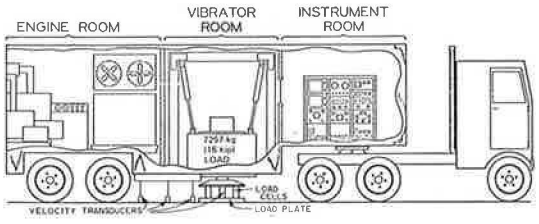

most of the pavements in the project area had been dual and dual tandem jet aircraft over 10 to 15 years.

PREVIOUS TESTS

During a 1970 preliminary evaluation, the pavements were tested with a model 400 road rater to assist in determining locations for destructive tests. In November 1972, WES made dynamic tests for their FAA research study on the newly constructed pavements of runway 9R-27L and taxiway AA. At the request of the Philadelphia Division of Aviation, additional tests were made at other locations, principally where destructive tests including CBRs had been made in 1970. In June 1973, WES returned to make research dynamic and destructive tests (through small-aperture borehole techniques) (3) at two additional locations on pavements completed in 1972. At this time, by contract with the city of Philadelphia and as directed by SITE Engineers, Inc., WES also made dynamic tests on the project reported here.

FIELD INVESTIGATIONS

Dynamic Testing Equipment

The WES 7257-kg (16-kip) vibrator, which is an experimental prototype model, is housed in an 11-m (36-ft) semitrailer that contains supporting power supplies and automatic data recording systems. The vibrator and mass assembly consists of an electrohydraulic actuator surrounded by a 7257-kg (16 000-lb) lead-filled steel box. The actuator uses up to a 5.1-cm (2-in) double-amplitude stroke to produce a vibratory load ranging from 0 to 66 723 N (0 to 15 000 lbf) with a frequency range of 5 to 100 Hz for each load setting.

Major items of electronic equipment are: a set of three load cells that measure the load applied to the pavement, velocity transducers located on the 45.7-cm-diameter (18-in-diameter) steel load plate and at points away from the load plate that are calibrated to measure deflections, a servomechanism that allows variation of frequency and load, an X-Y recorder that produces load versus deflection and frequency versus deflection curves, and a printer that provides data in digital form. Figure 2 shows the schematic view of the vehicle, major systems, and detection devices.

With this equipment, the vibratory load can be varied at constant frequencies and load versus deflection can be plotted. These load-deflection data are used to compute the dynamic stiffness modulus (DSM) for a pavement structure. The frequency can be varied from approximately 5 to 100 Hz at constant force levels to produce the frequency response of the pavement structure. Also, at any selected load or frequency, the deflection basin shape can be obtained.

Selection of the WES 7257-kg (16-kip) vibrator as a standard test to produce the DSM results has been somewhat arbitrary but is based on results of earlier research studies. The vibrator must be capable of applying static and dynamic loads sufficient to stress the entire pavement section under consideration. Also enough dynamic force must be applied to produce deflections large enough

to be accurately measured. Studies over instrumented pavement sections have shown that the stress distribution with depth at a loading frequency of 15 Hz is nearest that of slowly moving wheel loads (with that at other frequencies between 5 and 50 Hz). The 45.7-cm-diameter (18-in-diameter) load plate with contact area of 1638 cm^2 (254 in^2) was selected because it approximates the single-tire contact area of most large jet aircraft.

Test Procedures

A dynamic stiffness test is performed by centering the test apparatus over the test location, lowering the contact plate, and slowly sweeping the dynamic force to a maximum of 15 kips (66.7 kN). The load-deflection data are plotted automatically in graphical form as the test progresses. For deflection basin shape measurements, the selected load is briefly held constant and the data are printed out in digital form and then manually.

Dynamic Investigations

The nondestructive tests consisted primarily of DSM measurements but did include a few variable frequency and many basin shape measurements.

The initial tests were made on closely spaced points along widely spaced lines transverse to the centerlines. The locations for these lines were selected from a study of the available data concerning the type and thickness of existing pavement, base, and subgrade-in-depth sections. From these tests at Albany County and Oakland-Pontiac airports, the locations for tests along longitudinal lines were selected. At Philadelphia International Airport, subsequent tests were made adjacent to previous and concurrent borings and test pits, in distressed areas, along certain longitudinal lines, and at other points of particular interest. A partial investigation plan for Philadelphia International Airport is shown in Figure 3.

Further use of stiffness testing was made at Philadelphia International Airport by performing tests along several transverse lines after several series of passes with a 32-Mg (35-ton) vibratory compactor and a 45-Mg (50-ton) pneumatic-tired proof roller. The purpose of these tests was to determine whether changes in the strength of the pavement and subgrade system occurred because of the two types of rollers.

More than 650 stiffness tests and 760 deflection basin tests were made at Philadelphia International Airport in 6 days.

Conventional Investigations

At Philadelphia International Airport, a comprehensive investigation into destructive testing had been authorized to provide conventional information for the design of overlays, new construction, reconstruction, special treatments at junctures of existing and proposed pavements, and other related items. Details of the procedures and results are given in the report (4) and include the following: (a) deep borings (to below the organic silt) at approximately 305-m (1000-ft) centers; (b) shallow borings about 4.6 m (15 ft) deep and core borings at about 61-m (200-ft) centers longitudinally and at about 7.6-m (25-ft) centers transversely at pavement intersections; (c) CBR and nuclear moisture-density tests in boreholes and test pits; and (d) a detailed visual condition survey including rut depth measurements at typical locations and complete defect mapping in selected areas. Typical locations of these types of investigations are also shown in Figure 3.

TEST RESULTS

Adjustment of Dynamic Data

From the load deflection plot, the WES method of determining DSM is to calculate the inverse of the slope of the straight-line portion of the curve (Figure 4). The resulting value is in kilonewtons per centimeter. A stiffness value may also be calculated for any point along the plot, and, as can be seen on the typical graph for a flexible pavement (Figure 4), the plot is usually concave upward. This yields higher values at points below the straight-line portion. The amount of curvature is believed to reflect the relatively higher rigidity of the surface and base materials rather than that of the overall pavement, base, and subgrade system. Also, the stronger the pavement is, the flatter the slope is. For the purpose of these investigations only DSM as determined from the straight-line portion was used.

Another correction that should be made to put all the data on a more common basis is the adjustment for temperature of the BC to a uniform temperature such as 21.11° C (70° F). Methods available for making this correction necessitate either direct measurement of the temperature within the pavement or estimates of an average pavement temperature by measurements of the surface temperature during testing and knowledge of the average air temperature for several preceding days. Tentative procedures recommended by WES are given elsewhere (2, 5).

DSM Test Results

The corrected stiffness values were presented in a manner to assist visual assessment of the variations, note where changes in patterns occurred, and aid in selecting typical values for further analysis. The first step was to evaluate the transverse sections taken at selected stations along the major pavements that represented the various pavement and subgrade conditions. As shown in Figure 5, there were major variations in stiffness both longitudinally and transversely. The runway had been built in three stages, and the center 45 m (150 ft) of the earlier stages had been overlaid at various times to improve the load-bearing capacity. From the data for stations 36+14 and 90+16, the thickness of BC would appear to be the major factor affecting stiffness. However, examination of the data for station 119+04 reveals that, even where the thickness of BC is uniform, the stiffness near the outer edges is only about 65 percent of that in the central area. Therefore, a second cause of variation in stiffness must be the effect of additional compaction of the base and subgrade by traffic. Weakening of nontraffic areas due to frost action is also possible. The destructive tests indicated no such magnitude of difference in base and subgrade strength. Another cause of variation appears to be a deterioration in overall strength in the vicinity of the wheel paths. This may be seen particularly at stations 90+14 and 119+04.

Examination of the taxiway sections revealed similar conditions especially for the western end, which is the only area that had received a large volume of jet traffic before testing. The areas consisting of 1-year-old 30.5-cm (12-in) BC pavement (taxiway W to taxiway B) revealed rather large differences that are probably due to a combination of nonuniformity in the strength of the old fills and the thickness of the granular fill from the recent construction.

Examination of the longitudinal profile of the runway (Figure 6) revealed further the effect of subgrade conditions to depths of at least 3.05 m (10 ft). On the runway, the western extensions included 1.52 to 3.05 m (5 to 10 ft)

of controlled granular fill and had much higher DSMs than did the original portion, which has only 0.6 to 0.9 m (2 to 3 ft) of cinders over variable sand and silts. The eastern end contains some sand fill and tested somewhat higher than the central portion between runway 17-35 and taxiway C. The profile of taxiway A exhibited similar characteristics in that the western end is strongest and the thickness of reasonably dense granular fill appears to have the greatest affect. Two other observations were made.

1. Along taxiway W south of runway 9L-27R, the subgrade conditions are relatively uniform, but the thickness of BC in the wheel paths increases from about 13 to 76 cm (5 to 30 in) going southwest. The profile revealed an increase in stiffness of from about 700 to 3500 kN/cm (400 to 2000 kips/in).
2. On taxiway C, a difference of about 1050 kN/cm (600 kips/in) was noted from where there is only 30.5 cm (12 in) of portland cement concrete to where there is an overlay of about 13 cm (5 in) of BC.

For the Philadelphia International Airport project, longitudinal runs were not made; to analyze for representative stiffnesses in each area, a contour plan was drawn from the data. For Albany County and Oakland-Pontiac airports, profiles were used and the data were statistically analyzed to assist selection of significantly different areas. Low average DSM values for the load-bearing areas at Philadelphia International Airport are shown in Figure 1.

Deflection Basin Results

Typical deflection basins are shown in Figure 7 and indicate that the deflection slopes generally vary most significantly from the edge of the loading plate to sensor 2 15.24 cm (6 in) from the edge. Comparison of the basin shapes to pavement sections showed similarities among dissimilar pavement, base, and upper subgrade sections and differences among similar sections. Although they have not been analyzed in detail, the differences in shape are suspected to reflect the condition and strength of the lower portions of thick flexible pavements or the base and top of subgrade. Limited analyses show that there are general trends of increasing steepness of slope with decreasing DSM and that the trend varies with pavement composition. At Oakland-Pontiac Airport, a definite re-

Figure 3. Partial investigation plan.

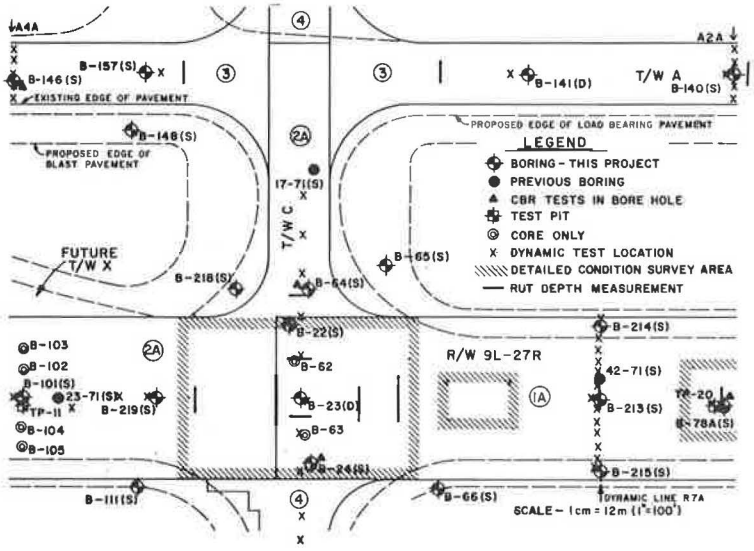

Figure 4. Field load deflection graph and DSM calculation.

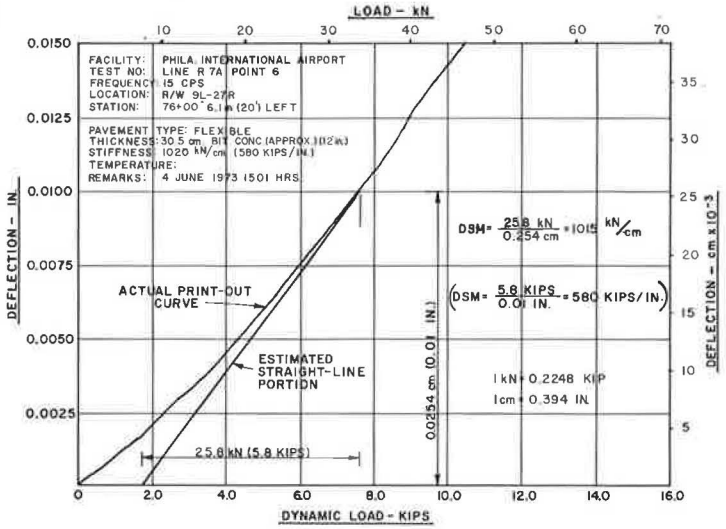

lationship was found between the slopes and the condition of the soil-cement base.

ANALYSIS

Evaluation of Allowable Load-Carrying Capacity

At each location where adequate thickness and CBR data were available, an allowable gross airplane load was calculated. The evaluation was based on FAA criteria in effect in 1973 for 6000 to 12 000 equivalent critical departures (ECDs)/year (design life of 120 000 ECDs) of DC-8-63 aircraft. This equals approximately 40 000 actual departures/year for the 1975 air carrier jet traffic mix at Philadelphia International Airport. Because measured subsoil CBRs varied from less (1 percent) to more (1 to 50 percent) than assumed in the FAA procedures (3 to 20 percent), it was necessary to develop a thickness versus CBR curve similar to that used by the U.S. Army Corps of Engineers (6).

The computed allowable loads were plotted against the DSMS, and a relatively good correlation as shown in Figure 8 was obtained.

Selection of Design DSM Values

For Philadelphia International Airport, conservative existing DSM values were selected for each of the more than 50 analysis areas to be overlaid by examining the contour plans, profiles, and sections. The analysis areas were determined on the basis of known differences in pavement and subgrade conditions, estimated future traffic volume, and offsets from centerline in accordance with keel section design concepts. Traffic volumes in terms of ECDs were developed by analyzing the aircraft

Figure 5. Transverse DSM sections on runway 9L-27R.

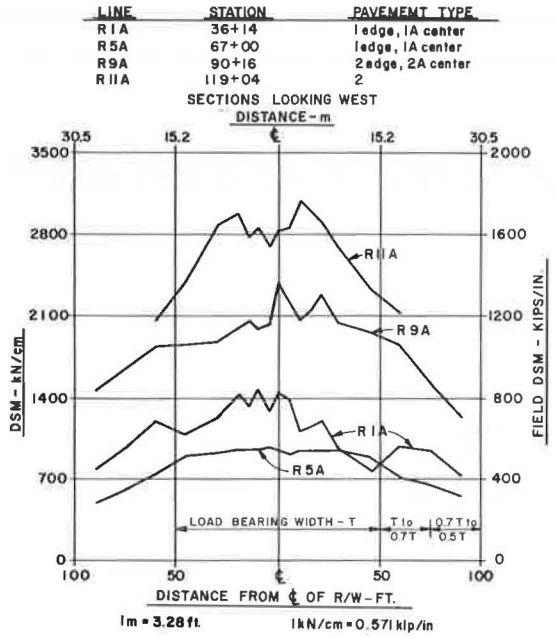

Figure 6. Profile of runway 9L-27R.

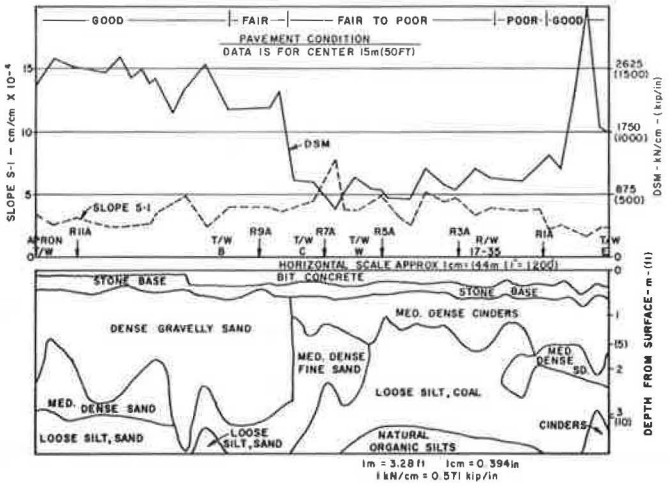

Figure 7. Typical deflection basins.

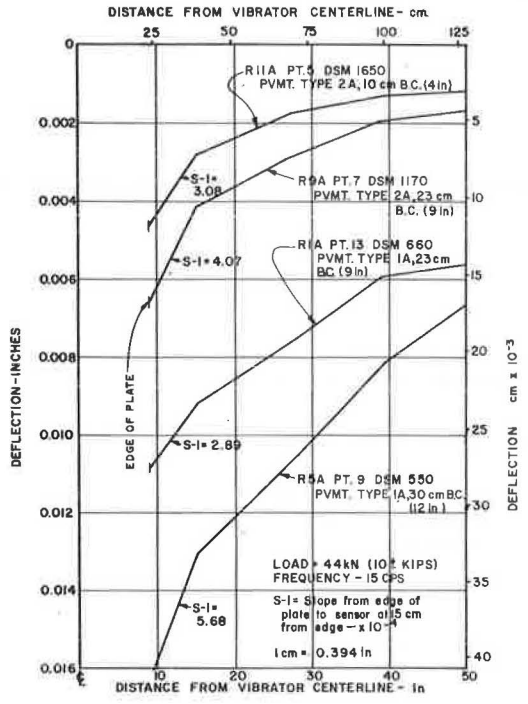

Figure 8. DSM versus allowable load.

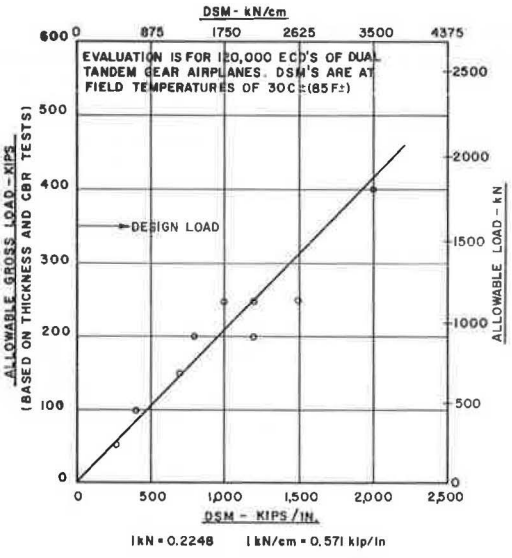

mix in each area and coverage versus actual departure ratios (7).

To use the DSM for overlay computations, we had to select design criteria values for the several levels of traffic volume. The DSM for a 1557-kN (350-kip) design load from Figure 8, 2977 kN/cm (1700 kips/in), was one possible value for 6000 to 12 000 ECDs/year, but the DSMs from a number of old and recent pavements that had either known design criteria or substantial evidence of good, fair, or poor performance were also examined. Figure 1 shows the existing DSMs for the areas tested.

Because a wide range of thicknesses of BC existed over most of the pavement and subsoil conditions, it was possible to plot DSM versus thickness of BC curves as shown in Figure 9. As may be noted from that figure, there is a similar curvature for each of the types of pavement. The intercepts on the DSM axis indicate the expected magnitude of the DSM on the several granular base and subsoil systems. These curves reveal increases in DSM of from 35 to 175 kN/cm of BC (20 to 100 kips/in of BC).

The next step was to calculate the required overlay by "standard" FAA methods. This entailed using equivalency factors to convert the existing sections to "conventional" flexible pavement sections and entering the CBR versus thickness curves developed for the project to determine the thickness of additional material required above each specific layer. A lower limiting CBR value of 2 percent was used for the very weak soils and an upper limit of 50 percent was used for the strongest subgrade. The required additional thicknesses of granular base, granular subbase, and granular fill were converted back to BC by using equivalency factors. The selected equivalency factors were based on evaluation of FAA standards and data in the Asphalt Institute Manual MS-11 (8).

The computed overlays were plotted against the DSM values for each of the specific test locations, and approximate curves were developed for one level of traffic. These curves were compared for shape and intercept values with the DSM versus thickness of BC curves. A final series of design DSMs and curves for each traffic level was selected from this comparison, and a typical set is given in Figure 10.

Figure 9. DSM versus bituminous concrete thickness.

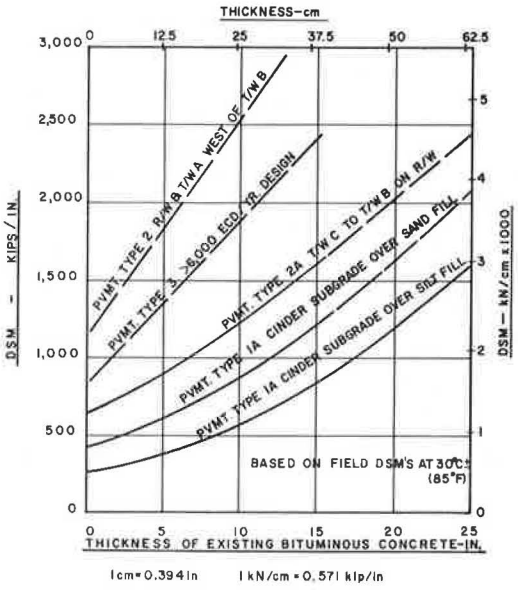

Figure 10. Typical DSM versus overlay thickness graph.

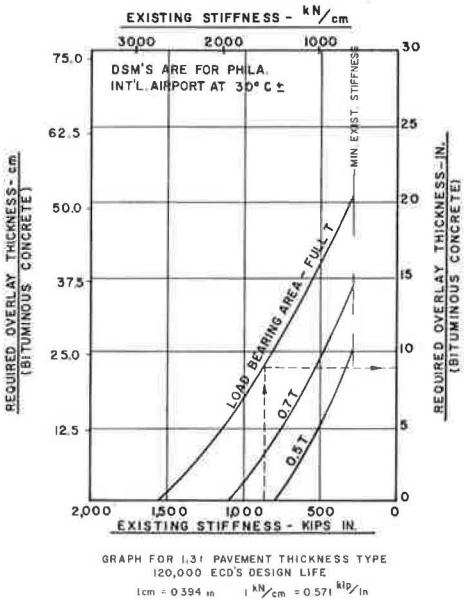

Selection of Recommended Overlays

To determine the overlay thicknesses to be recommended, we checked each analysis area by using average thickness, condition, and CBR data for the area. Overlay estimates were made by using the DSM versus overlay curves, the FAA equivalency method, and the Asphalt Institute MS-11 method (8) for design of new pavements.

Although the resulting three values were usually within 2.5 to 5 cm (1 to 2 in) of each other, there were a number of places where the thickness by DSM was several centimeters greater or less than by the other methods. The selected values were generally in conformance with the FAA method but were modified where the DSM or condition indicated a need. Minimum overlay thicknesses of FAA binder and surface requirements were recommended regardless of computed thicknesses because none of the existing BC was built to current specifications. Transition sections were recommended at certain locations, and the final overlay thicknesses were adjusted by the designers to achieve proper transverse and longitudinal grades.

CONCLUSIONS

Applicability of Dynamic Data

A review of the data and analysis from the 3 projects suggests four conclusions.

1. Data and correlations on bituminous pavements from different airports should not be too strictly compared unless all the data (deflections for stiffness, basin shape, and variable frequency) have been corrected to a uniform temperature and the subgrade conditions are similar.
2. A detailed knowledge of the construction history is necessary to develop an adequate investigation program. Knowledge of the current physical condition and strength of the pavement and soil layers is necessary to interpret the dynamic data. Special attention should be given to the soils below the upper portion of the subgrade that may never have been processed and that may be significantly weaker than the top of subgrade.

3. Dynamic testing with a heavy vibrator reveals ranges of strength far wider than would be expected from design and construction history.
4. The use of dynamic testing can limit shutdown time on a runway to 1 to 3 days (or nights) including time for destructive testing in boreholes depending on length, width, and variability of conditions.

Suitability of Stiffness Concept

The following comments apply primarily to DSM as measured by the WES 7257-kg (16-kip) vibrator and to the method of usage of the data on these projects, which were not research oriented.

Benefits and Advantages

1. The expression of strength by a single number is very attractive because it is derived from the overall pavement, base, and subgrade-in-depth system regardless of the thickness, compaction, and strength of the individual layers.
2. For a given set of design criteria (the FAA CBR versus thickness in this case), the DSM correlates reasonably well.
3. The potential ability to eliminate the cumbersome and questionably accurate material equivalency methodology will be a great asset.
4. Being able to perform several hundred tests per day and thereby obtain a significant number of tests in relatively small areas will assist the reliability of evaluation and design studies and will permit the detection and mapping of weaker areas.
5. The existing FAA procedures are applicable only to conventional rigid and flexible pavements, but current work by WES and correlations with destructive tests will enable analysis of stabilized base and composite pavements.

Disadvantages and Considerations for Improvement

1. The meaning of the DSM in more theoretical terms and in relation to actual aircraft loads and layered systems analyses is needed and has been under development by WES.
2. The shape of the deflection basin is not considered in the current FAA procedure but should be developed because work by others and by us indicates that it can be a significant factor.
3. Loading well into the straight-line portion of the load deflection graph may not be necessary, and the maximum dynamic load to be required should be defined as a function of the critical airplane gear load. This is important for the development of commercially available equipment and procedures.
4. The best frequency to use, or the need for frequency sweeps, should be firmly established. The variable frequency method is undergoing further investigation.
5. The current FAA data collection and analysis system does not permit determination of the thickness, condition, or strength of individual layers by nondestructive testing data alone. Further analysis of the curved portion of the load deflection plot and the deflection basins may be fruitful. Wave-velocity measurements are another approach. The significance of these determinations is in knowing where the controlling layers exist and being able to evaluate their effect on the pavement performance under future traffic. The ability to further minimize borings would also be helpful.

ACKNOWLEDGMENTS

We appreciate the cooperation of the Philadelphia Division of Aviation and their permission to use the data given here. Urban Engineers, Inc., of Philadelphia was the prime consultant.

The conclusions and opinions expressed are ours and do not necessarily represent those of our employers, the airport owners, or the project consultants.

REFERENCES

1. J. W. Hall. Nondestructive Testing of Pavements: Final Test Results and Evaluation Procedure. Air Force Weapons Laboratory, Technical Rept. AFWL-TR-72-151, June 1973.
2. J. L. Green and J. W. Hall. Nondestructive Vibratory Testing of Airport Pavements. Federal Aviation Administration, Vol. 1, Rept. FAA-RD-73-205-I, Sept. 1975.
3. J. W. Hall and D. R. Elsea. Small Aperture Testing for Airfield Pavement Evaluation. U.S. Army Engineer Waterways Experiment Station, Vicksburg, Miss., Miscellaneous Paper S-74-3, Feb. 1974.
4. Soil and Pavement Investigation for Improvements to Runway 9L-27R and Related Taxiways, Philadelphia International Airport. SITE Engineers, Inc., Sept. 18, 1974.
5. Use of Nondestructive Testing Devices in the Evaluation of Airport Pavements. Federal Aviation Administration, FAA Order 5370.7, Aug. 7, 1975.
6. Evaluation of Airfield Pavements Other than Army-Flexible Pavement Evaluation. Departments of the Army and the Air Force, Technical Manual 5-827-2 and Air Force Manual 88-24, Oct. 1968.
7. D. N. Brown and O. O. Thompson. Lateral Distribution of Aircraft Traffic. U.S. Army Engineer Waterways Experiment Station, Vicksburg, Miss., Miscellaneous Paper S-73-56, July 1973.
8. Manual MS-11. Asphalt Institute, College Park, Md.

Abridgment

Relationships Between Various Classes of Road Surface Roughness and Ratings of Riding Quality

Hugh J. Williamson, W. Ronald Hudson, and C. Dale Zinn, Center for Highway Research, University of Texas at Austin

This paper discusses the development of new methods for evaluating the riding quality of a road. Methods of this type are important because the ability to evaluate the present condition of a road is essential both for maintaining a system of high-quality roads now and for improving highway engineering practices in the future through research.

The new methods are based on evaluations of the quality of a road made by a panel using descriptors of different aspects of road roughness as predictor variables. Thus several predictive models are developed, each of which relates to a certain aspect of riding quality.

BACKGROUND

Serviceability

The present serviceability rating (PSR) introduced by Carey and Irick (1) is an evaluation of the present ability of a road to serve the public. The PSR is made by a panel of people and ranges from 0 (very poor) to 5 (very good).

Determining panel ratings, however, is very time-consuming. Another approach, which was introduced by Carey and Irick (1) and which has subsequently been taken by several other investigators (3, 4, 5), is to develop a regression model that can be used to predict PSR. The estimate of PSR so obtained is called the serviceability index (SI).

Roughness Measurement and Evaluation

A device such as the General Motors surface dynamics profilometer can be used to measure road surface elevation versus distance along the road in both the right and left wheel paths. Because of the large amount of data required to fully describe a road surface, most uses of the data require the calculation of a small set of characterizing measures of roughness.

In this study, the roughness was categorized on the basis of wavelength through digital filtering; four bands spanning the range from 1.219 to 30.48 m (4 to 100 ft) in wavelength were included. For each band, characterizing measures of both the most severe roughness and the average roughness of each road section were computed. The waves in both wheel paths were analyzed along with the surface profile elevation undulations of one wheel path relative to the other; the latter causes a vehicle rolling effect. The mathematical calculations are described explicitly elsewhere (6, 7).

RELATIONSHIP BETWEEN COMPONENTS OF ROUGHNESS AND PSR

An SI model provides a means for associating a riding quality index with a set of physical measurements and thus greatly facilitates interpretation of the measurements. Still, neither SI nor any other single number could reflect or characterize all of the important information in a measured road profile.

For this reason, a set of SI models was developed that can be used to transform the roughness measures corresponding to each wavelength band into a measure of riding quality that is directly related to PSR. This was achieved by regressing PSR on the roughness terms for each individual band. Then the model for 1.219 to 3.048-m (4 to 10-ft) wavelengths, for example, predicts whatever part of the variation in PSR is interpretable or explainable in terms of this class of roughness.

Separate models were developed for asphalt concrete (asphalt) and portland cement concrete (concrete) pavements. In addition to the roughness measures, the models also contain a dummy variable to account for any possible visual or auditory differences between types of pavements that may not be explainable in terms of roughness. The dummy variable was used to differentiate between continuous and jointed pavements in the concrete case and between surface-treated and hot-mix asphalt concrete pavements in the asphalt case.

The multiple correlations and other information about the models are given in Table 1. Space restrictions do

Publication of this paper sponsored by Committee on Pavement Condition Evaluation.

Table 1. Characteristics of the SI models.

Type of Pavement	Sample Size	Wavelength[a] (m)	Correlation With PSR	Standard Error	Number of Terms in Model[b]
Concrete	22	1.219 to 30.48 (overall)	0.91	0.32	6
		1.219 to 3.048	0.86	0.37	5
		3.048 to 7.620	0.85	0.38	4
		7.620 to 15.24	0.77	0.46	4
		15.24 to 30.48	0.75	0.46	3
Asphalt	50	1.219 to 30.48 (overall)	0.91	0.38	8
		1.219 to 3.048	0.86	0.45	6
		3.048 to 7.620	0.82	0.49	5
		7.620 to 15.24	0.81	0.52	6
		15.24 to 30.48	0.68	0.61	2

Note: 1 m = 3.28 ft.
[a]Type of roughness. [b]Including constant term.

not allow presentation of the models themselves here, but they are available elsewhere (7).

Stepwise regression, a method for choosing a subset of a collection of possible predictor variables, was used to develop the regression models (2). We note three points:

1. The multiple correlation of 0.91 for both overall models is very high, which indicates that there is a close relationship between roughness and PSR. This is consistent with other published results (1, 3, 4, 5).
2. For the models corresponding to the individual pass bands, the correlations decrease monotonically as wavelength increases. Although it is dangerous in general to assume automatically that a cause and effect relationship exists between two variables that are highly correlated, it seems reasonable in this case to infer from the correlations that the raters were more sensitive to short than to long waves. Further experimental work to assess the isolated effect of severe long waves caused by swelling clay would be valuable, however.
3. The correlation of 0.86 for both the concrete and asphalt models for 1.219 to 3.048-m (4 to 10-ft) wavelengths is almost as high as the 0.91 correlation for all roughness measures combined. This again suggests the close relationship between PSR and short waves.

Correlations among the roughness terms unquestionably cloud the relationships between PSR and individual types of roughness to some extent, but this problem would be difficult to eliminate.

TEST CASES

The SI models were applied to profiles measured on I-20 near Odessa, Texas, just before and just after a hot-mix overlay was performed. The overlay produced (a) an improvement of 1.12 in the overall SI value, (b) an improvement of 1.58 for 1.219 to 3.048-m (4 to 10-ft) wavelength roughness, and (c) steadily decreasing improvements [0.05 for 15.24 to 30.48-m (50 to 100-ft) wavelengths] for longer waves. The results are consistent with field observations, with effects seen in plots of the measured profiles, and with the nature of the roughness improvement that would be expected of any overlay performed with a 7.62-m (25-ft) skid.

This test case and others, along with the details of the model development, are discussed further elsewhere (7). Separate models for longitudinal and transverse roughness are also presented.

SUMMARY

This paper discusses the development and application of a set of riding quality indexes that characterize the road roughness with different ranges of wavelengths. The indexes are based on the relationship between road surface profile data and ratings made by a panel of riding quality and were derived through regression analysis.

ACKNOWLEDGMENTS

This study was carried out at the Center for Highway Research at the University of Texas at Austin. We wish to thank the sponsors, the Texas Department of Highways and Public Transportation and the Federal Highway Administration. The suggestions made by the Texas Department of Highways and Public Transportation contact representative, James L. Brown, have been very beneficial. The programming support provided by Randy Wallin and Jack O'Quin and the profile measurements made by Harold Dalrymple, Noel Wolf, and Leon Snider are also greatly appreciated.

The contents of this report reflect our views, and we are responsible for the facts and the accuracy of the data presented. The contents do not necessarily reflect the official views or policies of the Federal Highway Administration.

REFERENCES

1. W. N. Carey, Jr., and P. E. Irick. The Pavement Serviceability-Performance Concept. HRB, Bulletin 250, 1960, pp. 40-58.
2. N. Draper and H. Smith. Applied Regression Analysis. Wiley, New York, 1966.
3. L. F. Holbrook and J. R. Darlington. Analytical Problems Encountered in the Correlation of Subjective Response and Pavement Power Spectral Density Functions. HRB, Highway Research Record 471, 1973, pp. 83-90.
4. F. L. Roberts and W. R. Hudson. Pavement Serviceability Equations Using the Surface Dynamics Profilometer. Center for Highway Research, Univ. of Texas at Austin, Research Rept. 73-3, April 1970.
5. R. S. Walker and W. R. Hudson. Use of Profile Wave Amplitude Estimates for Pavement Serviceability Measures. HRB, Highway Research Record 471, 1973, pp. 110-117.
6. H. J. Williamson. Analysis of Road Profiles By Use of Digital Filtering. TRB, Transportation Research Record 584, 1976, pp. 37-54.
7. H. J. Williamson, W. R. Hudson, and C. D. Zinn. A Study of the Relationships Between Road-Surface Roughness and Human Ratings of Riding Quality. Center for Highway Research, Univ. of Texas at Austin, Research Rept. 156-5F, Aug. 1975.

A Comprehensive Pavement Evaluation System Applied to Continuously Reinforced Concrete Pavement

Eldon J. Yoder and Donald G. Shurig, Purdue University
Asif Faiz,* International Bank for Reconstruction and Development

This paper presents a comprehensive pavement evaluation system developed at the Joint Highway Research Project, Purdue University. In addition to the purpose of presenting the method, a secondary purpose is to demonstrate the use of the method as it was used to evaluate continuously reinforced concrete pavements (CRCPs) in Indiana. The evaluation system consists of a hierarchy of increasingly detailed pavement survey strategies—reconnaissance surveys, condition surveys, and evaluation surveys. The complete system, encompassing the three different types of surveys, permits an evaluation of maintenance priorities conveniently with the determination of the reasons for pavement deterioration. Although the demonstration of the evaluation system as applied to CRCP is incidental to the central theme of the paper, it contributes to the understanding of the comprehensive evaluation system. The paper presents a summary of the results obtained at the completion of each stage of CRCP evaluation. Some of the significant findings of the CRCP study and the resultant maintenance strategies are also included.

During the past several years, a great amount of research has been concentrated on methods of making condition surveys and on techniques for pavement rehabilitation. This is particularly important from the standpoint of the Interstate Highway System in the United States since, because of its age, there is a need to plan for its maintenance. Further, the states and counties have large investments in highways that are in need of maintenance.

The need for developing maintenance strategies has focused on development of methods for surveying and analyzing the condition of an existing pavement. These techniques have, by and large, centered on rapid methods of measuring pavement condition and have attempted to relate the condition of the pavement to the present serviceability index (PSI). Along parallel lines, but often not coordinated with condition survey methods, has been the development of techniques for optimizing design and maintenance of pavement systems.

The purpose of this paper is to present a comprehensive pavement evaluation system that was developed at the Joint Highway Research Project, Purdue University. Another purpose is to demonstrate the use of the method as it was used to evaluate continuously reinforced concrete pavements (CRCPs) in the state of Indiana.

SURVEY STRATEGIES

At the outset, various surveys that might be made must be defined. Each of the surveys has its use, and each has its limitation depending upon many factors. For purposes of this discussion, use will be made of terms relating to three basic types of surveys: reconnaissance surveys, condition surveys, and evaluation surveys.

Reconnaissance Surveys

Reconnaissance surveys are generally carried out on a routine basis by most highway departments. They consist of visual inspection and a qualitative judgment of the condition of pavements made by a qualified field engineer. Often, this type of survey is the only one required and conclusions can be derived from it.

Condition Surveys

Condition surveys, at a given time, are made to determine the condition of a pavement generally by use of roughometers, profilometers, and the like. This type of survey is not intended to evaluate the structural strength of the pavement, and generally no attempt is made to determine the reason for the pavement condition. Information from this type of survey can lead to the establishment of priorities and cost estimates for pavement rehabilitation.

Evaluation Surveys

The purpose of evaluation surveys is to determine the structural adequacy of the pavement and to determine causes for pavement defects that might be observed. These surveys are more comprehensive and include both laboratory and field tests; the resultant data can lead to evaluation of the pavement structure. Results

Publication of this paper sponsored by Committee on Pavement Condition Evaluation.

*Mr. Faiz was with Purdue University when this research was performed.

of evaluation surveys can be used for establishment of priorities and cost estimates, but, in addition, they permit recommendations relative to new designs and maintenance alternatives that might be considered.

SEQUENCE OF COMPREHENSIVE EVALUATION SYSTEM

The complete system encompasses all of the steps just defined and permits an evaluation of maintenance priorities concurrently with the determination of the reasons for pavement defects. Figure 1 shows the sequence that is followed in the comprehensive pavement evaluation system. This is a six-step process as outlined on the flow diagram. Each of the phases of the survey is self-explanatory.

The evaluation process can be stopped during any one of the phases depending on the needs of the highway department. For completeness, however, it is necessary to follow all of the phases sequentially.

The condition survey, as envisioned in Figure 1, has at its heart two principal steps. First, the data must be stratified on the basis of known conditions at the site. Second, the road sections falling under each combination of the strata are statistically sampled and only a predetermined number of randomly selected road sections are actually surveyed. Hence stratification of the data along with a statistical sampling procedure immediately dictates that a statistical analysis be made of the data.

In the condition survey analysis, the factors that significantly affect the observed condition of the pavement must be determined. Many of the factors listed in the stratification process can be shown to be statistically nonsignificant by appropriate tests and therefore may be dropped from further consideration. As indicated by the flow diagram, the significance tests can be bypassed if one wishes merely to obtain data that indicate the extent of pavement distress.

After the significant factors influencing performance are determined, it is possible to make an evaluation survey in which field tests are performed on statistically laid-out test sections and samples of pavement components are also obtained on a statistical basis. Appropriate field and laboratory tests can then be made on these samples and an evaluation made of the pavement as shown in phase V in Figure 1. The primary feature of the evaluation survey is, again, stratification and random sampling of pavement sections.

The process can be completed during any one of the phases listed on the flow diagram. The details of any given step depend on the results of the preceding phase. The decision whether to proceed through the comprehensive evaluation system is dependent on the needs of the particular situation.

ILLUSTRATION OF METHOD

Use of the method will be illustrated by means of a study made of CRCP in Indiana. The evaluation system, however, is equally applicable to other types of pavement. In 1972, a continuing study of the performance of CRCPs was initiated by the Joint Highway Research Project at Purdue University. The objective of the study was to evaluate and recommend design and construction techniques that would result in better performance of CRCPs. The evaluation of CRCP in Indiana followed the sequential steps outlined in Figure 1.

PHASE 1, RECONNAISSANCE SURVEY

Distress was noted on some sections of CRCP in Indiana as early as 1970. The development of distress reached alarming proportions at certain locations by 1972. It was at this time that the evaluation process was started.

A reconnaissance survey was conducted on a section of one road, I-65, and encompassed only the northbound lanes of the four-lane divided facility. The road at the location surveyed traverses glacial drift of Wisconsin Age and the subgrade is highly variable, ranging from sands and gravels to plastic clays. Subbase materials were largely nonstabilized gravels with some crushed stone and bitumen-stabilized gravel. A variety of construction and design variables were incorporated in the road with the result that several design and construction features affecting performance became immediately noticeable.

The results of the reconnaissance survey indicated, although not conclusively, that factors probably contributing to poor performance were (a) clay subgrades, (b) gravel subbases, (c) use of bar mats, and (d) slip-form paving. Because no definitive conclusions could be reached on the basis of the first survey, a statewide condition survey was subsequently planned. Note that these were tentative conclusions and that they were changed after further study.

PHASE 2, STATEWIDE CONDITION SURVEY

To arrive at definitive conclusions and to include a large range of construction and design variables, we set up the scope of the condition survey to include all CRCPs in Indiana. A sampling procedure was used to design the field survey, and statistical methods were used to analyze the resulting data.

Study Design

The intent of the study design was to ensure inclusion in the study of every CRCP contract that had been completed up to the time of the survey. A further purpose was to provide an inference space for the proposed analysis that would encompass all the factors under investigation.

Sampling Procedure

A stratified random sample of CRCPs was used in the field survey. Stratified random sampling is a plan by which the population under consideration (in this case, all the CRCP contracts in Indiana) is divided into strata or classes according to some principle significant to the projected analysis. This is followed by sampling within each class as if it were a separate universe. The aim in stratification is to break up the population into classes that are fundamentally different with respect to the average or level of some quality characteristics (3, pp. 213-214).

Only one simple random sample was obtained from each stratum or class. Such a sample or unit of evaluation was designated as a field survey section. Each field survey section was a 1524-m (5000-ft) length of pavement. The survey sections were stratified on the basis of the following factors: contract, method of paving, method of steel placement, method of steel fabrication, type of subbase, and type of subgrade. Data relative to these factors were obtained from construction records.

Statistical Design

A $2 \times 2 \times 3 \times 4 \times 2$ completely randomized factoral design with unequal subclass frequencies was used to study the factors influencing the performance of CRCPs. A

Figure 1. Sequential process of pavement evaluation.

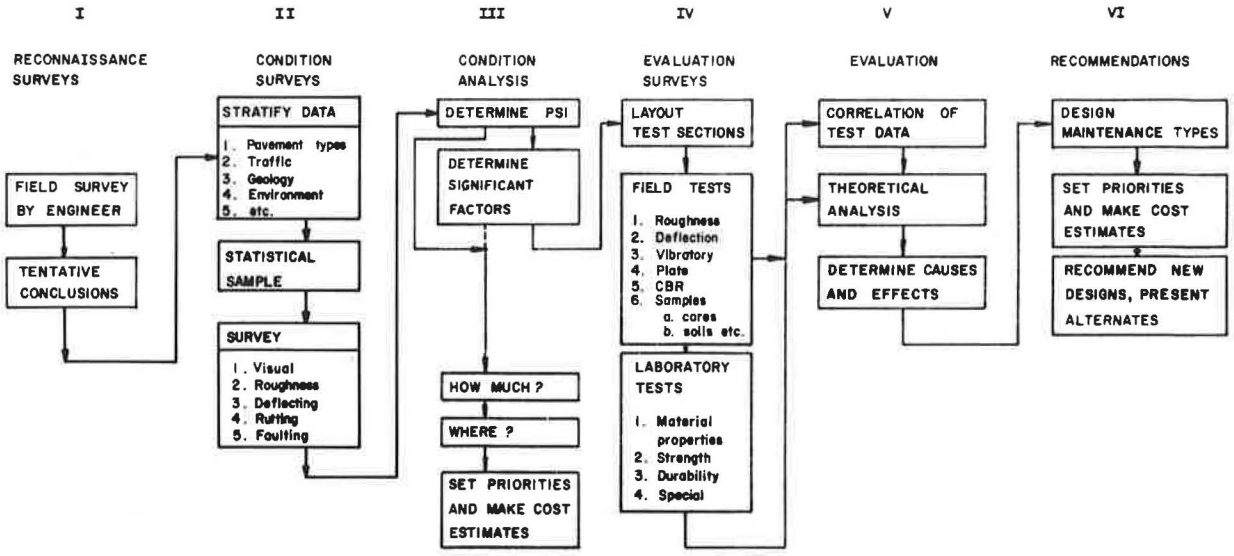

Figure 2. Factorial design for study of factors influencing CRCP performance.

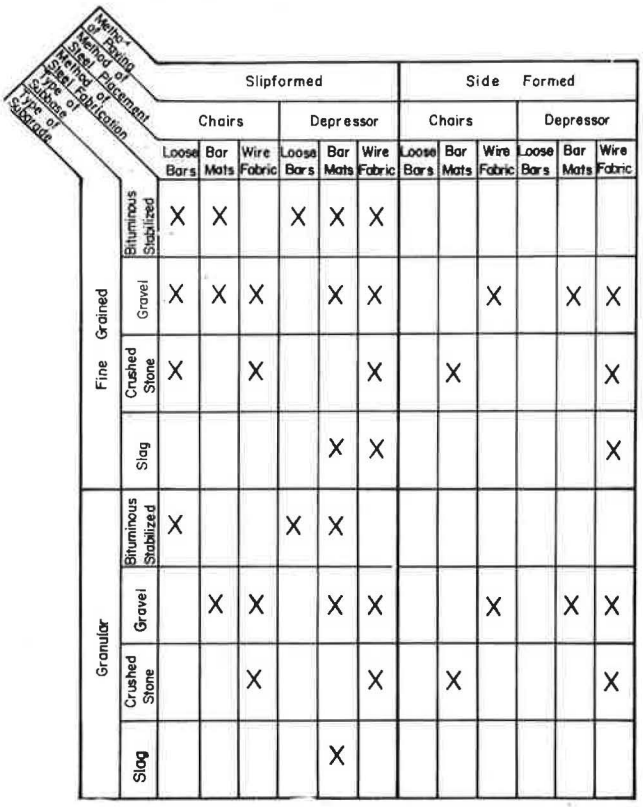

number of covariates or concomitant variables were superimposed on the factorial. The layout of the statistical design is shown in Figure 2, which also indicates the independent factors and their corresponding levels selected for this investigation.

Data Collection

The survey was conducted by five parties who were assigned survey sections at random. Subsequent statistical tests showed that no restriction on randomization had resulted from using five different survey parties.

PHASE 3, CONDITION ANALYSIS

The data obtained from the statewide CRCP condition survey were statistically analyzed by using a weighted least squares analysis of covariance procedure. The method of analysis and the supporting statistical package were the least squares maximum likelihood general purpose program of the Purdue University Computer Center.

Results From Statewide Condition Survey

The analysis of data collected during the statewide survey of CRCPs in Indiana revealed a number of significant results and correlations. The results of the statewide survey provided some definite indications relative to causes of distress in CRCPs.

With regard to just the extent of distress in the state, 69.7 percent of CRCP sections surveyed did not show any defects, 26.9 percent of the sections had from one to five defects, and 3.4 percent had more than five defects. This information was based on a stratified sample of 89 sections, each of which was 1524 m (5,000 ft) long and had equivalent two-lane or three-lane CRCP.

Gravel subbases showed the poorest performance; crushed stone and slag subbases showed good performance; and, at the time of the survey, bitumen-stabilized subbases showed little or no distress (since the condition survey, some structural failures have occurred on sections with bitumen-stabilized subbase). For most cases depressed steel performed better than preset steel on chairs. Better performance was indicated when loose bars were used compared to when bar mats and wire fabric were used. Pavements that were slipformed performed the same as did those that were side-formed. Relative to good performance, the optimum slump range was between 5.1 and 6.3 cm (2.0 to 2.5 in); slump values of 3.8 cm (1.5 in) and greater generally showed good results. Distress in CRCPs was found to be linked with traffic intensity. Subgrade parent material (granular or fine grained) was not a significant performance factor.

Summary Statement of Condition Survey

The conclusions reached from the results of the condition survey were valid from the standpoint of identifying significant factors that influenced performance of CRCP. The conclusions differed in some respects from those reached in the first survey. The data also showed the extent of distress of the pavements on a statewide basis. One could infer reasons for suspect performance on a comparative basis (for example, gravel subbases versus stone subbases or use of chairs versus depressed steel), but one could not determine them with certainty. Hence an evaluation survey was set up to delineate possible causes and effects for the relative performance.

PHASE 4, DETAILED EVALUATION SURVEY

With respect to the broad framework of the study, the detailed field investigation followed by a laboratory testing program constituted the fourth phase of the research. These two steps (field and laboratory tests) of the research are presented together because the results obtained from the two parts must be analyzed together. A primary purpose of phase 4 was to determine the effect of pavement materials on performance.

Study Design

The design of the detailed evaluation study was based on the results of the statewide condition survey. The factors that were found to be statistically significant in the condition survey were incorporated in the stratification criterion for sampling the test sections for the field study. The stratification scheme consisted of the following factors: method of paving (slip-formed, side-formed); method of steel placement (depressed steel, steel preset on chairs); type of steel reinforcement (wire fabric, bar mats, loose bars); and type of subbase (gravel, slag, crushed stone, bitumen stabilized).

A total of 31 test sections with the same thickness [23 cm (9 in)] and percentage of steel reinforcement (0.6 percent) were included in the field investigation. These CRCP sections are part of the Interstate Highway System in Indiana. Each test section was 300 m (1000 ft) in length.

Collection of Field Data

The typical layout and the data collected at each test section are shown in Figure 3.

The battery of tests performed at a test section consisted of

1. Deflection measurements,
2. Crack width measurements,
3. Crack interval measurements,
4. Subgrade and subbase evaluation, and
5. Concrete core testing.

Dynaflect (4) was used to obtain deflection measurements at 30-m (100-ft) intervals along the centerline of the traffic lane. In addition, at each test location, deflection measurements were obtained transversely at 0.3 m (1.0 ft), 1.07 m (3.5 ft), and 1.83 m (6.0 ft) from the pavement edge. At any point, deflection measurements were taken at both a crack position and an adjacent midspan position between two transverse cracks.

Crack width measurements were made at each test location by means of a 50x, direct-measuring pocket microscope.

Crack interval measurements were made along the pavement edge over a 30-m (100-ft) section centered on a test location. The number of crack intersections was also counted over the 30-m (100-ft) length.

In-place penetration tests were made on subbase and subgrade by means of the high load penetrometer (2, pp. 1-16) and the dynamic cone penetrometer (5) respectively. These tests were performed at both core-hole and shoulder positions at each of the two test locations. The two methods of penetration tests are shown in Figure 4. In addition to the penetration tests, in-place density and water content determinations were made on the subbase and the subgrade. At the completion of a series of tests on the subbase or subgrade, material was sampled from under the edge of the pavement slab for laboratory testing.

Concrete cores were taken at each test location from the traffic lane close to the point from which other pavement materials were sampled.

Laboratory Testing Program

Concrete cores, as obtained from the field, were tested for specific gravity, water absorption, bulk density, and pulse velocity. Next the cores were cut, and segments without any steel from above and below the level of reinforcement were subjected to specific gravity, water absorption, pulse velocity, bulk density, and splitting tensile strength tests.

The series of tests on subgrade soil and granular subbase samples included standard classification and compaction tests. Permeability tests, which used a constant head permeameter, were made on selected samples of slag, crushed stone, and gravel subbases. For bitumen-stabilized materials, grain-size distribution and asphalt content were determined.

PHASE 5, EVALUATION

Approach to Data Analysis

The characteristics of the design of the field study offered two dichotomies that could be profitably used in data analysis:

1. Comparison of failed test locations with good test locations within test sections showing significant distress and
2. Comparison of test sections showing distress (with failures as indicated by a breakup or a patch) with test sections in good condition and showing no apparent distress (without failures).

The primary aim of this comparative analysis was to identify material properties and performance characteristics that are indicators of potential distress in CRCP. Only data from structurally sound locations were included in the study. The objective of using such data was to isolate inherent deficiencies in the pavement structure even where no superficial evidence of distress was present.

Analysis of Data

The number of test sections in each of the without-failure and with-failure categories were 15 and 16 respectively. Differences between the two categories with respect to material properties and performance characteristics were tested by the t-test. In other cases, in which a factorial arrangement was used, data were analyzed within the framework of a nested factorial design (1). An equal number of randomly selected test sections were nested within each of the pavement condition categories.

Comparison of Types of Subbases

The data given in Table 1 describe the variation of subbase California bearing ratio (CBR), permeability, and degree of compaction with type of subbase. Although no clear differences in the properties of the gravel subbases were evident between sections with failures and sections showing no apparent distress, gravel subbases at structurally sound test locations were found to have a moderately high permeability but showed poor stability characteristics, probably a function of insufficient compaction. Crushed stone subbase at the section without failures was found to possess a high strength (CBR of 90 percent) and excellent internal drainage (over 0.71 cm/s or 2000 ft/day). The failure on another section with a crushed stone subbase was a function of poor stability (very low CBR), resulting from inadequate compaction. The good condition of pavements on slag subbases, despite relatively poor water transmission characteristics of this type of subbase, was probably due to its very high stability (CBR of more than 100 percent).

Figure 3. Typical layout of test sections.

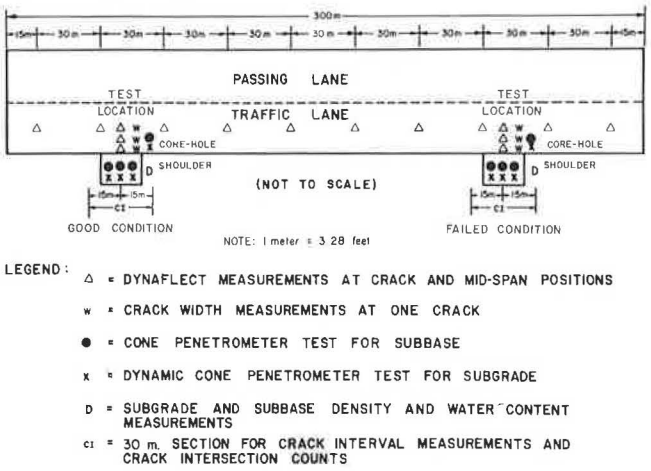

Interaction of Permeability and Strength

It is worthwhile to note that concrete pavement performance is also a function of the interaction between subbase permeability and strength (CBR). In Figure 5, estimated field permeability values from 46 test locations of the detailed field study are plotted against field subbase CBR values measured at the shoulder-slab interface. Test data for crushed stone and slag subbases are shown with separate indicators. In addition, values obtained at failed test locations are differentiated from the values at good test locations. The data were grouped

Figure 4. Two methods of rapid CBR tests.

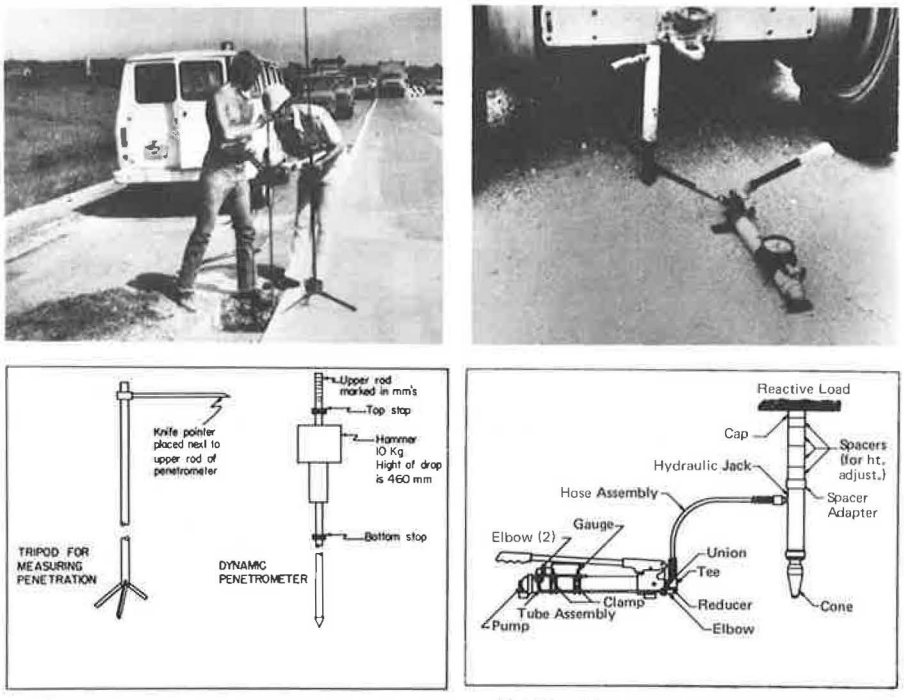

(a) DYNAMIC CONE (FINE GRAINED SOILS)

(b) HIGH LOAD CONE (GRANULAR SOIL)

Table 1. Effect of type of subbase on pavement condition.

Type of Subbase	Condition of Test Sections	Number of Test Sections	Subbase CBR (%)		Permeability (cm/s)	Compaction (%)
			Shoulder	Core		
Gravel	With failures	13	33.5	38.0	0.345[a]	91.5[a]
	Without failures	10	35.9	45.2	0.247[b]	93.2[b]
Slag	With failures	1	95.0	100.0	0.01	117.2
	Without failures	3	81.0	96.6	0.05	100.6
Crushed stone	With failures	1	32.0	41.0	0.483	89.9
	Without failures	1	90.0	59.0	0.880	85.3

Notes: 1 cm/s = 2835 ft/day.
Data are from structurally sound test sections.
[a]Average of values from nine test sections. [b]Average of values from ten test sections.

in nine categories corresponding to three levels each of subbase CBR and permeability. For low subbase strength (CBR less than 40 percent) in mainly gravel subbases, the percentage of failed test locations decreased from 53 percent in the low permeability group to 25 percent in the high permeability group. For medium subbase strength (CBR between 40 and 80 percent), no failures were observed where permeability was high. Where subbase strength was high (CBR greater than 80 percent, applicable only to slag and crushed stone subbases) no failures were indicated irrespective of permeability.

Deflection as Predictor of Performance

The major interest in the analysis of deflection measurements, taken over the total extent of each test section at

Figure 5. Effect of subbase strength and permeability on CRCP performance.

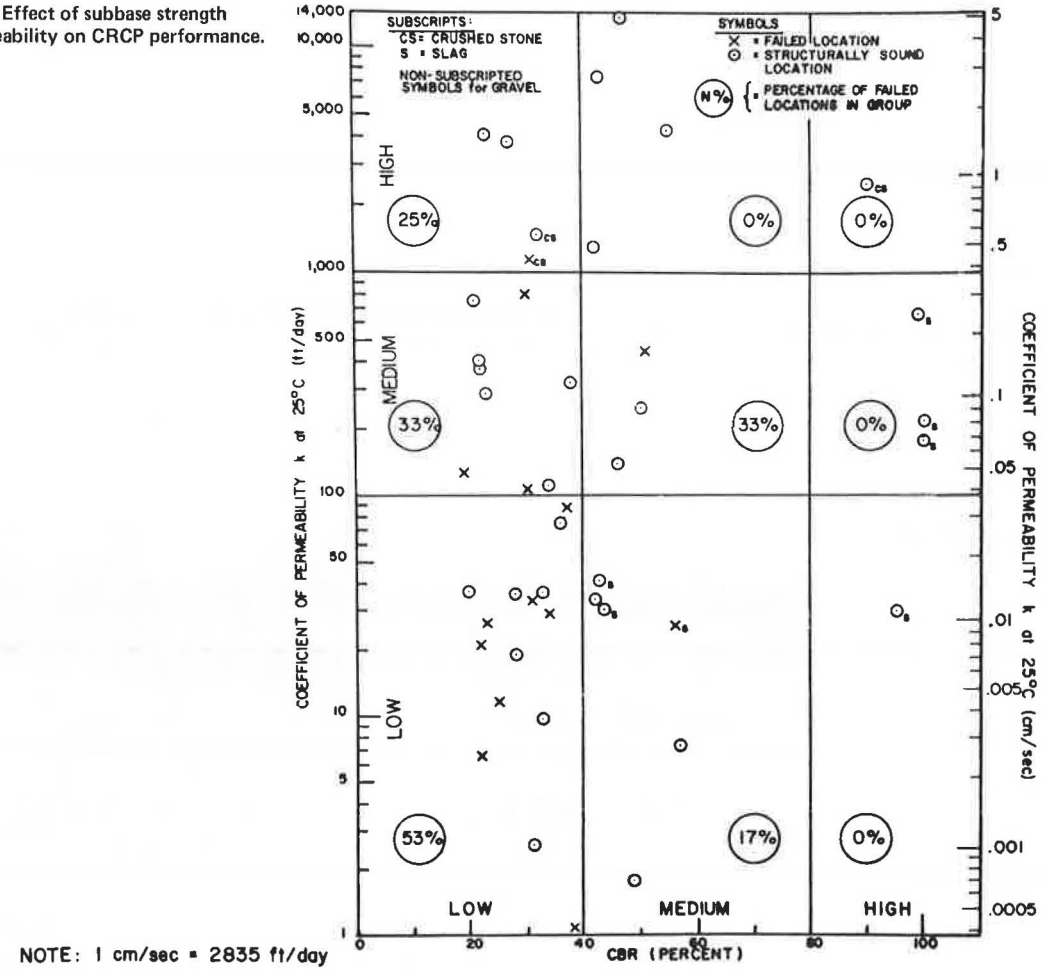

NOTE: 1 cm/sec = 2835 ft/day

Figure 6. Rating of test sections.

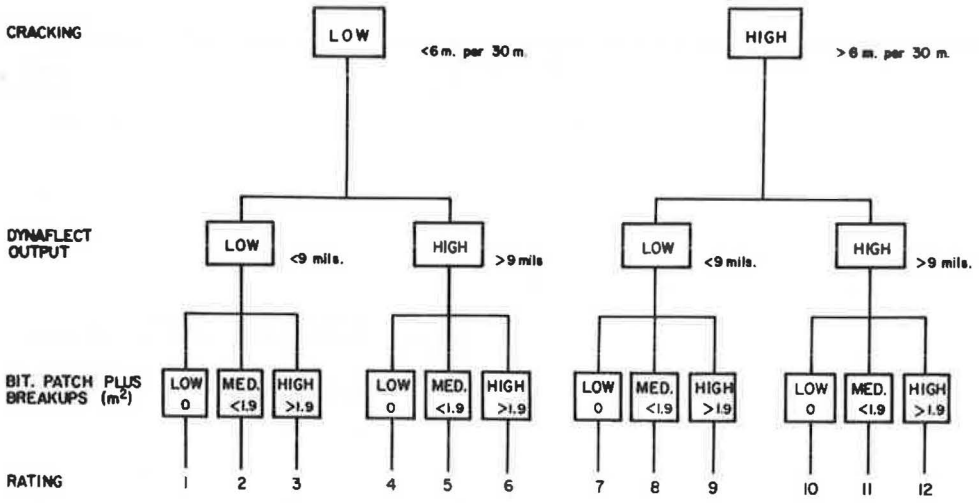

NOTE: 1 meter = 3.28 feet

Table 2. Possible maintenance.

Rating Number	Total Number of Sections Involved	Maintenance Type	Maintenance Number of Sections Involved
1	7	None	7
2	10	None	5
		Patch	5
3	2	None	1
		Patch	1
4	5	None	1
		Underseal and overlay	2
		Underseal	0
		Overlay	1
		Concrete shoulders	1
		Drain	0
5	11	None	1
		Patch, underseal, and overlay	4
		Patch and underseal	1
		Patch and overlay	1
		Patch and concrete shoulders	0
		Patch and drain	3
		Patch, drain, and concrete shoulders	1
6	3	None	½
		Patch, underseal, and overlay	½
		Patch and underseal	1
		Patch and overlay	0
		Patch and concrete shoulders	0
		Patch and drain	1
7	3	None	1
		Drain	1
		Overlay	1
8	5	None	1
		Patch and overlay	1
		Patch and concrete shoulders	1
		Patch and drain	2
		Patch	0
9	7	None	2
		Patch and overlay	2
		Patch and concrete shoulders	2
		Patch and drain	1
		Patch	0
10	2	None	½
		Underseal and overlay	½
		Concrete shoulders	1
		Drain	0
11	0	None	0
		Patch, underseal, and overlay	0
		Patch and drain	0
		Patch and concrete shoulders	0
		Full-depth bitumen	0
12	5	None	1
		Patch, underseal, and overlay	0
		Patch and drain	1
		Patch and concrete shoulders	½
		Full-depth bitumen	1
		Patch, underseal, overlay, drain, and concrete shoulders	1
		Patch, drain, and concrete shoulders	½

Note: This list of possible maintenance is considered a "shopping list" of various procedures. These were greatly reduced in number based on length of sections and the like.

30-m (100-ft) intervals, was to determine whether pavement condition, as indicated by the presence or absence of failures, could be differentiated by such sectionwide measurements.

Deflection profiles were developed for sections that were in excellent condition, those showing signs of distress, and those that, according to crack patterns and the like, indicated potential failures.

As a rule, pavement sections showing signs of potential distress had higher deflections than those that had already failed. Therefore, it was concluded that pavement deflections, if used judiciously, are a good indicator of potential distress. After the continuous slab breaks up into discrete segments, the usefulness of deflection measurements is impaired.

Using measurements taken at 1.8 m (6 ft) from the pavement edge for 23-cm (9-in) CRCP, Dynaflect readings of less than 0.012 mm (0.5 mil) are indicators of good pavement condition. Values in the range of 0.015 to 0.022 mm (0.6 to 0.9 mil) spell a potential distress condition; values above 0.025 mm (1.0 mil) are indicators of severe distress with a high probability of pavement breakups.

PHASE 6, DESIGN OF MAINTENANCE STRATEGIES

The evaluation of significant factors relating to performance of CRCP led to recommendations for altering future CRCP designs. These recommendations are not included here. As a part of these recommendations, however, it became obvious that there was a need to recommend maintenance strategies that might be adopted.

Data relative to the most economical maintenance were meager; as a result, a field experiment was established to evaluate this factor. This field experiment was evolved on the basis of known factors that have significantly influenced performance of CRCP in Indiana (poor drainage condition, high deflections, and the like).

The end point of the research could only be accomplished by dividing a section of highway into smaller units with similar characteristics. A pavement section of I-65 7.4 km (4.6 miles) in each direction was selected as the test pavement because it contains all of the significant features identified as major contributors to performance of CRCP. It has a gravel subbase and bar mats on chairs. This pavement has shown, as predicted, very poor performance.

Objective of Research

The types of maintenance considered were determined on the basis of results of the evaluation. Therefore, the types of maintenance considered were directed at three principal factors:

1. Improvement of drainage of subbase,
2. Methods of reducing pavement deflection, and
3. Methods of patching failed areas.

Initial Tests

Deflection readings were taken in the fall of 1974 with Dynaflect at 7.6-m (25-ft) intervals over the study area. At the same time, a condition survey of the pavement was made noting the locations of breakups, patches, intersecting cracks, and combination cracks.

Method of Selecting Study Sections

Using the data derived from the above tests, we chose three factors as indicative of the overall condition of the pavement. These were (a) linear meters of cracks spaced less than 76 cm (30 in) plus linear meters of intersecting

cracks per 30-m (100-ft) section, (b) total area of patching or breakups per section, and (c) maximum deflection per 30-m (100-ft) section.

By using this technique, we then stratified the pavement sections and assigned rating numbers of 1 to 12 as shown in Figure 6.

Selection of Maintenance Methods

An attempt was made to apply as many types of appropriate maintenance as possible to the various ratings. Table 2 gives the types of maintenance that were considered appropriate for the given rating numbers. Input into this selection was provided by Federal Highway Administration, Indiana Highway Commission, and Purdue University personnel.

Layout of Study Sections

The layout of study sections for a given type of maintenance was governed by four criteria.

1. A section of one type of maintenance was made as long as possible.
2. At least one no-maintenance control section for each of the rating numbers, 1 to 12, was retained.
3. As many different types of maintenance methods as possible were used for each rating number.
4. The maintenance to be used was allocated first to the rating categories having the fewest actual sections with that rating. (Note that this criterion is a means for attaining the first three criteria.)

SUMMARY

In this paper a comprehensive system for pavement condition evaluation has been outlined. It has been the primary purpose to present principles that can be used for a variety of pavements. The method has been illustrated by using an evaluation of continuously reinforced concrete pavements. The techniques, however, are not unique to this type of pavement but have application to all types of pavements under a variety of traffic and environmental conditions.

The heart of the method lies in stratification of the known factors surrounding the pavement and, along with this, a statistical analysis of the data. The sequential series of events must be followed although the process can be concluded at any of the several stages depending on the needs of the engineer.

REFERENCES

1. V. L. Anderson and R. A. McLean. Design of Experiments—A Realistic Approach. Marcel Dekker, Inc., New York, 1974, 418 pp.
2. High Load Penetrometer Soil Strength Tester. Commercial Airplane Division, Boeing Co., Renton, Wash., Document D6-24555, 1971.
3. W. E. Deming. Some Theory of Sampling. Dover Publications, New York, 1950.
4. F. H. Scrivner, R. Peohl, W. M. Moore, and M. B. Phillips. Detecting Seasonal Changes in Load-Carrying Capabilities of Flexible Pavements. NCHRP, Rept. 76, 1969, 37 pp.
5. D. J. Van Vuuren. Rapid Determination of CBR With the Portable Dynamic Cone Penetrometer. Rhodesian Engineer, Paper 105, 1969.

Development of a Pavement Management System

R. Kulkarni and F. N. Finn, Western Region, Woodward-Clyde Consultants
R. LeClerc and H. Sandahl, Washington State Department of Highways

The objective of this paper is to describe an investigation by the Washington State Department of Highways to determine the feasibility of developing a pavement management system. A pavement management system, as envisioned by this investigation, should provide systematic and reasonably objective information regarding the optimum economic maintenance strategy on a project-by-project basis. The system is concerned primarily with the development of a performance prediction model and a cost model, both to be based on the data bank of information that has been collected by Washington during the past 6 to 8 years. This paper describes two approaches to the performance model: a regression equation and a probability transition matrix. Efforts to develop a prediction model by regression techniques were unsuccessful. The transition matrix appears promising and relatively simple. General procedures for development and use of this model are given in the paper. A cost model is developed that includes considerations of routine maintenance costs, construction costs, interest, inflation, and excess user costs. The pavement management system framework as developed provides an objective procedure for comparing the performance and cost models of several maintenance strategies and selecting the strategy that will be the most economical for any designated time period.

The investigation described here was implemented in an effort to determine the feasibility of developing a pavement management system for the Washington State Department of Highways. The basic objective of a pavement management system is to develop a systematic procedure that would predict the most economical maintenance strategy for a particular pavement within Washington's network of highways. In effect, the system should provide information on what maintenance to perform and when such maintenance should be started. Thus the system would maximize the effective use of money to be programmed for maintenance on any specific project. In analyzing maintenance strategies, the management system was expected to give specific consideration to the economic advantages of preventive maintenance (generally applied before pavement deteriorates to some unsatisfactory state) over corrective maintenance (generally applied after pavement has deteriorated to an unsatisfactory state).

Publication of this paper sponsored by Committee on Theory of Pavement Design.

RESEARCH OBJECTIVES

The pavement management system considered by this investigation contains four basic features: (a) ability to predict performance; (b) ability to compute costs for various maintenance strategies; (c) ability to be adaptive (dynamic), that is ability to respond to uncertainties associated with actual performance as compared to predicted performance; and (d) ability to make internal changes (system updating) with regard to features a, b, and c.

Performance Model

The purpose of the performance model is to predict the future condition of a given roadway (pavement). Such a prediction is necessary to estimate when major maintenance would be required, predict performance after major maintenance is completed, and relate user costs to pavement performance.

Two specific performance models were studied—the regression model and the Markov chain model. The latter was selected as the most reasonable procedure at this time. The details of the Markov chain model will be given.

Cost Model

The cost items included in the model are:

1. Routine maintenance,
2. Cost of preparation associated with major maintenance,
3. Cost of major maintenance,
4. Cost of shoulder improvements,
5. Interest and inflation,
6. Salvage value,
7. Excess user costs associated with major maintenance, and
8. Excess user costs associated with traffic slowdown due to pavement deterioration.

In determining economic cost of a maintenance strategy, we discounted all the future costs to their present

worth at a specified time by using an appropriate interest rate.

Adaptive Characteristics

The management system is based on the ability to predict future performance of pavements on a kilometer-by-kilometer basis. The prediction model provides an estimate of the expected performance value of the pavement at some future time. It has been recognized that specific kilometer-by-kilometer sections may not perform as predicted. Parts of this variation can be attributed to errors in field evaluation; unusual circumstances (severe climate, construction variations, or change in traffic pattern); and unexplained factors that influence performance. Thus the management system must be adaptive or responsive to deviations from predicted values.

System Updating

One of the requirements of the management system is the need for it to be updated, which allows for changes in the performance model associated with factors such as new construction methods, new design practices, or new legal load limits. In general, the scheme adopted for system updating would result in the accumulation of field data for approximately 6 years in the data bank. As more information is obtained from the field, the older data would be eliminated in determining parameters of the performance model.

RESEARCH APPROACH

The procedure for implementation of this investigation was as follows:

1. Determine the desired goals for a management system by discussion with the personnel of the Washington Department of Highways;
2. Discuss with department personnel current operating procedures for materials, design, construction, and maintenance;
3. Review with department personnel specific data potentially available for use in management system;
4. Combine information from items 1, 2, and 3 into a hypothetical system and illustrate the operational characteristics with hypothetical data;
5. By using sample information provided by the department, generate performance and cost models; and
6. Develop computer programs to (a) determine the maintenance strategy that will result in the minimum total expected cost, (b) predict the expected value of pavement condition and standard error of the performance prediction, and (c) calculate the budget requirements for each 2-year period for the selected maintenance strategy.

SCOPE

Because of space limitations, implementation of all the steps presented in the research approach cannot be described in this paper. Details on all aspects of the investigation are available elsewhere (1).

This paper emphasizes a summary of the completed investigation. Details of the performance model and the cost model are given, and the operational logic of the search method employed in determining optimum maintenance strategy for a given pavement section is discussed. The adaptive characteristics of the system, the scheme of updating information, and details of the computer programs are not discussed.

PERFORMANCE MODEL

Two specific performance models were studied—the multiple regression model and Markov chain model. In both models, the pavement condition was described by a pavement rating number R_R between 0 and 100. The R_R used by the Washington Department of Highways combines objective measurement of pavement roughness G_R and the subjective measurement of physical distress G_D into a single number. Pavement condition surveys are made every 2 years over the entire state system, and data are currently available on most pavements since 1968. Details regarding computation of R_R can be found elsewhere (2).

Multiple Regression Model

The multiple regression approach has the potential of individualizing pavement performance on a kilometer-by-kilometer basis depending on those physical factors known to engineers to influence significantly the performance of a pavement. The pertinent factors for regression analysis, chosen in consultation with the department personnel, are given in Table 1.

The results of the regression analysis were considered to be unacceptable for use as a prediction model. The multiple correlation coefficients were 0.718 for rigid pavements and 0.846 for flexible pavements. The standard error of estimate for R_R was approximately 7 for rigid pavements and 11 for flexible pavements. An analysis of variance indicated that time was the only factor that affected average R_R significantly. For rigid pavements, the partial regression coefficient for time was 2.9 with a standard error of ±0.4. Thus, annual change in R_R could be estimated to range between 1.7 and 4.1 (± three times the standard error) with the expected value being 2.9. For flexible pavements, the partial regression coefficient was 4.6 with a standard error of ±0.7. The annual change in R_R for these pavements could range from 2.5 to 6.7. These average rates of change in R_R were significantly higher than those currently being estimated by the department.

Markov Chain Model

The Markov chain model uses a one-step probability transition matrix in predicting future pavement conditions. The theoretical background of this approach can be found in probability textbooks (3, 4).

The essential requirement needed to develop a prediction model is the probability transition matrix such as that shown in Figure 1 for maintenance alternative 1 for asphalt pavement. For this matrix, reducing the pavement rating from discrete values to condition states as defined by intervals of R_R was found to be convenient. The interval selected was 10 points on the R_R scale. This interval was selected based on the general confidence interval believed to be associated with the field determination of the pavement rating. Thus in Figure 1 a condition state of 7 indicates an R_R value between 70 and 79.

The tabulation summarizes the field data for any 2-year period for which field observations were made on a series of roadway sections. For example, for a particular section, the condition of a particular roadway has changed from a condition state of 6 to a condition state of 5. By combining data from all pavement sections within a particular district, one can obtain a distribution of the probable transitions or a probability transition matrix for that type of pavement in that district.

Again, in Figure 1, the numerical values indicate the probability associated with each transition. For example, the data used to develop this matrix have indicated that, when a pavement is in condition state 7, there is a 5

Table 1. Factors included in regression analysis to predict pavement conditions.

Type of Pavement	Factors for Regression Analysis
Rigid and flexible	R_R values for four condition surveys Average daily truck traffic Thickness of treated layers Thickness of untreated layers Resistance value of subgrade materials Time in years Number of days below 0°C
Rigid	Average modulus of rupture for PCC Range in modulus of rupture for PCC
Flexible	Average void content in asphalt concrete Range in void content in asphalt concrete

Note: 1°C = (1°F - 32)/1.8.

Figure 1. Probability transition matrix for alternative 1.

FROM CONDITION STATE	TO CONDITION STATE 9 (100-90)	8 (89-80)	7 (79-70)	6 (69-60)	5 (59-50)	4 (49-40)	3 (39-30)	2 (29-20)	1 (19-10)
9 (90-100)	0.90	0.10							
8 (80-89)	0.05	0.65	0.30						
7 (70-79)		0.05	0.60	0.25	0.10				
6 (60-69)			0.05	0.45	0.25	0.20	0.05		
5 (50-59)				0.05	0.25	0.40	0.30		
4 (40-49)					0.05	0.20	0.75		
3 (30-39)						0.05	0.65	0.30	
2 (20-29)							0.10	0.80	0.10
1 (10-19)								0.05	0.95

Figure 2. Performance prediction obtained from probability transition matrix.

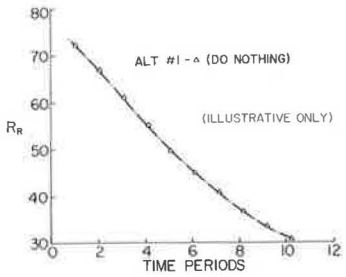

Figure 3. Performance trends for various maintenance alternatives.

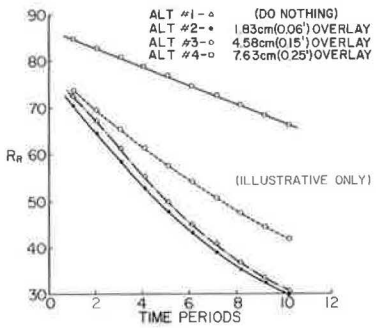

Figure 4. Constraint for mandatory action.

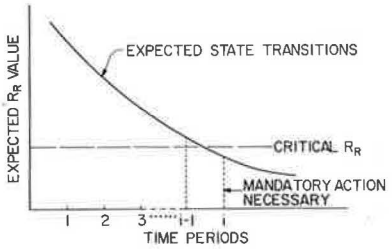

Figure 5. Subset of feasible maintenance strategies.

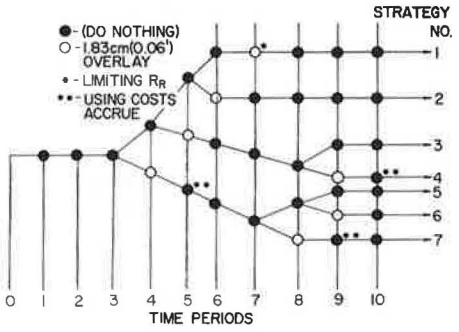

percent chance that it will be in condition state 8 after 2 years, a 60 percent chance that it will remain in state 7, a 25 percent chance that it will be in state 6, and a 10 percent chance that it will be in state 5. The matrix indicates there is no chance of being in those states for which no value is indicated.

From the probability transition matrix and initial condition of a pavement, one can find the expected R_R value of the pavement at any future time. The mathematics involved in this procedure can be found elsewhere (1). Figure 2 shows the expected performance trend for the information contained in Figure 1. This model is associated with the performance of the original construction aided only by routine maintenance. The continuation of routine maintenance is a valid maintenance strategy and is referred to here as the do nothing alternative.

From Figure 2 the performance trend line is observed to be curvilinear. The annual drop in R_R is approximately 3 points until the pavement reaches a value of 40 when the rate of change drops to 2 points/year. These rates are in keeping with the experience of department personnel.

For the pavement management system to function properly, three general types of transition matrices had to be developed for (a) performance after original construction, (b) condition immediately after major maintenance (initial state vector), and (c) performance after each alternative major maintenance.

For purposes of the feasibility study, matrices such as that shown in Figure 1 were developed in consultation with department personnel. Initial state vectors that specify pavement condition immediately after an overlay were also estimated. The performance trends for the various maintenance alternatives based on these matrices are shown in Figure 3. Alternative 1 in this figure represents the performance trend of the original construction with routine maintenance.

COST MODEL

A detailed economic analysis of road maintenance for use in the maintenance system can be found elsewhere (1). In this section, a brief summary of the elements of the analysis is provided.

Two kinds of costs are considered in the analysis: costs to the highway department and costs to the user. Costs to the highway department can be classified as direct and indirect. Direct costs (cash flow) would be those associated with the actual cost for personnel, materials, and equipment required to accomplish maintenance, including provision for inflation. Indirect costs would be those associated with interest. Excess user costs are those incurred by the user because of time delays resulting either from construction or from the condition of a particular roadway (5).

User costs have a significant effect on the selection

of an optimum maintenance strategy. The only incentive for keeping pavements in smooth condition is the reduction in user costs. If these costs are neglected, the optimum maintenance strategy would almost always be to do nothing until the pavement reaches a totally unsatisfactory condition. Every effort should be made to obtain reasonable numbers for the user costs. In the initial implementation, the numbers suggested by Finn, Kulkarni, and Nair (1) may be used.

DETERMINATION OF OPTIMUM MAINTENANCE STRATEGY

The objective of the pavement management system is to provide information useful to the decision maker in the selection of the optimum maintenance strategy for a given pavement section. A maintenance strategy, as defined here, consists of two components: type of maintenance alternative to be adopted (such as type of overlay) and timing of that maintenance alternative.

The procedure used in determining the optimum maintenance strategy consists of the following steps:

1. Selection of a set of feasible maintenance strategies,
2. Prediction of pavement condition under each feasible maintenance strategy within the analysis period, and
3. Calculation of total expected cost of each feasible maintenance strategy.

Selection of a Set of Feasible Maintenance Strategies

To make the management system compatible with the current operating procedures of the state, the constraint of a mandatory action at a preselected critical R_R value is adopted. Thus, if at any time period the R_R value of a given pavement is expected to fall below the specified critical R_R value, it is assumed that one of the given maintenance alternatives will be adopted (Figure 4). Each time period in the analysis consists of 2 years.

Within the constraint of minimum R_R, a number of maintenance strategies can be obtained. In theory, one should consider all the given maintenance alternatives at each time period in the analysis. With only a few maintenance alternatives and a relatively short analysis period, the total possible maintenance strategies following this scheme become very large. Fortunately, from the optimization viewpoint, several of these possible strategies can be discarded as being very remote from the potential region of optimum solution. The set of the possible maintenance strategies can therefore be reduced to a much smaller set of feasible maintenance strategies.

The implementation of the search for feasible maintenance strategies can be best explained by an example. In the following discussion, K_1 denotes the time period since the start of the analysis at which the first overlay is scheduled and K_2 denotes the time period since K_1 at which a second overlay is scheduled.

Consider the following example in which, for the sake of illustration, only two maintenance alternatives are studied: (a) alternative 1, the do nothing alternative (normal rate of deterioration with routine maintenance), and (b) alternative 2, in which an overlay of 1.83 cm (0.06 ft) is used. In the example the following values apply:

Item	Value
Initial R_R value of the pavement	75
Critical R_R value (RCRI)	40
Level at which user costs start occurring (UCLEVEL)	50
Analysis period, time periods of 2 years each	10

Let the prediction of the expected R_R values of the pavement be as follows:

	Expected R_R Value			Expected R_R Value	
Time Period	Alternative 1	Alternative 2	Time Period	Alternative 1	Alternative 2
1	71	68	6	42	41
2	67	64	7	39	38
3	62	60	8	32	33
4	55	53	9	27	27
5	49	44	10	22	23

Three considerations are used in the selection of feasible maintenance strategies.

1. A mandatory action is necessary at time period 7 after the start of the analysis if alternative 1 is adopted throughout.
2. At time period 5, the expected R_R goes below 50, the level at which user costs start occurring; to avoid user costs, an overlay at time period 4 should be considered.
3. If an overlay of 1.83 cm (0.06 ft) is scheduled, mandatory maintenance becomes necessary again at time period 7 following the overlay.

With this information, values of 7, 6, 5, and 4 are successively chosen for K_1. Values higher than 7 cannot be considered because of the constraint of mandatory action; values lower than 4 are not considered because such values would only increase construction costs and not significantly reduce user costs.

Next, consider the selection of K_2 values for this example. Suppose that K_1 is 7; 3 time periods still remain within the analysis period of 10. The expected R_R values for these 3 time periods are 68, 64, and 60. Because the last value is greater than both RCRI and UCLEVEL, a second overlay is not scheduled and K_2 is set to zero. On the other hand, if K_1 is 4, the expected R_R values for the remaining 6 time periods are 68, 64, 60, 53, 44, and 41. Because the expected R_R goes below 50 at time period 5, a second overlay at time period 4 is considered and K_2 is set to 4.

All the feasible strategies selected for the illustrative example are shown in Figure 5. These can be enumerated as follows:

Maintenance Strategy	K_1 Value	K_2 Value	Maintenance Strategy	K_1 Value	K_2 Value
1	7	0	5	4	0
2	6	0	6	4	5
3	5	0	7	4	4
4	5	4			

Prediction of Pavement Conditions Under Each Feasible Strategy

The Markov chain model is employed to predict future conditions of a given pavement under each of the feasible maintenance strategies selected in the previous step. The Markov model requires the initial condition of a pavement immediately after the adoption of a given maintenance alternative and the one-step transition matrix for the alternative. From this information, the model

finds the expected state of the pavement and its expected R_R value.

Calculation of Total Expected Cost of Feasible Maintenance Strategies

For each feasible maintenance strategy, routine maintenance costs, construction costs, preparation costs, traffic interruption costs during construction, excess user costs due to slower traffic, and salvage value at the end of the analysis period are calculated. The total expected cost is then found from the following

$$\text{Total expected cost} = \text{routine maintenance cost} + \text{construction cost} + \text{preparation cost} + \text{traffic interruption cost} + \text{excess user cost} - \text{salvage value} \quad (1)$$

All the costs are discounted to bring them to their present worth values. The discount factors are calculated from the following formula:

$$\beta(I) = 1/(1 + i_e)^{2I} \quad (2)$$

where

$\beta(I)$ = present value of \$1 spent at the end of the Ith time period and
i_e = effective interest rate = interest rate - inflation rate

The salvage value is calculated as follows:

$$\text{Salvage value} = (\text{usable life left in last overlay} \div \text{total expected life of last overlay}) \times \text{construction cost of last overlay} \quad (3)$$

Preparation cost, excess user cost, and salvage value depend on pavement conditions; construction cost and traffic interruption cost depend on type of maintenance alternative and method of handling traffic during construction; and routine maintenance cost depends only on time periods since the last overlay.

CONCLUSIONS

The investigation described here indicates that a pavement management system is feasible and can be implemented by the Washington State Department of Highways. The major requirements for such a system can be satisfied within the constraints of existing operating procedures. The major benefits from the system will be in the optimum usage of funds. It must be noted that the implementation of the system may not reduce the funds required for maintenance of the total network. The management system will, however, provide a systematic and reasonably objective procedure for using maintenance funds in the most efficient way possible. This could result in a general upgrading of the network without an increase in the total budget requirements.

A limited parametric evaluation of the system indicates the crucial role of user costs in the selection of optimum maintenance. A major effort for the implementation of the system will be in developing realistic user costs.

Parts of the management system that may require improvement are treatment of uncertainties and consideration of time-dependent transition matrices in the Markov model.

REFERENCES

1. F. Finn, R. Kulkarni, and K. Nair. Pavement Management System: Feasibility Study. Washington Highway Commission, final rept., Aug. 1974.
2. R. LeClerc and T. R. Marshall. A Pavement Condition Rating System and Its Use. Proc., AAPT, Feb. 1969, pp. 280-295.
3. R. Howard. Dynamic Probabilistic Systems. Wiley, New York, 1971.
4. J. Benjamin and C. A. Cornell. Probability, Statistics, and Decision for Civil Engineers. McGraw-Hill, New York, 1970.
5. R. Winfrey. Economic Analysis for Highways. IEP, New York (formerly International Textbook Company, Scranton), 1969.

Effects of Pavement Roughness on Vehicle Speeds

M. A. Karan and Ralph Haas, Department of Civil Engineering, University of Waterloo
Ramesh Kher, Ontario Ministry of Transportation and Communications

Vehicle speeds on highways as affected by a variety of factors, such as geometric characteristics of the roadway and traffic conditions, have been extensively studied. One factor that has received little attention is that of pavement condition. This report describes a study conducted in the summer of 1974 to develop relationships between average vehicle speed and pavement condition for two-lane highways. The condition factor chosen was roughness, and 72 sites covering a wide range of roughness were selected. Measurements included speed, roughness, geometric characteristics, and traffic counts. Capacities and volume-capacity ratios of the sections were calculated. A regression model relating average speed to roughness in terms of riding comfort index, volume-capacity ratio, and speed limit was developed. The model is simple and plausible and has a reasonable multiple correlation coefficient (0.77).

The operating speed of a highway is one of the major indicators of the level of service provided to the user and one of the major factors to be used in the analysis and justification of highway projects. A number of studies have been conducted to establish vehicle speed characteristics for different highways and conditions. These have shown that operating speeds are affected mainly by the following five groups of variables:

1. Driver characteristics,
2. Vehicle characteristics,
3. Roadway characteristics,
4. Traffic conditions, and
5. Environmental conditions.

Driver characteristics include age, occupation, sex, and experience as well as trip length, trip purpose, and presence or absence of passengers. Vehicle characteristics include engine size and power, type, age, weight, and maximum speed.

Roadway characteristics such as geographic location, sight distance, lateral clearance, frequency of intersections, gradient length and magnitude, and type of surface have been shown to be important in speed analysis.

Traffic volume and density, composition, access control, and passing maneuvers are the most important variables related to traffic.

Time of day and climatic conditions are the major environmental factors. Although the effects of time and weather on speed have not yet been well established, experience has shown that they cannot be neglected.

One of the major unknowns in speed studies is the effect of pavement condition or roughness on operating speed. Recent improvements in the economic evaluation component of pavement design and management suggest that all agency and user costs need to be included (1). As a consequence, an existing pavement condition that significantly affects operating speeds can have significant economic implications in terms of extra user time and vehicle operating costs and potential extra accident and discomfort costs.

SCOPE AND OBJECTIVES OF STUDY

The basic purpose of this study was to establish initial relationships of speed and roughness for rural highways through a field study of a range of representative highway sections. Riding comfort index (RCI) was chosen as the indicator of roughness. [RCI is the Canadian equivalent of present serviceability index (PSI) except that a scale of 0 to 10 is used instead of a scale of 0 to 5 as for PSI values.]

Highways with both 80-km/h (50-mph) and 96-km/h (60-mph) speed limits were chosen for the study. These represent speed limits for many highway sections in Canada, and they encompass the current, common 88-km/h (55-mph) speed limit in the United States.

The following sections describe the scope and results of the field study, the analysis of the data, and the potential use of the relationships developed in pavement design and management systems.

FIELD STUDY

Selection of Study Sites

In selecting the location of the sites, we made an attempt

Publication of this paper sponsored by Committee on Theory of Pavement Design.

to obtain as many sections as possible for each range of RCI values. RCI was taken in 10 groups (0.0 to 0.9, 1.0 to 1.9, . . . , 9.0 to 10). Actual measurements of the sections were taken by Ontario Ministry of Transportation and Communications (MTC) personnel with a roughness meter, which had been correlated with RCI. It was thought that the results of the study would be mainly used for pavements with an RCI value between 4.0 and 7.0. Therefore, special consideration was given to finding sections in this range. Sections with very low and very high RCIs were also needed, however, to establish a complete range of conditions and for regression analysis. Figures 1 and 2 give the general geographic location of the study sites in southern Ontario and the number of sections used in this study for each group of RCIs respectively.

Many potential sites were initially selected from scaled maps. However, because the sections were required to have certain characteristics (level, tangent, good sight distance, an RCI within the desired range), the final selection was made by extensive field observations.

All sections selected were on two-lane paved highways with both 80- and 96-km/h (50- and 60-mph) speed limits so that the effect of speed limit on actual highway speed could be determined. Information concerning type of surface and other physical roadway characteristics occurring at the various sites is given in Table 1.

Traffic counts were also taken because traffic characteristics can have a significant influence on speeds. These counts were made during the speed measurements. Capacities and volume-capacity (V/C) ratios were calculated [by using the Highway Capacity Manual (14)]. Table 2 gives detailed information on the traffic characteristics of the sites.

Figure 1. Area of speed station locations.

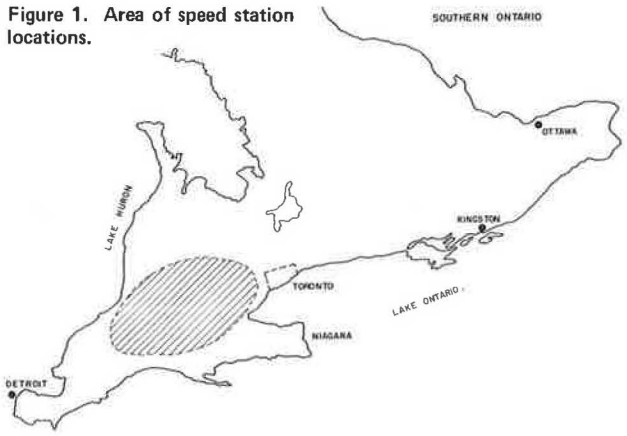

Figure 2. Distribution of roughness for sections used in speed studies.

F3

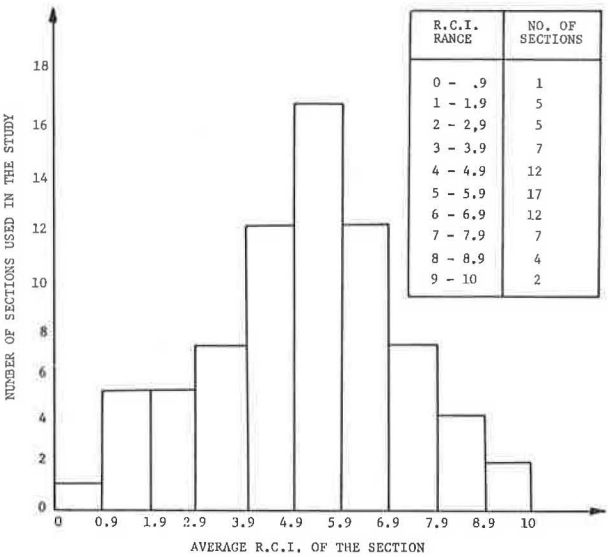

Speed Measuring Equipment

The two most important features of speed measuring equipment for field studies are that

1. It should be easy to use and be reliable and accurate so that measurements can be obtained easily and with reasonable accuracy and
2. It should be of such a nature that it can be camouflaged and thus not influence the motorist.

After taking these factors into consideration, we decided that an electromatic radar speed meter would be most suitable for the study. A graphic recorder was also used to obtain permanent records and more accurate readings.

To ensure the reliability of the equipment, several preliminary tests were run. The effect of the position of the receiver was checked. The receiver was set on the dash, rear window ledge, and outside the side windows facing to the front and rear of the vehicle. The right window position was found to be the best. The receiver was therefore installed at the outside of the right rear window, facing the traffic approaching from the rear of the test vehicle. It was not noticeable to motorists; moreover, the test vehicle was an older type of car

Table 1. Roadway characteristics at speed stations.

Section Number	Lane Width (m)	Shoulder Width (m)	Section Number	Lane Width (m)	Shoulder Width (m)
1	3.20	0.61	37	3.35	1.83
2	3.20	0.61	38	3.35	1.83
3	3.05	3.35	39	3.35	3.35
4	3.05	3.35	40	3.35	3.35
5	3.35	2.59	41	3.35	2.59
6	3.35	2.59	42	3.35	2.59
7	2.74	0.91	43	3.35	2.44
8	2.74	0.91	44	3.35	2.44
9	2.74	0.61	45	3.35	2.44
10	2.74	0.61	46	3.35	2.44
11	3.05	0.91	47	3.66	2.44
12	3.05	0.91	48	3.66	2.44
13	3.35	1.52	49	3.35	2.44
14	3.35	1.52	50	3.35	2.44
15	3.66	0.61	51	3.35	3.05
16	3.66	0.61	52	3.35	3.05
17	2.90	2.13	53	3.35	3.05
18	2.90	2.13	54	3.35	3.05
19	3.35	3.35	55	3.35	3.35
20	3.35	3.35	56	3.35	3.35
21	3.35	3.05	57	3.05	2.74
22	3.35	3.05	58	3.05	2.74
23	3.35	3.96	59	3.05	2.59
24	3.35	3.96	60	3.05	2.59
25	3.35	2.74	61	3.05	0.76
26	3.35	2.74	62	3.05	0.76
27	3.66	3.05	63	3.05	0.91
28	3.66	3.05	64	3.05	0.91
29	3.05	0.91	65	3.05	0.30
30	3.05	0.91	66	3.05	0.30
31	3.35	2.44	67	3.35	0.91
32	3.35	2.44	68	3.35	0.91
33	3.05	3.05	69	3.35	1.52
34	3.05	3.05	70	3.35	1.52
35	3.35	2.13	71	3.81	0.91
36	3.35	2.13	72	3.81	0.91

Notes: 1 m = 3.28 ft.
Each section has two lanes; all pavements are asphalt; and all shoulders are gravel.

with no resemblance to police vehicles.

After several test runs, it was found that traffic in both directions could be observed from the single position. As a consequence, speeds in both directions were measured at the same time, at each study site. Traffic volumes did not create any difficulty because they were relatively low (free-flow conditions). In the case of two vehicles passing the station at the same time, the data were canceled by the observer sitting on the front seat of the test vehicle simply by putting a mark on the records.

As a check on the reliability of the radar during the field study, tuning forks were used to simulate speeds of 48, 80, and 112 km/h (30, 50, and 70 mph). Adjustments were made before the actual speed measurements.

Field Measurements

After the selection of speed stations for the study, roughness was measured at each station on a 0.4-km (0.25-mile) section. The measurements were taken with a BPR roughometer, and the readings were converted to RCI from a previously established correlation with mean panel ratings. Table 3 gives roughness readings and RCI values for each study station.

The next step consisted of speed measurements. For these, the test vehicle was parked on the far edge of the shoulder at each station. In the case of inadequate shoulder widths, private driveways were used. The radar and recorder were set, and the receiver was placed in position. Standard field sheets were used to record traffic and roadway data. The following information was obtained from each station:

1. Speeds of vehicles by type and direction;
2. Hourly traffic volumes by type and direction; and
3. Roadway characteristics (land and shoulder widths, type of pavement, and the like).

It should be noted that all observations were made during daytime but not in a specific time period. Rush hours, when traffic volumes are very heavy, were avoided. The speed measurements were generally made under free-flow conditions so that the effect of slow-moving vehicles or congestion could be minimized.

Motorcycles were excluded from the study. Similarly, "unusual" drivers (such as very slow-moving, elderly drivers) were not taken into account. When a vehicle was felt to be influenced by such a slow-moving vehicle or opposing traffic, the measurement was omitted.

The sample size was calculated by the formula given in the Manual of Traffic Engineering Studies (2). An attempt was made to observe 60 vehicles at each station; however, at some stations (especially those on secondary county roads), this number could not be obtained in a reasonable length of time because of the very low traffic volumes.

ANALYSIS OF FIELD DATA

A total of 4105 vehicle speeds were measured during the field studies. Although measurements were made by type of vehicle, the data were combined for the final analysis and an overall average speed for each station was calculated. Because the objective of the study was to determine the relationship between average highway speed and roughness of the pavement, this approach was considered reasonable. The calculated mean speeds and standard deviation of the speed distributions at each station are given in Table 4.

Figure 3, which was obtained from the information given in Table 4, shows the speed measurements determined by the field studies. It shows that, on county roads with a speed limit of 80 km/h (50 mph), a high proportion of the motorists usually drive somewhat too fast, even on very rough pavements. This situation may be partially explained by the lack of speed limit enforcement on these facilities. On main highways, most drivers tend to obey the speed limit.

The data given in Table 5 and plotted in Figure 3 were first analyzed separately for each group of speed limits and capacity levels. Various regression models were tested. Because of the data limitations, however, a generally acceptable model could not be developed.

The data for 80- and 90-km/h (50- and 60-mph) speed limits were then combined, and one general regression model was tested. Several different forms of models were checked. The final four equations considered are as follows:

$$y = 34.4718 + 0.0199x_1x_4 + 0.0044x_4^2 \quad (1)$$

$$y = 32.9584 + 0.0183x_1x_4 + 0.0055x_4^2 - 0.0075x_2x_3 \quad (2)$$

$$y = 2.596x_1^{0.0928} \times x_3^{-0.0275} \times x_4^{0.704} \quad (3)$$

$$y = 30.7368 + 1.0375x_1 - 11.2421x_3 + 0.0062x_4^2 \quad (4)$$

where

y = average highway speed in kilometers per hour,
x_1 = RCI,
x_2 = total capacity of roadway in vehicles per hour,
x_3 = V/C ratio, and
x_4 = speed limit in kilometers per hour.

Statistical characteristics of these models, as indicated by the data given in Table 5, are similar. All coefficients are statistically significant; constant terms are alike; and all of them have similar multiple correlation coefficients. Mean, absolute mean, and standard deviation of residuals were calculated for further analysis. However, the results were not particularly helpful for selecting the best model.

Subjective, logical tests were then applied. Model 3 was eliminated because of the production nature of the equation. It would give zero speeds for zero RCI value, which means no vehicle movement on very rough sections. This is unrealistic.

The remaining models were then studied thoroughly. Model 4 was finally selected mainly because of its simplicity. Caution should, however, be exercised in use of the x_3 term in the model. The reason for this is that field measurements were conducted mostly under free-flow conditions. The effect of V/C ratio in speed, therefore, is perhaps not accurately represented by the model over the whole range of possible V/C ratios (from 0.0 to 1.0). Thus the recommended model should not be used for highway sections with very high traffic volumes. Similarly, the model is not too accurate for RCI values of less than 2.0.

COMPARISON OF RESULTS

Figure 4 compares the data of this investigation with those of previously presented relationships.

The relationships used by the Ontario MTC in their pavement management system OPAC (1) are represented by heavy solid lines for various speed limits between 80 and 112 km/h (50 and 70 mph). Also shown are the linear regressions (model 4) for data from the 80-km/h (50-mph) speed limit roads and the 96-km/h (60-mph) speed limit roads.

The MTC relationship for the 80-km/h (50-mph) speed limit roads compares reasonably well with the observed

Table 2. Traffic characteristics at speed stations.

Section Number	Total Capacity (vehicles/h)	Directional Volume (vehicles/h)	Volume-Capacity Ratio	Speed Limit (km/h)	Section Number	Total Capacity (vehicles/h)	Directional Volume (vehicles/h)	Volume-Capacity Ratio	Speed Limit (km/h)
1	1253	7	0.01	80	37	1531	51	0.07	80
2	1253	12	0.02	80	38	1531	63	0.08	80
3	1409	17	0.02	80	39	1531	120	0.16	96
4	1409	16	0.02	80	40	1531	108	0.14	96
5	1531	35	0.05	96	41	1531	108	0.14	96
6	1531	49	0.06	96	42	1531	72	0.09	96
7	1183	33	0.06	80	43	1531	96	0.13	96
8	1183	34	0.06	80	44	1531	96	0.13	96
9	1131	25	0.04	80	45	1531	72	0.09	96
10	1131	24	0.04	80	46	1531	84	0.11	96
11	1262	28	0.04	80	47	1740	84	0.10	96
12	1262	111	0.18	80	48	1740	96	0.11	96
13	1496	69	0.09	80	49	1531	96	0.13	96
14	1496	78	0.10	80	50	1531	120	0.16	96
15	1479	203	0.27	80	51	1531	156	0.20	96
16	1479	225	0.30	80	52	1531	144	0.18	96
17	1357	94	0.13	96	53	1531	96	0.12	96
18	1357	69	0.10	96	54	1531	192	0.25	96
19	1531	336	0.43	96	55	1531	156	0.20	96
20	1531	252	0.33	96	56	1531	228	0.29	96
21	1531	108	0.14	96	57	1409	216	0.31	96
22	1531	144	0.19	96	58	1409	156	0.22	96
23	1531	131	0.17	96	59	1409	156	0.22	96
24	1531	125	0.16	96	60	1409	144	0.20	96
25	1531	69	0.09	80	61	1253	48	0.06	80
26	1531	63	0.08	80	62	1253	48	0.06	80
27	1740	70	0.08	96	63	1262	36	0.06	80
28	1740	88	0.10	96	64	1262	48	0.08	80
29	1262	42	0.07	80	65	1140	33	0.06	80
30	1262	37	0.06	80	66	1140	39	0.07	80
31	1531	156	0.20	96	67	1375	47	0.07	96
32	1531	120	0.16	96	68	1375	61	0.09	96
33	1409	96	0.14	96	69	1496	58	0.08	80
34	1409	132	0.19	96	70	1496	40	0.05	80
35	1531	132	0.17	96	71	1557	156	0.20	80
36	1531	132	0.17	96	72	1557	144	0.18	80

Note: 1 km/h = 0.621 mph.

Table 3. Roughness data for speed stations.

Section Number	Roughness Index (mm/km)	RCI[a]	Section Number	Roughness Index (mm/km)	RCI[a]
1	4762	0.5	37	1080	6.9
2	3493	1.8	38	1016	7.2
3	—	3.4	39	762	8.4
4	—	3.6	40	826	8.1
5	572	9.7	41	953	7.5
6	699	8.8	42	1016	7.2
7	2858	2.7	43	1080	6.9
8	3175	2.2	44	1651	5.1
9	3556	1.7	45	1397	5.8
10	3874	1.4	46	1524	5.4
11	3747	1.5	47	1461	5.6
12	3175	2.2	48	1143	6.7
13	2032	4.2	49	1016	7.2
14	1588	5.2	50	889	7.8
15	4064	1.2	51	1080	6.9
16	3366	2.0	52	1080	6.9
17	2032	4.2	53	1080	6.9
18	2223	3.8	54	1461	5.6
19	1016	7.2	55	2159	4.0
20	1016	7.2	56	2096	4.0
21	2032	4.2	57	1524	5.4
22	2096	4.0	58	1461	5.6
23	2413	3.4	59	1588	5.2
24	2159	3.9	60	1651	5.1
25	1080	6.9	61	1715	4.9
26	1143	6.7	62	1524	5.4
27	635	9.2	63	1651	5.1
28	699	8.8	64	1461	5.6
29	1715	4.9	65	1651	5.1
30	1905	4.4	66	2032	4.2
31	1588	5.2	67	1778	4.7
32	1334	6.0	68	1270	6.2
33	1651	5.0	69	1842	4.6
34	1461	5.6	70	2223	3.8
35	1270	6.2	71	2667	3.0
36	1270	6.2	72	3302	2.1

Notes: 1 mm/km = 15.78 mm/mile.
The length of each section is 0.40 km (0.25 mile).
[a]RCI = 25.25 - 10.0093 log R where R = roughness index.

Table 4. Speed data for speed stations.

Section Number	Mean Speed (km/h)	Standard Deviation (km/h)	Section Number	Mean Speed (km/h)	Standard Deviation (km/h)
1	67	8.79	37	82	10.06
2	67	9.10	38	83	8.72
3	86	14.76	39	98	10.90
4	85	10.32	40	101	12.08
5	96	9.24	41	94	12.49
6	96	9.34	42	99	12.17
7	77	8.52	43	91	15.39
8	78	8.97	44	94	12.99
9	78	10.34	45	94	11.95
10	78	14.04	46	96	11.56
11	62	4.59	47	94	10.59
12	61	7.65	48	98	12.70
13	78	17.23	49	98	10.77
14	78	11.59	50	94	10.21
15	69	11.51	51	93	14.52
16	72	8.77	52	94	11.09
17	91	17.36	53	91	11.85
18	90	11.90	54	86	9.26
19	93	10.21	55	85	9.74
20	91	8.65	56	83	9.35
21	99	9.27	57	90	9.19
22	93	10.21	58	88	12.77
23	88	10.42	59	91	9.68
24	93	10.18	60	88	9.97
25	91	11.11	61	83	12.48
26	88	10.79	62	77	10.79
27	96	14.81	63	86	11.79
28	93	12.30	64	82	11.74
29	78	10.90	65	85	13.09
30	86	14.57	66	85	13.15
31	91	12.06	67	93	12.99
32	91	11.33	68	91	14.31
33	86	11.22	69	72	12.59
34	86	12.08	70	72	10.13
35	85	10.14	71	75	11.16
36	90	11.22	72	74	10.92

Note: 1 km/h = 0.621 mph.

data although its slope could be adjusted. For the 96-km/h (60-mph) speed limit roads, it also compares reasonably well with the data, but again the slope could be adjusted. The MTC relationship also appears to reduce speed too severely for the lower RCI values (vehicles travel somewhat faster on very rough roads under free-flow conditions than originally postulated).

Finally, McFarland's original postulated relationship for 96-km/h (60-mph) speed limit roads (11) is also shown in Figure 4. It agrees reasonably well with the observed data for high RCI values (greater than about 7), but it reduces speed too severely for the lower RCI values.

Figure 3. Distribution of mean vehicle speeds.

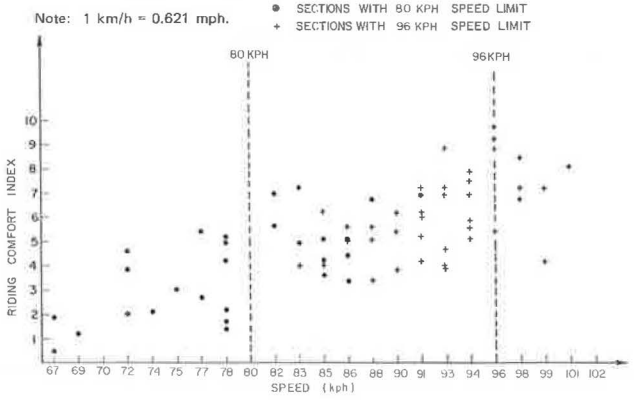

Table 5. Statistical characteristics of regression equations.

Model Number	Multiple Correlation Coefficient	Student's t-Values[a]	Standard Error of Estimate	Goodness of Fit
1	0.73	t_1 = 5.87	2.67	96.78
2	0.77	t_1 = 5.56 t_2 = 6.41 t_3 = 2.67	2.56	72.77
3	0.79	t_1 = 7.40 t_2 = 2.90 t_3 = 8.54	0.05	85.16
4	0.77	t_1 = 5.74 t_2 = 2.67 t_3 = 8.25	2.52	60.41

[a]Theoretical t = 2.32.

Figure 4. Speed-riding comfort index data and relationships.

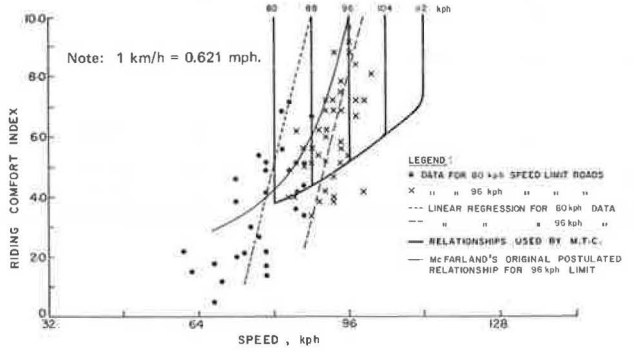

USE OF SPEED-ROUGHNESS RELATIONSHIPS IN PAVEMENT MANAGEMENT

General Implications

The pavement design and management concept that has been used recently for developing real working systems within various highway agencies (3, 4, 5, 6, 7, 8, 9, 10) includes the generation and analysis of alternative design strategies. In the analysis procedure, the performance output of each strategy is predicted. Then the cost and benefit implications of these performance outputs are determined and compared for selecting the optimal strategy.

Today many pavement authorities have agreed that both agency costs (initial capital, resurfacing, and maintenance costs) and user costs (traffic delay, vehicle operation, travel time, accident, and discomfort) need to be considered in the economic evaluation of alternative pavement design strategies. Recent studies (1, 11) have quantitatively illustrated the importance of the user costs component.

User costs vary significantly with pavement performance. This variation is a function of roughness, which affects vehicle speeds and operating costs. As the pavement deteriorates, the lower speeds result in higher user costs. Therefore, a pavement strategy that provides a low level of serviceability over a longer period of time causes higher user costs than a strategy that serves the traffic on a smoother surface for most of the time.

Figure 5. Speed profiles for two example strategies.

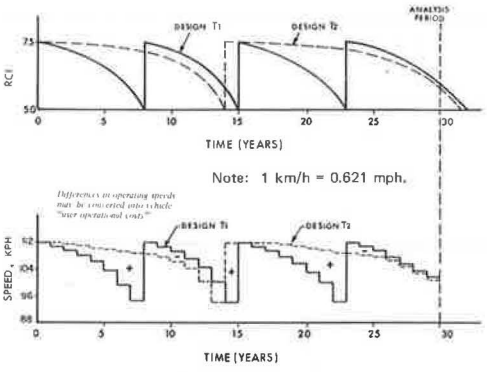

Figure 6. Unit costs (excluding taxes) of speed reductions at different RCI levels on a rolling tangent in Ontario.

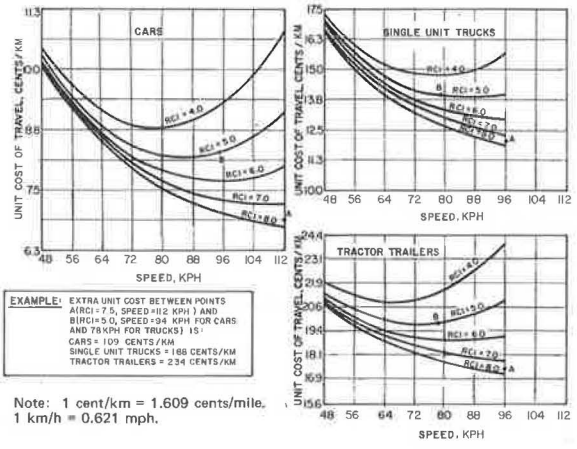

As a consequence, determination of speed profiles during the life of a pavement becomes extremely important because it provides a means for relating user costs to pavement performance.

When the performance history of a pavement design strategy is determined, as shown in the upper portion of Figure 5, the speed profile of the strategy can then be easily found by the types of relationships shown in Figure 4. An example is shown in the lower portion of Figure 5, which is patterned after Kher, Phang, and Haas (1). The corresponding user costs can be calculated from data available in the literature (12, 13) or from relationships such as those shown in Figure 6, also patterned after Kher, Phang, and Haas (1). (In Figure 6, unit costs = vehicle operation and travel time.)

The effect of the traffic volume on vehicle speeds should also be considered in the analysis for more accurate results because speed reductions may occur as a result of increased traffic volumes as well as low pavement serviceability levels. Therefore, speed versus roughness and traffic (combined) relationships should be the object of future research for more comprehensive user cost analysis.

Example

A simple example can serve to illustrate the economic implications of speed-roughness variations.

Suppose that a two-lane highway with an annual average daily traffic (AADT) of 5000 and a 96-km/h (60-mph) speed limit has reached a terminal serviceability (i.e., RCI) level of 4.5. The extra user costs involved in delaying the resurfacing (which is expected to raise the RCI level to 8.0) by 1 year should be calculated.

If we assume that the 5000 AADT represents all passenger cars, then Figure 4 indicates an 88-km/h (55-mph) average speed for an RCI of 4.5 and a 96-km/h (60-mph) average speed for an RCI of 8.0. Figure 6 then indicates user costs of 8.8 and 6.9 cents/km (14.1 and 11.2 cents/mile) respectively for the before and after resurfacing conditions.

For a 1.6-km (1-mile) section and 350 days, the extra user costs of delaying resurfacing are $5000 \times 350 \times (0.141 - 0.112)$, which is $50 750. This would be reduced slightly by the delay in the extra user costs due to resurfacing (using present worth of costs analysis), but it still represents quite a significant extra cost. Of course budget restrictions of the agency involved might require many such resurfacing delays despite the extra user costs. Nevertheless, these extra user costs should be determined and used as a factor in determining investment priorities.

The foregoing example has been chosen to cover a fairly narrow range and conditions in which the observed data of Figure 4 agree quite closely with the relationship that the Ontario MTC uses in its pavement management system. Allowing the serviceability to drop to lower levels than those of the example would result in higher extra user costs as well as possible extra capital costs for resurfacing (i.e., extra thickness).

CONCLUSIONS

Three major points of this paper can be summarized.

1. Speeds of motor vehicles on highways are significantly affected by pavement condition. Neglecting this effect may result in major errors in the economic evaluation of alternative pavement design strategies.
2. Field observations were made at 72 selected stations in southern Ontario. Vehicle speeds were measured for various roughness levels (which were transformed into RCI values). Geometric characteristics of the roadway section at each station were also determined. Traffic counts were conducted and V/C ratios were calculated.
3. A regression equation was developed for two-lane rural highways to express vehicle speeds in terms of RCI, V/C ratio, and speed limit. The relationship has potential application to individual pavement projects or to a series of projects within a network. It compares reasonably well with previously postulated relationships over a certain range of conditions.

ACKNOWLEDGMENT

The study on which this paper is based was supported by the Ontario Ministry of Transportation and Communications.

REFERENCES

1. R. K. Kher, W. A. Phang, and R. C. G. Haas. Economic Analysis of Elements in Pavement Design. TRB, Transportation Research Record 572, 1976, pp. 1-14.
2. D. E. Cleveland. Manual of Traffic Engineering Studies. ITE, Arlington, Va., 1964.
3. W. R. Hudson and others. A Systems Approach Applied to Pavement Design and Research. Texas Highway Department, Center for Highway Research, and Texas Transportation Institute, Research Rept. 123-1, March 1970.
4. W. R. Hudson, R. K. Kher, and B. F. McCullough. Automation in Pavement Design and Management Systems. HRB, Special Rept. 128, 1972, pp. 40-53.
5. J. L. Brown. Texas Highway Department Pavement Management System. TRB, Transportation Research Record 512, 1974, pp. 16-20.
6. W. A. Phang and R. Slocum. Pavement Investment Decision Making and Management System. Ontario Ministry of Transportation and Communications, Rept. RR174, Oct. 1971.
7. W. A. Phang. Flexible Pavement Design in Ontario. TRB, Transportation Research Record 512, 1974, pp. 28-43.
8. D. E. Peterson. Utah's Pavement Design and Evaluation System. TRB, Transportation Research Record 512, 1974, pp. 21-27.
9. W. T. Kenis and T. F. McMahon. Pavement Analysis System: VESYS II. AASHO Design Committee Meeting, Oct. 1972.
10. R. L. Lytton and W. F. McFarland. Implementation of a Systems Approach to Pavement Design. TRB, Transportation Research Record 512, 1974, pp. 58-62.
11. W. F. McFarland. Benefit Analysis for Pavement Design Systems. Texas Highway Department, Center for Highway Research, and Texas Transportation Institute, Research Rept. 123-13, April 1972.
12. P. J. Claffey. Running Costs of Motor Vehicles as Affected by Road Design and Traffic. NCHRP, Rept. 111, 1971.
13. R. Winfrey. Economic Analysis for Highways. IEP, New York (formerly International Textbook Company, Scranton), 1969.
14. Highway Capacity Manual—1965. HRB, Special Rept. 87, 1965.